Solid phase microextraction coupled to comprehensive two-dimensional gas chromatography–time-of-flight mass spectrometry for metabolite profiling of apples: Potential of non-invasive *in vivo* sampling assay in characterization of metabolome

by

Sanja Risticevic

A thesis

presented to the University of Waterloo

in fulfillment of the

thesis requirement for the degree of

Doctor of Philosophy

in

Chemistry

Waterloo, Ontario, Canada, 2012

Author's Declaration

I hereby declare that I am the sole author of this thesis. This is a true copy of the thesis, including any required final revisions, as accepted by my examiners.

I understand that my thesis may be made electronically available to the public.

Abstract

The objective of the current research project relies on implementation of solvent-free, green and environmentally friendly solid phase microextraction (SPME) sample preparation alternative in the area of complex sample characterization. The advantages that the technique offers in comparison to traditional methods of sample preparation including solvent-free implementation, short sample preparation times, small sample amount requirements, advanced automation capability and minimization of matrix effects are effectively employed during *ex vivo* and laboratory investigations of complex samples. More important, the underlying features of the technique including miniaturized format, nonexhaustive extraction recoveries and on-site compatibility were fully exploited in order to investigate the metabolome of biological systems directly on the site. Hence, *in vivo* SPME extraction format was employed in direct immersion SPME sampling of biological systems, hence eliminating the crucial prerequisites associated with multiple preparative steps and incorporation of metabolism quenching that are encountered during implementation of traditional sample preparation methods in global metabolite analysis. Furthermore, *in vivo* sampling format was hyphenated to comprehensive two-dimensional gas chromatography – time-of-flight mass spectrometry (GCxGC-ToFMS) for high-resolution sampling of volatile and semivolatile metabolites in 'Honeycrisp' apples.

The initial stages of the project involved evaluation of performance characteristics of commercial SPME extraction coatings in terms of extraction selectivity, extraction sensitivity and desorption efficiency by employing headspace SPME analysis of both aqueous standards spiked with representative volatile and semivolatile metabolites as well as the apple homogenate. DVB/CAR/PDMS coating was selected on the basis of optimum metabolite coverage and extraction sensitivity and was consequently employed during *ex vivo* and *in vivo* sampling assays corresponding to determination of volatile and

semivolatile metabolites. The former extraction methodology incorporated appropriate sample preparation steps for quenching metabolic activity so that the relevant metabolome profile is not biased against unstable metabolites and those that are susceptible to inter-metabolite conversions which adversely impact preservation of metabolite identity. The two sample preparation assays were compared in terms of metabolite coverage and analytical precision in order to identify SPME route toward characterization of more representative metabolome and determination of instantaneous and more 'true' metabolism snapshoot. This is the first report illustrating the implementation of *in vivo* direct immersion SPME assay for non invasive determination of endogenous fruit metabolites whose profiles and contents are highly correlated to a multitude of influential fruit quality traits.

Acknowledgements

I am very grateful to many many people from University of Waterloo and external industrial and government organizations for completion of this wonderful project.

First of all, I am thankful to my supervisor, Dr. Janusz Pawliszyn for giving me the opportunity to have such a wonderful and exciting PhD project, the project whose completion has not only been rewarding contribution to the field of analytical chemistry and his research group, but also has been important in extending the range of my own expertise. Throughout the years, I have been intensively and continuously learning new concepts from all possible dimensions that were composing my project, including sample preparation, *in vivo* SPME, comprehensive two-dimensional gas chromatography and time-of-flight mass spectrometry. I am proud of the extent of knowledge and level of excellence that I acquired during my PhD years and how much I have matured as a scientist and an analytical chemist during the period of my PhD program. Thank you professor Pawliszyn for giving me time to learn new methodology and to comprehensively investigate the effects of many experimental conditions and variables on the quality of the analytical method. Thank you so much, because I realize that my instrumental investigations not only made me learn and learn and learn but also resulted in the development of robust and high-quality SPME-GCxGC-ToFMS method that I am proud of and that has been impressing me on daily basis with acquisition of reliable data sets. I am also very grateful for the financial support that you offered, for the opportunity to engage and be responsible for SPME course coordination and organization, for having your support to participate in international meetings and conferences and for the assignment of laboratory manager role. Thank you for allowing me to be comprehensive and detailed, for trusting in reliability and accuracy of my results and for believing in me and my capabilities in encountering daily challenges.

I am also very grateful to my advisory committee member, Dr. Jennifer DeEll from Ontario Ministry of Agriculture, Food and Rural Affairs (OMAFRA) (Simcoe, ON, Canada) for allowing the access to representative and reliable metabolomics sample sets, for editing my manuscripts and giving me valuable feedback on improving my written thesis document. It was my pleasure to have Dr. Michael Chong on my advisory committee and I am grateful to him about discussions on differential metabolites and their uniqueness to *ex vivo* and *in vivo* SPME modes of sampling. It was my pleasure to have Dr. Wojciech Gabryelski, Dr. Simon Chuong and Dr. Hans-Gerd Janssen on my committee and I thank them for contributing to improvement of my written thesis document. I am thanking my committee members for providing the excellent feedback about the organization, quality and structure of my thesis, for indicating that my results were valuable to the field of analytical chemistry and for nominating my thesis for award.

I would also like to acknowledge Mr. Olivier Niquette and Mr. Chris Warren from LECO (St. Joseph, MI, USA) for allowing the cost-effective addition of GCxGC-ToFMS instrument to our InFAReL laboratory to be employed in my PhD project. I am thankful for your support during installation, configuration and maintenance of the instrument during all the years of my PhD project. I am grateful to Mr. Olivier Niquette for listening about my research, for being interested in and enthusiastic about my results, and for spending long hours and days trying to resolve a particular instrumental problem in the light of me being able to proceed with experiments and to have a more reliable method. I am also very grateful to Mr. Chris Warren and Dr. Tomas Kovalczuk for approving and organizing my participation at EUROanalysis conference in Belgrade (Serbia, September 2011) as it was my pleasure to do so and to present my results on LECO Pegasus 4D GCxGC-ToFMS system.

I am grateful to Mr. Len Sidisky from Supelco (Bellefonte, PA, USA) for providing Supelcowax second dimension column for second dimension separation on GCxGC-ToFMS system. Special acknowledgment and

gratefulness goes to Dr. Jack Cochran from Restek (Bellefonte, PA, USA) for carefully listening to my concerns about retention time stability in second dimension and providing the column on which such challenges were overcome. The possibility of performing automated data processing and alignment of metabolites greatly enhanced the speed of processing and generation of data matrices compatible with subsequent multivariate analysis.

I am thankful to personnel from Gerstel (Linthicum, MD, USA), including Mr. Edward Pfannkoch, Mr. Jim Daley and Mr. Tim Pence for configuration of MultiPurpose Sampler (MPS 2), for considering the issues with autosampler configuration a high priority and for helping resolve multiple problems with autosampler configuration, installation and operation in impressively efficient and timely manner.

I thank the two hard working people in the chemistry department at University of Waterloo, Mr. Kenneth Gosselink and Mr. Matthew Sternbauer from Chem Stores for going out of their way many times to assist me in organizations and preparations for *in vivo* sampling.

I thank Erica Silva, my coworker and friend for attending on-site sampling sessions and for being inspired by my project and the results I was acquiring. I will never forget how much your presence has meant to me. I thank you for being a good friend and a great listener.

I thank my two very best ‘coworker’ friends and amazing coworkers, Dr. Dajana Vuckovic and Dr. Rosalba Vatinno, for unconditional support and friendship, for being always there, for enjoying the collaborative activities that we were involved in, and for constantly impressing me with their dedication, motivation, enthusiasm, positive energy, hard work and amazing research potential. It has been my pleasure to work with both of you and I am so grateful that our friendship continued despite the fact we were working in different institutions. Special acknowledgment goes to Dr. Dajana Vuckovic for being an amazing coworker and the hardest working person that I have ever known.

I thank my family, my parents, Bozo and Gora Risticevic and my brother, Aleksandar Risticevic for unconditional support and love, for being my

very best friends and role models and for inspiring me always with their unconditional love, loyalty, honesty, dedication, motivation and hard work. Thank you for believing in me and being proud of my accomplishments.

Table of Contents

List of Figures

List of Tables

1. Introduction

1.1 *Metabolomics: emergence, platforms and food metabolomics perspective*

1.1.1 *Introduction to metabolomics*

Metabolomics currently represents one of the fastest growing high-throughput molecular analysis platforms that refer to the simultaneous and unbiased analysis of metabolite pools constituting a particular biological system under investigation. The goal of metabolomics lies in the comprehensive analysis and simultaneous relative quantification of all or at least as many as possible metabolites (small molecules having molecular weights lower than 1000 D) in cells, tissues or body fluids [1-3]. Therefore, it is regarded as the systematic study of metabolite profiles and their compositional levels which are highly dependent on factors including, for example, genetic modifications, physiological stimuli, environmental conditions and supply of nutrition. Metabolomics analyses strive toward complete characterization of metabolome which is regarded as the ultimate expression of genotype in response to environment [4]. The term 'metabolome' was first described as the set of metabolites synthesized by an organism [5]. However, later on, the definition of metabolome was transformed to 'the quantitative complement of all of the low molecular weight molecules present in cells in a particular physiological or development state' [5]. The cellular processes controlling the biochemical phenotype of the cell, tissue or organism as a whole are reflected in metabolome composition [6]. Qualitative and quantitative analysis of a complete and accurate metabolomic profile represents one of the major goals of quantitative systems biology and metabolic pathway engineering considering the crucial role of metabolism in the context of the overall cellular function. Whether metabolomics encompasses qualitative profiling or quantitative measurements of intra-cellular metabolites, it reveals the biochemical status of an organism

[6]. The quest for systematic coverage of all metabolites can allow a contemporary analytical chemist to comprehend a variety of biological processes that a multitude of fields including (agri-)biotechnology, disease progression, drug development, toxicology, clinical trial monitoring, organism's response to a treatment or the effect of environmental stimuli on developmental processes can benefit from. The technique has demonstrated a great promise in biomarker detection, identification and/or quantification and subsequent correlation to selected metabolic perturbations.

Since the technology has rapidly become established and technological developments continue to create new opportunities, it is important to define and summarize different types of metabolomics investigations that can be carried out to address a particular question of biological relevance [7]. In general terms, two different conceptual approaches of carrying out a metabolomics investigation exist: targeted and non-targeted [8]. Non-targeted approaches provide a global snapshoot of readily detectable metabolites. Hence, the type of data acquisition technology influences the spectrum of detectable metabolites that can be obtained using this approach. Targeted approaches on the other hand, are focused on selected metabolites and/or metabolic pathways and the outcome of such a limited metabolomic workflow is as predicted improved quantitation and data interpretability. From a more specific perspective, metabolomics investigation may involve one and/or combination of metabolite fingerprinting and profiling [6,9]. Metabolic fingerprinting involves high throughput qualitative screening of metabolome constituents and it uses signals from hundreds to thousands of metabolites for sample comparison and discriminative analysis [6,9]. Therefore, the approach does not require metabolite identification and does not necessitate optimization of sample preparation, separation and detection procedures. The goal of analytical methodology is simplicity and speed. On the other hand, metabolic profiling involves metabolite identification and quantification, a process which is feasible for a limited number of compounds and is practically possible for classes of chemically related metabolites having chemical properties that facilitate

simultaneous analysis [6,9-10]. Subsequent to broad-scale metabolomics analyses, targeted metabolomics approach can be implemented in greater detail on selected groups of metabolites following thorough optimization of extraction, separation and detection procedure.

Biology is an informational science and as such, biological interpretation of living organisms has benefitted greatly with the emergence of metabolomics [9]. With the advancements in analytical instrumentation including design of the instruments with improved sensitivity, selectivity and specificity, the capacity of an analytical chemist to generate data on the molecular organization of biological systems has never been greater. In fact, recent technological advances have revolutionized our visualization of biological systems [11]. Metabolomics also necessitates multidisciplinary approaches and combination of complementary divergent expertise for appropriate analytical methods implementation and analysis, statistical evaluation and data interpretation from a biological standpoint. The plant community has adopted the technique fairly rapidly for the obvious reason of its promising contribution to a wide range of both scientific and applied fields.

1.1.2 *Plant metabolomics and its role in understanding plant systems*

While there is evidence that at least 270,000 plant species exist worldwide, researchers believe in the existence of more than 400,000 species and in fact plants account for 90% of the biomass on Earth [12]. From a historical point of view, plants provide critical nutritional and valuable life resources for both humans and animals [13]. It is well known that animals and humans exploit plants as a source of carbon and the photosynthetic process plays a role in fixing organic carbon to edible organic forms. Apart from this, plants represent a valuable source of nitrogen and in fact herbivorous and omnivorous animals rely on plants for the supply of essential amino acids. These processes of photosynthesis and respiration in plants function to maintain a balance of oxygen, carbon dioxide and water in the atmosphere. More

important, plants provide trace nutrients and vitamins such as folate and vitamins A, C and E. Therefore, apart from visually appealing characteristics, plants provide irreplaceable resources that are of biological and economic importance to humans [13-14]. Industries require plant products for ensuring their supply of industrial products (polymers, fibers, latex, packaging materials, industrial oils, paper, textiles, building materials, binders, emulsifiers, adhesives) and fuels including hydrogen, biodiesel, methane and ethanol. The medicines and herbal remedies are either derived from plants or plant extracts. The production of food commodities is dependent on plants in food and beverage industries. Therefore, there is an ever increasing interest in plant research efforts both from scientific (understanding the biochemical complexity of plants) and applied (identification of bioactive compounds) perspectives [15].

Over the years, plants have been developing a complex collection of metabolites and it has been reported that the total number of metabolites produced in the plant kingdom is in the range 100,000 – 200,000 [6,9]. These compounds range from relatively simple primary compounds to highly complex and chemically diverse secondary products [16]. These compounds are synthesized within a complex biochemical network and they may comprise a wide spectrum of chemical families including amino and other organic acids, sugars, volatile metabolites and diverse secondary metabolites such as alkaloids, phenolic compounds and terpenoids. Plant secondary metabolites are compounds that are produced by plants but they are not involved in the growth and development processes [14]. The function of these metabolites, often involving highly complex structures, is not known in majority of cases. On the other hand, the confirmed functions that were assigned to some of these molecules involve roles in pollination, seed dispersal, flavours and fragrances for foods and cosmetics, quality of agricultural products, plant survival, insect resistance and defense against herbivorous and microbial attack [14,17]. Their involvement in interactions between plants, between plants and arthropod herbivores and between plants and microorganisms have also been well documented. The medicinal, anti-carcinogenic, anti-malarial, anti-ulcer,

hapaticidal, antimicrobial and diuretic properties of secondary metabolites have been reported as well [17]. Terpenoids are produced in plants in higher numbers than in any other organisms and the number of plant terpenoids was estimated to about 22,000. Isoprenoid biosynthetic pathway generates primary metabolites such as *i)* phytohormones (gibberellic acid, abscisic acid, cytokinins), carotenoids, chlorophylls and plastoquinones that are involved in photosynthesis; *ii)* ubiquinones required for respiration and *iii)* sterols responsible for structure of the membranes [17]. Terpenoids on the other hand comprise monoterpenoids (C_{10}), sesquiterpenoids (C_{15}), diterpenoids (C_{20}) and triterpenoids (C_{30}) [17]. Terpenoids are derived from the mevalonate pathway or from the 2-C-methyl-D-erythritol-4-phosphate pathway. Both of these pathways result in formation of the C5 units isopentenyl diphosphate and dimethylallyl diphosphate, the two of them representing the basic terpenoid biosynthesis building blocks.

The afore-mentioned biosynthesis of terpenes is just an example of the complex networks that are involved in biosynthesis of selected plant metabolites. It is worth noting that there are still gaps in the knowledge and comprehension of biochemical pathways and their regulation [9]. Largely, plant biochemistry can still be defined in terms of unidentified components derived from poorly understood pathways. Therefore, more comprehensive information on the biochemical composition is necessary to broaden our understanding of how a plant exists, functions and responds to environmental perturbations [7]. Plant metabolomics as one of the relatively new analytical strategies has been regarded as a promising technology when it comes to answering the poorly understood concepts in plant biochemistry. The field has expanded significantly since the first scientific application and early studies focused on model systems including *Arabidopsis*, tomato and potato have been applied to many other species. Plant metabolomics has therefore found a widespread relevance for understanding the influence of the effects including mutations, environmental perturbation and organ development on plant metabolism [15].

1.1.3 *Food metabolomics: another research initiative*

1.1.3.1 Perspectives in application of metabolomics in food analysis

Plants provide the main component of human food intake in most diets. It has been reported that diets that are rich in fresh fruits and vegetables are correlated with increased longevity, promoting health, maintaining metabolic homeostasis and fulfilling energy requirements [18,19]. Food components have also been associated with reduced incidence of diseases including Type 2 diabetes, cardio-vascular disease, obesity and cancer [18]. Therefore, there is an ever increasing demand for improved food commodities from both the health and safety-related aspects. The quality of crop plants in terms of its nutritional value and stability, fragrance, taste, appearance, flavour, shelf-life and physical attributes is directly correlated to the overall biochemical composition. Each of these characteristics can be fully defined in terms of metabolome composition [9,18]. Therefore, there is great interest in using metabolomic technologies in the field of improvement of food product quality and authenticity.

In the field of food nutrition, there are reports that rather than focusing on carbohydrates, proteins and lipids, significant research efforts should be directed toward analyses concerning physiologically active compounds [7]. Plant metabolomics is thought to play an important role in the future for indicating potential links between bioactive molecules and long-term human health. The presence of selected components in the food has been shown to induce direct or indirect effects on health- and disease-related processes in human body. Metabolomics approaches have been implemented in analysis of bioactive compounds including isoprenoids (including carotenoid pigments, monoterpene volatiles) and polyphenolics (flavonoids, anthocyanins) [7]. In addition, nutraceutical evaluation of for example green tea cultivars, which was carried out by Fujimura et al. suggested that metabolic profiling represents an useful approach for determination of health promoting effects in green teas [20]. Plant metabolomics has also been largely applied in investigating the effects of

genetic modification which is increasingly applied in order to enhance nutritional value and increase the levels of nutritionally relevant compounds. Rice and tomato with enhanced provitamin A and lycopene levels, respectively are good examples. Genetic modification, even though still a controversial concept is applied in other areas of plant research apart from nutrition. For example, monoterpene profile was altered in plants and quantitative changes in monoterpene levels for compounds including 1,8-cineole and β-ocimene were detected [20]. The implementation of genetic modification was also carried out in order to elevate tryptophan production in plants as it not only represents an essential amino acid, but also the precursor of various metabolites of pharmaceutical value [21]. Metabolomics fingerprinting was also employed to demonstrate substantial compositional similarity between genetically modified and conventional potato crops [22]. On the other hand, in a study by Roessner et al., metabolic profiling of wild-type and transgenic lines modified in sucrose catabolism and starch synthesis, revealed unexpected changes in disaccharides and sugar alcohols [23]. While genetic modification certainly holds promise in improving food-quality traits, it also poses a threat for disturbing normal metabolism and gene expression [24]. In fact, it is believed that metabolomics holds great promise in revealing unintended effects in genetically modified foods [25]. The nutrition related food metabolomics may involve studying for example the effects of genotype-environment interaction, since external factors including environmental conditions during crop protection and storage considerably influence nutritional quality [7]. Metabolomic analysis of plant-host and plant-pathogen interactions is becoming increasingly important as it is well known that plants offer a nutrient-rich environment to microbial pathogens, herbivores and insects [6]. Considering the huge variability in the biochemical responses of the plant after the interaction with pathogenic and non-pathogenic organisms, plant-host interactions are interesting due to high metabolite richness as well as huge diversity of different chemical classes. For example, Slisz et al. examined the effect of Citrus infection by *Candidatus* Liberibacter on citrus fruit metabolism and fruit juice quality [26]. The authors observed

concentration differences for sugars, amino acids, organic acids, adenosine, limonin glucoside and limonin between fruit trees obtained from infected and non-infected trees. Metabolite profiling of potato (*Solanum tuberosum* L.) was performed to wound-healing tubers after they were induced to suberize (form suberin, a cell wall-associated biopolymer functioning to prevent plants from desiccation and pathogen attack) [27]. The results provided new insights into the complexity of the process and global rearrangement of metabolism in response to wounding. In addition to nutrition and metabolic engineering perspectives, plant metabolomics applications in food-related fields have been applied for population screening purposes considering that metabolic differences between genotypes are not externally visible [9]. Consequently, minor qualitative variations in metabolome may imply differences having major biological impacts and this increases the demand for metabolomics methods ensuring coverage of a broad chemical spectrum in a high-throughput manner. Metabolomics can also lead to more comprehensive understanding of plant physiology and its dependence on multiple genetic, physical and chemical environmental factors. Plants survival on exposure to suboptimal growth conditions and initiation of protective responses under biotic and abiotic stress circumstances are examples of studies requiring metabolomics approach. For example, the effect of sulphur/nitrogen stress on *Arabidopsis* plants was investigated and the effect of single gene mutation in tomato fruit was examined by performing both targeted as well as non-targeted analyses of primary and secondary metabolites (including volatile compounds) [9]. In addition, metabolomic analysis of soil- and *in vitro*-grown potato tubers revealed major differences in contents of amino acids as the *in vitro*-grown tubers were found to have a much higher amount of amino acids in comparison to soil-grown ones [23]. It is also expected that plant metabolomics will provide insight into the modes of action of externally applied procedures during postharvest period as well as crop-protecting chemicals including pesticides and herbicides [9]. The responses of crops to such perturbations will lead to more accurate determination of their suitability for such purposes and will definitely aid in

discovery of new herbicides with more efficient and less invasive modes of action. For example, gamma-irradiation of *Psoralea corylifolia* L. seeds resulted in enhancement of phenylpropanoids furanocoumarins and consequently, Jan et al. suggested that the plant is under stress [28].

From a food metabolomics perspective, at this point it is beneficial to summarize the potential of metabolomic fingerprinting and profiling in addressing a variety of questions since most of the afore-mentioned parameters are closely inter-related [18,29-31]:

i) Metabolomic approach in food quality. This approach may be based on determination of metabolite profile associated with preharvest (maturity at the time of harvest, fruit development and ripening), postharvest and storage issues of fruit-based plants. Monitoring of quality attributes during postharvest processes (including climatic modulation, modified/controlled atmosphere storage) can aid in broader understanding of the undergoing chemical transformations in the food matrix. Comprehensive metabolite profiling may also result in improvement of food quality attributes by taking into account consumer perception and subsequently improving flavour, fragrance, aroma and visually-appealing traits. The identification of bioactive metabolites and correlation of metabolite profiles to nutritional quality are also subsets of interest in this category.

ii) Metabolomic approach in food processing. The production of processed food products through milling, extrusion, steaming, and frying/baking requires understanding of chemical processes and reactions that are taking place in food matrix and altering the final composition.

iii) Metabolomic approach in food safety and food microbiology. This approach may rely on determination of metabolome profile following inoculation of food products with pathogens and following the process of genetic modification. Bacterial and

fungal contaminations as well as the modes of herbicide actions can also be comprehensively studied with the focus on food safety.

iv) Metabolomics for compliance with food regulations. This approach relies on establishing differences in food metabolite profile as affected by genotype and growing (climate, soil composition, irrigation, fertilization) conditions. Obtaining baseline varietal and regional variability in metabolite profiles is subsequently employed in determining food authenticity in terms of declared geographical and region-specific attributes.

Based on these examples, plant- and food-based metabolomics investigations are rapidly evolving as reliable technologies not only for increasing the scope of our understanding of complex metabolomic pathways but also for representing promising tools in applied food and agricultural sector fields. It is well known that agricultural crops are considered as a starting point for plant-based economy, which relies on exploitative processing of plants in order to produce food with enhanced quality, stability, safety and nutritional characteristics [29]. In addition to its input in improved food quality, metabolomics will also aid the development of targeted breeding strategies for agricultural foods. In addition to identifying the association between biochemical composition and particular quality-traits (disease resistance, taste, flavour, consumer perception), the implementation of comprehensive metabolomic profiling approaches will also add a considerable predictive value for production of foods of enhanced quality.

1.1.3.2 Food metabolomics: correlation between fruit development and food quality

Fruit development and ripening processes are specific to plants and they represent the terminal stage of development in which matured seeds are

released. The changes associated with the synthesis, transport, accumulation and breakdown of metabolites that are initiated during fruit development and ripening processes influence the compositional and nutritional characteristics of food products [8]. It is well known that during crop developmental and ripening stages, the induced changes in compositional biochemistry alter the whole biological system with a multitude of components affecting each other [31]. A more comprehensive understanding of these metabolic transitions should aid to implementation of improved approaches for enhancement of food quality. For example, a non-targeted screening platform implemented by Tarpley et al. allowed identification of a large number of metabolites among which 21 compounds accounted for 83% of metabolite variance associated with developmental changes in the metabolome [32]. Consequently, the authors concluded that these biomarkers comprising organic acids, sugars and amino acids, the contents of which were altered during developmental stages can be employed in future studies. Fruit developmental studies have so far been limited to fleshy species due to their importance in the human diet [33]. Hence, tomato has often represented a model crop for investigation of metabolome alterations during fruit development. During the ripening process in tomato and other fleshy fruits, the biochemistry, physiology and organ structure are developmentally modified consequently inducing considerable alterations in appearance, flavour, texture and aroma [33]. These changes in visual characteristics and biochemical composition of ripening plants usually result in attraction of seed-dispersing organisms.

Mounet et al. examined the metabolic profiles of tomato flesh and seeds during fruit development and they detected the prominent differences in composition of seeds and flesh at all developmental stages [34]. They also reported that compositional differences were more pronounced during development from 8 to 45 days and increases in glucose, fructose, free amino acids and isoprenoids in flesh were accompanied by their suppression in seed. Finally, it was concluded that organ-dependent differences in the metabolome can provide further insight into the optimization of breeding approaches. In

another study, metabolite analysis of Cabernet Sauvignon grape berries during developmental stages revealed accumulation of key metabolites including tartrate, malate and proline [35]. On the other hand, metabolite fingerprints corresponding to developing potato tubers, in which eight different field-grown genotypes were analyzed at two harvest times, revealed the discrimination of two distinct groups [9,36]. Discriminative analysis illustrated differentiation of potato tubers based on developmental stage (as seen in Figure 1.1) and the authors were able to identify the specific metabolites whose contents were significantly altered in immature tubers.

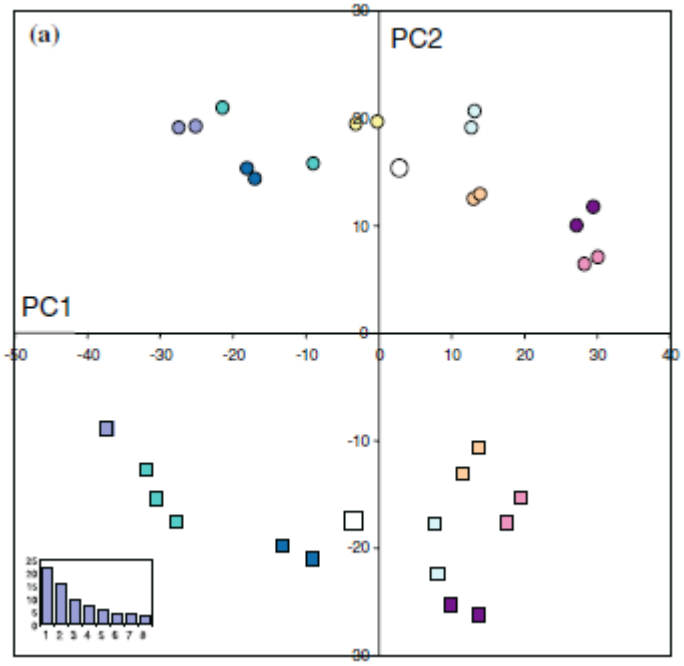

Figure 1.1. Principal component analysis of metabolite profiles of potato tubers from eight potato genotypes at two harvest times. Symbol shape corresponds to harvest time (circles represent early harvest, squares represent late harvest). The insert shows the percentage of variance explained for each of the first eight PCs [36].

The biochemical alterations associated with ripening are species-dependant, however it has been reported that the following changes take place: *i)* alterations in chlorophyll, carotenoid and/or flavonoid accumulation result in colour modifications; *ii)* textural modifications associated with alteration of cell wall structure and metabolism; *iii)* alterations in contents of sugars, acids and

volatile compounds influence nutritional value and flavor characteristics and *iv)* loss of cell wall integrity leads to enhanced pathogen susceptibility [33]. From the plant physiology perspective, fruit species are defined on the basis of the presence (climacteric) or absence (nonclimacteric) of enhanced synthesis of the gaseous hormone ethylene and increased respiration at the onset of ripening. However, independent of the ripening regime, fruits tend to undergo the afore-mentioned processes during development [33]. While tomato, apple, avocado, banana and other stone fruits are climacteric, ripening without increased ethylene synthesis occurs in non-climacteric fruits, such as grape, strawberry and citrus [37]. Based on this and examples stated above, it can be seen that the biochemical changes in fruits and crops during ripening and development have a pronounced effect on a variety of food quality traits including flavour, fragrance, taste, consumer perception, nutritional quality and disease/pathogen susceptibility. Therefore, the wide applicability of comprehensive plant metabolomics approaches in the area should be expected in order to allow for better characterization of biochemical developmental processes and their relevance to food-quality influencing parameters.

1.1.4 *Choosing apple as a metabolomics system*

1.1.4.1 Current trends in metabolite profiling of apples

Apple (*Malus* ×*domestica* Borkh.) represents one of the most ubiquitously cultivated and diverse fruit species [38-40]. In addition, apple is among the global crops of high economic importance and commercial distribution [38-40]. Apple production in the United States is worth approximately 1.6 billion dollars annually, and Canada produced 346,677 metric tonnes in 2010 with Quebec, Ontario, British Columbia, Nova Scotia and New Brunswick being the main apple-producing provinces [40-41]. Considering its significant contribution to human health and the ‘five a day’

healthy diet regime in assuring the supply of key bioactive molecules, the consumer demand for apples necessitates the breeding and production of high-quality fruit, a year-round availability as well as the cultivation of diverse and improved apple varieties [39]. Therefore, various plant metabolomics approaches were carried out by using apple as the investigated system. These include, but are not limited to the following topics [38,40,42-49]:

i) Applications in functional genomics, systems biology, human nutrition and agriculture.

ii) The characterization of metabolome for 'Protected Designation of Origin' (PDO) and newly cultivated crops.

iii) Understanding the biochemical nature of complex processes involving postharvest pathogen attack, effect of different crop management systems, development of postharvest physiological disorders, effectiveness of storage regimes, comparisons between genetically modified and conventionally bred genotypes and metabolic networks involved in fruit ripening and development.

The objective of the proceeding sections is to provide a scope on current research trends in the area of metabolite profiling of apples by summarizing several studies for which gas chromatography-mass spectrometry (GC-MS) and liquid chromatography-mass spectrometry (LC-MS) were employed (instrumentation aspects introduced in more detail in Sections 1.2 and 1.3). In the field of genetic modification, Vogler et al. compared the volatile emissions from transgenic apples and compared them to those obtained for two representative classically bred cultivars [46]. The authors were interested in targeting resistance against a key fungal pathogen, apple scab (*Venturia inaequalis*), as this target organism is the focus of resistance breeding programs. The apple set involved in the study was composed of scab susceptible cultivar and transgenic lines and scab resistant cultivar and transgenic lines. After the apples were submitted to inoculation with pathogen, infestation with herbivore

and combined pathogen-herbivore perturbation, the authors concluded that volatile emission was significantly dependent on apple genotype, infection type and genotype-infection type interaction [46]. Apple quality during shelf-life was investigated by Saevels et al. by looking at the changes in volatile profile [50]. The apples were stored in small containers for up to 8 months under three different storage atmospheres: ultra low oxygen, controlled atmosphere and cooled air. The authors were able to detect alterations in volatile composition with respect to storage regime. Several metabolomics studies were also carried out in order to detect and identify the varietal biomarkers of apple fruits and/or to characterize the biochemical composition in terms of volatile metabolite profile for novel and more recently introduced apple varieties as well as those recognized as PDO products. For example, Aprea et al. identified characteristic markers for each of the examined apple varieties including Golden Delicious, Granny Smith, Pinova and Stark Delicious with the implementation of principal components analysis (PCA) which was performed to reveal patterns in the data and correlations among samples [39]. Similarly, Reis et al. established the volatile profile of 'Bravo de Esmolfe' apple variety and detected α-farnesene and several esters as major constituents of volatile composition [42]. These authors also established sample classifications based on the alterations in volatile composition (esters and terpenoids) between apples obtained immediately after harvest and those stored for up to 4 months at 4 ^{o}C. Ferreira et al. characterized the volatile metabolite profile in apples originating from three different geographical regions at Madeira Islands by identifying approximately 100 different compounds in pulp, peel and entire fruit [49]. The major components comprising the volatile composition were ethyl esters, terpenes and alcohols, while the authors established variety-based sample characterizations based on the relative levels of characteristic biomarkers including ethyl hexanoate, hexyl 2-methylbutanoate and E-2-hexenal. On the other hand, Young et al. submitted relative levels of 40 esters and α-farnesene to multivariate analysis in order to differentiate apples based on skin colour [51]. The authors concluded that total ester contents were most enhanced in red-

coloured apples, while the composition of green-coloured apples was dominated by α-farnesene. In another interesting study, Róth et al. implemented a metabolomics approach to facilitate determination of postharvest quality of organic and integrated produced 'Jonagold' apple fruit, since apples grown under organic conditions have been reported to have an altered internal quality, lower growth rate and smaller fruit size [48]. Fruits were stored in air and under controlled atmosphere for 6 months at 1 ^{o}C. Their study demonstrated that the quality attributes of apples were not affected significantly by the nature of production system neither at harvest nor after storage. Rudell et al. conducted metabolic profiling of 'Granny Smith' apple peel in order to evaluate metabolomic alterations resulting from prestorage Ultraviolet – white light irradiation. Apples were submitted to irradiation for 0-48.5 hr and stored for 6 months at 0 ^{o}C. The PCA classification model that they obtained showed significant temporal changes in primary and secondary metabolic pathways before and after storage as a result of prestorage irradiation [52]. The authors reported irradiation-induced alterations in metabolic pathways associated with ethylene synthesis, flavonoid pigment synthesis, acid metabolism and fruit texture. Hern et al. studied the effect of infestation with *Cydia pomonella* on the induction of volatile emissions from ripening apple fruit [53]. The authors concluded that the volatile profiles obtained for healthy, artificially damaged and infested fruits differed with emission of β-ocimene being induced by *Cydia pomonella* infestation. Vikram et al. developed a method for volatile metabolite profiling of McIntosh apples, non-inoculated and inoculated with four different fungi including *Botrytis cinerea* Pers, *Penicillium expansum* Link, *Mucor piriformis* Fischer and *Monilinia* sp [54]. Even though the study allowed the detection of a large number of metabolites, among them, 20 were specific to one or more inoculation agents/diseases and seven were unique to apples inoculated with different pathogens. For instance, fluoroethene and 3,4-dimethyl-1-hexene were specific to *Penicillium*, butanoic acid butyl ester, 4-methyl-1-hexene and 2-methyltetrazole relevant to inoculation with *Mucor* and the contents of acetic acid methyl ester and fluoroethane were relevant to apple inoculation with

Botrytis and *Monilinia*. The authors suggested the application of the method for detection of the onset of diseases at an early stage of disease progress and before significant losses are incurred.

1.1.4.2 Fruit development and ripening in apples: correlation to disorder susceptibility

Apart from the afore-mentioned research trends involving apple as an investigated metabolomics system, in recent years, considerable efforts have been made in identifying and characterizing diseases and disorders that this crop is susceptible to. More importantly, in addition to visual symptoms, and quality attributes including firmness, acidity and soluble solids, rewarding attempts have been made to correlate the onset of diseases to metabolome composition. Several published applications underlying this particular topic in metabolomics are worth summarizing.

The postharvest regime for apples involves storage at 0 ^{o}C and for some cultivars at -1 to 4 ^{o}C [44,47]. Browning disorders that have been attributed to chilling stress at low storage temperatures have been reported to take place within weeks or months following the initiation of a storage treatment [44]. Two prominent storage disorders that induce significant apple losses to growers worldwide are superficial scald and bitter pit [47]. Superficial scald is an apple fruit peel storage disorder manifested by necrosis of the first 4-6 hypodermal cell layers of susceptible cultivars [43].

Rudell et al. performed global metabolite profiling in 'Granny Smith' apples that were exposed to artificial UV-white light after harvest, stored in air at 1 ^{o}C for 6 months and held for 4 days at 20 ^{o}C [43]. The authors hypothesized that postharvest UV-vis irradiation would reduce scald susceptibility, as some previous reports indicated reduced scald incidence with enhanced sunlight exposure. Indeed, it was determined in this study that scald was eliminated on the side of the fruit directly exposed to artificial light and as far as the opposite fruit side was concerned, the scald was reduced with

increasing treatment time. The classifications accomplished with principal component analysis revealed correlations between scald status and light treatment duration as well as induced changes in the metabolome. Based on principal component analysis, hyperin, reynoutrin, avicularin, catechin, and (-)epicatechin levels increased for unexposed peel and decreased with increased scald severity. The α-farnesene content diminished with light treatment duration. In another study conducted by Pesis et al., the occurrence of superficial scald and bitter pit was investigated for 'Greensleeves' apples placed in cold storage at 0 ^{o}C [47]. Considering that ethylene plays a major role in the development of superficial scald in apple fruit during cold storage, the authors investigated the incidence of disorders (superficial scald and bitter pit) for untransformed and transformed lines, the latter being suppressed for ethylene synthesis. After the period of 4 months at 0 ^{o}C and 1 week at 20 ^{o}C, untransformed apples exhibited highest incidence of superficial scald. On the other hand, the transgenic apples even though suppressed for ethylene biosynthesis still produced α-farnesene, a compound whose oxidation in peel tissues is thought to play a key role in scald development [44,47]. Rudell et al. conducted untargeted metabolomic profiling in order to characterize the changes in metabolome as a result of superficial scald development in 'Granny Smith' apples [44]. Moreover, they inspected the progress of disease development following the treatment of fruit with ethylene action inhibitors, diphenylamine (DPA) and 1-methylcyclopropene (1-MCP). Multivariate analysis was implemented to find correlations between scald, postharvest treatment and storage duration. The authors concluded the occurrence of extensive metabolomic changes between untreated controls and fruit treated with ethylene inhibitors.

On the basis of intensified research efforts, the occurrence of superficial scald is correlated to autoxidation of α-farnesene in peel tissues [44]. The levels of this secondary metabolite increase with respect to apple ripening in many scald-resistant and scald-susceptible cultivars [44]. Alterations in the metabolome as a result of initiation of scald development and its progress have

not been elucidated so far, but it is thought that the volatile end products of α-farnesene oxidation including 6-methyl-5-hepten-2-one, 6-methyl-5-hepten-2-ol as well as conjugated triene hydroperoxides can increase coincidently with scald [44]. Furthermore, the increasing levels of these metabolites have been correlated to the discoloration and death of hypodermal cells which lead to development of scald symptoms [55]. For example, exogenously applied 6-methyl-5-hepten-2-one induced scald-like browning in peel tissue of susceptible apple cultivars [55].

'Honeycrisp' apple represents one of the relatively new cultivars that was released by the Minnesota Agricultural Experiment Station in 1991 [56]. The cultivar has been encountering increasing consumer and market enthusiasm for availability and positive consumer perception has mainly resulted from its outstanding flavour characteristics as well as the ability of the fruit to remain crisp for 6 months in cold storage. However, the fruit also demonstrated high degree of susceptibility to diseases and storage disorders including soft scald, soggy breakdown, bitter pit, low temperature breakdown and cork spot [56-58]. The effect of preharvest 1-methylcyclopropene treatment on 'Honeycrisp' quality at harvest and after storage as well as on susceptibility to soft scald was examined by DeEll and Ehsani-Moghaddam [56]. Soft scald is a low-temperature disorder characterized by irregularly shaped and sharply defined brown lesions on the apple skin. The disorder can extend beneath the skin into the flesh, giving rise to occurrence of secondary infections [56]. The authors found that application of preharvest 1-methylcyclopropene treatment reduced the incidence of soft scald. Several other maturity and storage problems associated with variability in fruit colouration, uneven maturity (multiple harvests are necessary) and incomplete maturity leading to poor eating quality were reported to be characteristic of this apple cultivar. In fact, harvesting 'Honeycrisp' apples at optimum maturity is very challenging as the traditional maturity indicators such as ethylene, starch, soluble solids and firmness sometimes fail to administrate the best harvesting time [58]. Variability in fruit colouration is most likely attributed to environmental stresses, genetic variation

and virus expression [58]. Also fermentation products acetaldehyde and ethyl acetate develop in apples during late harvests, contributing to initiation of disagreeable flavour after late harvest and especially during storage [58]. The initiation of off-flavour production is difficult to predict especially since external visual symptoms fail to indicate its presence. In addition, high degree of disorder susceptibility requires mild postharvest storage conditions (2.5-3 ^{o}C) and controlled atmosphere storage is therefore not recommended. Considering the facts mentioned above about 'Honeycrisp' apples, which include: *i)* high degree of disorder susceptibility; *ii)* high consumer acceptance, market value and growers' interest resulting from exceptional flavour characteristics; and *iii)* demand for comprehensive metabolome characterization for newly introduced cultivars; unbiased and comprehensive metabolomics approaches should be developed and executed.

It has also been reported that disorder occurrence in susceptible apple cultivars is impacted by a number of factors, including fruit maturity, storage atmosphere, temperature during fruit growth and storage, preharvest light environment and ethylene biosynthesis and activity [43]. In particular at this point, it is important to further establish a correlation between disorder incidence and fruit maturity, the latter being impacted by fruit development and ripening processes. Fruit development is a plant-specific process controlled by complex interactions of endogenous and environmental factors [59]. Although the specific function of climacteric respiration during the developmental and ripening processes occurring in fruit remains unclear, it is proven that ethylene involvement facilitates rapid and coordinated ripening. In fact, ethylene is the major effector of ripening in fleshy fruits and in apples, and its addition initiates a climacteric burst of respiration, softening of flesh and increase in biosynthesis of flavor compounds. For example, Schaffer et al. generated a transgenic line of 'Royal Gala' apples in order to prevent ethylene biosynthesis and produce apples absent of ethylene-induced ripening attributes [60]. After the application of external ethylene, the authors detected increasing concentrations of ester, polypropanoid and terpene volatile compounds over an 8-day period. Through

the application of genomics approach, the authors evidenced that the first and last steps of aroma biosynthesis pathways were regulated by ethylene. In another study of similar focus, Defilippi et al. attempted to understand the biochemical processes that occur in 'Greensleeves' apples from transgenic line with a high suppression of ethylene biosynthesis [61]. The activity of volatile-related enzymes including alcohol acyltransferase (AAT), alcohol dehydrogenase (ADH) and lipoxygenase (LOX) and levels of amino acid and fatty acid volatile precursors in peel and flesh were monitored. The authors concluded that enzyme and precursor activities were differentially affected: *i)* AAT enzyme activity and levels of amino and fatty acids were dependent on ethylene regulation and *ii)* ADH and LOX enzymes were independent of ethylene regulation [61]. As it can be seen from examples mentioned above, the concept of biosynthesis of volatile metabolites and its relevance to fruit quality are influenced by many factors such as genome, harvest maturity, environmental factors (temperature, light, etc.) and postharvest handling and storage [62]. The levels of flavour compounds increase substantially during fruit ripening, which takes place toward the end of 20-21 weeks of fruit development [63]. However, a correlation between enhanced production of volatile metabolites and marked increase in cell wall, starch breakdown and disorder incidence, all being the processes initiated by autocatalytic burst of ethylene late in fruit development, opens up a multitude of opportunities from plant metabolomics perspective. In fact, relatively few studies have provided comprehensive investigation of apple fruit quality traits through unbiased metabolomic profiling, hence limiting our understanding of apple fruit development, physiology and biochemistry [38]. The enormous diversity in fruit-related traits among the large number of cultivars and related wild genotypes facilitates additional interest in execution of comprehensive approaches that allow simultaneous analysis of metabolite pools at a particular point in time. All of these points were detrimental to selection of objectives and direction of research initiatives in the current project.

1.1.5 *Volatile metabolites: biologically active roles and functions*

Based on the comprehensive list of above summarized literature resources, it can be seen that volatile organic compounds are not only the end products of secondary metabolomic pathways but also play a pronounced role in determination of fruit quality and fruit deterioration. Therefore, the functions and properties of these biologically relevant compounds will be reviewed prior to introducing the section on methodologies that are implemented in their analysis.

Volatile organic compounds (volatiles) comprise a chemically diverse group of organic compounds that are generally characterized by small molecular weights (50-200 Daltons) and appreciable vapour pressure under ambient conditions [64]. Volatile metabolites are generated from both primary and secondary metabolites and as mentioned before, they are synthesized in plant tissues at specific developmental stages during ripening, flowering and fruit maturation [65]. Essentially all plant parts such as leaves, stems, roots, flowers and fruits emit volatiles that possess a diverse array of biochemical and ecological functions [66]. Compounds emitted by flowers serve to guide and attract pollinators and specific sensory impressions for the pollinators are imparted by the overall qualitative and quantitative composition of flavour, rather than the presence of individual molecules [66]. Many volatiles have also been found to contain anti-microbial and anti-herbivore activities which are advantageous in protecting reproductive plant parts from enemies [66-67]. In fact, in line with previously emphasized topics, many plants have the ability to release volatiles following the herbivore attack and plant damage initiated by pathogen attack and other environmental aggressors. These compounds are operated internally as defensive signaling systems employed to modulate levels of systemic acquired resistance to pests and heal the adverse effects of heat and oxidative stress [64]. Defensive chemicals operate either in indirect defensive manner by for example attracting arthropods that pray upon herbivores, while other may represent direct toxicants for herbivores and pathogens that increase

the ecological competitiveness of the plant [66-67]. Volatile emission from fruits on the other hand likely facilitates seed dispersal by animals and insects. Interestingly, phytohormones such as ethylene, methyl salicylate and jasmonate send signals associated with triggering of defensive responses upon herbivore attack to other neighboring plants to communicate the presence of a threat [64]. As mentioned in previous sections, fruit volatiles are signaling fruit ripeness and maturity considering that specific compounds and/or groups of compounds are either present in low levels or absent from non-developed fruits [66]. For humans and other animals, volatiles are important as scents and they contribute to flavour and aroma perception of foods. Among the wide spectrum of volatile compounds biosynthesized in plants, only a small subset is known to contribute to 'flavour fingerprint' which is attractive to humans and animals. For example, the chemistry of tomato fruit and its relevance to positive consumer feedback were studied by Tieman et al., who implemented a targeted metabolomics approach for examining natural variation in flavor-attributing acids, aroma compounds and sugars in order to come to reliable conclusions [68]. The authors concluded that the majority of the most abundant volatiles did not influence consumer perception, whereas some minor constituents did. Goff et al. suggested that plant volatile compounds are indicators of nutritional value in plant-based food commodities [69]. They made such conclusions by relying on the mechanism of volatile metabolite biosynthesis which is regulated by the presence of essential nutrients, including amino acids and fatty acids and antioxidants, such as carotenoids [69]. Having tomato as the metabolomics model, they attempted to establish the relationship between volatile composition at appropriate maturity level and nutritional makeup (Figure 1.2).

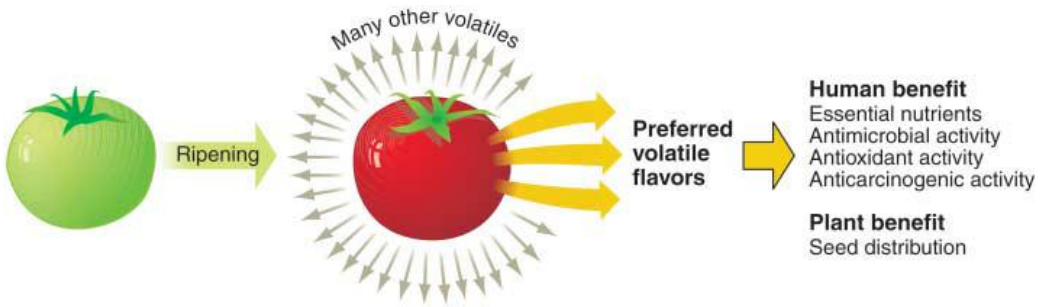

Figure 1.2. Tomato fruits produce a volatile emission profile indicative of fruit quality and ripeness degree. Many of volatile compounds are produced from nutritionally relevant precursors [69].

From the chemical perspective, volatile metabolites constitute a heterogeneous group of compounds having a diverse spectrum of structures ranging from straight-chain backbones to branched-chain, aromatic and heteroaromatic ones [66]. These volatile metabolites are also composed of various functional groups including hydroxyl, carbonyl, carboxyl, ester, lactone, amine and thiol [66]. For example, over 300 different volatile metabolites have been reported to constitute the biochemical composition of apple [70]. The most active 'character impact' odourants attributing to exceptional flavor attributes belong to esters, alcohols, aldehydes, norisoprenoids and terpenoids. In apple, the biosynthesis of these compounds has been reported to occur via at least four pathways [60,70]:

i) Fatty acid pathway derives straight chain esters from fatty acids such as linoleic and linolenic acids;

ii) Isoleucine pathway contributes to biosynthesis of branched chain esters;

iii) Mevalonate pathway allows biosynthesis of α-farnesene;

iv) Phenylpropanoid pathway contributes to biosynthesis of estragole.

The qualitative and quantitative levels of these compounds depend on genotype, ripening, maturation, preharvest environmental conditions and

postharvest processing and storage practices. However, the biological activities of these volatile compounds are also regulated by their physicochemical properties, since their high vapour pressure and low molecular weights enhance the rates of diffusion through the gas phase and within biological systems [64]. In fact, these characteristics result in their implementation as *i)* signaling molecules (semiochemicals), which pass the information both within and between organisms; *ii)* defense compounds upon the invasion of external stimuli and *iii)* compounds affecting flavor perception and overall quality of food [64]. Emissions of volatile metabolites at various stages during the lifespan of the plant can be successfully implemented for facilitation of targeted and non-targeted metabolomics approaches in the field of plant biology. However, three limitations are associated with the implementation of volatile emission approach: *i)* the method is selective and sensitive for highly volatile compounds; *ii)* release and emission of selected volatile metabolites can only be initiated after the disruption of cells (this is especially relevant to vegetative tissues and non-ripe fruits) and *iii)* gene expression is directly related to endogenous, rather than emitted volatiles [66,71]. In accordance to the last point emphasized, it is important to clarify that so far studies focused on volatile metabolite identification, their biosynthetic regulation and elucidation of metabolome networks in apple have been conducted by establishing the relationship between emitted compounds and gene expression [71]. However, what is often overlooked is the quality and quantity of endogenous volatiles that influence the volatile emission process and are directly correlated to gene expression because genes function in the tissues where also biosynthesis of endogenous volatiles is taking place [71]. For example, Ban et al. attempted to elucidate the mechanism of ester and α-farnesene formation in 'Tsugaru' apple by including both emitted and endogenous volatile compounds in their evaluation [71]. The authors concluded that only nine compounds were common to volatile fingerprints corresponding to volatile emissions and endogenous compound analyses, hence fingerprints were both qualitatively and quantitatively impacted by the method of volatile analyte collection. The

differences in profile composition were partly attributed to boiling points of selected analytes since higher emission rates were detected for compounds having lower boiling points. On the other hand, a number of lower boiling point analytes such as (E)-2-hexenal were not detected in volatile emissions despite the fact they were present at high concentrations endogenously. The authors suggested that in addition to boiling point, an array of different factors and networks such as temperature and enzyme activity may be influencing the process of volatile metabolite emission. Based on this example, it is obvious that future plant metabolomics platforms should be designed accordingly in order to include endogenous metabolites and accomplish a reasonable coverage for such compounds.

1.2 *Analytical technologies for acquisition of metabolomics data*

Many significant technological developments and advancements in analytical instrumentation that were occurring in the past decade have attributed to increased capacity to simultaneously and unbiasely analyze and interpret hundreds and in some cases thousands of metabolites and metabolite interactions [9]. However, despite the promising and bright future, the metabolomics community recognizes that gaining a complete overview of the entire metabolomic complement in a particular biological system under investigation is currently an inconceivable task. These limitations, which even current state-of-the-art technologies have, are resulted by [9-11]:

i) Large number of metabolites at any given time;

ii) Biochemical complexity of the metabolites encountered in plant tissues in terms of possessing a diverse array of physicochemical properties;

iii) Biological variance inherent in most living organisms;

iv) Wide concentration levels that may be manifested by variations as big as 7-9 orders of magnitude between individual components present in plant extracts.

The enormous biochemical diversity of a typical metabolome requires multiple approaches for sample preparation and analysis to account for variations in solubility, reactivity and other physicochemical properties [10]. Wide dynamic range of metabolite concentrations on the other hand requires efficient separation strategies such that major compounds do not hinder the detection and quantification of metabolites present in trace amounts. Therefore, the major limitation of metabolomics is attributed to its current inability to comprehensively profile a metabolome. However, even though no analytical platform facilitates the vision of complete metabolite analysis, acceptable metabolite coverage can be achieved by employing currently available analytical tools and/or combinations of different platforms. Several major platforms will be introduced in the following sections with particular emphasis being placed on methodologies employed in volatile analyte analysis.

Mass spectrometry (MS) is the most widely applied analytical platform in metabolomics, especially if it is hyphenated to chromatographic instrumentation [72]. The most important advantages of MS implementation in metabolomics investigations involve high-throughput, high sensitivity and enhanced selectivity [72-73]. The ability to elucidate structural conformation and annotate metabolite identity from collected fragmentation patterns of analytes have also contributed to the convenience in utilizing this approach as it provides an excellent tool for identification of unknown and unexpected compounds. Furthermore, the hyphenation of the technique to the chromatographic instrument tremendously expands the capability of the chemical analysis of highly complex biological samples. Metabolites are hence separated from matrix interferences and the resultant higher mass spectral purity increases the identification capability of mass spectrometer.

Gas chromatography, which has been named the 'gold standard' of metabolomics, is currently the most popular global analysis method. It involves the separation of volatile, less polar and thermally stable analytes, which are subsequently submitted to electron ionization (EI) mass spectrometry [16]. The technique is biased against non-volatile, highly polar, thermally labile and high molecular weight metabolites, which can on the contrary still be analyzed with this approach provided that chemical derivatization is employed to convert them to GC-amenable analytes [72]. While chemical derivatization increases sample preparation time through multiple and complex sample handling procedures which overall result in increased variance of the method, the GC-MS approach provides excellent performance characteristics when naturally volatile metabolites having boiling points lower than 300 ^{o}C and including monoterpenes, alcohols, esters, aldehydes and hydrocarbons are of interest [9]. The characteristics that render GC-MS advantageous for global metabolomics studies include *i)* high sensitivity that decreases the amount of biological material required; *ii)* high chromatographic resolution; *iii)* affordability and robustness of operation; *iv)* high detection specificity; *v)* quantification of compounds in complex mixtures; *vi)* metabolite identification potential via retention time comparison; *vii)* annotation of analyte identity via comparison of characteristic experimental mass spectra with widely available commercial spectral databases [1,64,73]. Historically, GC-MS has been regarded as one of the most valuable bioanalytical tools due to the ability to resolve complex mixtures in a single analysis. GC-MS is a more mature and established technique in analysis of complex biological mixtures and as a consequence, the technique has encountered a broad application interest in the area of global metabolite analysis. In the past decade, development of rewarding methods for qualitative and quantitative determinations of volatile analytes has been possible due to the design of relatively inexpensive but sensitive bench-top instruments.

1.2.1 *New advancements in GC-MS, high resolution GC instrumentation and introduction to comprehensive two-dimensional gas chromatography*

Traditional GC instrumentation has been subjected to a number of advancements over the past years, one of them being increased analysis throughput. The implementation of traditional GC capillary columns (25-30 m length, 0.25-0.32 mm internal diameter) while achieving satisfactory separations on simple-medium complexity samples, is also characterized by a substantial drawback associated with increased analysis time [74]. In fact, typical run times required in analysis of food samples range between 0.5 to 1.5 hr, which represents an unacceptable condition, especially when laboratories having high daily sample throughput and requiring the analysis of large numbers of samples are concerned. Therefore, there was an ever growing interest within the chromatographic community in the introduction of fast gas chromatographic methods. This concept has been effectively exploited with the implementation of narrow-bore columns as one of the widely acknowledged and accepted approaches of increasing analysis speed [74-75]. As a result, the application of fast gas chromatography to global metabolomics studies in complex samples has become routine over the past 10 years and has been greatly facilitated by high sensitivity and the possibility of obtaining rich metabolite coverage that time-of-flight (ToF) mass spectrometers have offered [76]. In such cases, high data acquisition rates and absence of spectral skew allow the mass spectral deconvolution of chromatographically overlapping analyte peaks to be accomplished with the employment of appropriate deconvolution softwares that are readily available from instrument manufacturers while simultaneously decreasing GC resolution requirements [6,72].

Single column (one-dimensional) chromatographic analysis has been the method of choice and a standard separation tool in a broad variety of fields including food analysis and plant metabolomics [77-78]. One-dimensional gas

chromatography provides satisfactory separations and rewarding analytical results for samples of low to medium complexity and it has been capable of resolving 100-150 peaks in a single run [79]. However, the heterogeneous nature and impressive complexity of many naturally occurring matrices exceeds the capacity of any single separation system whose implementation in other words does not suffice resolution requirements for qualitative and quantitative determinations of organic compounds in complex biological mixtures [78]. In response to the demand for more selective separations and increased resolution power, and especially for situations in which technological improvements such as new column technologies seem to be reaching their maximum level, multidimensional approaches facilitating the combination of independent techniques with the aim of strengthening resolving power have become conceivable solutions [77-78]. Among them, comprehensive two-dimensional gas chromatography coupled with ToF (GCxGC-ToFMS) is the most popular option due to its capability to submit the entire sample to separation on two independent mechanisms, rather than subjecting limited numbers of fractions eluting from the first column to further separation [79]. The later approach termed as multidimensional gas chromatography is suitable for targeted analysis or in other words relies on prior knowledge of target analytes/metabolites of interest [77,79-80]. GCxGC on the other hand permits the separation of the entire sample through coupling of two separation dimensions having independent and complementary separation mechanisms [78]. In another words, the whole effluent from the first dimension column is periodically cryotrapped and then remobilized with the employment of increased temperature gradient into narrow bands to the second dimension column for further separation. Therefore, inefficiently resolved and chromatographically coeluted analytes on the first dimension column may be potentially separated on the second dimension column, provided that the system is equipped with optimum column ensembles. Hence the technique is theoretically capable of producing improved separation of complex mixtures [81]. The instrumental setup for GCxGC methodology involves the employment of a tandem set of

columns having different separation principles that are connected in series through the specially designed interface device (the illustration of main instrumental components is presented in Figure 1.3) [78,81]. The interface device, referred to as a modulator functions to continuously during first dimension separation sample, refocus and inject first dimension eluate into a second dimension for further separation [78-79].

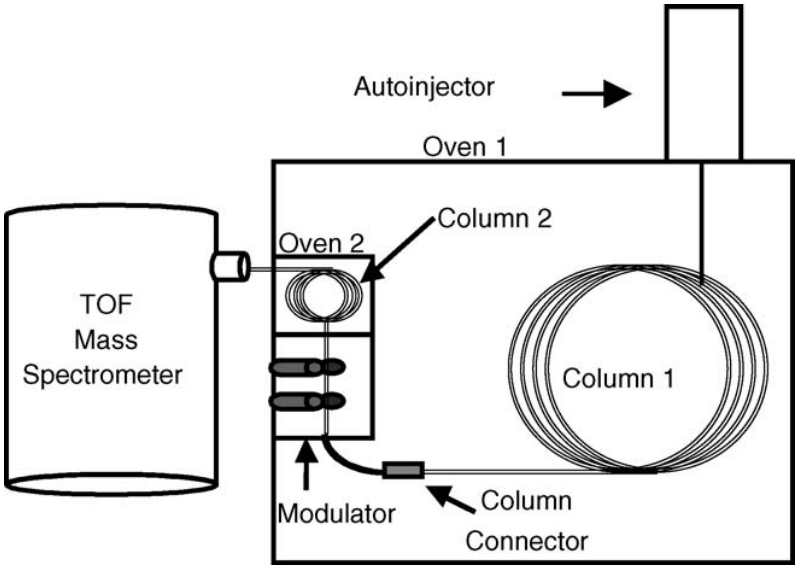

Figure 1.3. Schematic of the GCxGC system and its main components including first dimension column, second dimension column and modulator.

In a standard configuration, GCxGC setup involves the implementation of non-polar capillary GC column (15-30 m length, 0.25-0.32 mm internal diameter) in the first dimension where separation of analytes takes place according to their volatility [79,81]. The polar second dimension short and narrow-bore column (typical dimensions 0.5-2 m length, 0.1 mm internal diameter) then employs specific interactions with the stationary phase such as for example, hydrogen bonding and π- π interaction for analyte separation. Considering that second dimension separations are super fast and in terms of length on the order of 2-8 s, they are considered essentially isothermal for

analytes of equal volatility, i.e. the analytes in each individual isolated fraction eluting from first dimension column [79]. Hence, the boiling point contribution in second dimension separation is eliminated and this non-polar x polar column combination set is considered orthogonal since only specific interactions are governing the separation and retention in second dimension. This classical GCxGC setup has been adopted to many studies since the retention behaviour on non-polar first dimension column is well known from huge compilations of one-dimensional GC separations, hence convenient optimization of first dimension separation in GCxGC is facilitated. The benefits of 'reversed polarity mode' have also been realized in the GCxGC separation of food samples, particularly in achieving better overall chromatographic behaviour and separation of the polar sample constituents [82].

In comparison to classical one-dimensional gas chromatography experiment, the employment of GCxGC has proved advantageous in many different aspects that are essential for resolving some of the most challenging issues that are encountered in analysis of naturally complex samples and that the contemporary analytical chemist is faced with. These include: *i)* effluent refocusing during modulation (compression) process leading to improved analyte detectability and increased signal-to-noise ratio (S/N), hence measurement of lower analyte amounts is enabled; *ii)* dual-column combination resulting in increased separation power and selectivity; *iii)* higher throughput separations resulting in higher number of peaks separated per unit time; *iv)* presence of structured separations [83-84]. The last point here is related to chemical structure-dependent distribution of analytes over the two dimensional separation space that enables a trained analyst to recognize structural patterns on the basis of retention time coordinates of peaks of interest [84]. The implementation of two principal and complementary separation components allows the separation plane to be defined in terms of structural properties of analytes, rather than just a collection of analyte peaks. Therefore, GCxGC enables deconvolution of conventional one-dimensional chromatograms and their convenient interpretation leading to rapid and accurate elucidation of

compositional characteristics. These molecular structure – retention relationships provide next to mass spectral comparison another dimension to the analyte identification procedure hence, enabling development of novel screening approaches for which annotation of analyte identity is essential [84-86].

1.2.1.1 General overview of GCxGC metabolomics applications

GCxGC-ToFMS offers unique possibilities for high-resolution metabolite profiling and fingerprinting of complex samples [85]. In fact, the technique has become a method of choice in complex sample characterization and various research studies that strive to detect unique chemical fingerprints and biomarkers indicative of sample normality/abnormality. Several targeted and global metabolomics studies have been reported in the literature and will be briefly summarized in this section, whereas on the other hand, a number of selected food- and plant-metabolomics applications will be also presented, after completing the sections associated with introduction of technical concepts corresponding to the most important steps of the appropriate metabolomics workflow.

GCxGC-ToFMS instrumentation has been exploited in a variety of metabolomics based fields, which include metabolomic fingerprinting and profiling of biofluids (studies on the blood metabolome and urinary metabolome); cell cultures and tissue extracts; bacteria and yeast; plants; herbivore-induced plant emissions and foods [87-90]. With the objective of confirming the expected superiority of GCxGC-ToFMS in terms of improved signal intensity and increased resolving power, metabolic fingerprinting of *E. coli* strains was performed on both one-dimensional and two-dimensional platforms [90]. The implementation of two-dimensional platform resulted in superior chromatographic resolving power and baseline separation of key metabolites such as glycerol and leucine [90]. The number of detected and

statistically significant features was thus significantly higher when GCxGC platform was implemented (Figure 1.4) [87,90].

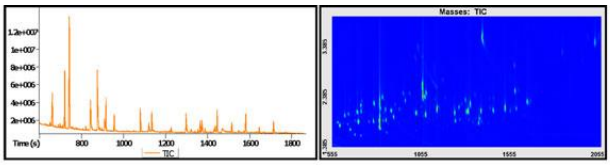

	GC-TOFMS	GC×GC-TOF-MS
Total features	624	2625
Reduced features[1]	181	422
Significant features[2]	28	53
Metabolites identified that distinguished the two *E. coli* strains	11 cis-aconitate, caproate, citrate, fumarate, glucose-6-phosphate, glycine, α-ketoglutarate, proline, putrescine, pyruvate, valine	27 cis-aconitate, caproate, citrate, fumarate, glucose-6-phosphate, glycine, α-ketoglutarate, proline, putrescine, pyruvate, valine aminoadipate, furoate, GABA, glucose, indole, myo-inositol, isoleucine, itaconate, leucine, lysine, malate, orotate, pyroglutamate, succinate, sucrose, tartrate

Figure 1.4. Comparison of one-dimensional and two-dimensional GC platforms in metabolic fingerprinting of a wild-type versus a double mutant strain of *Escherichia coli* [87,90].

Also, as part of the METAbolomics for Plants Health and OutReach (META-PHOR) project, Allwood et al. performed metabolomic profiling of three complex sample matrices, including: *i)* melon selected for its matrix complexity and enhanced presence of sugars in extracts; *ii)* broccoli selected for its extreme complexity and metabolite richness and *iii)* rice representing nutraceutical-rich food commodity [76]. The authors compared performance characteristics between one-dimensional and two-dimensional metabolomics methods and concluded that in contrast to one-dimensional method, the implementation of GCxGC-ToFMS resulted in significantly higher wealth of information and enhanced level of resolution. Terpenoid metabolic profiling analysis of transgenic *Artemisia annua* L., a famous herb in the traditional Chinese medicine was also conducted on GCxGC-ToFMS platform equipped with polar x moderate polar column combination [88]. The authors produced two lines of transgenic plant, one being over-expressed with amorpha-4,11-

diene synthase, an important enzyme which catalyzes the committed step of artemisinin biosynthesis, while the other transgenic line was suppressed with the enzyme. The authors concluded that as a result of enzyme over-expression, the content of artemisinin, an important component of anti-malarial drugs and the amounts of its precursors increased [88]. While the authors had issues with establishing quality group separations, they were able to detect 500 compounds, among which after proper filtering and data reduction, there were about 200 monoterpenoids and sesquiterpenoids. Kusano et al. employed a combination of one-dimensional and GCxGC methodologies in order to conduct metabolomic phenotyping of natural variants in rice [91]. The authors did not exclude the implementation of one-dimensional method, which was employed for increasing throughput rather than providing complementary aspects to GCxGC analysis. Consequently, statistical analysis was being performed on one-dimensional data in order to elucidate main differences in terms of metabolome composition between extracts corresponding to brown rice varieties. The results revealed clear classifications between the varieties of non-glutinous and glutinous rice and differential metabolites were further profiled in 'high-resolution' GCxGC manner to provide complementary information on analyte identification. In another study, Pierce and coworkers evaluated the quality of quantitative GCxGC-ToFMS results by submitting large volumes of multidimensional data corresponding to 54 chromatograms obtained on extracts from three different species of plants including *Ocimum basilicum* (basil), *Mentha piperita* (peppermint) and *Stevia rebaudiana* (sweet herb stevia) [92]. The multivariate analysis illustrated that main differentiator analytes between three different plant species were amino acids, carboxylic acids and carbohydrates.

1.2.1.2 GCxGC data processing and implications to metabolomics

In addition to representing the findings of some feature applications, it is crucial to summarize the current status of GCxGC implementation in global

metabolomics studies. The technique generates multidimensional data sets that can be easily spanned over four dimensions of separation, including: *i)* first dimension time, *ii)* second dimension time, *iii)* mass spectral fragmentation specificity, *iv)* mass spectral deconvolution as a mathematical model for separation of spectra of chromatographically overlapping peaks, *v)* molecular structure – retention relationships. The first four dimensions also affect the efficacy of the software to combine all individual second dimension peaks into appropriate one dimensional entries and this GCxGC-specific data processing requirement is essential for accurate quantitative analysis. Consequently, novel strategies for data mining are highly demanded in order to extract the information of highest and most valuable biological relevance as the quality of data processing largely impacts the reliability of biological information extracted from the data [2]. In fact, the major limitation of the technique at its current state is inability of current data processing and software tools to handle multidimensional data arrays. From the qualitative comparison aspect, Shellie et al. suggested among other methods, direct chromatogram comparison and visual inspections of extracted ion chromatograms [85]. While this approach provides an indication of presence or absence of a particular analyte, the main drawback is that the procedure is impossible to be performed for large quantity metabolomics experiments compiled with 100s and sometimes 1000s of metabolites and/or samples. In addition, concentration differences for metabolites of interest in comparison samples are indicative by change in colour intensities, which is also a significant disadvantage of this approach. These authors also suggested bubble plot representation in which bubbles represent the individual peaks and bubble sizes correspond to integrated peak areas. However, bubble sizes needed to be scaled accordingly in order to detect changes in concentration levels for compounds present in trace amounts. In terms of peak alignment and generation of quantitative and/or semi-quantitative data, often detected inconsistencies in peak tables make it difficult to place the metabolite information into a suitable matrix format where rows represent individual peaks, columns represent individual chromatograms and values

relative peak levels [85]. The 'automated sample comparison' feature has been very often implemented in such processing methodologies for one-dimensional platform and has been also employed for example by Wojtowicz et al. in a GCxGC-based metabolomics study on pathological metabolites in urine for the diagnosis of inherited metabolic disorders [93]. The automated data processing strategy consisted of building the reference table by importing selected pathological metabolites from different samples where the given metabolites were present. The authors were able to implement this automated procedure for confirming the metabolite presence/absence based on mass spectral quality and retention time coordinates match. However, the method was based on determination of few known targeted metabolites of inherited metabolic disorders and likely would find limited application in non-targeted global metabolomics studies where several hundreds of metabolites are required to be screened for biomarker potential. Majority of these alignment procedures on software able to handle GCxGC-ToFMS data rely on deconvolution to mathematically separate spectra of coeluted peaks [78]. However, in a study by Allwood et al., the authors reported outlying deconvolutions and cautioned against non-critical use of deconvoluted mass spectral intensities for relative quantification [76 and reference therein]. Also, Koek et al. confirmed that despite the development of novel custom-made software tools for alignment and quantification, there have been unsurprisingly relatively few studies that were focussed on quantification of all or at least as many as possible peaks in global metabolomics studies [2]. They implemented a semi-automated non-targeted processing approach in which heavy reliability was placed on deconvolution capability of commercial software. They found that second dimension peak width and the mass spectral match necessary to combine two dimensional peaks into their corresponding one-dimensional entries were the most important parameters of the data processing method. Therefore, despite outstanding performance characteristics of GCxGC as compared to one-dimensional GC which were also reflected in relative standard deviation (RSD) for manually integrated internal standard peaks, GCxGC provided poorer RSD when manual

integration was eliminated and automated analysis enabled in data processing procedure. All of these examples illustrate that development of new and automated software tools for data mining, data alignment and relative quantification is absolutely necessary in order to both decrease manual intervention and increase processing speed as well as to ensure accurate quantification required for reliable deduction of biological interpretation.

1.3 *Sample preparation considerations in metabolomics*

1.3.1 *Sample preparation and its role in complex sample analysis*

Modern analysis of complex samples requires undertaking each step of a complete analytical workflow, starting with sampling and ending with critical interpretation of acquired analytical data. The combination of sample preparation and appropriate chromatographic methodology impacts our understanding of multi-phase heterogeneous systems and is regarded as the bridge between the two afore-mentioned steps. In particular, the choice of sampling and sample preparation methodology has the potential to affect the quality of data and sample preparation is undoubtedly quoted as the slowest step in the analytical procedure for quantitative determinations in complex matrices [94-95]. The concentration levels of trace organic analytes in complex samples are generally too low to allow for direct injection into a chromatographic system. As a result, the main objective of sample preparation relies on generating extract compatible with chromatographic method employed by isolating target analytes from very complex media while simultaneously ensuring acceptable degree of selectivity and overcoming sensitivity limitations of direct injection.

The importance of sample preparation in complex sample analysis results from the complexity and nonhomogeneity of many natural systems composed by a large number of chemical constituents characterized by varying degrees of

structural diversity. For example, in the determination of flavour and off-flavour compounds, the sample preparation is complicated due to a variety of factors including trace levels of investigated analytes, their wide concentration ranges and enormous chemical diversity of target as well as non-target constituents encompassing wide range of polarities, volatilities, solubilities and matrix-binding activities [96]. In such cases, the isolation and concentration steps are performed following sampling and laborious sample manipulation steps which typically require analyte liberation from intracellular compartments through mincing and homogenization as well as the performance of centrifugation [96-97]. Generation of the extract compatible with subsequent instrumental analysis usually requires appropriate clean-up steps, as the importance of their implementation has not been underestimated in the era of emergence of highly selective and sensitive analytical instrumentation [98-99]. In fact, the adverse impacts of matrix on chromatographic behaviour, ionization efficiency, method sensitivity, instrument condition and structural conformation capability of the detection system require more than ever careful selection and optimization of sample preparation strategy. Optimum sample preparation is necessary in order to minimize the required sample preparation time, but also to reduce the number of matrix manipulation and sample preparation steps and method uncertainty, as each step adds a potential source of error [99]. A reduction in uncertainty also requires the implementation of automated and attendance free sample preparation procedures. Recent trends in sample preparation feature the implementation of small sample volumes and minimized consumption of organic solvents in order to promote the use of green and environmentally friendly sample preparation alternatives [99]. The objective of the following section is to place the significance of sample preparation in the context of metabolomics.

1.3.2 *Sample preparation considerations in plant metabolomics*

Biochemical complexity, metabolic heterogeneity and development of a suitable extraction methodology persist to be the main challenges in developing an appropriate metabolomics platform [9]. The current extraction protocols irrespective of their high potential in covering specific metabolite classes are likely biased toward other groups of metabolites [72]. No single extraction methodology is therefore capable of envisioning a truly complete metabolome coverage. In addition to the analytical platform used, sample preparation has a vital contribution in defining the array of metabolite classes covered [100]. Sample preparation will therefore be addressed in line with objectives and goals of a plant metabolomics assay in the current research project.

Preparing a plant sample for a metabolomic study involves several steps including harvesting, drying and extracting the metabolites [101]. Prior to harvesting, it is essential that the biological materials are grown under controlled conditions since alterations in environmental conditions have a pronounced effect on metabolome. Harvesting of plant material requires special considerations since this process itself can initiate enzymatic degradation and oxidation and therefore induce a significant impact on metabolome. Hence in order to ensure collection of as representative metabolome as possible, harvesting should be conducted very rapidly [101]. In addition, the exact timing of harvesting is of utmost importance as well as avoidance of perturbation of metabolism during harvesting [102]. Freezing of the harvested material should be carried out immediately after harvest in order to again minimize the metabolome changes caused by enzymatic reactions that are associated with handling and wounding of the plant [101]. In fact, metabolic processes are rapid and reaction times as low as 1 s and less were reported resulting in the important requirement of fast inhibition of enzymatic processes [72].

Therefore, a metabolism quenching step becomes an essential part of any metabolomics workflow and the most important prerequisite for stopping the enzymatic reactions rapidly and simultaneously and hence ensuring instantaneous snapshot of metabolite concentrations [5]. Typical approaches to metabolism quenching of plant tissues include freezing with liquid nitrogen,

freeze drying, and addition of alcohol or acid [5]. Acid treatment is undesirable and it should be avoided unless there are positive aspects of its use. This method is very efficient for extraction of amines and amides, however it has been reported that a multitude of metabolites are not stable in extreme pH conditions [73]. Freezing with liquid nitrogen was recommended as the best method for quenching enzyme activity in plant tissues since it ensures relatively fast termination of cell metabolism and extremely low temperature (- 196 ^{o}C) [73]. While effectively stopping enzymatic activity, freezing in liquid nitrogen is also disadvantageous because the freezing process itself is not homogeneous and the procedure also gives rise to a number of issues, including loss of metabolites, the emission of touch- or wound-induced metabolites and non-reversible loss of metabolites by absorption to cell walls [72-73]. For example, freezing produced substantial changes in the glucoside composition of leaves [5]. Following freezing, homogenization should be conducted immediately or the transportation of the plant material to the laboratory should be carried out as quick as possible at – 80 ^{o}C before homogenization is possible [15]. Sample transport to the analytical laboratory usually requires dry ice for samples already frozen in liquid nitrogen. Homogenization is required for optimization of extraction recovery, but it has been reported that the process can induce contamination and volatilization of certain components [15]. In addition to the freezing process, the thawing of plant sample can also trigger undesirable metabolite conversions and lead to loss of extract integrity [5]. For example, among various thawing processes including refrigerator, room temperature and microwave thawing, the later method produced the most reliable results in the analysis of anthocyanins in berries.

The second step involved in the preparation of plant material prior to metabolomics analysis is drying. Drying is performed before extraction for a variety of reasons, which are related to water providing the medium for enzyme-mediated reactions during sample preparation, which may initiate metabolite decomposition [101]. Drying can be conducted by implementing a variety of methods, such as ambient air-drying, oven-drying, freeze drying and

trap drying. Oven-drying is disadvantageous in analysis of volatile metabolites as it can lead to severe losses [5]. In general, the implementation of drying methods has been associated with alterations of concentrations of some metabolites [5]. The effect of various drying treatments was for example examined in the analysis of biophenols from birch [5]. Significant concentration differences translated into lower levels of majority of biophenols after application of drying treatments. The observations were attributed to the effect of drying temperature on the rate of enzyme inactivation and issues with thermostability of the biophenols. Among these methods, freeze drying is the most popular method of choice since it is relatively fast and mild, and it also does not require the use of heat to evaporate and eliminate water. With freeze drying, the material is first frozen and then exposed to low pressure in order to sublime frozen water in the material [101]. However, complete removal of all water might not be easy or possible in many cases. Only free water molecules can be removed, but those tightly bound to for example hydroxyl groups of polysaccharides and carbonyl and amino groups of proteins are more difficult to remove. Since biological activity is restricted during freeze drying, the degradation of cellular metabolites is believed to be minimized [103]. However, this process also damages the cellular structure by for example the increase in cell volume during freezing. Freeze drying has been reported to initiate volatile metabolite losses and metabolite losses through irreversible binding to cell walls and membranes [15]. The effect of incorporating this sample preparation step in a plant metabolomics workflow was examined by Oikawa et al. [103]. The authors detected significant decreases in the levels of succinate and choline in *Arabidopsis* and pear, respectively and the extent of metabolite alterations following the application of treatment was dependent on the plant system investigated [103]. The effect of freeze drying was also investigated during the metabolomics workflow focused on the fingerprinting and profiling of volatile metabolites in apples [39]. According to their results, freeze drying process altered the contents of volatile metabolites causing reduction and elimination of some important biomarkers of food quality traits

[39]. For example, for important varietal biomarker, 3-methyl-1-pentanol, freeze drying resulted in an average decrease of 95% among the five fruits investigated. Multivariate analysis also revealed significant differences between fresh and freeze dried samples as illustrated in Figure 1.5.

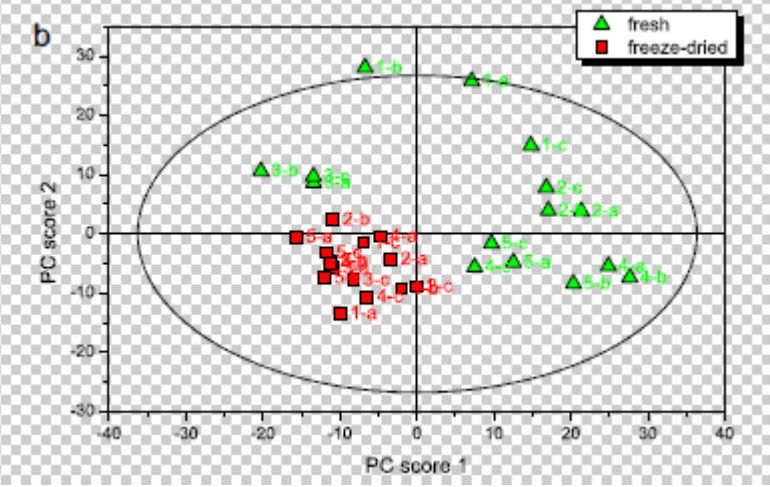

Figure 1.5. PCA scores plot of data originating from HS-SPME-GC-ToFMS analysis of five Golden Delicious apples extracted fresh and after freeze-drying [39].

Finally, after metabolism quenching and sample preparation and prior to extraction, the samples are often required to be stored, but issues such as leakage, cross-contamination, and loss of sample integrity may be encountered during deep freeze storage [5]. Storage conditions have to be controlled as stability during storage is an important parameter to consider. However, such studies focused on examining the effect of long-term storage are rare, even though it was reported that for example the volatile metabolite composition of fruit was significantly altered with respect to storage time [15].

The extraction step must prevent hydrolytic, oxidative, photodegradative, and enzymatic conversions of metabolites. This may involve the use of inert atmospheres, manipulation in the dark and addition of enzyme

inhibitors or antioxidants. However, the addition of exogenous substances should be avoided, unless absolutely necessary. Isolation of metabolites from the sample matrix is essential in any comprehensive metabolomics scheme and the main objective of extraction is to obtain uniformly enriched extract with all metabolites. Since metabolomics aims to quantify all or at least as many as possible metabolites in a biological system, the extraction process should be unselective and unbiased for optimum metabolite coverage. An exception to this is targeted metabolomics platform, which necessitates thorough optimization of extraction protocol for optimum recovery and possibly exhaustive extraction. Generally, the extraction method implemented is a compromise between extraction recovery and minimizing inter-metabolite conversion and labile metabolite destruction. For non targeted and global metabolomics platforms, chemical and structural metabolite diversity and their effects on physicochemical properties that control extraction efficiency and recovery imply a number of challenges encountered during the search for and optimization of an appropriate extraction methodology.

It is widely acknowledged that the anatomical and physiological complexity of plants has to be considered in studies focused on plant metabolism [14]. Potential sources of uncontrolled variability include plant and organ age and developmental stage, duration of harvest and sample processing and all these steps should be carefully standardized [15]. This is especially important when multiple harvests are required and/or different operators need to be involved in order to decrease the duration [15]. From a plant anatomy point of view, each plant organ and tissue is composed and characterized by a specific set of metabolites that are present in specific distributions and are very often differentially affected by external stimuli. Each of the plant compartments is characterized by their own array of metabolites and concentration levels. However, in order to improve sensitivity of a metabolomics assay, different cell types and tissues are usually combined per each biological specimen in order to profile metabolites effectively [14]. Alternatively, only selected plant organs or small pieces of plant tissue can be investigated in terms of metabolome

composition [12]. In addition to inter-compartmental variations in plant metabolome, the metabolite content is also found to vary within the same organ and/or compartment [101]. The metabolome analysis conducted in this way may lead to rewarding results, however, it lacks the information regarding intertissue translocation of metabolites and the functional differentiation of various types of plant cells [12]. Therefore, no information is collected with respect to metabolome composition within and between compartments and this poses a significant drawback of majority of sample preparation methods not only due to inability to examine compartment-specific responses to external variations, but also impossibility to locate sources of for example nutritionally-related and disorder-specific features summarized in sections above. The inter-compartmental distribution of metabolites also plays a major role in determining pathway activities and metabolic fluxes.

In addition to plant anatomy, significant emphasis needs to be placed on the physiological aspects of plant metabolism [9,14]. For example, gene expression and enzyme activity associated with photosynthesis, respiration and energy metabolism are rapidly affected by changes in environmental conditions [102]. In the context of harvesting, it must be kept in mind that levels of plant metabolites vary throughout the day and that metabolome composition of the leaf and fruit alters with respect to progression of a day [15,101]. Levels of several primary metabolites such as malic acid and sugars fluctuate during a daily plant cycle, and secondary metabolites are not excluded from this phenomenon either [101]. For example, several plants of *Cannabis sativa* harvested at different times during the day, as well as in the morning and afternoon, were showing completely different profile of metabolites with respect to harvest time [101]. Again, the differences both in primary and secondary metabolite profiles with respect to harvest time were apparent (Figure 1.6).

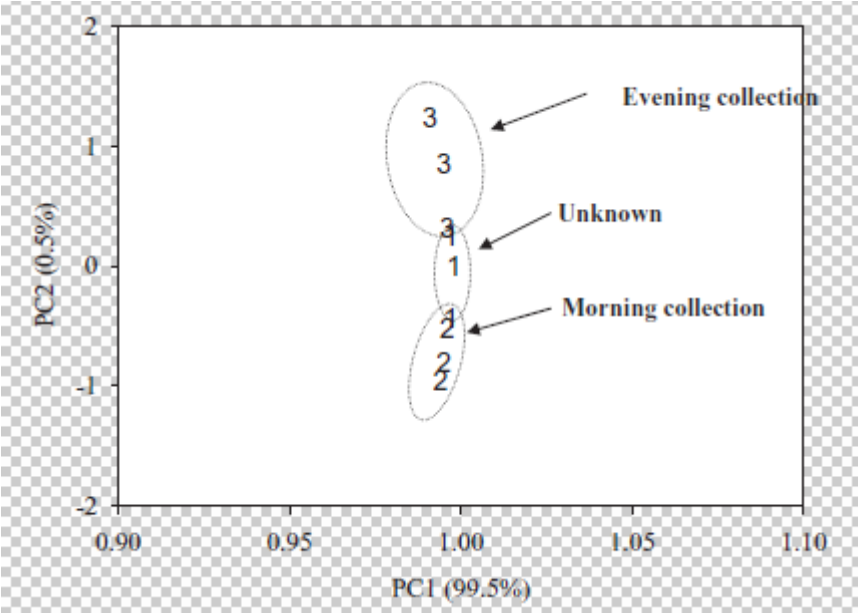

Figure 1.6. Principal component analysis score plot of *Cannabis sativa* collected at different time points. 1 – collection time unknown; 2 – collected in the morning; 3 – collected in the evening [101].

Also, significant changes in leaf metabolome caused by temporal resolution when plants were harvested at sunrise and sunset were reported and a number of authors cautioned against differences in day and night metabolome [31, and references therein]. Temporal distribution is large with variations ranging across an organism's lifespan and during seasonal rhythms and environmental oscillations and therefore should be taken into account and controlled for if possible [10].

In conclusion, selection of sampling and sample preparation method impacts the quality and reliability of metabolomics data. The sample preparation and extraction methodology employed should be non-selective and unbiased for optimum metabolome extraction coverage and for ensuring the minimum degree of discrimination toward metabolite classes present in the investigated biological system. Therefore, the role of sample preparation in defining the array of metabolite classes covered should not be underestimated. On the other hand, apart from metabolite coverage, the optimum sample preparation protocol should provide an extract compatible with subsequent

instrumental analysis. Finally, the most important prerequisite of any sampling and sample preparation platform is the incorporation of a metabolism quenching step in order to terminate enzymatic activity, prevent enzyme-mediated metabolite conversions and eliminate chemical and physical breakdown of labile metabolites. The metabolite profile obtained under the circumstances in which these prerequisites are not fulfilled can not be regarded as a true representation of the biological system and its biochemical state.

1.3.3 *Traditional sample preparation methods for analysis of volatile metabolites*

The measurement of a volatile profile encountered in a specific biological system requires a substantially different approach from targeted and selective quantitative analysis where the objective is maximizing analyte recovery. Rather than focusing on few selected analytes and adjusting parameters that control extraction sensitivity and selectivity, the goal of global metabolite analysis is optimum extraction coverage, hence the implementation of unselective approaches is required. Therefore, the diverse range of physicochemical properties that these compounds possess therefore may represent a challenge and no single analytical extraction method has been capable of achieving the complete profile. Furthermore, the profile is highly dependent on the technique employed, so complementary and parallel extraction methodologies are simultaneously used for broad-spectrum profiling purposes [64]. The objective of this section is to introduce the sample preparation and extraction techniques that are most commonly applied in studies involving targeted and non-targeted profiling of plant metabolites. Even though the field of sample preparation has been subjected to many advancements in the recent years which attributed to introduction of novel, improved and more environmentally friendly techniques, only the most common and least invasive methods will be addressed here.

The isolation and concentration of volatile metabolites from food and plant matrices is generally carried out by employing solvent extraction or headspace analysis [104]. Solvent based extraction methods have been traditionally implemented in various areas of analytical chemistry. Extraction with organic solvents generally gives a more complete profile of volatile metabolites and the method is also capable of providing a reasonable metabolite coverage for some important polar and hydrophilic species present in various types of food and plant matrices. These include, but are not limited to lower molecular weight alcohols, thiols, acids as well as flavour compounds such as acetoin, methionol and furaneol [64]. Despite the reasonable completeness in extraction coverage, the method does also introduce a number of non-volatile matrix components including leaf waxes, triterpenes, sterols, triglycerides as well as impurities from laboratory apparatus [64]. The solvent mixtures used for extraction employ pentane-ether mixture and dichloromethane [9,64]. For example, endogenous volatile compounds from apple skin were analyzed by submitting 5 g of skin to grinding in liquid nitrogen and extracting with pentane twice [71]. The extract was subsequently dehydrated with anhydrous sodium sulphate and concentrated to 15 μL at 40 ^{o}C in a water bath. As it can be seen, solvent extracts are frequently concentrated by evaporation before analysis and this presents a significant drawback as it leads to losses of important volatile metabolites [64,104]. Insufficient sensitivity is resulted by the injection of only a small portion of solvent extract (1 μL) [64]. Additional limitations are related to long sample preparation times, the deterioration of sample composition leading to formation of artifacts, extensive organic solvent consumption, high cost and environmentally unfriendly nature of the analytical technique [105].

In order to address the requirement for reduction of toxic organic solvent use and encourage the implementation of ‘green chemistry’ sample preparation alternatives, environmentally friendly methods have attracted increasing attention and have been subjected to major developments [105]. Among them, headspace methods have been frequently employed in the analysis of environmental and food samples [99,104-106]. Headspace analysis is generally

defined as a vapour-phase extraction, which involves the partitioning of analytes between a liquid or solid sample containing target analytes and the vapour phase above the sample [106]. Therefore, the use of solvents can be avoided by analyzing the headspace of the sample. The sample preparation is simple and these techniques generate clean chromatograms as only the vapour phase is injected. Hence, accumulation of high-molecular weight and non-volatile components in the GC system is eliminated, which is an advantage, considering that their buildup results in poor instrument and analytical performance. Static headspace sampling involves employing optimum temperature to heat an aliquot of a liquid or solid sample in a sealed vial for a given period of time [99,106]. Subsequently, a known volume of headspace is collected usually in a gas-tight syringe and injected into GC. This extraction method has been a primary tool for analysis of volatile organic compounds in food and environmental samples [106]. However, the technique suffers from sensitivity limitations since the extract is not preconcentrated prior to GC injection and usually high part per billion (ppb) levels are targeted [106]. An illustrative example of the importance of sampling and sample preparation in defining the metabolome coverage and array of functional groups constituting a particular biological system is presented in Figure 1.7. The figure effectively demonstrates the dependence of volatile profile in apple skin on the extraction methodology implemented. Static headspace sampling was more selective for analysis of highly volatile metabolites and it showed a pronounced bias toward butyl acetate, 2-methylbutyl acetate and hexyl acetate [64]. On the other hand, diethyl ether extract of apple skin showed richer coverage for higher molecular weight terpenes and hydrocarbons.

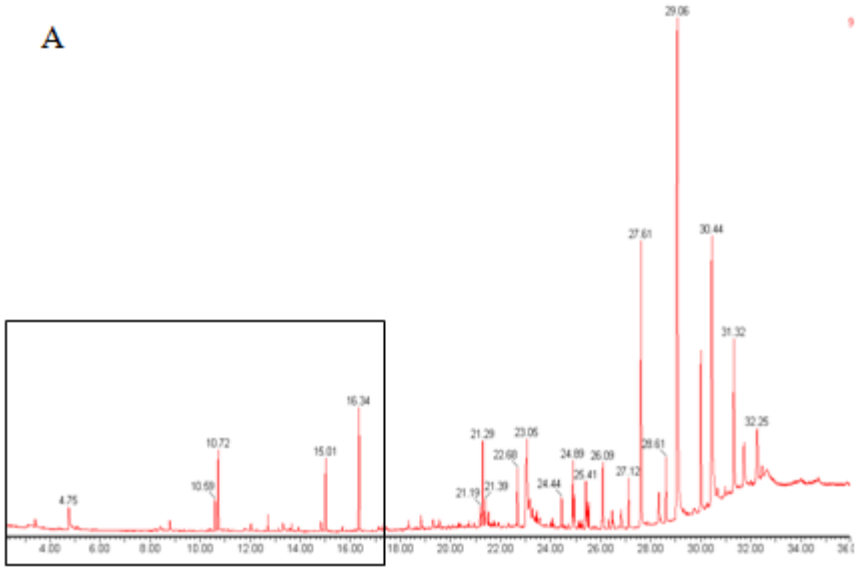
A
4.75
10.59
10.72
15.01
16.34
21.19
21.29
21.39
22.68
23.05
24.44
24.89
25.41
26.09
27.12
27.61
28.61
29.06
30.44
31.32
32.25

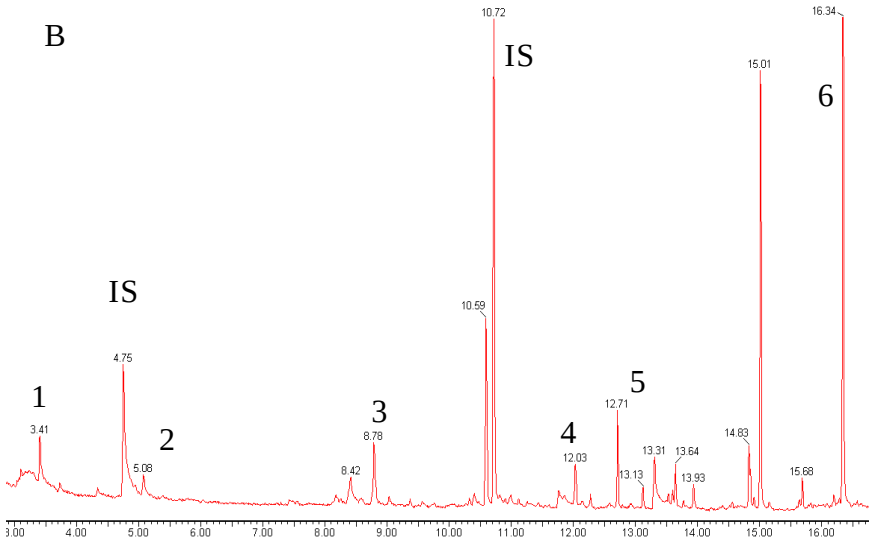
B
IS
IS
1
2
3
4
5
6
3.41
4.75
5.08
8.42
8.78
10.59
10.72
12.03
12.71
13.13
13.31
13.64
13.93
14.83
15.01
15.68
16.34

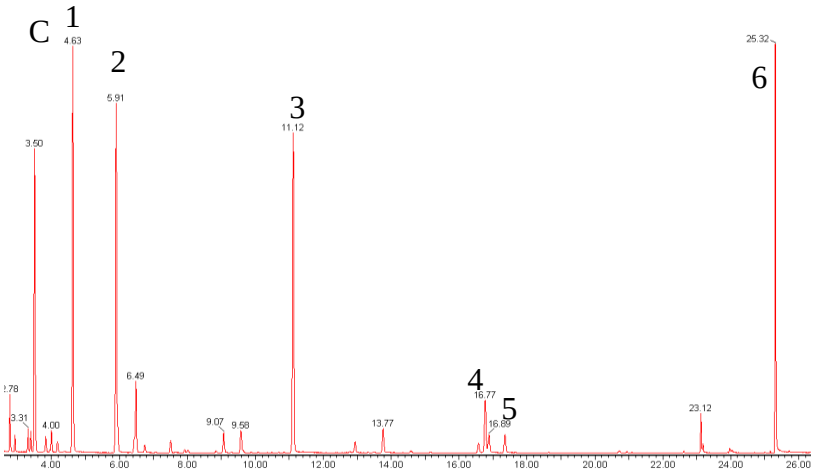

Figure 1.7. GC-MS chromatographic profiles of volatile metabolites in apple skin and their dependence on extraction methodology used. A - diethyl ether extract; B - 3–16 min region of diethyl ether extract; C - headspace volatile profile. Labeled peaks are butyl acetate (1), 2-methylbutyl acetate (2), hexyl acetate (3), butyl hexanoate (4), hexyl 2-methylbutanoate (5), α-farnesene (6) and internal standard (IS) [64].

Dynamic headspace on the other hand involves the continual sampling of the gas phase above the sample by flushing the sample with an inert gas [99]. The most frequently employed dynamic headspace method is purge and trap. In purge and trap, the volatile compounds are flushed from the sample with a gas stream and then enriched in a cold trap or on appropriate adsorbent that is directly transferred into the GC using thermal desorption [106]. This method is more sensitive than static headspace since with the removal of gas, the equilibrium will re-establish and subsequently exhaustive extraction may be achieved. However, the adsorbents employed for enrichment are nonselective and the obtained extracts are frequently quite complicated.

The importance of static and dynamic headspace sampling methods mentioned here in extraction of volatile metabolites has been realized in the analysis of headspace surrounding specific plant parts and/or whole plants [107]. Major research fields in this area have investigated the role of floral volatiles in pollination biology, the alterations of volatile emissions released

from photosynthetic tissues in response to changes in light and temperature and emissions induced by herbivore damage. Volatile emission and profile measurement can be conducted with static and dynamic headspace techniques in a non-destructive manner by collecting headspace around the undamaged living specimens [107]. Therefore, it is important to address the advantages and limitations of such sampling approaches.

All methods for the analysis of volatile metabolites from plants strive toward obtaining the authentic volatile profile emitted from an investigated specimen [107]. For static headspace sampling, the plant or its parts can be placed in a sealed container and the emitted volatiles may be collected in a gas-tight syringe and introduced into GC instrument. However, this approach is not recommended as it requires a sufficiently high concentration of volatiles in the headspace. In addition, static headspace may accumulate humidity and heat, especially when samples are analyzed under illumination. Consequently, the sampling design, which is implemented in laboratory investigations when plants and/or plant parts are enclosed in sealed containers may interfere with normal physiological processes of plant that affect the emission of volatiles [107]. Alternatively, in-field evaluations are possible provided that plants are surrounded by closed containers, but issues with transportation of collected gas from the sampling site to the laboratory and the stability of collected components limit their applicability. Similarly, the dynamic headspace method can be employed for volatile metabolite collection from plant parts and/or whole plants when they are enclosed in sealed containers. Sensitivity limitation is compensated for by trapping and enriching the volatiles on adsorbents as mentioned before. Application of a continuous air stream addresses some of the limitations of static headspace sampling including interference of heat and humidity on measurements. Dynamic headspace collection of volatiles emitted from intact greenhouse grown transgenic and classically bred apple cultivars was performed by Vogler and coworkers [46]. The plants were packed in a polyester bag construct and wrapped at the shoot with cotton wool and Teflon tape. The polyester bags were provided with an attached glass funnel and

continuous circulation of charcoal filtered air was supplied during volatile collection. The volatiles were adsorbed on trap filled with Tenax TA adsorbent and after collection, thermal desorption was employed to introduce the extract into GC-MS instrument. Similarly, Ban et al. analyzed volatile emissions by implementing a dynamic headspace method that required collecting volatile analytes for 1 hr onto Tenax TA traps after placing apple fruit in Tedlar bags and applying a constant stream of air [71]. The trapped analytes were eluted from adsorbent by applying consecutive portions of pentane and diethyl ether. Also, harvested apple fruit were analyzed for volatile profile by dynamic headspace method after weighing the fruit, placing them in 2-L vessel and waiting for 1 hr at 24 ^{o}C for accumulation of volatiles in headspace of the sampling chamber [60]. Subsequently, dried air was introduced to sweep the headspace and volatiles were collected for 1 hr onto Chromosorb 105 sorbent. After drying the traps for 15 min with nitrogen, thermal desorption was conducted for GC-MS analysis. With regards to dynamic headspace method, it must be noted that the application of an external gas stream may also induce a drastic alteration in functioning of natural physiological processes and therefore, result in collection of nonrepresentative volatile profile. The in-field employment of the technique is also hindered by insufficient miniaturization and on-site incompatibility. Considering the lack of portability and inconvenient on-site implementation of these extraction methodologies, the subsequent sampling and sample preparation design permits the performance of laboratory investigations only, in which the placement of sealed chambers around living plants and their ruptured parts affects physiological processes and volatile profile collected in response to such perturbations. The representativeness of metabolome collected under such conditions is questionable and the employment of novel non-invasive, miniature and portable sampling and sample preparation devices is more than ever required.

1.3.4 *Introduction to solid phase microextraction*

Solid phase microextraction (SPME) was developed by Pawliszyn and coworkers in 1989 to promote rapid sample preparation, for both laboratory and on-site arrangements and provide an efficient way toward integration of sample preparation with separation and detection systems [108]. In accordance to microextraction principle, the technique employs a small volume of polymeric extracting phase coated on the outside of a fused silica or metal alloy solid support [94-95]. The manual SPME device is presented in Figure 1.8. The most important part of this device is a fibre solid support coated with a thin layer of a polymeric stationary phase which is used to extract the analytes by concentrating them from the sample matrix [94,109-110]. The fibre is housed inside the needle which serves to protect the fibre/fibre coating from damage during vial/injector septa penetrations [94,109]. Traditionally, SPME has been used routinely in combination with GC and GC-MS. However, in order to analyze non-volatile and thermally labile compounds not amenable to GC or GC-MS, significant improvements were made in direct coupling of SPME with high-performance liquid chromatography (HPLC) and liquid chromatography – mass spectrometry (LC-MS). Today, SPME is widely applicable in both targeted and non-targeted qualitative and quantitative analyses of organic compounds from various gaseous, solid and liquid environmental, biological and food matrices.

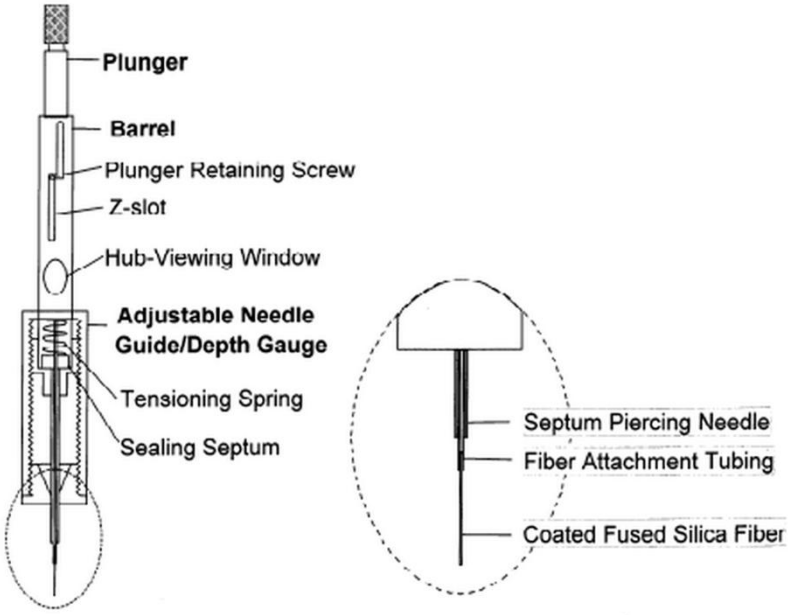

Figure 1.8. Commercial fibre-SPME device for manual operations available from Supelco.

SPME principle relies on placing a thin polymeric coating coated on the outside of a fused-silica fibre directly to the sample matrix or to the headspace above it for a pre-determined period of time (Figure 1.9) [94]. As soon as the coated fibre is placed in contact with the sample matrix, analytes partition by adsorption or absorption from the sample matrix to the extracting phase [94,111]. At the instance when the analyte concentration reaches the distribution equilibrium between the sample matrix and the fibre coating, SPME extraction is considered to be complete. Upon reaching equilibrium, the amount of analyte extracted by the SPME coating does not further increase with extraction time within the limits of experimental error. This means that sampling under equilibrium conditions provides maximum sensitivity achievable with SPME [95]. However, SPME extraction can be interrupted at any time before equilibrium, provided that sufficient sensitivity is achieved for a particular application of interest. Once the extraction process is completed, concentrated extracts are transferred onto the separation system either *via*

thermal desorption in GC injection port or by solvent desorption in the case of HPLC [95, 112].

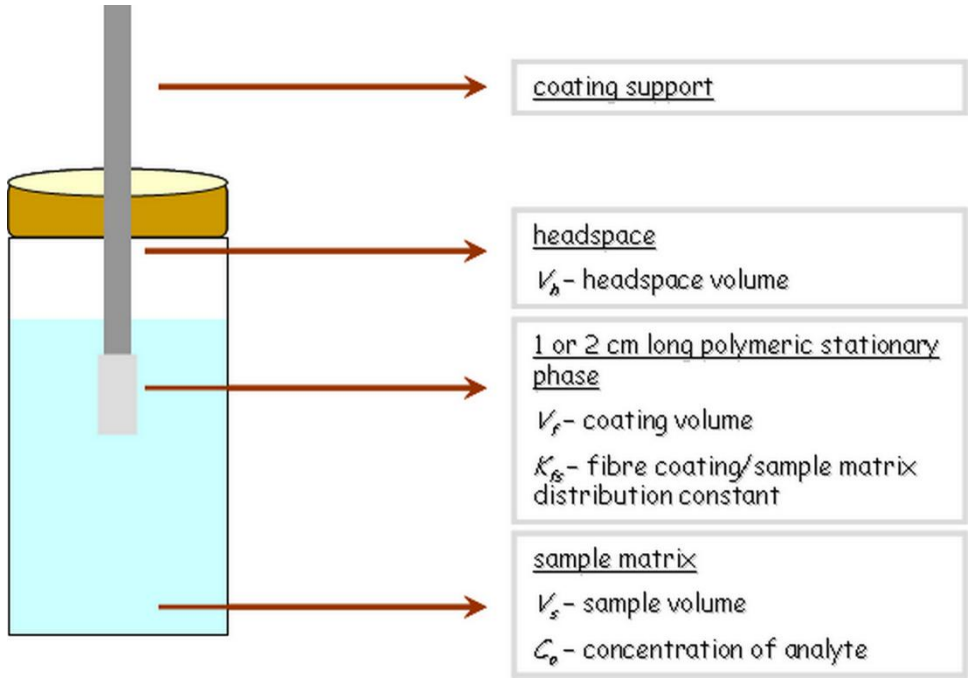

Figure 1.9. The basic principle of SPME extraction. Fibre coating is immersed in the sample matrix for a pre-determined extraction time. After the completion of extraction process, the coating is introduced into the analytical instrument for subsequent desorption of analytes, separation and detection.

The main parameter affecting SPME extraction efficiency is fibre coating (extracting phase)/sample matrix distribution constant of the target analyte (K_{fs}) as it reflects the chemical composition of the extracting phase and determines the magnitude of enrichment factors possible through the use of SPME technique [95,113-114]. Distribution constant between the liquid extraction medium and the sample matrix is expressed by the following equation:

$$K_{fs} = C_f^{\infty} / C_s^{\infty} \qquad \textbf{Equation 1.1}$$

where C_f^{∞} and C_s^{∞} are the equilibrium concentrations of the target analyte in the fibre coating and sample matrix, respectively [94]. Equation 1 is also applicable when solid is used as a extraction medium, provided that C_f is replaced by solid extraction phase surface concentration of adsorbed analytes [115]. The parameters that influence the magnitude of K_{fs} are sample temperature and sample matrix conditions, such as salt, pH and organic solvent composition [114]. The number of moles of analyte extracted at equilibrium (n_e) in a two-phase system (sample matrix and extraction phase) can be determined through the following equation:

$$n_e = \frac{K_{fs}\, V_f\, V_s\, C_o}{K_{fs}\, V_f + V_s} \qquad \textbf{Equation 1.2}$$

where V_f is the fibre coating volume, V_s is the sample volume and C_o is the initial concentration of a target analyte in the sample matrix [94,109].

However, the extraction process becomes more complicated in multi-phase heterogeneous systems, where more than two phases are present such as for example headspace, immiscible liquids and solids. Equation 1.2 results in Equation 1.3 when the investigated system involves the extraction phase, gas phase and a homogeneous matrix such as pure water:

$$n_e = \frac{K_{fs}\, V_f\, V_s\, C_o}{K_{fs}\, V_f + K_{hs}\, V_h + V_s} \qquad \textbf{Equation 1.3}$$

where K_{hs} is the headspace/sample matrix distribution constant and V_h is headspace volume [95,116].

Kinetic parameters affect the rate of extraction and their understanding gives indication on how to increase the overall speed and decrease the time of extraction [94-95]. In order to enhance mass transfer of analytes from the sample matrix to the vicinity of the fibre, some level of agitation is usually

required. Agitation (convection) conditions are critical in increasing the rate of mass transfer from the sample matrix to the fibre coating. This in turn leads to shorter equilibration times, increased overall speed of analysis and higher mass of analyte extracted in pre-equilibrium conditions.

In the practical application of SPME, a variety of experimental factors need to be considered and addressed for a particular system under investigation. The selection of parameters that affect SPME extraction efficiency is mainly dependent on the target analytes of interest, sample matrix and objectives of analysis [110]. Selection of fibre coating is usually the first stage in SPME method optimization. As demonstrated in Equation 1.2, the sensitivity of SPME method is proportional to fibre coating/sample matrix distribution constant (or in another words the chemical composition of the extraction phase), as this parameter determines coating sensitivity and selectivity toward target analyte of interest versus other components present in the sample matrix [94,98,110]. Up to now, the only producer of commercial fibre assemblies is Supelco (Bellefonte, PA, USA) and it offers single-polymer and mixed-polymer coatings of different polarities, thicknesses (7-100 μm range) and lengths (1-cm and 2-cm lengths available) [117]. Fibre selectivity for the particular analytes of interest is determined on the basis of the principle 'like-dissolves-like' [95]. Hence, successful exploitation of SPME technique has been attributed to commercial availability of a variety of extraction phases, including single-phase absorbents such as polydimethylsiloxane (PDMS), polyacrylate (PA), carbowax (CW) and mixed-phase sorbents such as carboxen/polydimethylsiloxane (CAR/PDMS), polydimethylsiloxane/divinylbenzene (PDMS/DVB), divinylbenzene/carboxen/polydimethylsiloxane (DVB/CAR/PDMS) and carbopack Z/PDMS [94-95]. While PDMS provides good extraction efficiency for non-polar compounds, the use of PA and CW gives rise to better selectivity in polar compound determinations [94-95]. On the other hand, the implementation of solid and mixed-phase sorbents has been favourable in volatile and small molecular weight compound analysis [94-95,118]. In addition to selection of fibre coating, extraction time plays a critical role in

obtaining desired sensitivity, method precision and accuracy in complex sample analysis. As mentioned previously, the maximum sensitivity is achievable with SPME methods when equilibrium conditions are applied. Therefore, the choice of optimum extraction time depends on the particular application under consideration and is always a compromise between sensitivity, speed and precision required [95]. The preferred extraction mode of SPME implementation in complex sample analysis is headspace-SPME (HS-SPME), where fibre coating is exposed to headspace above the simple or complex aqueous sample or solid sample [94-95]. Besides accelerated extraction rates (hence selectivity and sensitivity) for volatile compounds as well as compounds characterized by high Henry's law constants, the convenience in its utility arises from the introduction of a barrier of gas for protection of extraction phase from high molecular weight matrix interferences and/or compounds that are not amenable to GC analysis [94-94,109]. The sensitivity limitation of HS-SPME when high-molecular weight and highly polar compounds are concerned may be overcome by increasing extraction temperature [94-95]. With direct immersion SPME (DI-SPME), the fibre coating is exposed and completely immersed inside the sample matrix. Therefore, this extraction mode is favourable toward analytes having low to medium volatility and high to medium polarity [95]. Finally, it is important to make sure that desorption efficiency is optimized and that the extracted analytes are completely desorbed from the fibre coating.

Besides the ease of utility, minimized organic solvent consumption and short sample preparation times, SPME technique features small sample amount requirements, automation capability and the ability to produce high-quality qualitative and quantitative analytical results for gaseous, aqueous and solid real-life samples of high complexity. Therefore, the technique has been capable of overcoming several drawbacks encountered during implementation of traditional sample preparation methods. Several applications demonstrating rewarding performance characteristics of the technique in advanced fingerprinting and profiling studies of apple matrix and a number of complex food/plant matrices will be underlined in this section. The metabolomics

studies conducted on hyphenated SPME-GCxGC-ToFMS system will be also introduced to highlight the advantages of this multidimensional analytical approach in complex sample characterization.

1.3.4.1 Feature SPME applications: analysis of apple matrix with HS-SPME

SPME technique featuring rapid and solvent-free sample preparation, small sample amount requirements and automation compatibility contributing to high-throughput qualitative and quantitative determinations has frequently been employed in the area of volatile metabolite profiling. In particular, considering the complexity of many naturally existing food and plant matrices attributed by hundreds of GC-amenable, thermally labile and non-volatile compounds, ever since its inception, HS-SPME extraction mode has been gaining increasing interest. Consequently, the full exploitation of the advantages offered by HS-SPME including high sensitivity and selectivity for highly volatile analytes and enhanced fibre coating lifetime resulted in a multitude of published studies illustrating rewarding method performance characteristics both in terms of sensitivity and sample characterization [110, 119-120]. In the context of feasibility of SPME technique for profiling of volatile metabolites in apples, several studies were published in the literature and the main findings of biological relevance were already summarized in Section 1.1.4.1 and 1.1.4.2. At this point it is beneficial to summarize SPME conditions employed in those studies and briefly highlight the main research achievements. Dunemann et al. employed HS-SPME method by exposing 100 μm PDMS fibre for 15 min to the headspace of sodium chloride (NaCl) saturated apple slurry [70]. Desorption was carried out for 2 min at 250 ^{o}C and the GC-MS chromatographic profiles containing up to 100 distinct peaks were processed to accomplish the identification of 20 analytes. The identified compounds were comprised of 6 alcohols, 11 esters, 1 terpenoid compound and 2 analytes from miscellaneous

chemical groups. The volatile profile collected was strongly reflective of genotype, which allowed the examination of genetic and molecular basis of apple aroma. Ferreira and coworkers thoroughly optimized HS-SPME procedure in order to depict the effects of coating type, sample temperature, extraction time, sample amount, dilution factor, ionic strength and desorption time on extraction sensitivity and desorption efficiency [49]. The optimum settings for major extraction efficiency influencing parameters consisted of DVB/CAR/PDMS fibre, 30 min extraction time and 50 ^{o}C sample temperature. The authors added calcium chloride ($CaCl_2$) solution to apple pieces before homogenization to inhibit the enzyme activity. A quite extensive list containing up to 100 identified compounds was composed and analyte relative levels were used for characterization of different Madeira Islands apple varieties according to origin (Figure 1.10).

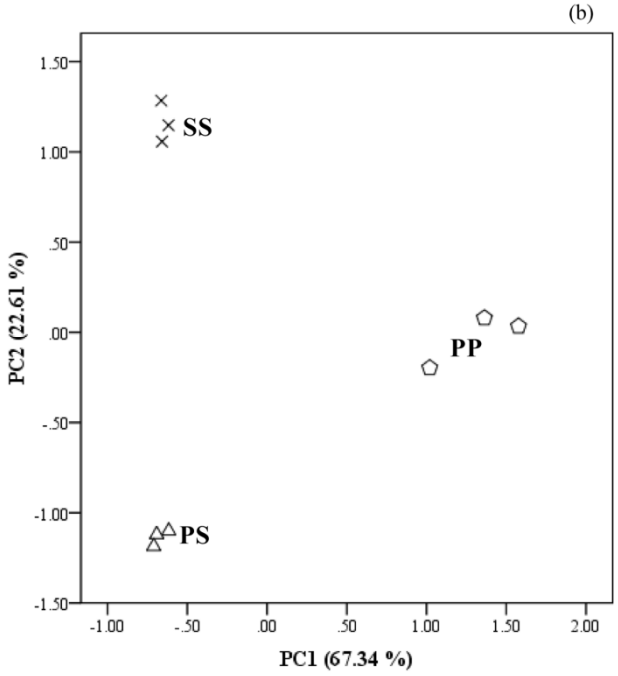

Figure 1.10. Principal component analysis of three different Madeira Islands apple varieties illustrating differentiation according to geographical origin for apples from Ponta do Pargo (PP), Porto Santo (PS), and Santo da Serra (SS) [49].

Young et al. applied HS-SPME method toward determination of 40 esters and α-farnesene in 13 apple varieties [51]. The authors differentiated the samples based on the skin colour by employing a method consisting of 100-μm PDMS fibre coating exposed to samples for 25 min at 23 ^{o}C. Róth et al. investigated the postharvest quality of integrated and organically produced apple fruit by employing a PDMS/DVB fibre coating in HS-SPME mode for 10 min over homogenate kept at 35 ^{o}C and consisting of apple sample and saturated NaCl [48]. Superficial scald and bitter pit development in cold-stored transgenic apples suppressed for ethylene biosynthesis was also examined by applying a HS-SPME method [47]. The method consisted of exposing a 100-μm PDMS fibre coating to the headspace of NaCl saturated apple sample for 20 min after a quite extensive incubation procedure performed for 2 hr at 30 ^{o}C. Finally, in addition to traditional fingerprinting and profiling of volatile metabolites with the intention of accomplishing establishment of compositional characteristics and/or disorder incidence, HS-SPME has also been applied for elucidation of volatile profile with respect to apple fruit development and ripening. For example, HS-SPME method employing a PDMS/DVB fibre coating for 30 min at 50 ^{o}C was applied in a study by Defilippi and coworkers in order to examine relationships between ethylene biosynthesis and production of volatile compounds [61]. The majority of these and other published metabolomic fingerprinting and profiling studies incorporated a metabolism quenching step in liquid nitrogen and further prevention of enzymatic activity associated with volatile biosynthesis was assured by adding high contents of salts such as NaCl and $CaCl_2$ prior to homogenization and extraction steps [47]. The addition of salts also functions to decrease aqueous solubility and subsequently increase fibre coating/sample matrix distribution constant of certain analytes, hence, extraction recovery may significantly be improved [94-95]. In such sample modifications, more enhanced salting out effect and less viscous final homogenate were obtained after NaCl addition and these observations resulted in preferred use of NaCl over $CaCl_2$ [48]. Nevertheless, extensive and labour

intensive pre-extraction sample preparation steps are required to assure that the final extract is as close to true metabolome composition as possible.

1.3.4.2 Analysis of food and plant samples with SPME combined with high-speed GC and GCxGC-ToFMS

Several underlying aspects that will be covered in the proceeding section will address the suitability of laboratory SPME investigations combined with high-speed gas chromatography and GCxGC-ToFMS in the areas of metabolomics fingerprinting, targeted metabolomics and global metabolite analysis.

Traditionally, HS-SPME approach has been widely implemented in semi-quantitative fingerprinting and profiling studies involving volatile and semivolatile analytes, as it assures good sensitivity and selectivity for determination of volatile and non-polar to mid-polar compounds, including flavours and off-flavours. In fact, the more recent advancements and/or features of SPME methodology, including fast sample preparation and introduction and increased selectivity and sensitivity (in both equilibrium and pre-equilibrium regimes) of HS-SPME extraction for volatile analyte determination, have attributed to the wide implementation of HS-SPME in combination with high-speed gas chromatography [119,121-122]. In addition, the employment of automated systems for ensuring repeatable timing periods and robust superelastic fibre assemblies have resulted in increasing interest for SPME use in studies involving rapid determination of food quality. For example, Setkova et al. employed a fast SPME-GC-ToFMS method consisting of applying short exposure 5 min HS-SPME extraction at 45 ^{o}C to isolate volatile and semivolatile constituents in ice wines [121,123]. While GC run time was less than 5 min, the authors emphasized enhanced durability of metal SPME fibre assembly reflected in completion of 627 injections without significant loss in extraction sensitivity [121]. Finally, a comprehensive list of more than 200

compounds was composed and the authors established rewarding differentiations of samples according to several quality attributes including geographical origin and grape variety [121]. Tranchida et al. employed automated HS-SPME extraction of volatile compounds in a bergamot essential oil with the use of low-capacity PDMS fibre coating for fast equilibration of analytes and subsequent separation on narrow-bore (12.5 min run time, 10 m x 0.1 mm internal diameter) column [124]. Confirmation of the authenticity of fruit-flavoured foods and beverages was performed by adopting a Total Analysis System (TAS) in which on-line integration of pre-equilibrium HS-SPME, enantioselective GC-MS and statistical multivariate methods was accomplished [125]. The application of short SPME extraction times (10-20 min depending on the matrix) contributed to the overall feasibility of the TAS system to reduce total analysis time from 150 to 20 or 50 min [125]. Based on these and numerous applications in related areas of research, HS-SPME has been capable of achieving a reasonably satisfactory overview of food composition and such high-throughput GC-EI-MS food profiling studies have been greatly facilitated by high data acquisition rates and absence of spectral skew to allow the mass spectral deconvolution of chromatographically overlapping analyte peaks that unit-resolution high-speed time-of-flight detectors have offered [74,122]. As a result, narrow chromatographic peaks generated in a fast gas chromatography set-up are properly constructed and GC resolution requirements are greatly reduced [76,81]. Apart from analysis of volatile and less polar compounds, the limitations of HS-SPME mode are encountered however, when polar and/or high boiling point analytes are considered, necessitating matrix adjustment and increase in sample temperature to increase mass transfer rates from sample matrix to headspace [94-95].

Even though the application of SPME in combination with traditional and fast GC-MS instrumentation in metabolomics has become routine, a continuous strive toward quantitative methods offering higher sensitivity and specificity has demanded the use of high-resolution gas chromatographic instrumentation including GCxGC-ToFMS, which has become the method of

choice in the area of complex sample characterization. In relation to metabolomics fingerprinting and profiling, and relevant studies attempting to establish a more complete sample characterization, rewarding results were obtained when the technique was hyphenated to SPME. SPME-GCxGC approach was employed in comprehensive volatile profile characterization for a number of food and plant matrices including wines, grapes, honey, basil (*Ocimum basilicum* L.), Brazilian sugar spirit (cachaça), coffee, barley coffee, strawberry, butter, olive oil, roasted hazelnut, cacao, roast beef, pepper and Malaysian soursop [78,81,86,126-138]. For example, Weldegergis et al. reported 206 positively or tentatively identified compounds in South African Pinotage wines encompassing large range of chemical functionalities including esters, alcohols, carbonyls, acids, acetals, furans, lactones, sulphur compounds, nitrogen containing compounds, terpenes, hydrocarbons, volatile phenols and pyrans [127]. SPME step was performed in HS mode with CAR/PDMS fibre coating placed above 10 mL of wine sample (accompanied by sodium chloride addition, magnetic stir bars for agitation and sample temperature of 23 ^{o}C) for 10 min, followed by 5 min desorption at 275 ^{o}C. Similarly, Robinson et al. characterized wine profile composition and they reported simultaneous detection of over 350 tentatively identified constituents belonging to potent aroma compound classes including monoterpenes, norisoprenoids, sesquiterpenes and alkyl-methoxypyrazines [126]. The following steps were performed in SPME sequence: 10 min incubation and 60 min extraction steps at 30 ^{o}C with metal alloy DVB/CAR/PDMS fibre coating, followed by desorption at 260 ^{o}C for 5 min. Čajka et al. developed a method focused on reducing GCxGC-ToFMS analysis time and their setup provided a relatively fast and selective screening approach (164 identified compounds) by allowing additional separation efficiency through utilization of second dimension [81]. The methodology was hyphenated with HS-SPME (20 min extraction) in a number of follow-up studies on honey traceability determination and authentication [139]. Rocha et al. reported rewarding results with implementation of SPME (CW/DVB coating, 60 min HS-SPME extraction at 40 ^{o}C) and GCxGC-ToFMS

in the establishment of monoterpenoid profile of *Vitis vinifera* L. white grapes (cultivar Fernão-Pires). A comprehensive database of 56 identified monoterpenoids, including 20 analytes that were reported for the first time in grapes was superior as compared to performance of traditional one-dimensional GC-MS systems [78]. Through the use of extracted ion chromatograms, bidimensional separation space was efficiently defined by monoterpenoid elution profile featuring structured retentions for monoterpene hydrocarbons and monoterpene oxygen-containing compounds (Figure 1.11) [78].

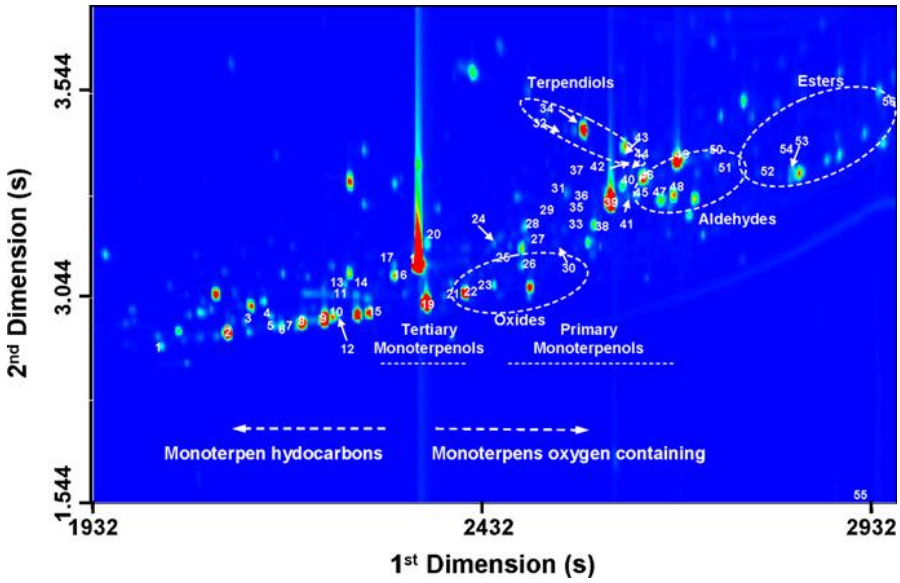

Figure 1.11. Contour plot of GCxGC extracted ion chromatogram for *m*/*z* 93, 121 and 136 obtained after submitting HS-SPME extract obtained with CW/DVB fibre coating to GCxGC-ToFMS analysis. Bands or clusters formed by structurally related compounds are emphasized [78].

An interesting application of SPME with GCxGC-ToFMS was conducted by Marriott et al., who determined the volatile compounds in Brazilian distilled cachaça by employing HS-SPME with PA fibre coating for 25 min at 60 ^{o}C [86]. The authors exploited peak apex plots with retention time coordinates of several structurally related compounds in order to study the

effects of various industrial processes on the quality of the beverage. For example, significant differences in obtained volatile profiles were detected for different processing procedures in cachaça production (Figure 1.12).

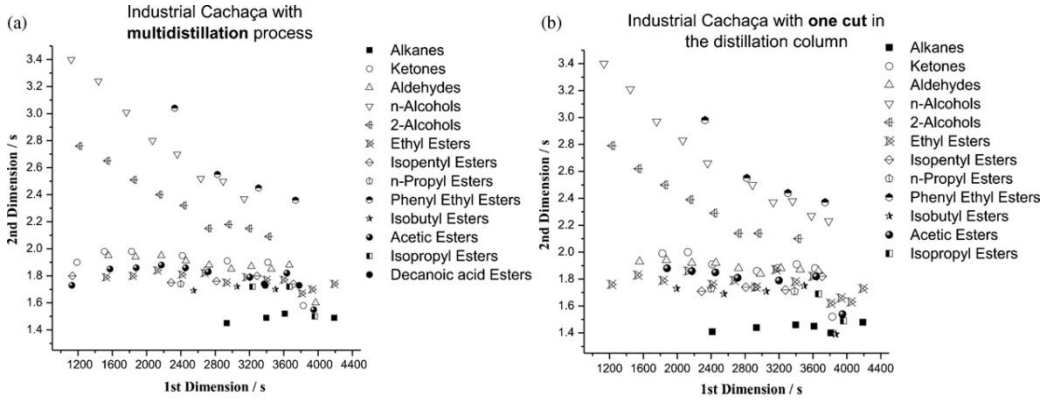

Figure 1.12. Peak apex plot interpretation for comparison of cachaça samples and their differentiation according to processing procedure. The profiles were obtained by HS-SPME performed with PA fibre coating [86].

The hyphenation of SPME and GCxGC-ToFMS has to the best of author knowledge not been reported for advanced metabolomic fingerprinting of apple samples and undoubtedly such study would benefit from this powerful multidimensional analytical approach.

1.3.4.3 *In vivo SPME*: powerful technique for metabolome collection

As a microextraction technique that features solvent-free sample preparation as one of the major prerequisites for in-field analysis, the miniaturized format of SPME along with non-exhaustive analyte recovery make SPME an ideal candidate sampling and sample preparation method for *in vivo* analysis of biological systems in their natural environments. In addition,

according to fundamental principles, the amount of analyte extracted by SPME becomes independent of sample volume under the condition of negligible depletion. Negligible depletion of analyte from sample matrix is fulfilled in the analysis of large sample volumes and/or analytes having low fibre coating/sample matrix distribution constants [94-95]. In such circumstances, when the product of K_{fs} and V_f becomes insignificant as compared to the sample volume, Equation 1.2 (Section 1.3.4), which illustrates that the number of moles of analyte extracted is proportional to the sample volume and indicates the possibility of enhancing the method sensitivity by increasing sample amount is transformed to Equation 1.4 [94-95].

$$n_e = K_{fs}\, V_f\, C_o \qquad \textbf{Equation 1.4}$$

This principle is advantageous in the context of eliminating the need of collection of defined and representative sample volume prior to analysis using an *in vitro*/*ex vivo* assay, which is a fairly difficult task when biologically relevant systems are concerned. More importantly sample volume-independence allows the measurements to be performed *in vivo*. Therefore, considering *i)* the small dimensions of the SPME probe relative to the size of many naturally occurring systems, *ii)* negligible extraction of free analyte concentration contributing to minimized invasion and *iii)* sample volume-independent enrichment factors, *in vivo* format of SPME has been explored in many interesting application areas. These research investigations include, but are not limited to determinations of environmental pollutants such as pharmaceuticals and personal-care products in tissues and biological fluids of living, freely moving animals as well as investigations on biologically active compounds in for example, plant, animal and insect emissions [140-143]. Alternatively, as several studies indicated, *in vivo* SPME approach may represent an important tool for determination of food quality traits and subsequent authentication of food products. The proceeding sections will focus

on summarizing the various application areas of *in vivo* SPME and highlighting the feasibility of such an approach in global metabolomics studies.

The quantitation of allelochemical uptake by plants is important for hypothesizing allelopathic effects, but the performance of systematic research studies in the area has been hindered by the unavailability of appropriate *in vivo* methods. In a study by Loi et al., *in vivo* SPME was employed for measurement of allelochemical uptake by tomato plants and uptake rates of exogenously applied chemicals including 1,8-cineole, camphor, menthol, coumarin and carveol were measured with PDMS fibre inserted into the stem of the test plant 1 to 72 hr after treatment application [144]. Given the dynamic nature of cineole concentrations, the authors explored temporal resolution advantages of SPME and spatial resolution of the technique revealed that the cineole concentrations in tomato stem decreased linearly with sampling height. All of these findings suggest the suitability of technique for direct measurement of compounds *in planta*. Odour gradients and patterns in grapefruit (*Citrus paradise* L.) volatile emission were sampled *in vivo* with the implementation of SPME during the whole vegetative cycle of the plant [145]. Volatile extracts were subsequently introduced into GC-MS and involvement of profile-characteristic analytes in entomophilous pollination was verified. Multivariate statistical analysis highlighted a multitude of differences in volatile emissions collected from different plant parts and developmental stages. Similarly, different volatile profiles were found in the emissions of yellow-coloured *Viola etrusca* flowers, as opposed to violet-coloured ones when PDMS fibre coating was exposed for 15 min to headspace of three living flowers inserted into a 100 mL glass conical flask [146]. Volatile and semivolatile metabolites of semiepiphytic vegetable species of the *Aristolochia ringens* Vahl were determined by sampling the flower scent with *ex vivo* and *in vivo* SPME [147]. The authors implemented HS-SPME mode with PDMS or PDMS/DVB fibre coating exposed for 30 min above 2.5 g of manually sliced fresh leaves (*ex vivo* assay) or to the headspace inside the cylinder surrounding a complete living flower. The authors found that *in vivo* extract was composed mainly of

chemicals imparting unpleasant odour such as undecanal, nonanal, decanal, and 2-methylbutanoic acid, while small molecular weight aldehydes were absent in the extract obtained using *ex vivo* assay on chopped flowers. Based on this study, it is obvious that the volatile scent emissions of damaged and live specimens differ significantly and that *in vitro* assay may not be able to representatively reveal the dynamic metabolite fluxes taking place in complex systems.

1.4 *Research objectives*

As it can be seen from the findings collected from a huge compilation of literature resources, the selection and optimization of sampling and sample preparation represent crucial aspects during the design of reliable metabolomics workflow. In the context of plant metabolomics, the requirements of sample collection at the natural location site of a biological system are of utmost importance and the performance of harvesting itself may adversely affect the representativeness of metabolome. Hence, even the very initial step of sample collection can lead to enzymatic degradation, oxidation and metabolism perturbation. Subsequent steps associated with metabolism quenching in liquid nitrogen which represents the most popular metabolism quenching step in plant metabolomics, are not free of limitations that impose serious threat to obtaining the instantaneous snapshot of true metabolome. Issues associated with metabolite losses, degradation, inter-metabolite conversions and failure of preserving metabolite identity during transportation, storage, homogenization and extraction process itself are well documented. Therefore and in consideration with limitations of current volatile collection methods, the objective of the current project is implementation of *in vivo* SPME and exploitation of its miniaturized format, on-site compatibility and consequent eliminated perturbation toward investigated metabolomics system in metabolomics profiling of apples. The technique, hyphenated to GCxGC-

ToFMS was exploited in the area of advanced metabolic fingerprinting for the purposes of identifying the SPME route toward comprehensive characterization of representative and true metabolome. This is the first report describing the employment, utility and feasibility of *in vivo* DI-SPME sampling assay in global and high-resolution profiling of plant metabolome and the first report on hyphenation of *in vivo* DI-SPME with GCxGC-ToFMS. The extraction selectivity and sensitivity performance characteristics of commercial SPME coatings were first evaluated and their limitations in analysis of complex food samples identified. Following the development of extraction and GCxGC protocols, the *in vivo* SPME implementation on-site was followed by a series of comparative studies on metabolome coverage and analytical precision between *in vivo* and *ex vivo* sampling assays. The latter sampling protocol was performed with employment of a suitable metabolism quenching step, so that the metabolome coverage is not biased against metabolite groups that are affected by factors arising when metabolic and enzymatic activity is not terminated. High-resolution metabolite fingerprinting and profiling of the 'Honeycrisp' apple cultivar at various stages of maturity were facilitated, as the biochemical changes in fruits and crops during ripening and development have a pronounced effect on a variety of food quality traits.

2. Experimental conditions

2.1 *Systematic evaluation of performance characteristics of commercial SPME coatings in analysis of spiked water samples*

2.1.1 *Chemicals and materials*

HPLC grade methanol and acetone were obtained from Caledon Laboratories (Georgetown, Canada). Analyte standards were obtained from Sigma-Aldrich (Oakville, Canada) and they were all of purity > 97% (except for > 95% purity for heptanal, nonanal, citral isomers, farnesol isomers, dodecanal, tridecanal and linalool). Commercial SPME fibre assemblies in 23-gauge needle sizes and automated formats (100 µm PDMS (fused silica), 85 µm PA (fused silica), 60 µm CW (metal), 65 µm PDMS/DVB (stableflex), 85 µm CAR/PDMS (stableflex), 50/30 µm DVB/CAR/PDMS (stableflex) and 16 µm carbopack Z/PDMS (metal)) were obtained from Supelco (Oakville, Canada). Automated SPME holder and 10- and 20 mL screw cap vials were purchased from Supelco (Oakville, Canada).

2.1.2 *Standards and samples preparation*

Stock individual solutions of target metabolites were prepared in acetone and methanol, followed by preparation of a spiking standard mixture in methanol. The concentrations of metabolites in the standard mixture were carefully adjusted to reach the compromise between the following effects: *i)* eliminate overloading of second dimension column/modulator when using highly selective fibres; *ii)* enhance amount extracted for poorly selective fibres and *iii)* not exceed aqueous solubility of the metabolites (with the exception of farnesenes, ethyl palmitate, ethyl stearate and 1-heptadecanol). Stock solutions and spiking mixture were stored at – 30 ^{o}C and protected from light. Extraction

standards were prepared by spiking 4 µL of the metabolite mixture in 3 mL nano pure water (purified to 18.3 MΩ quality level using NANOpure water system from Barnstead International (Dubuque, USA)), placed in 10 mL amber screw cap vials. The liquid injection standards were prepared in methanol from individual stock solutions and a series of dilutions (stored at – 30 ^{o}C and protected from light) at 15 concentration levels (0.5, 1, 2.5, 5, 10, 25, 50, 100, 250, 500, 1000, 2500, 5000, 10000, 20000 ng/mL). Out of this range of calibration curve standards, appropriate calibration points were used to calibrate each individual obtained SPME response to mass extracted in pg.

2.1.3 *SPME procedure*

Coatings were conditioned according to the manufacturer's recommendations and they were pre-conditioned before usage at the appropriate desorption temperature for 10 min. The extraction standards were prepared and analyzed fresh by HS-SPME at 30 ^{o}C and 500 rpm agitation speed and using 15 min and 60 min incubation and extraction times, respectively (triplicate analysis per each coating type). Desorption was performed for 10 min in splitless mode at a desorption temperature set at 5 ^{o}C lower setpoint than maximum recommended coating temperature. The desorption efficiency was tested by sealing the needle of the SPME assembly with a Teflon cap immediately after the performance of initial extraction-desorption cycle, keeping it at 5 ^{o}C and injecting after GC ready status initiation (triplicate analysis per coating type). In addition to 60 min extraction, 90 min extraction time was employed in order to assess whether an equilibrium state has been achieved and to properly interpret SPME enrichment data.

2.1.4 *GCxGC-ToFMS equipment, analysis conditions and data processing specifications*

The instrument employed in this study was a LECO Pegasus 4D GCxGC-ToFMS system equipped with Agilent 6890N GC and high-speed ToF mass spectrometer (LECO, St. Joseph, MI, USA). The instrument was also equipped with a dual-stage quad-jet cryogenic modulator (licensed from Zoex, Houston, TX, USA) and a MultiPurpose Sampler (MPS 2) autosampler (Gerstel GmbH, Mulheim an der Ruhr, Germany). The primary and secondary dimension columns employed were Rxi-5SilMS (30 m x 0.25 mm ID x 0.25 µm) and Supelcowax (1.15 m x 0.10 mm ID x 0.10 µm) from Restek (Bellefonte, PA, USA) and Supelco (Bellefonte, PA, USA), respectively. The GC injector was equipped with 0.75 mm internal diameter narrow-bore liner available from Supelco (Oakville, Canada) and high-pressure Merlin Microseal septumless injection kit from Merlin Instrument Co. (Half Moon Bay, CA, USA). Carrier gas was helium at 1.5 mL/min and 31.5 mL/min after purge flow activation (10 min) flow rates. The primary dimension oven temperature programming was set at 35 ^{o}C (5 min), 3 ^{o}C/min rate to 245 ^{o}C (3 min), while the secondary oven programming was equivalent except for the 15 ^{o}C oven temperature offset above the primary oven. The modulation parameters consisted of modulator temperature offset of 35 ^{o}C, 3 s modulation period, 0.6 s hot pulse time and 0.9 s cool time. The transfer line and ion source temperatures were set to 240 and 220 ^{o}C, respectively. The mass spectrometer was operated in electron ionization mode with mass acquisition range 33-450 u, 200 spectra/s acquisition rate and 1650 V detector voltage. Data acquisition and processing were performed with ChromaTOF (version 4.24) software, with S/N threshold for peak finding of 50 and automated National Institute of Standards and Technology (NIST, version 2.05) Terpene and Wiley 8 library searching procedure.

2.2 *Ex vivo headspace solid phase microextraction coupled with comprehensive two-dimensional gas chromatography – time-of-flight mass spectrometry for metabolite profiling in apples: Implementation of GCxGC structured separations for optimization of SPME procedure in complex samples*

2.2.1 *Analytical reagents and supplies*

Commercially available SPME fibre assemblies in 23-gauge needle sizes and automated formats (100 µm polydimethylsiloxane (PDMS) [fused silica], 85 µm polyacrylate (PA) [fused silica], 60 µm carbowax (CW) [metal], 65 µm polydimethylsiloxane/divinylbenzene (PDMS/DVB) [stableflex], 85 µm carboxen/polydimethylsiloxane (CAR/PDMS) [stableflex], 50/30 µm divinylbenzene/carboxen/polydimethylsiloxane (DVB/CAR/PDMS) [stableflex] and 16 µm carbopack Z/PDMS [metal]) were purchased from Supelco (Oakville, Canada). Ten and 20 mL screw cap vials and an automated SPME holder were obtained from Supelco.

2.2.2 *Samples and sample preparation*

The determination of experimental linear temperature-programmed retention indices (RI) in the first dimension was carried out by analysing aqueous standards spiked with 52 metabolites (sample preparation conditions already summarized in Section 2.1.2), including straight chain hydrocarbons C_8-C_{19}. 'Honeycrisp' apples (with a diameter of approximately 6-7 cm), were harvested on September 14, 2010 at 20 ^{o}C from a mature commercial orchard in Simcoe (Norfolk County), Ontario, Canada. Immediately after harvesting, the metabolism quenching step was performed by soaking the fruit in liquid nitrogen followed by the storing of apples in dry ice (-70 ^{o}C) during

transportation to the laboratory. In the laboratory, individual fruit were rinsed with distilled water and dried with Kim Wipe, followed by apple core removal and slicing of the frozen fruit in random positions from all possible sides of the fruit cortex. One hundred grams of disrupted frozen apple tissue was submitted to 250 mL of saturated sodium chloride solution (providing an additional metabolism quenching step, termination of enzymatic activity and decrease in the aqueous solubility, leading to potential enhancement of SPME enrichment factors for selected compounds), followed by 1.5 min homogenization. Subsequently, an additional 250 mL aliquot of nano pure water was added to the homogenate followed by the introduction of an additional 1 min homogenization period. This was performed to lead to a more enhanced release of metabolites during extraction and decreased matrix effects. The final homogenate was transferred into 20 mL vials (protected from light) which were stored in freezer at – 30 ^{o}C until the time of analysis when they were thawed individually in a temperature controlled water bath maintained at 30 ^{o}C for 20 min. Three mL portions of thawed homogenate were transferred into 10 mL screw-cap amber vials and submitted to HS-SPME procedure.

2.2.3 *SPME methodology*

Commercially available SPME coatings were conditioned as *per* the manufacturer recommendations and were also preconditioned at the appropriate desorption temperature for 10 min prior to the start of the relevant analysis sequence. The aqueous RI standards and apple samples were submitted to 5 min and 60 min incubation and extraction procedures, respectively, using HS-SPME extraction mode at 30 ^{o}C sample temperature and 500 rpm agitation speed (triplicate analysis per fibre coating). Desorption was performed for 10 min in splitless mode at a desorption temperature set at a 5 ^{o}C lower set point than the maximum recommended coating temperature in order to allow for better desorption efficiency of higher molecular weight and/or analytes having higher

affinity for the relevant polymeric coating. For the analysis of real apple samples with DVB/CAR/PDMS coating, 25 min splitless desorption at 270 ^{o}C was used.

2.2.4 *GCxGC-ToFMS equipment and analysis conditions*

LECO Pegasus 4D GCxGC-ToFMS system equipped with Agilent 6890N GC and high speed ToF mass spectrometer (LECO, St. Joseph, MI, USA) was employed in the study. Modulation was performed with dual-stage quad-jet cryogenic modulator (licensed from Zoex, Houston, TX, USA) and a MultiPurpose Sampler (MPS 2) autosampler was used for automation of SPME procedure (Gerstel GmbH, Mulheim an der Ruhr, Germany). In order to assure a substantially different separation principle in the second dimension, two column ensembles were tested during the optimization of GCxGC-ToFMS conditions and they both consisted of 5% diphenyl 95% dimethylpolysiloxane Rxi-5SilMS (30 m x 0.25 mm internal diameter x 0.25 µm film thickness) capillary column (Restek, Bellefonte, PA, USA) in the first dimension coupled to either medium-polar 50% phenyl methylpolysiloxane DB-17 (Agilent Technologies, CA, USA) or polar polyethylene glycol Supelcowax (Supelco, Bellefonte, PA, USA) and BP 20 (SGE Incorporated, Austin, USA) second dimension columns (dimensions 1.12 m x 0.10 mm internal diameter x 0.10 µm film thickness). Helium was the carrier gas used at 1.5 mL/min and 31.5 mL/min after purge flow activation (10 min) flow rates. The GC injector was kept at 270 ^{o}C and was equipped with a high-pressure Merlin Microseal septumless injection kit purchased from Merlin Instrument Co. (Half Moon Bay, CA, USA) and 0.75 mm internal diameter liner available from Supelco (Oakville, Canada) for optimum desorption efficiency. The primary dimension temperature programming was initiated at 40 ^{o}C (5 min hold), followed by 3 ^{o}C/min rate to 240 ^{o}C (10 min hold), while the secondary oven programming was equivalent except for the 10 ^{o}C oven temperature offset above the primary

oven. Modulator temperature offset was set to 30 ^{o}C and additional modulation parameters consisted of a 5 s modulation period (1 s hot pulse time and 1.5 s cool time). The transfer line temperature and ion source temperature were set to 240 ^{o}C and 220 ^{o}C, respectively. The mass spectrometer was operated in EI mode with mass acquisition range 33-550 u, 200 spectra/s acquisition rate and 1700 V detector voltage. Data acquisition and processing were performed with ChromaTOF (version 4.24) software with S/N threshold for peak finding of 50, unless specified otherwise followed by manual inspection of generated peak tables as described in the results and discussion section. Automated library searching procedure employed National Institute of Standards and Technology (NIST, version 2.05), Terpene and Wiley 8 commercial mass spectral libraries. For peak apex plot data presentation, the tables generated by ChromaTOF software were manually filtered taking into account system blanks and mass spectral similarity. Consequently, the retention time coordinates of true metabolite features were included in apex plots and used for further data interpretation.

2.3 *Ex vivo headspace and direct immersion solid phase microextraction in advanced metabolite fingerprinting of apples*

Refer to Sections 2.2.1, 2.2.2, 2.2.3 and 2.2.4 for information on analytical reagents used, sample preparation, SPME extraction conditions and GCxGC-ToFMS analysis conditions. For comparison purposes, water sample analysis was also submitted to one-dimensional GC-ToFMS carried out under equivalent conditions, except for disabled modulation and employment of 3 spectra/s acquisition rate for data collection. Extraction time uptakes for HS-SPME analysis were conducted on freshly prepared samples at a series of time points including 1, 5, 15, 30, 60, 120 and 180 min. Direct immersion SPME was performed by transferring 10 mL portions of thawed homogenate into 10 mL screw-cap amber vials and submitting homogenate to 5 min incubation and 60

min extraction at 30 ^{o}C. Direct extraction was followed by a brief immersion of SPME phase into 10 mL of nano pure water prior to desorption to remove interferences from the coating surface that could potentially adversely affect SPME coating lifetime, extraction efficiency, repeatability and integrity of investigated extracts.

2.4 *In vivo SPME sampling: determination of analytical precision and metabolite coverage of the analytical platform*

2.4.1 *Sampling and sample preparation*

The *ex vivo* assay for HS-SPME and DI-SPME analyses conducted for comparative purposes was following the procedure from Section 2.2.2 (HS-SPME analysis and metabolism quenching) and Section 2.3 (DI-SPME analysis). The *ex vivo* HS- and DI-SPME analyses were performed on the same apples that were sampled *in vivo* and quenched in metabolism after *in vivo* extraction in order to draw comparisons in terms of metabolite coverage. Following metabolism quenching steps described in Section 2.2.2, the final homogenate was transferred into 20 mL vials (protected from light) which were stored in a freezer at – 30 ^{o}C until the time of analysis when they were thawed in a temperature controlled water bath maintained at 30 ^{o}C for 20 min (October 2009 and September 2010 sampling, as samples were not analyzed fresh due to delays caused by GCxGC-ToFMS instrumental problems). Alternatively, following metabolism quenching steps described in Section 2.2.2, the final homogenate was transferred into 20 mL vials (protected from light) which were either immediately analyzed without freezing and thawing processes or depending on instrument wait time were kept frozen at – 70 ^{o}C before thawing and SPME extraction (September 2011 sampling).

The preparations for *in vivo* sampling started with conditioning of SPME fibre coatings as per the supplier recommendation. Prior to sampling, additional 5 min conditioning was performed for each fibre coating, followed by sealing of needles of SPME assemblies with the Teflon caps. The plunger of SPME assemblies was marked with 1.3 cm total distance which was designed to incorporate 0.3 cm of plunger exposure and exposure of 1 cm long coating. The sampling depth of 3 cm was marked on the needle of SPME fibre assembly with a piece of septum. After penetrating the apple tissue with 3 cm distance, the needle of each fibre assembly was withdrawn by 1.5 cm, leaving 1.5 cm safe distance for exposure of coating and plunger past the tip of the needle. Subsequently, the 1.3 cm mark on the plunger was followed to expose a 1 cm long coating and 0.3 cm length of plunger. In sampling of a particular apple, the sampling sequence started with penetration of all three needles and was followed by 1.5 cm withdrawal length and after withdrawal, the three coatings were exposed for 60 min long extraction process. Following the extraction, a brief dipping wash step in water solution was implemented, coatings were wiped by kim wipes, and withdrawn into needles, which were then sealed with Teflon cap (October 2009 and September 2010 sampling). For sampling conducted in harvesting year 2011, after extraction, coatings were wiped with kim wipe, exposed to aqueous solution for 10 s and wiped with kim wipe again. Following the withdrawal of coatings into respective needles, Teflon caps were placed onto the needle tips. All coatings were stored in dry ice at – 70 ^{o}C during transportation. Upon arrival to the laboratory, fibre coatings were stored in freezer at – 30 ^{o}C before analysis (October 2009 and September 2010 sampling) and analysis of fresh extracts was not possible because of GCxGC-ToFMS instrumental problems. However in September 2011 sampling season, immediately after arrival to the laboratory, the extracts were submitted to GCxGC-ToFMS analysis.

The sampling in year 2009, which was the very first sampling conducted was performed on October 8, 2009 when the in-field temperature was 16 ^{o}C. Intra-fruit repeatability was assessed by penetrating three SPME fibre coatings

into apple cortex from directions that were perpendicular with respect to the fruit stem. The coatings were kept as far as possible from each other as to allow metabolome sampling from three distinct sides of apple fruit.

The sampling in harvesting year 2010 was performed on September 14, 2010 when the in-field temperature was ranging from 24 ^{o}C at the beginning of sampling to 21 ^{o}C at the end of experiment. In harvesting year 2011, the sampling was done on September 23, 2011 and temperature on the site of sampling was 18 ^{o}C. In September 2010 and 2011 samplings, the three coatings employed in extractions of apple metabolome were placed close to each other and small inter-fibre distance of 1.5 cm was implemented. All sampling positions were facing west during sampling design carried out in 2010 and were facing east during sampling that was conducted in 2011. In total, during sampling conducted in September 2010, five apples of earlier harvest maturity (HC-O apples with codes 1-5) and 5 apples of later harvest maturity (HC-L apples with codes 1-5) were sampled with triplicate analysis per apple. HC-L apple coded with number 1 was used for comparative studies between *ex vivo* and *in vivo* assays in terms of metabolite coverage. On the other hand, HC-O-2-5 and HC-L-2-5 apples were employed in statistical interpretation of data in order to elucidate differences in metabolome as a result of harvest maturity.

2.4.2 *GCxGC-ToFMS conditions for analysis of in vivo SPME extracts*

Following 2009 sampling, the samples were submitted to the following GCxGC-ToFMS procedure. The primary and secondary dimension columns employed were Rxi-5SilMS (30 m x 0.25 mm ID x 0.25 µm) and Supelcowax (1.06 m x 0.10 mm ID x 0.10 µm) from Restek (Bellefonte, PA, USA) and Supelco (Bellefonte, PA, USA), respectively. The GC injector was kept at 265 ^{o}C and was equipped with 0.75 mm internal diameter narrow-bore liner available from Supelco (Oakville, Canada) and high-pressure Merlin Microseal septumless injection kit from Merlin Instrument Co. (Half Moon Bay, CA,

USA). Carrier gas was helium at 1.0 mL/min and 31 mL/min rates after purge flow activation (5 min). The primary dimension oven temperature programming was set at 35 ^{o}C (5 min), 3 ^{o}C/min rate to 245 ^{o}C (5 min), while secondary oven programming was equivalent except for the 10 ^{o}C oven temperature offset above primary oven. The modulation parameters consisted of modulator temperature offset of 35 ^{o}C, 3 s modulation period, 0.6 s hot pulse time and 0.9 s cool time. The transfer line and ion source temperatures were set to 260 and 220 ^{o}C, respectively. The mass spectrometer was operated in electron ionization mode with mass acquisition range 33-550 u, 200 spectra/s acquisition rate and 1625 V detector voltage. Data acquisition and processing were performed with ChromaTOF (version 4.24) software and automated National Institute of Standards and Technology (NIST, version 2.05) Terpene and Wiley 8 library searching procedure.

Following 2010 sampling, the samples intended for comparative studies between metabolome obtained in *ex vivo* and *in vivo* (HC-O-1 and HC-L-1) assays were submitted to GCxGC-ToFMS procedure outlined in Section 2.2.4. On the other hand, *in vivo* extracts corresponding to HC-O-2-5 and HC-L-2-5 and intended for statistical interpretation of data were analyzed on a different GCxGC setup. The primary and secondary dimension columns employed were Rxi-5SilMS (30 m x 0.25 mm ID x 0.25 µm) and Stabilwax (1 m x 0.25 mm ID x 0.25 µm) both from Restek (Bellefonte, PA, USA). The GC injector was kept at 270 ^{o}C and was equipped with 0.75 mm internal diameter narrow-bore liner available from Supelco (Oakville, Canada) and high-pressure Merlin Microseal septumless injection kit from Merlin Instrument Co. (Half Moon Bay, CA, USA). Carrier gas was helium at 2.0 mL/min and 32 mL/min after purge flow activation (25 min) flow rates. The primary dimension oven temperature programming was set at 40 ^{o}C (5 min), 5 ^{o}C/min rate to 235 ^{o}C (10 min), while the secondary oven programming was equivalent except for the 20 ^{o}C oven temperature offset above the primary oven. The modulation parameters consisted of modulator temperature offset of 25 ^{o}C, 3.5 s modulation period, 0.7 s hot pulse time and 1.05 s cool time. The transfer line and ion source

temperatures were set to 240 and 220 ^{o}C, respectively. The mass spectrometer was operated in electron ionization mode with mass acquisition range 33-550 u, 200 spectra/s acquisition rate and 1700 V detector voltage. Data acquisition and processing were performed with ChromaTOF (version 4.24) software and automated National Institute of Standards and Technology (NIST, version 2.05) Terpene and Wiley 8 library searching procedure.

Following sampling in September 2011, the following GCxGC conditions were employed. The primary and secondary dimension columns employed were Rxi-5SilMS (30 m x 0.25 mm ID x 0.25 µm) and BP 20 (1.11 m x 0.10 mm ID x 0.10 µm) from Restek (Bellefonte, PA, USA) and SGE Incorporated (Austin, USA), respectively. The GC injector was kept at 270 ^{o}C and was equipped with 0.75 mm internal diameter narrow-bore liner available from Supelco (Oakville, Canada) and high-pressure Merlin Microseal septumless injection kit from Merlin Instrument Co. (Half Moon Bay, CA, USA). Carrier gas was helium at 1.5 mL/min and 31.5 mL/min after purge flow activation (25 min) flow rates. The primary dimension oven temperature programming was set at 40 ^{o}C (5 min), 5 ^{o}C/min rate to 250 ^{o}C (10 min), while the secondary oven programming was equivalent except for the 10 ^{o}C oven temperature offset above the primary oven. The modulation parameters consisted of modulator temperature offset of 30 ^{o}C, 4 s modulation period, 0.8 s hot pulse time and 1.20 s cool time. The transfer line and ion source temperatures were set to 240 and 220 ^{o}C, respectively. The mass spectrometer was operated in electron ionization mode with mass acquisition range 33-550 u, 250 spectra/s acquisition rate and 1750 V detector voltage. Data acquisition and processing were performed with ChromaTOF (version 4.24) software and automated National Institute of Standards and Technology (NIST, version 2.05) Terpene and Wiley 8 library searching procedure.

3. Systematic evaluation of performance characteristics of commercial SPME coatings in analysis of spiked water samples: results and interpretation of data

3.1 *Background and objectives of research*

Fibre coating/sample matrix distribution constant (K_{fs}) is a physicochemical constant (dependent on sample temperature, ionic strength and organic solvent composition) that governs enrichment factors achievable by SPME as well as extraction selectivity [94,110]. In order to 'tune' both extraction sensitivity and selectivity, Supelco has been offering a wide range of commercially available SPME assemblies, including: *i)* liquid absorbents (polydimethylsiloxane (PDMS), polyacrylate (PA) and carbowax (CW)) and *ii)* solid adsorbents (polydimethylsiloxane/divinylbenzene (PDMS/DVB), divinylbenzene/carboxen/polydimethylsiloxane (DVB/CAR/PDMS), carboxen/polydimethylsiloxane (CAR/PDMS) and carbopack Z/polydimethylsiloxane (carbopack Z/PDMS)). Considering that the introduction of solid sorbents has offered significant advantages in terms of improved sorbent strength, extraction capacity as well as the retention capability for volatile analytes, the determination of relevant K_{fs} values for as many compounds as possible is a must [104,118]. However, the adsorption mechanism of extraction requires that solid extraction phase surface concentration (S_e) of adsorbed analytes is considered rather than the extraction phase concentration [95]. Therefore, the calculation of K_{fs} for SPME adsorbents requires the determination of S_e values or alternatively since S_e can be expressed as the ratio of amount extracted and the active surface of the fibre coating (S_a), the knowledge of S_a constants which are quite tedious to determine experimentally [148]. Therefore, a new constant, termed fibre constant, f_c representing the products $K_{fs}V_f$ and $K_{fs}S_a$ for liquid and solid sorbents,

respectively has been introduced for the estimation of SPME enrichment factors at equilibrium [148]. f_c can be represented by Equations 3.1 and 3.2 for DI-SPME and HS-SPME modes of extraction, respectively:

$$f_c = \frac{n_e V_s}{V_s C_o - n_e} \qquad \text{Equation 3.1}$$

$$f_c = \frac{n_e K_{hs} V_h + n_e V_s}{V_s C_o - n_e} \qquad \text{Equation 3.2}$$

Besides the existence of basic guidelines including the use of PDMS for nonpolar chemicals and the use of PA and CW for polar analytes, so far solid SPME coatings have not been comprehensively evaluated for their suitability in extraction of organic compounds constituting a diverse spectrum of molecular weights, volatility and polarity characteristics. Such systematic evaluations are of utmost importance for allowing a *priori* judgment of a suitability of particular SPME extraction phase(s) for particular analyte(s)/application(s) of interest. For example, studies requiring determination of molecular weight thresholds where the choice of particular solid coating provides best retention capacity and simultaneous effective removal of analytes during thermal desorption are lacking in current SPME literature. In fact, a review of recent SPME literature suggests that the choice of the fibre coating is frequently based on trial and error, analytical intuition or alternatively a majority of published studies involve preliminary experimental setups focused on SPME coating selection, which is time-consuming, costly, considering the need for fibre availability, and misleading [149-153]. The latter comment is mainly associated with the inconsistency in published data due to several factors, such as *i)* variations in experimental extraction, desorption and analysis conditions, *ii)* improper experimental designs for coating selection experiments, and *iii)* inclusion of small analyte sets such that the main turning points cannot be identified [153].

The current investigation addresses the requirement for systematic evaluation of SPME coatings by considering a wide analyte set composed of 52 components frequently encountered in food and environmental samples and utilizing GCxGC-ToFMS instrumental set-up. The analytes considered belong to several homologous groups of compounds (*n*-alkanes, ethyl esters, aldehydes, 2-ketones, 1-alcohols, 2-alcohols, terpene hydrocarbons and oxygenated terpenes) and were selected on the basis of meeting the following criteria: *i)* wide range of physicochemical properties (log K_{ow} range 1.26-8.72), *ii)* amenability to GC analysis, *iii)* occupation of a wide range of primary and secondary dimension retention times on orthogonal GCxGC setup, and *iv)* reasonable chemical diversity leading to potential identification of analyte structure-SPME enrichment relationships. To this end, seven commercially available SPME coatings were compared in terms of extraction capacity (fibre constants), extraction selectivity and desorption efficiency. The current investigation is unique as compared to existing published data since it provides for the first time the most comprehensive evaluation of existing coatings including solid sorbents that were characterized in terms of molecular weight-SPME extraction efficiency relationships and desorption efficiency when high molecular weight and strongly retained analytes come in contact with strong sorbent. Finally, DVB/CAR/PDMS coating providing the optimum extraction coverage and sensitivity for widest molecular weight range exploited in targeted-metabolite mix was used for determination of linear dynamic range (LDR) to assess the feasibility of its use in quantitative metabolomics studies.

3.2 *Target metabolites and their physicochemical properties*

Target metabolite names along with their physicochemical properties, chromatographic and mass spectrometric data (including retention times in primary and secondary dimension, experimental and literature RI in first

dimension, molecular weight, boiling point, log K_{ow}, EI fragmentation pattern and quantification ion) are presented in Table 3.1 and Table 3.2. These metabolites belong to a diverse chemical functionality set (MW range 88.15-312.54 g/mol, boiling point range 115.64-360.59 ^{o}C, log K_{ow} range 1.26-8.72) and in addition to these properties were chosen on the basis of their occurrence in volatile metabolome profiles.

Table 3.1. Target metabolite names and chromatographic properties on Rxi-5SilMS/ Supelcowax column ensemble. Literature RI data was obtained from references [81,86,154-155].

functional group	analyte name	$^{1}t_R$; s	$^{2}t_R$; s	RI; exp	RI; lit
Alkanes	octane	642	0.655	800	800
	nonane	960	0.655	900	900
	undecane	1605	0.665	1100	1100
	tridecane	2178	0.655	1300	1300
monoterpene hydrocarbons	*alpha*-pinene	1065	0.705	932	933
	limonene	1380	0.805	1029	1030
sesquiterpene hydrocarbons	(*Z*)-*β*-farnesene	2505	0.810	1426	1439
	(*E*)-*β*-farnesene	2568	0.825	1451	1452
	(*E,E*)-*α*-farnesene	2694	0.850	1503	1504
2-ketones	2-hexanone	606	1.095	787	na
	2-heptanone	924	1.095	888	898
	2-nonanone	1569	1.030	1090	1093
	2-undecanone	2151	0.980	1291	1294
	2-tridecanone	2670	0.950	1493	1495
	2-pentadecanone	3132	0.935	1696	1697
	2-heptadecanone	3549	0.920	1899	1906
Aldehydes	hexanal	639	1.065	800	801
	heptanal	963	1.065	901	906
	octanal	1296	1.035	1002	1006
	nonanal	1614	1.000	1103	1107
	undecanal	2193	0.960	1307	1309
	dodecanal	2457	0.955	1407	1410
	tridecanal	2709	0.955	1509	1516
ethyl esters	ethyl butanoate	645	0.910	801	na
	ethyl heptanoate	1590	0.885	1096	1101
	ethyl nonanoate	2160	0.865	1295	1297
	ethyl undecanoate	2667	0.855	1493	1498

	ethyl tridecanoate	3120	0.845	1692	1700
	ethyl palmitate	3723	0.835	1991	1993
	ethyl stearate	4083	0.850	na	na
1-alcohols	**1-pentanol**	552	2.455	766	759
	1-heptanol	1191	1.995	971	970
	1-nonanol	1815	1.590	1172	1176
	1-undecanol	2367	1.380	1373	1379
	1-tridecanol	2859	1.245	1575	1580
	1-pentadecanol	3303	1.165	1779	1784
	1-heptadecanol	3708	1.115	1981	1981
2-alcohols	**2-pentanol**	390	1.675	702	700
	2-hexanol	648	1.780	803	802
	2-octanol	1293	1.485	1002	1004
	2-dodecanol	2442	1.140	1401	1417
	2-hexadecanol	3360	1.015	1806	na
monoterpene ketones	**(*R*)-(-)-carvone**	2019	1.590	1243	1246
monoterpene aldehydes	***cis*-citral; neral**	2001	1.395	1237	1238
	***trans*-citral; geranial**	2085	1.435	1266	1268
monoterpene oxides	**eucalyptol**	1389	0.810	1031	1032
	***cis*-linalool oxide**	1509	1.225	1070	1069
	***trans*-linalool oxide**	1560	1.255	1086	1086
monoterpene alcohols	**linalool**	1599	1.485	1099	1101
	***trans*-geraniol**	2037	2.065	1250	1255
sesquiterpene alcohols	***cis, trans*-farnesol**	3120	1.555	1692	na
	(*Z,Z*)-farnesol	3171	1.550	1716	1716

Table 3.2. Target metabolite names, physicochemical properties and mass spectrometric data. Physicochemical properties were obtained from reference [156].

analyte name	EI fragmentation	*m/z*	MW; g/mol	log K_{ow}	BPT; °C
octane	43, 85, 57	57	114.230	5.18	119.87
nonane	43, 57, 85	57	128.260	5.65	142.69
undecane	43, 57, 85	57	156.310	5.74	185.61
tridecane	43, 57, 85	57	184.370	6.73	224.91
***alpha*-pinene**	93, 77, 121	93	136.240	4.44	157.25
limonene	68, 93, 136	68	136.240	4.58	167.66
(*Z*)-β-farnesene	69, 93, 133	69	204.400	7.17	254.57

(*E*)-β-farnesene	69, 93, 133	69	204.400	7.17	254.57
(*E,E*)-*a*-farnesene	93, 69, 107	93	204.400	7.10	261.11
2-hexanone	43, 58, 100	58	100.160	1.38	118.79
2-heptanone	43, 58, 71	58	114.190	1.98	141.64
2-nonanone	58, 43, 71	58	142.240	3.14	184.65
2-undecanone	58, 43, 71	58	170.300	4.09	224.03
2-tridecanone	58, 43, 71	96	198.350	4.68	259.80
2-pentadecanone	43, 58, 71	58	226.400	5.66	291.95
2-heptadecanone	43, 58, 71	58	254.450	6.64	320.49
hexanal	44, 56, 57, 72	56	100.160	1.78	132.20
heptanal	70, 55, 57, 96	70	114.190	2.29	154.53
octanal	41, 57, 84	57	128.220	2.78	175.95
nonanal	57, 70, 98	57	142.240	3.27	196.48
undecanal	41, 57, 82	57	170.300	4.25	234.81
dodecanal	57, 82, 96	57	184.320	4.75	252.62
tridecanal	57, 82, 96	57	198.350	5.24	269.53
ethyl butanoate	71, 88, 60	88	116.160	1.85	125.79
ethyl heptanoate	88, 60, 113	88	158.240	3.32	190.83
ethyl nonanoate	88, 60, 101	88	186.300	4.30	229.67
ethyl undecanoate	88, 101, 60	115	214.350	5.28	264.89
ethyl tridecanoate	88, 101, 60	88	242.400	6.27	296.50
ethyl palmitate	88, 101, 157	88	284.480	7.74	337.13
ethyl stearate	88, 101, 157	88	312.540	8.72	360.59
1-pentanol	42, 55, 70	55	88.150	1.33	136.95
1-heptanol	41, 70, 55	55	116.200	2.31	180.33
1-nonanol	41, 55, 70, 98	55	144.250	3.30	220.09
1-undecanol	55, 69, 83	55	172.310	4.28	256.24
1-tridecanol	55, 69, 97	55	200.370	5.26	288.77
1-pentadecanol	43, 55, 69, 97	55	228.420	6.24	317.69
1-heptadecanol	55, 69, 97	70	256.470	7.23	342.98
2-pentanol	45, 55, 73	45	88.150	1.26	115.64
2-hexanol	45, 55, 69	45	102.180	1.75	138.62
2-octanol	45, 55, 69	45	130.230	2.73	181.87
2-dodecanol	45, 55, 69	45	186.340	4.70	257.51
2-hexadecanol	45, 55, 69	45	242.450	6.66	318.68
(*R*)-(-)-carvone	82, 54, 93	82	150.220	2.27	230.5 [a]
***cis*-citral; neral**	41, 69, 109	69	152.240	3.45	217.44
***trans*-citral; geranial**	69, 41, 109	69	152.240	3.45	217.44
eucalyptol	43, 111, 93	111	154.250	2.82	174 [a]
***cis*-linalool oxide**	59, 93, 111	59	170.250	1.99	218.99
***trans*-linalool oxide**	59, 93, 111	59	170.250	1.99	218.99
linalool	71, 55, 93, 121	93	154.250	3.38	204.05
***trans*-geraniol**	69, 55, 93	69	154.250	3.47	239.89
***cis, trans*-farnesol**	69, 41, 93	69	222.370	5.77	319.11

(Z,Z)-farnesol	69, 41, 93	69	222.370	5.77	319.11

3.3 *Rationale behind the experimental setup*

As mentioned, the investigated model system for commercial coating comparison consisted of spiked water samples and eliminated matrix effects in order to effectively study extraction phase-analyte relationships and eliminate the influences of analyte transport mechanisms through and/or binding affinity to different phases in complex sample matrices. The experimental setup involved the use of automated sample preparation conditions, in particular 500 rotations per minute (rpm) agitation speed setting of MPS 2 autosampler considering that this condition has been standardized as to not allow significant amount of stress on SPME fibre assembly [119,157]. The selected sample preparation conditions were mild (employment of 40 and 30 ^{o}C sample temperatures) and sub-optimum in terms of extraction efficiency for some of the target analytes, however, they were considered optimum when it comes to representativeness of sample extracts (reduction in artifact production during extraction), which is a critical requirement in rapidly growing metabolomics field [81,101]. Under these conditions, mostly two to three highest molecular weight analogues of each homologous series did not reach equilibrium within 60 min and as longer extraction times were not feasible considering the poor robustness of employed GCxGC-ToFMS instrument and from practical considerations as they outweigh any gain in analytical sensitivity, their reported fibre constants can be considered 'apparent'. While extraction time was selected to allow high-throughput analysis, desorption was carried out at desorption temperature set at value 5 ^{o}C lower than the maximum recommended fibre operating temperature as to allow for more complete desorption of higher molecular weight analytes and/or analytes having higher affinity to a particular extraction phase. The rationale behind GCxGC-ToFMS equipment use is not only related to well-known benefits of improved separation efficiency,

eliminated chromatographic coelution and increased sensitivity (important for detection of trace carryover peaks), but also to the ease of confirmation of metabolite identity. Namely, considering the existence of analyte structure-GCxGC retention relationships, the analyte identification and postprocessing of generated peak tables was more convenient [86]. Most important, the GCxGC structurally related chromatograms were able to provide a deeper insight into extraction phase selectivity characteristics and subsequent better visualization/interpretation of potential analyte structure-SPME enrichment relationships.

3.4 *Results and discussion*

3.4.1 *GCxGC-ToFMS method considerations*

Since spiked aqueous standards can be considered relatively clean sample matrices, only selected GCxGC parameters were included in optimization, one of them being modulator temperature offset. Varying modulator temperature offset had the most significant effect on sensitivity improvement in GCxGC analysis, particularly when detectability of high molecular weight and high boiling analytes is concerned. Three modulator temperature offset values tested in the analysis of spiked water samples are 25, 30 and 35 ^{o}C (results shown in Figure 3.1). It is clear from the presented data that increasing modulator temperature offset resulted in an improvement of sensitivity with the effect being more prominent with increasing molecular weight in a particular homologous series of structurally related compounds. In fact, varying modulator temperature offset from 25 ^{o}C to 35 ^{o}C resulted in a 41% and 67% improvement in signal intensity for ethyl palmitate and ethyl stearate, respectively. Indeed, more efficient remobilization of the trapped solute into the secondary dimension column was permitted with the use of higher modulator temperature offsets; thus, a 35 ^{o}C condition was adopted for

future analyses (unless the secondary column maximum operating temperature did not permit so).

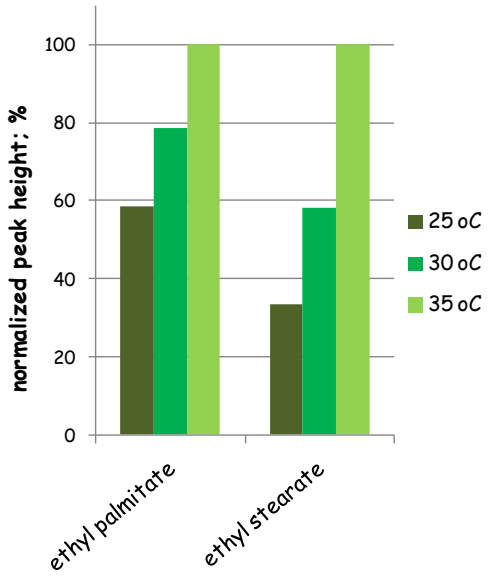

Figure 3.1. The effect of varying modulator temperature offset on detectability of higher molecular weight metabolites for 60 min HS-SPME analysis of spiked aqueous standards.

The adjustment of this parameter was especially important considering the discriminative features of SPME toward high molecular weight analytes that are attributed by slow mass transport from sample to headspace (in case of HS-SPME) and slow extraction kinetics, both resulting in poor recovery in pre-equilibrium conditions [94-95]. In addition, poor recovery for such compounds is caused by competitive adsorption onto vessel walls and the presence of an additional 'competing' phase in heterogeneous complex sample matrices which decreases the free concentration of target metabolites [94-95, 114]. The GCxGC surface plot of extracted ion chromatogram of water sample spiked with 52 metabolites (plus C_{15}, C_{17} and C_{19} hydrocarbons for RI confirmation, for a total of 55 analytes) is presented in Figure 3.2.

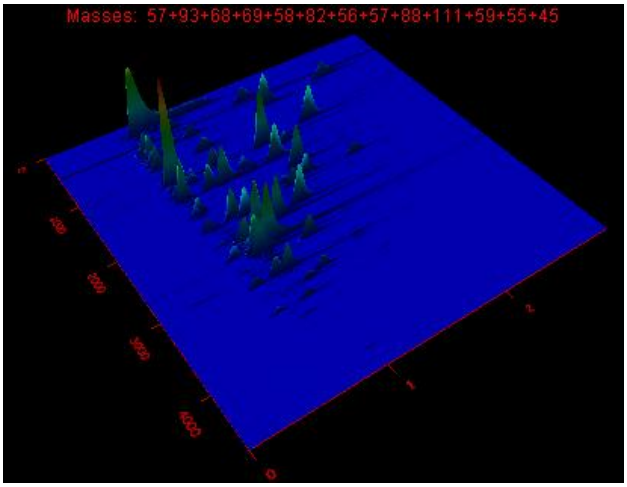

Figure 3.2. GCxGC surface plot of extracted ion chromatogram of water sample spiked with 52 metabolites (plus C_{15}, C_{17} and C_{19} hydrocarbons for RI confirmation, for a total of 55 analytes) and submitted to 60 min HS-SPME extraction using DVB/CAR/PDMS coating.

3.4.2 *Coating evaluation method performance characteristics*

Prior to the final coating evaluation, the precision of the employed SPME method was evaluated on both an intra- and inter-day basis, using the most commonly employed and universal DVB/CAR/PDMS coating [123]. These experiments included the analysis of 10 replicates prepared at the same time and required to assure at least 12 hrs of instrument running for acceptable degree of throughput. The results of the intra-day repeatability experiment were not satisfactory for the spiked water samples aged on the autosampler tray and extracted at 40 ^{o}C: 34.6% of peaks had precision (expressed as relative standard deviation, RSD) > 15%. The metabolites with unacceptable precision were those analytes with large K_{ow} values in each homologous group of components, with the effect of decreased precision being more prominent as the hydrophobicity increased as illustrated by the example of ethyl esters and alcohols in Figure 3.3 a-b as well as oxygenated terpenes and sesquiterpene hydrocarbons. In order to understand the phenomenon of unstable response over time (whether increasing as in the case of ethyl palmitate, ethyl stearate and 1-heptadecanol or decreasing as in the case of ethyl nonanoate, undecanoate

and tridecanoate, refer to Figure 3.3 a-b), several attempts were made: *i)* glassware silanization, *ii)* addition of small amount (20 µL) of methanol, and *iii)* spiking of 1 µL of methanolic solution directly into empty vial. These experiments resulted in 30.8, 40.4 and 9.8% of metabolites with precision > 15%, respectively. Therefore, significant improvements were being observed for analytes of mid to high log K_{ow} values (17.3 to 15.0%, 28.7 to 14.9%, 21.4 to 14.9%, 29.0 to 13.0% and 20.4 to 12.0% for 2-tridecanone, ethyl undecanoate, dodecanal, ethyl stearate and tridecanal, respectively), oxygenated terpenes and sesquiterpene hydrocarbons (38.6 to 9.7%, 28.4 to 9.8%, 31.0 to 8.3%, 24.1 to 9.9%, 18.5 to 7.5%, 19.8 to 9.7%, 17.8 to 11.7% for (*E*,*E*)-*α*-farnesene, *cis*,*trans*-farnesol, (*Z*,*Z*)-farnesol, (*E*)-*β*-farnesene, (*Z*)-*β*-farnesene, neral and *trans*-geraniol, respectively) in the case in which water aging was eliminated. Obviously, SPME technique suffers from losses of hydrophobic compounds during spiking because of precipitation and competitive adsorption of hydrophobic compounds to glassware. The latter was pointed out in the study by Langenfeld *et al*. to reduce the effective concentration of *n*-alkanes in aged water and unsilanized glassware, however for them glassware silanization resulted in improvement of recovery and reproducibility [158]. Since the aging of water obviously had an effect on precision and long-term stability of both less and more hydrophobic spiked metabolites whether due to reactivity of components with each other or potential activity toward the extraction apparatus (glassware walls, septa), an additional experiment was designed in order to determine whether a similar trend was observed for spiked water samples submitted to extraction procedure at 30 ^{o}C, or in other words to deduce whether the observed phenomenon was related to initiation of thermolysis-related extraction artifacts in the aqueous solution. The resulted outcome led to 27.5% of peaks with RSD > 15%, which still represents a significant improvement compared to 34.6% obtained for aged water samples submitted to 40 ^{o}C extraction temperature. The components for which better long-term stability was achieved upon decreasing extraction temperature in aqueous solution are members of the series of oxygenated terpenes, namely, *cis*,*trans*-farnesol (28.4

to 12.0%), (*Z,Z*)-farnesol (31.0 to 9.4%), neral (19.8 to 8.9%), *trans*-geraniol (17.8 to 7.8%) and geranial (14.0 to 10.2%) (Figure 3.3 c) as well as surprisingly some high MW homologues, such as ethyl stearate (29.0 to 11.8 %).

Based on these results, it is obvious that even in a system, which at a first glance looks relatively simple, long-term stability of samples and SPME measurements are affected by several phenomena potentially attributed by the production of thermolysis-initiated reactions in the aqueous medium at 40 ^{o}C, which can be still regarded as a considerably mild extraction condition. However, considering that significant % of water participates in the composition of plants and plant-based foods and that fibre coating/water distribution constant primarily determines the efficacy of SPME process, water as a sample matrix can not be neglected [148,150]. Also, considering that the precision was still not acceptable for some components either due to adsorption or activity of components towards the extraction apparatus in aqueous solution at 30 ^{o}C or the combination of all different factors (Figure 3.3 d, note the response increase initially for ethyl stearate in aqueous solution at 40 ^{o}C slowly leveling off, the response decrease in the absence of water at 40 ^{o}C, while the response in aqueous solution at 30 ^{o}C is stable over time), the calculation of SPME enrichment factors in this particular study was performed for freshly prepared samples at 30 ^{o}C.

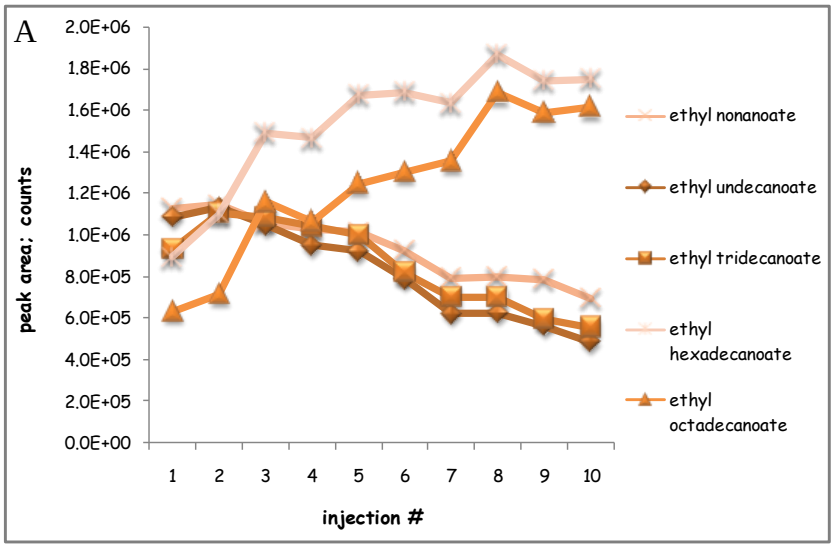
A
2.0E+06
1.8E+06
1.6E+06
1.4E+06
1.2E+06
1.0E+06
8.0E+05
6.0E+05
4.0E+05
2.0E+05
0.0E+00
peak area; counts
1 2 3 4 5 6 7 8 9 10
injection #
ethyl nonanoate
ethyl undecanoate
ethyl tridecanoate
ethyl hexadecanoate
ethyl octadecanoate

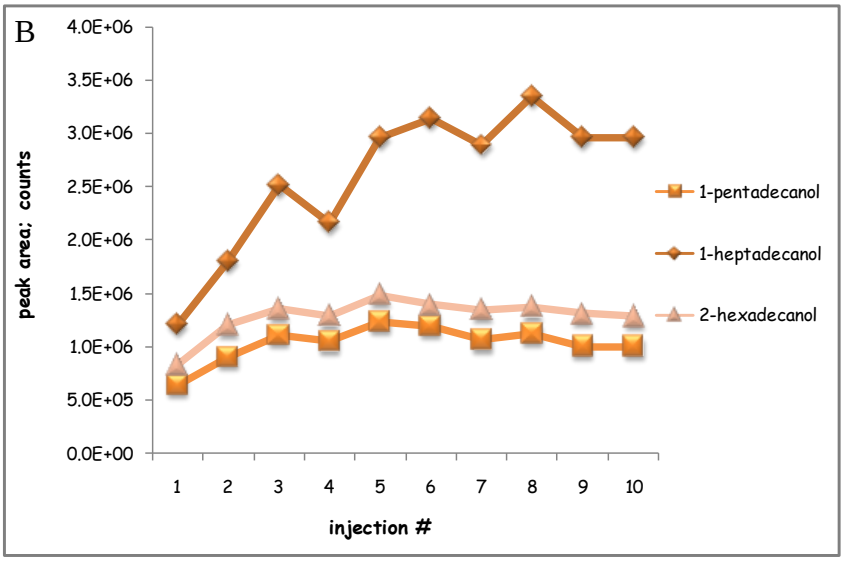
B
4.0E+06
3.5E+06
3.0E+06
2.5E+06
2.0E+06
1.5E+06
1.0E+06
5.0E+05
0.0E+00
peak area; counts
1 2 3 4 5 6 7 8 9 10
injection #
1-pentadecanol
1-heptadecanol
2-hexadecanol

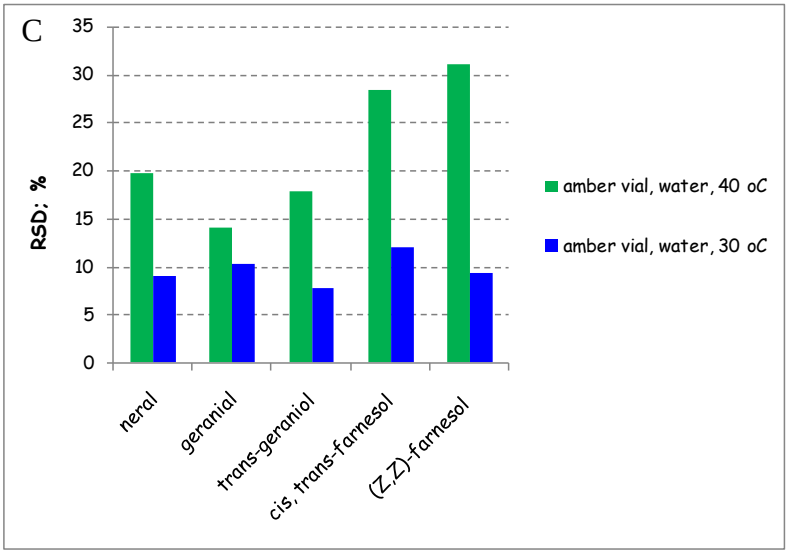
C
35
30
25
20
15
10
5
0
RSD; %
neral
geranial
trans-geraniol
cis, trans-farnesol
(Z,Z)-farnesol
amber vial, water, 40 oC
amber vial, water, 30 oC

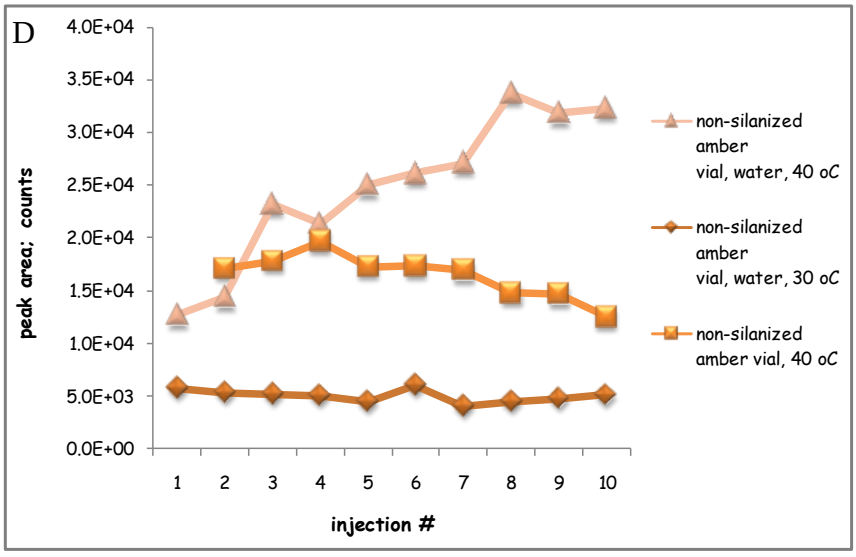

Figure 3.3. The evaluation of performance characteristics of the coating evaluation method indicating sample/analyte instability over time. Legend: A and B – long-term stability for spiked aqueous solutions extracted at 40 ^{o}C; C – comparison of precision (expressed as relative standard deviation; RSD %) for spiked aqueous solutions extracted at 40 ^{o}C and 30 ^{o}C; D – long-term stability for ethyl stearate in aqueous solution at 40 ^{o}C and 30 ^{o}C as well as after spiking empty amber vial with 1 µL of metabolite methanolic solution and extracting at 40 ^{o}C.

Under those conditions of freshly prepared sample analysis, intra-day repeatability and inter-day repeatability were characterized by 3.8% and 9.6% of peaks having RSD > 15%, respectively which was a satisfactory condition considering that overall precision is affected by water sample preparation, actual extraction and GCxGC analysis [158].

3.4.3 *Trends in coating selectivity and number of collected metabolites*

In general, the commercial coatings demonstrated poor group-type selectivity; however, some minor features can still be effectively identified by taking a closer look at GCxGC peak apex plots generated from retention time data and representing the metabolites found above S/N threshold of 50 in Figure 3.4. Based on the number of peaks satisfying this sensitivity criterion, PDMS,

PDMS/DVB and DVB/CAR/PDMS coatings were able to successfully capture all of the investigated metabolites (peak apex plot in Figure 3.4 a), while only 47, 50, 44 and 39 peaks were extracted with PA, CAR/PDMS, CW and carbopack Z/PDMS extraction phases, respectively (peak apex plots in Figure 3.4 b-e, respectively).

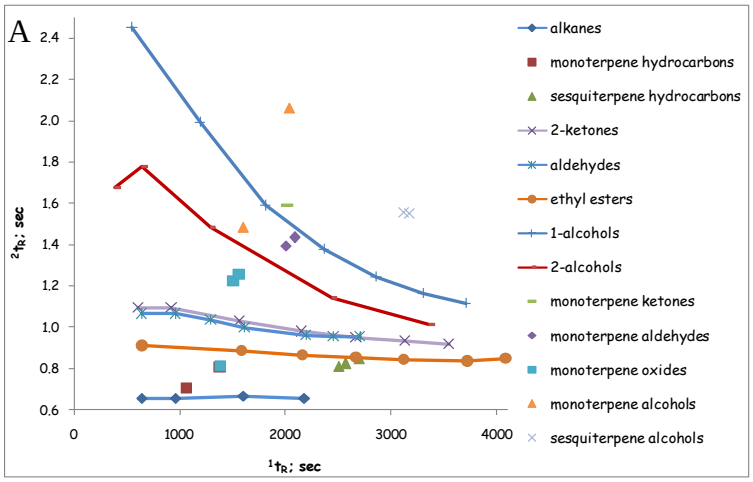

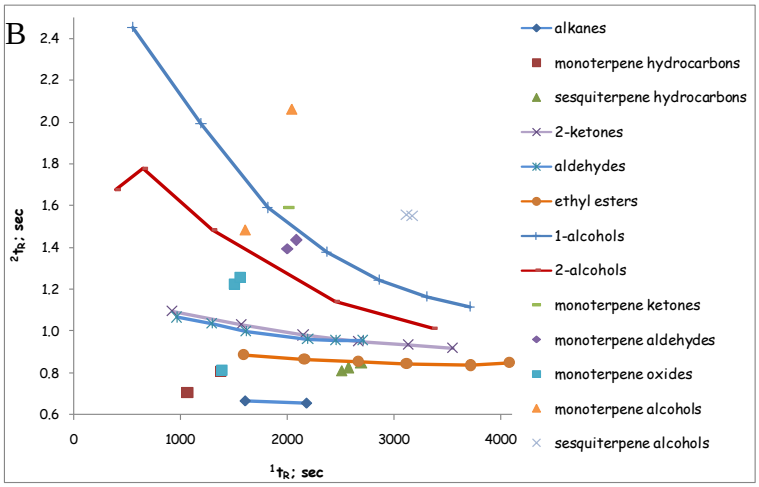

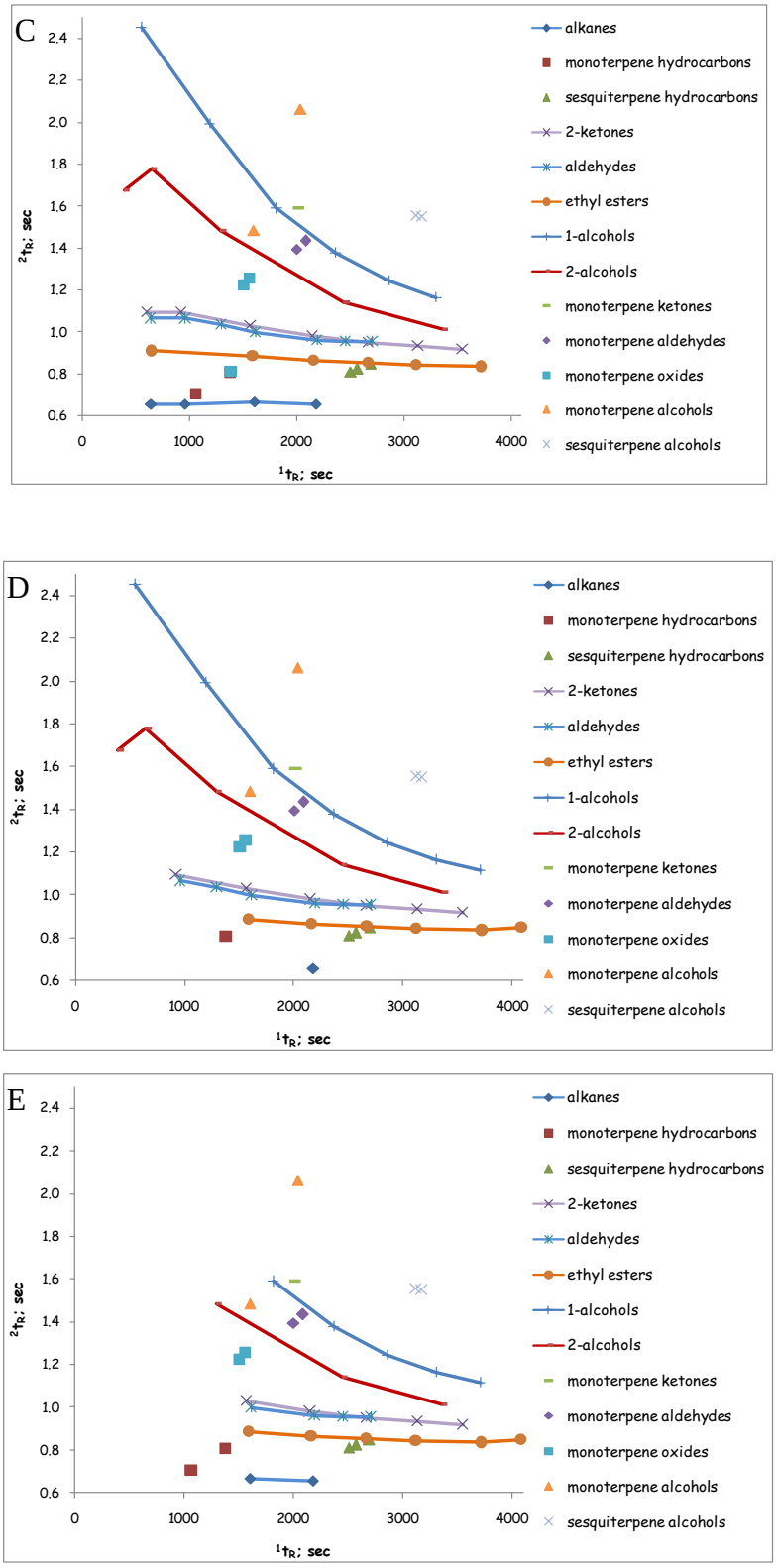

Figure 3.4. GCxGC peak apex plots of spiked water samples generated from retention time coordinates and representing the metabolites found above S/N threshold of 50 for DVB/CAR/PDMS, PDMS/DVB and PDMS coatings (plot

A), PA coating (plot B), CAR/PDMS coating (plot C), CW coating (plot D) and carbopack Z/PDMS coating (plot E).

No significant extraction selectivity trends were observed with adsorbent coatings, which consist of a solid material (porous polymer or porous carbon) suspended into a liquid polymer except for distribution according to analyte molecular weights that will be comprehensively addressed in one of the following sections. This is in accordance with relevant adsorption extraction mechanism as these coatings extract organic molecules based on physical trapping and the interaction of analyte with a solid particle [94-95]. However, some important trends can be identified with absorbent-type coatings, in particular PA and CW. In the case of PA, some nonpolar components such as octane and nonane, as well as moderately polar 2-hexanone, hexanal and ethyl butanoate were not captured, which, based on the extraction sensitivity data discussed later in this document, does not hold true for other members of these homologous series. Namely, the use of PA extraction phase was giving rise to a very strong background signal in a chromatogram, which was chromatographically coeluting with the above mentioned analytes to such extent that reliable identification and accurate quantification of these analytes could not have been assured even with the use of GCxGC. The corresponding peak apex plot for CW phase illustrates that this coating did not capture nonpolar analytes (octane-undecane), moderately polar analytes (2-hexanone, hexanal and ethyl butanoate) as well as *alpha*-pinene and eucalyptol. However, this is mainly due to the nonselectivity of this phase toward nonpolar and moderately polar analytes, as will be discussed later. An interesting version of peak apex plot is shown for carbopack Z/PDMS coating. As is well known, adsorbent ability to retain analyte is dependent on the total surface area, the amount of porosity (pore volume per gram of adsorbent) and the size of the pores. The earliest versions of adsorbents used in SPME fibres such as DVB and carboxen 1006 are both characterized with three pore categories: macro- (> 500 Å), meso- (20-500 Å) and micropores (2-20 Å) [94-95]. Carbopack Z being porous graphitized carbon black with the pore size of approximately 100 Å, possesses a

low degree of microporosity and consequently since the average size of the micropore diameter determines the strength of adsorbent, this phase is not suitable for the extraction of small molecular weight analytes. This trend was pretty consistent across the entire evaluated molecular weight range and independent of analyte polarity.

3.4.4 *Desorption efficiency of commercial coatings*

Desorption efficiency data revealed significant molecular weight-relevant memory effects of examined coatings only in the case of carboxen-based coatings. The trend for a series of ethyl esters is illustrated in Figure 3.5. DVB/CAR/PDMS coating demonstrated memory effects for ethyl undecanoate, ethyl tridecanoate and ethyl palmitate, with unacceptable carryover of 16.3% in the case of ethyl palmitate. So obviously the smaller CAR/PDMS layer thickness in the case of DVB/CAR/PDMS coating, as compared to CAR/PDMS coating is indicative of better desorption efficiency. In the case of CAR/PDMS coating, the initial increasing memory effects with increasing boiling point in a homologous series are eventually leveling off until the point the response is undetectable. These results translate into stronger irreversible adsorption effects with increasing molecular weight and are nicely correlated with enrichment data, considering that 1-heptadecanol and ethyl stearate were not detected when this coating was used (Figure 3.4). Furthermore, fibre constants were showing a decreasing trend with increasing molecular weight in each homologous series of investigated compounds. In fact, the desorption efficiency results corresponding to CAR/PDMS coating indicate the presence of memory effects across investigated homologous series starting with C_7 member. For example, % carryover of 1.6 and 1.2% were detected even in the case of 2-heptanone and 1-heptanol, respectively, which are relatively small molecular weight analytes. Significant efforts were being made to improve the desorption efficiency, such as the introduction of a tapered ‘throughput’ pore with two openings per

carboxen 1006 particle, thus allowing the carrier gas to enter a pore and enhance desorption [95]. However, these results illustrate that the upper analyte molecular weight limit for accurate quantification with CAR/PDMS coating is still extremely low even though aggressive 305 ^{o}C desorption temperature was applied. However, memory effects were not detected for two representative smallest molecular weight analytes including 1-pentanol and 2-pentanol, which allows the estimation of 88 g/mol upper molecular weight limit for this coating. This is in contrast with the Supelco recommendation for CAR/PDMS coating which involves upper molecular weight limit of 225 g/mol [95].

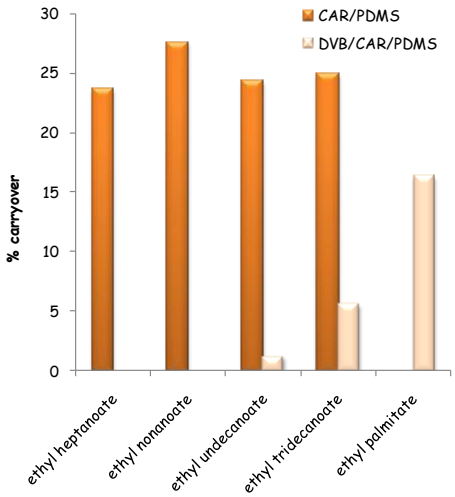

Figure 3.5. Desorption efficiency evaluation reported in terms of % carryover for wide molecular weight homologous series of ethyl esters and carboxen-based coatings DVB/CAR/PDMS and CAR/PDMS.

In order to attempt increasing MW range of DVB/CAR/PDMS coating, several desorption efficiency parameters were varied, and in addition to already implemented 265 ^{o}C/10 min condition, 270 ^{o}C desorption temperature was attempted in combination with 10 min and 25 min desorption times. The relevant results for a series of ethyl esters and alcohols are illustrated in Figure 3.6 and in general they are indicative of 19.2, 15.4 and 11.5% of peaks with carryover % above 1% for the afore-mentioned conditions, respectively. So

obviously, rather than desorption time, the strongest parameter leading to more effective desorption is desorption temperature, which resulted in promising improvements when raised to maximum operating limit, thus increasing the molecular weight range of this 'universal' coating. However, the fact that high molecular weight compounds are still not efficiently desorbed from the DVB/CAR/PDMS coating but are from the PDMS/DVB coating is indicative of the possibility that these components are not retained in the DVB/PDMS layer as originally thought, but rather partition to CAR/PDMS layer of the DVB/CAR/PDMS coating.

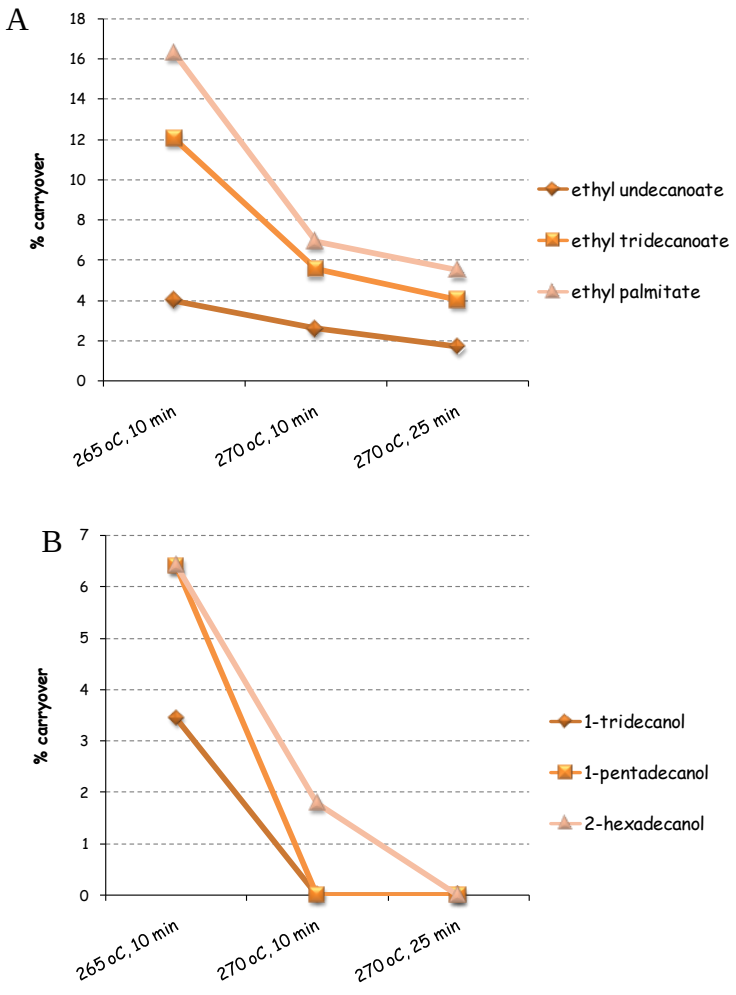

Figure 3.6. DVB/CAR/PDMS desorption efficiency evaluation reported in terms of % carryover for high MW compounds, including A – ethyl esters and B – alcohols at various desorption conditions.

3.4.5 *Comparison of coatings in terms of extraction sensitivity*

The generated SPME detector responses were converted to amounts extracted in pg followed by the calculation of fibre constants (Table 3.3, note that underlined values represent 'apparent' fibre constants or those obtained in pre-equilibrium conditions) for all of the investigated metabolites. In this table, fibre constants are reported for PDMS, PA, DVB/CAR/PDMS and PDMS/DVB coatings and the implementation of these coatings in spiked water analysis resulted in satisfactory reproducibility. On the other hand, the employment of CAR/PDMS, carbopack Z/PDMS and CW coatings resulted in poor method precision to such an extent that it was impossible and inaccurate to rely on 60 min and 90 min extraction time points in order to determine whether equilibrium was achieved in the system. Unsatisfactory method reproducibility in the case of CAR/PDMS and carbopack Z/PDMS coatings is attributed to non-Gaussian first dimension peak profiles, the cause of which was investigated later with the inclusion of additional experiments/samples, whereas in the case of CW coating, stripping of the polymeric extraction phase from solid support was externally visible. Nonetheless, as can be seen in Table 3.3 for the coatings that exhibited good performance characteristics, the RSD on measured $K_{fs}V_f$ values in the worst case scenario was ranging from 0.9% for linalool with PA coating to 25.4% for ethyl stearate (issues with solubility and detectability) with the same coating. Minimum and maximum RSD values on the collective set of daily quality control standards (PDMS fibre, n = 9) were 4.3 for (*E*)-β-farnesene and 25.5% for ethyl stearate, respectively.

Table 3.3. Fibre constants of target metabolites extracted from spiked water samples and obtained with PDMS, PA, PDMS/DVB and DVB/CAR/PDMS commercial coatings. Underlined values represent enrichment factors in pre-equilibrium conditions and nq implies that a particular component was not quantifiable.

	log $K_{fs}V_f$							
analyte name	PDMS	RSD; %	PA	RSD; %	PDMS/DVB	RSD; %	DVB/CAR/PDMS	RSD; %
octane	**5.05**	3.6	**nq**	nq	**6.96**	0.2	**7.09**	0.2
nonane	**5.20**	3.7	**nq**	nq	**6.51**	0.5	**6.61**	0.5
undecane	**5.62**	0.7	**4.34**	0.9	**6.17**	0.4	**6.55**	0.1
tridecane	**5.24**	1.7	**4.62**	1.5	**5.86**	0.5	**6.08**	0.3
alpha-pinene	**4.00**	3.2	**3.00**	5.2	**4.71**	1.9	**5.37**	0.5
limonene	**3.79**	2.6	**3.47**	2.6	**4.57**	0.7	**4.74**	0.7
(*Z*)-β-farnesene	**5.00**	2.7	**4.89**	1.7	**5.16**	2.1	**4.96**	0.8
(*E*)-β-farnesene	**5.11**	2.2	**4.99**	2.0	**5.25**	2.0	**4.96**	1.4
(*E,E*)-α-farnesene	**4.98**	2.4	**4.84**	2.2	**5.15**	2.4	**4.64**	2.1
2-hexanone	**0.91**	6.4	**nq**	nq	**2.36**	5.8	**2.94**	0.8
2-heptanone	**1.49**	4.8	**1.53**	1.6	**2.88**	2.1	**3.30**	0.4
2-nonanone	**2.47**	2.9	**2.29**	2.1	**3.62**	1.6	**3.78**	0.4
2-undecanone	**3.35**	1.4	**3.12**	1.7	**4.09**	0.9	**4.14**	0.3
2-tridecanone	**3.72**	1.0	**3.52**	4.5	**4.19**	0.9	**3.99**	0.5
2-pentadecanone	**3.11**	3.2	**3.11**	3.0	**3.21**	4.6	**3.04**	7.0
2-heptadecanone	**2.38**	2.3	**2.44**	5.9	**2.45**	4.8	**2.19**	8.8
hexanal	**1.33**	4.4	**nq**	nq	**2.80**	4.4	**3.31**	1.3
heptanal	**1.69**	4.3	**1.88**	4.9	**3.04**	1.8	**3.40**	0.9
octanal	**2.30**	6.6	**2.51**	5.3	**3.55**	1.5	**3.77**	0.5
nonanal	**2.79**	5.2	**2.80**	1.7	**3.85**	1.3	**3.86**	0.8
undecanal	**3.35**	2.1	**3.20**	1.5	**3.89**	0.8	**3.82**	0.8
dodecanal	**3.18**	2.1	**3.13**	1.4	**3.44**	1.6	**3.26**	1.2
tridecanal	**3.32**	2.0	**3.21**	1.8	**3.50**	1.9	**3.27**	2.4
ethyl butanoate	**0.98**	4.6	**nq**	nq	**2.68**	2.7	**3.16**	1.3
ethyl heptanoate	**2.75**	3.3	**2.47**	3.0	**3.79**	1.3	**3.92**	0.5
ethyl nonanoate	**3.41**	1.7	**3.13**	1.3	**3.94**	1.1	**3.93**	0.4
ethyl undecanoate	**3.82**	0.9	**3.67**	3.5	**4.08**	0.6	**4.03**	0.6
ethyl tridecanoate	**3.36**	2.0	**3.29**	1.9	**3.48**	2.9	**3.32**	4.7
ethyl palmitate	**2.34**	4.0	**2.38**	11.2	**2.41**	9.7	**2.23**	2.8
ethyl stearate	**1.27**	20.6	**1.34**	25.4	**1.42**	24.9	**0.96**	19.8
1-pentanol	**0.01**	3.8	**0.39**	5.1	**1.23**	4.7	**1.86**	2.7
1-heptanol	**1.31**	1.9	**1.55**	3.2	**2.50**	4.3	**2.68**	2.4
1-nonanol	**2.27**	2.3	**2.40**	1.9	**2.90**	3.6	**2.92**	2.1
1-undecanol	**2.83**	2.6	**2.88**	1.4	**3.09**	3.3	**3.03**	2.2

1-tridecanol	**2.63**	3.0	**2.68**	2.6	**2.70**	5.1	**2.60**	3.7
1-pentadecanol	**1.92**	8.6	**2.00**	6.4	**1.99**	10.6	**1.75**	10.2
1-heptadecanol	**0.75**	2.4	**0.80**	11.0	**0.79**	5.2	**0.58**	7.5
2-pentanol	**-0.65**	11.4	**-0.50**	4.8	**0.63**	6.4	**1.68**	2.2
2-hexanol	**0.37**	0.5	**0.82**	3.3	**1.77**	5.2	**2.36**	1.4
2-octanol	**1.62**	1.7	**1.73**	3.6	**2.89**	2.7	**3.04**	1.9
2-dodecanol	**3.00**	2.1	**2.98**	1.7	**3.21**	3.3	**3.19**	1.5
2-hexadecanol	**1.73**	8.3	**1.79**	6.0	**1.82**	10.8	**1.62**	10.0
(*R*)-(-)-carvone	**1.68**	2.0	**1.63**	2.1	**2.28**	3.7	**2.27**	2.1
cis-citral; neral	**2.63**	6.8	**2.42**	2.3	**3.53**	6.3	**3.28**	4.4
trans-citral; geranial	**2.68**	10.6	**2.49**	4.6	**3.41**	8.3	**3.29**	2.7
eucalyptol	**2.02**	7.6	**1.21**	5.4	**2.89**	2.1	**3.25**	0.6
cis-linalool oxide	**0.59**	3.4	**0.76**	3.7	**1.61**	2.5	**1.80**	5.0
trans-linalool oxide	**0.48**	1.6	**0.22**	1.8	**1.31**	5.0	**1.46**	3.8
linalool	**1.67**	1.5	**1.79**	0.9	**2.72**	1.9	**2.75**	2.1
trans-geraniol	**1.67**	0.2	**1.74**	1.6	**2.03**	4.9	**1.89**	5.4
cis,trans-farnesol	**2.07**	5.1	**2.21**	4.7	**2.17**	7.8	**1.79**	6.8
(*Z,Z*)-farnesol	**2.00**	5.5	**2.18**	5.3	**2.13**	7.6	**1.63**	9.3

Fibre constant data follow the general increasing trend with analyte hydrophobicity, which is widely acknowledged to be strongly associated with hydrophobic partitioning [159-160]. This trend is obviously less prominent for solid adsorbents, as the quality of the correlation between the experimentally determined fibre constants and analyte hydrophobicities is poor (for example, the linear regression coefficient for PDMS/DVB coating being 0.86 for a series of ethyl esters with fibre constant data measured under equilibrium conditions, while for the same set of analytes the linear correlation coefficient was 0.95 for PDMS coating), as reported in several previously published studies [161]. However, this is to be expected with solid coatings, as the retention of the analyte is dependent on the size of both the adsorbent pores and target analytes and in the case of mixed-phase solid coatings (such as DVB/CAR/PDMS), different analytes preferentially sorb to different phases [95]. When considering liquid coatings, such as PDMS and PA, there is overall a positive correlation between experimentally determined log $K_{fs}V_f$ values and literature log K_{ow} data

for all considered homologous groups of components up to a particular group member, at which point the fibre constant data start to decrease mainly because equilibrium condition has not been achieved. This positive correlation has already been reported for PDMS and PA coatings, indicating the possibility of estimating the K_{fs} data from well-known physicochemical properties for components across a given family of analytes [159-164]. The corresponding plots illustrating the association between log $K_{fs}V_f$ and log K_{ow} for all the investigated analytes for which equilibrium was reached within 60 min of extraction are illustrated in Figure 3.7 for PDMS and PA coatings. As can be seen from the data illustrated, the quality of correlation between log $K_{fs}V_f$ and log K_{ow} is excellent and characterized by linear correlation coefficients of 0.89 and 0.91 for PDMS and PA coatings, respectively. This confirms the validity of experimentally determined fibre constant data set across the investigated chemical spectrum. Furthermore, the dependence of fibre constants on analyte volatilities and overall positive log $K_{fs}V_f$ - log K_{ow} correlation that is observed for all coatings and all analytes imply that commercially available coatings are non-selective. For the investigated target metabolite mix, rather than specific analyte-extraction phase interactions, volatility and hydrophobicity are the main parameters governing the extraction recoveries under equilibrium conditions.

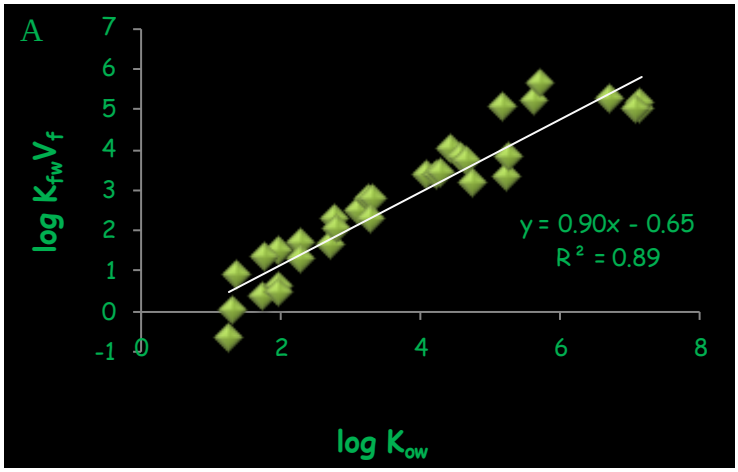

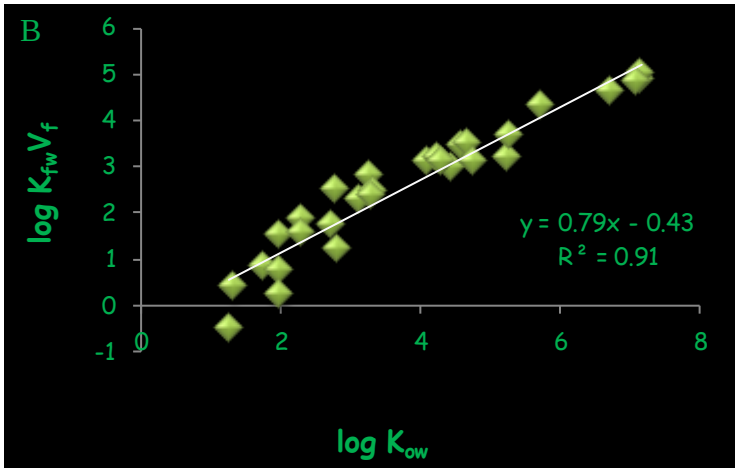

Figure 3.7. The relationship between fibre constants and analyte hydrophobicities for compounds in equilibrium within 60 min of extraction with A – PDMS coating and B – PA coating.

However, it is important to at least determine the degree of improvement in extraction recoveries when polar PA coating is compared to nonpolar PDMS for extraction of polar analytes. Figure 3.8 is illustrating such a comparison and it reveals improved extraction recoveries when PA is compared to PDMS in extraction of primary and secondary alcohols. Therefore, in accordance to already established coating selection rules, PA extraction phase is slightly more selective for the extraction of polar compounds and improvement in extraction sensitivity that it exhibits is more prominent as the analyte polarity increases [94-95]. It should be emphasized that the improvement in selectivity would be even more prominent if the experimentally obtained $K_{fs}V_f$ values were corrected for differences in volume of extraction phase since commercially available PA coating is thinner (85 μL) than PDMS coating (100 μL).

On the other hand, the most drastic improvements for nonpolar PDMS phase as compared to polar PA were observed in the case of nonpolar analytes including *n*-alkanes and monoterpene hydrocarbons. For *n*-alkanes, with respect to PA, the observed improvement of 19- and 4-x for undecane and tridecane was demonstrated, respectively. For monoterpene hydrocarbons, PDMS illustrated 10-x and 2-x improvement in $K_{fs}V_f$ as compared to PA for

alpha-pinene and limonene, respectively. In summary, PDMS should be considered for analysis of nonpolar *n*-alkanes and monoterpene hydrocarbons, whereas PA should be implemented for analysis of polar components having log K_{ow} < 3.30, such as 1-alcohols and 2-alcohols illustrated here.

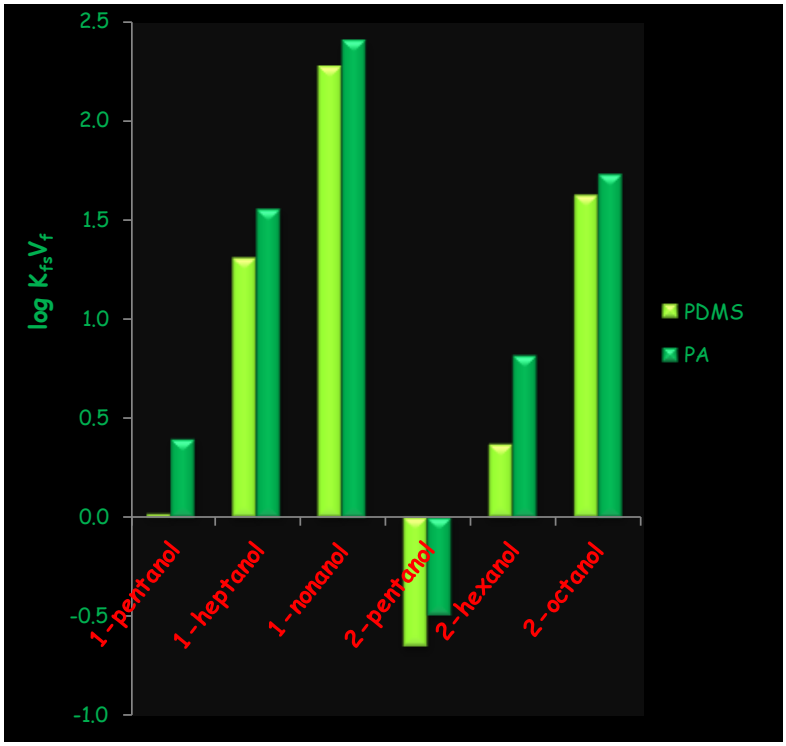

Figure 3.8. The comparison between nonpolar PDMS coating and polar PA coating in the extraction of polar analytes included in target metabolite mix.

Across the entire volatility range (see Figure 3.9 for homologous series of 2-ketones and ethyl esters, the data was log-transformed for simplicity since the $K_{fs}V_f$ values spanned over several orders of magnitude), the enrichment factors for volatile analytes could be correlated to adsorption capacity and retention capability of examined sorbents. As the degree of retention is higher with solid coatings due to increased interaction with the adsorbent surface, the performance of solid sorbents for volatile analyte capture was outstanding as compared to the liquid ones [95,104].

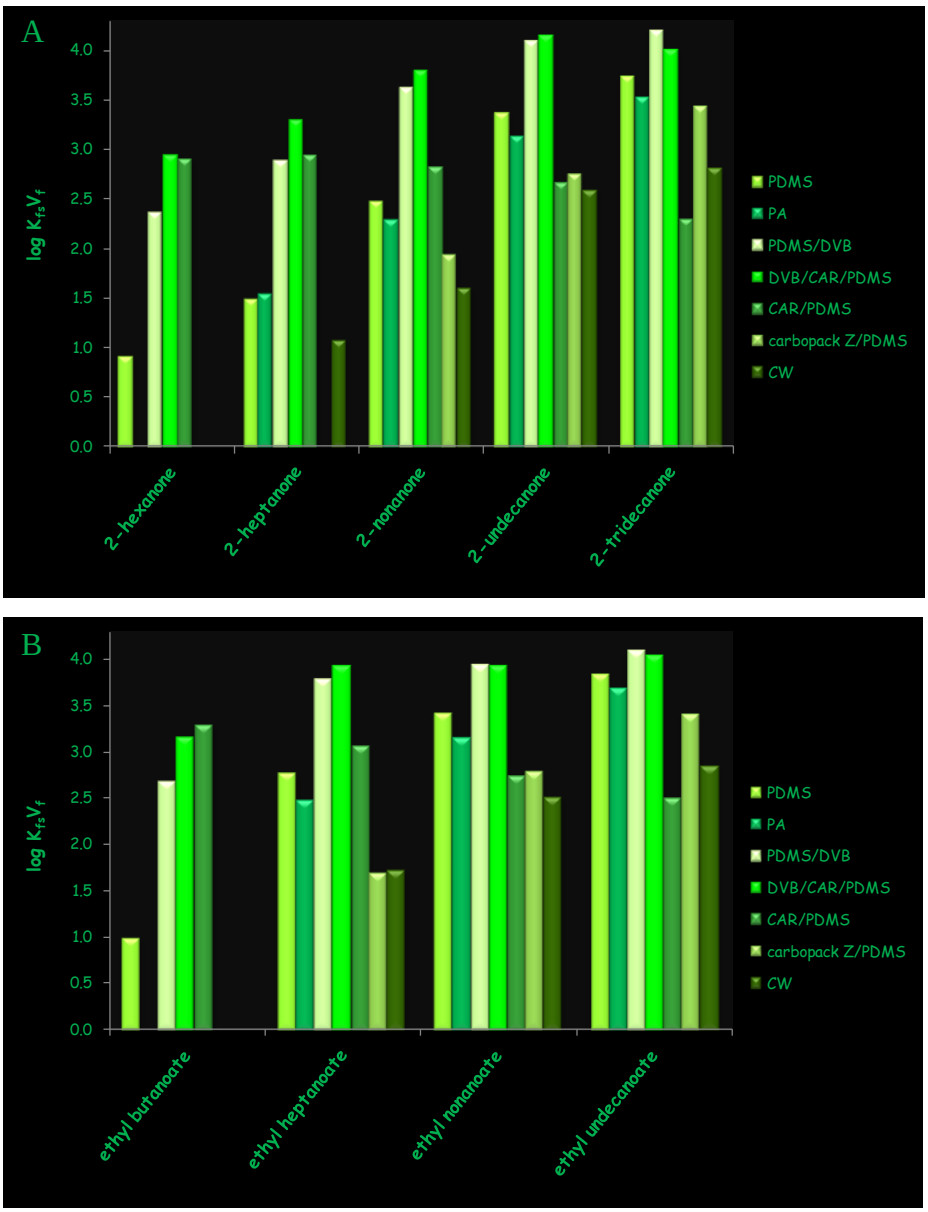

Figure 3.9. Experimentally determined fibre constants for homologous series of 2-ketones (plot A) and ethyl esters (plot B).

The $K_{fs}V_f$ data obtained show insignificant effect of fibre polarity on the extraction of small molecular weight polar analytes when solid coatings are compared to liquid ones as illustrated in the case of 1-pentanol with log $K_{fs}V_f$ of 0.01, 0.39, 1.23 and 1.86 and 2-pentanol with log $K_{fs}V_f$ of -0.65, -0.50, 0.63 and 1.68 for PDMS, PA, PDMS/DVB and DVB/CAR/PDMS coatings, respectively. Furthermore, in addition to total surface area and the amount of porosity, the

ability of adsorbent to retain a particular analyte is strongly dependent on average size of the micropore diameter [94-95]. Consequently, since the average sizes of the micropore diameter for carboxen 1006 in DVB/CAR/PDMS coating and DVB in PDMS/DVB and DVB/CAR/PDMS coatings are 12 and 16 Å, respectively, coatings containing carboxen 1006 showed superior performance in volatile analyte extraction enrichment as compared to PDMS/DVB [95]. For example, higher affinity to carboxen 1006-PDMS layer of DVB/CAR/PDMS coating resulted in the enhancements of 11 x for 2-pentanol, 4 x for alpha-pinene, 1-pentanol, 2-hexanone and 2-hexanol, 3 x for hexanal, ethyl butanoate and 2-heptanone and 2 x for heptanal, eucalyptol, 1-heptanol, tridecane, octanal and *cis*-linalool oxide as compared to PDMS/DVB in experimentally determined $K_{fs}V_f$ values. It is worth mentioning that not all above-mentioned components are in equilibrium (for example, eucalyptol is in equilibrium for PDMS/DVB coating but not for DVB/CAR/PDMS), therefore, for selected compounds for which DVB/CAR/PDMS fibre constants are 'apparent', DVB/CAR/PDMS is anticipated to have higher enrichment factors in equilibrium. The example extraction time profile for eucalyptol obtained with DVB/CAR/PDMS and PDMS/DVB coatings is illustrated in Figure 3.10. From the point of view of extraction kinetics, equilibrium was not achieved for DVB/CAR/PDMS coating due to higher K_{fs} value of the analyte in the CAR/PDMS layer of the DVB/CAR/PDMS coating as opposed to the PDMS/DVB layer of both examined coatings. This is resulted by the fact that more solute material needs to be transferred from sample matrix through boundary layer to the extraction phase [94-95].

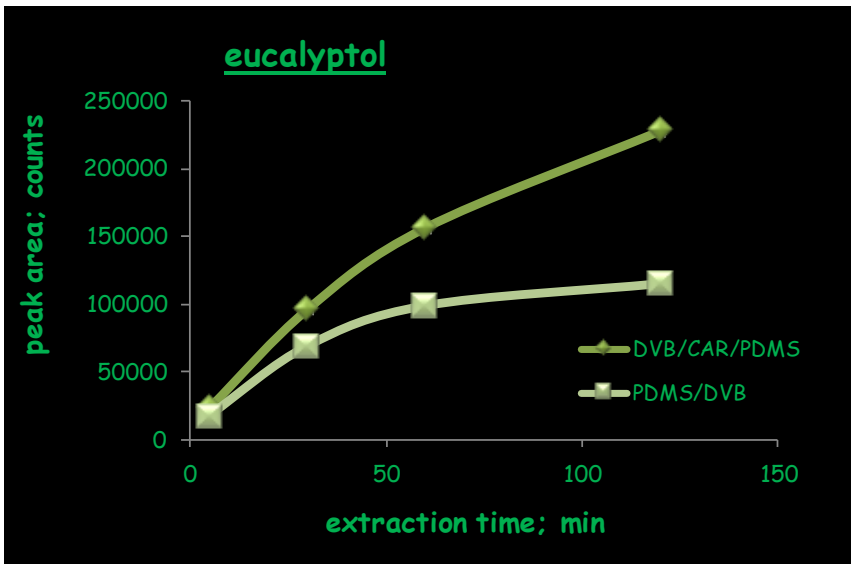

Figure 3.10. Extraction time profile for eucalyptol obtained with DVB/CAR/PDMS and PDMS/DVB coatings.

Based on the physicochemical properties of analytes mentioned above and plots in Figure 3.11, which show the distribution of experimentally determined $K_{fs}V_f$ values for subsets of analytes created on the basis of their molecular weights, the best sensitivity enhancement is achieved with DVB/CAR/PDMS coating as compared to PDMS/DVB for analytes having molecular weight < 185 g/mol. It is critical to emphasize at this point that above this molecular weight threshold, the performance of the two coatings is equivalent across the volatility and hydrophobicity range, followed by the slight enhancement of PDMS/DVB $K_{fs}V_f$ values (see Table 3.3), which was significant for one or at most two last members of each homologous series (for example, 3 x improvement for ethyl stearate is the most drastic example).

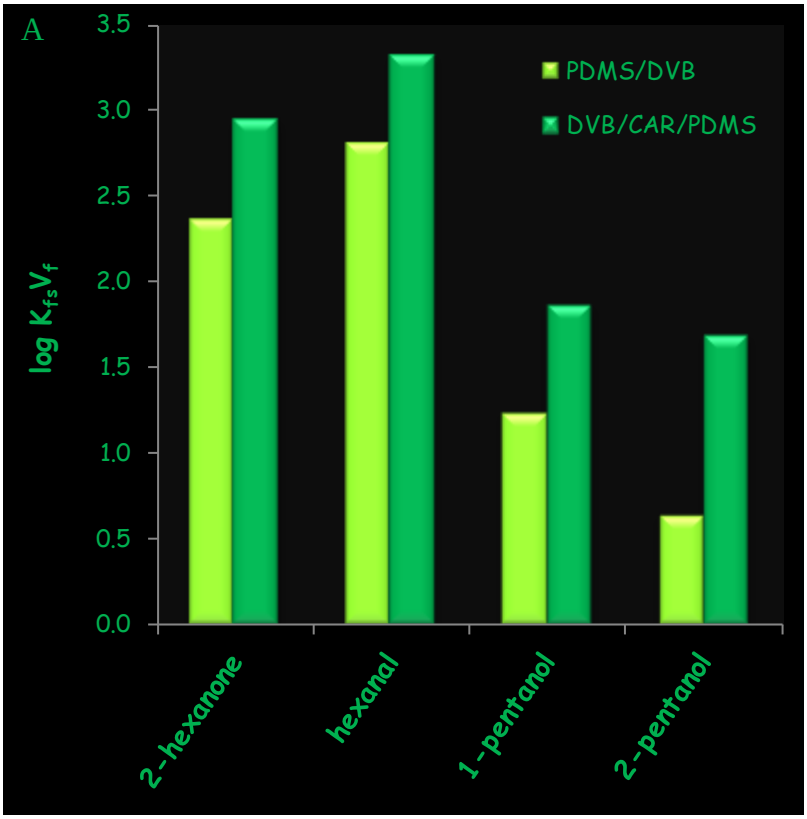
A
3.5
3.0
2.5
2.0
1.5
1.0
0.5
0.0
log $K_{fs}V_f$
PDMS/DVB
DVB/CAR/PDMS
2-hexanone
hexanal
1-pentanol
2-pentanol

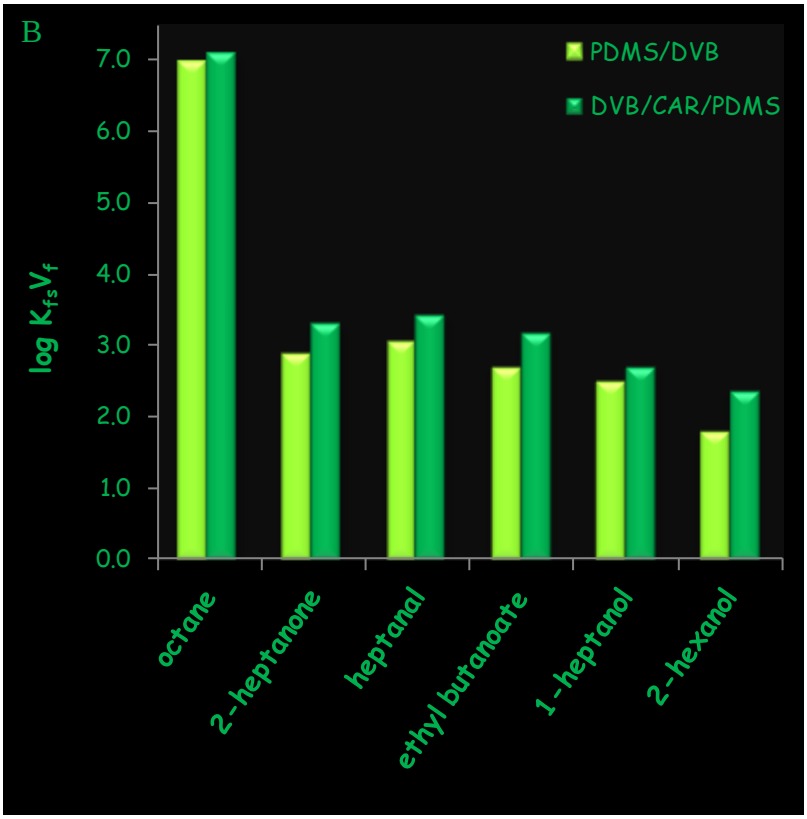
B
7.0
6.0
5.0
4.0
3.0
2.0
1.0
0.0
log $K_{fs}V_f$
PDMS/DVB
DVB/CAR/PDMS
octane
2-heptanone
heptanal
ethyl butanoate
1-heptanol
2-hexanol

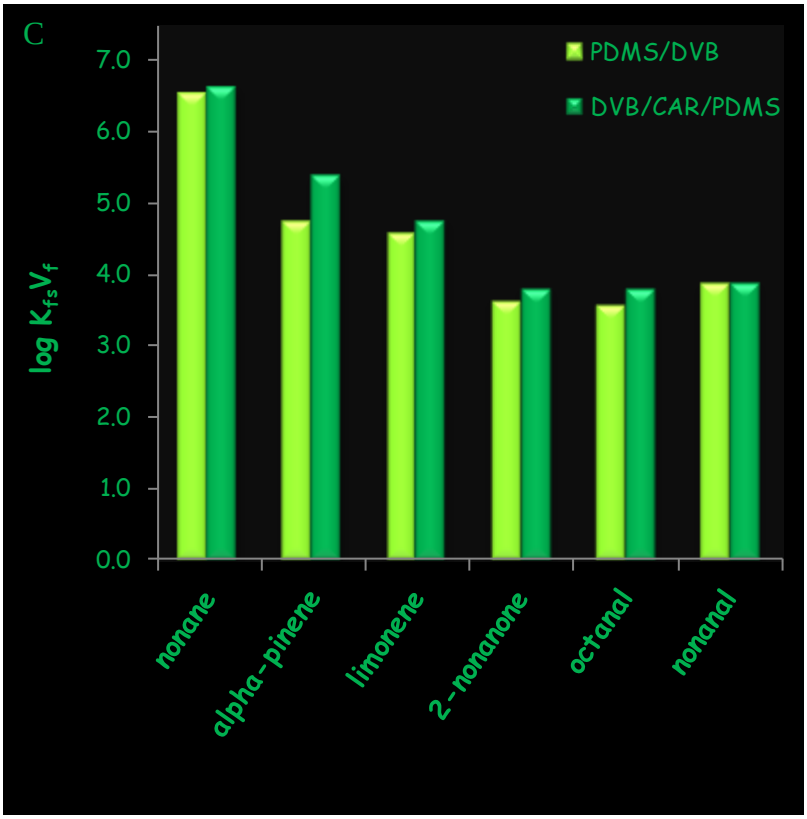
C
PDMS/DVB
DVB/CAR/PDMS
log $K_{fs}V_f$
7.0
6.0
5.0
4.0
3.0
2.0
1.0
0.0
nonane
alpha-pinene
limonene
2-nonanone
octanal
nonanal

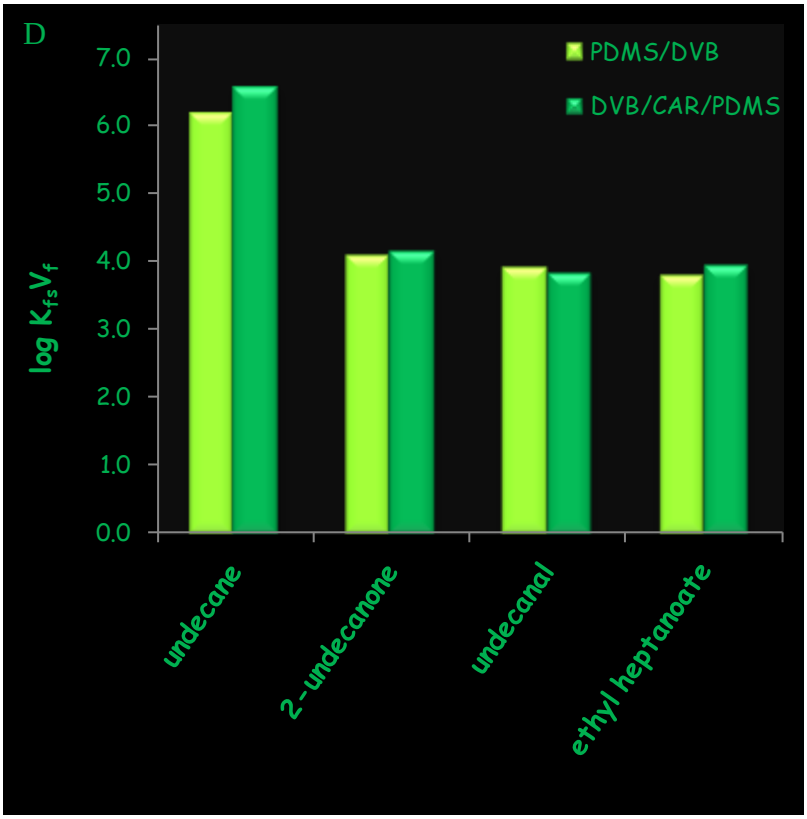
D
PDMS/DVB
DVB/CAR/PDMS
log $K_{fs}V_f$
7.0
6.0
5.0
4.0
3.0
2.0
1.0
0.0
undecane
2-undecanone
undecanal
ethyl heptanoate

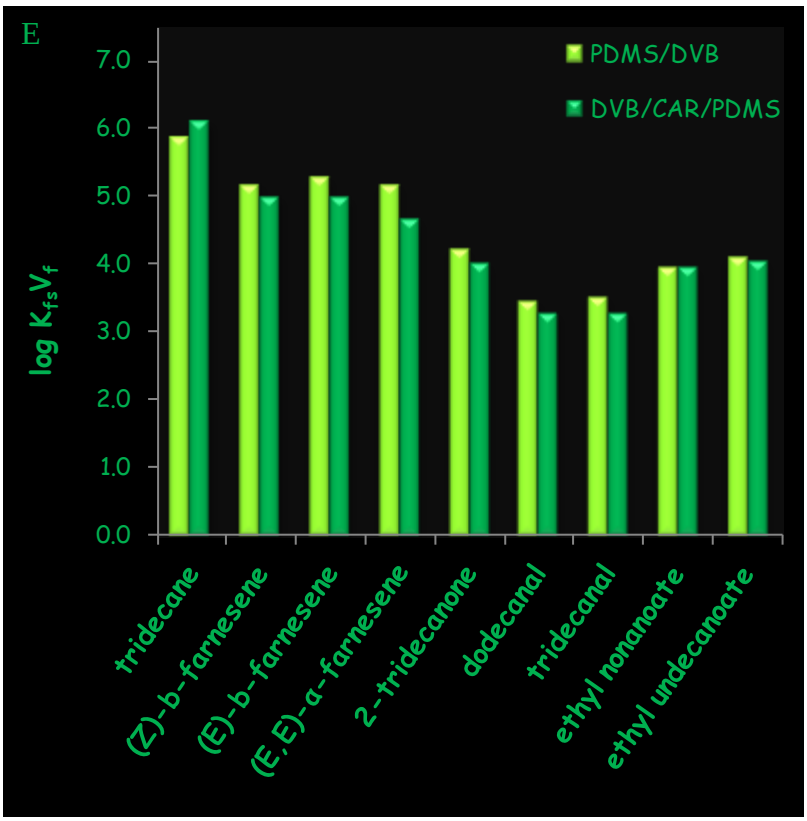

Figure 3.11. Experimentally determined $K_{fs}V_f$ values obtained for DVB/CAR/PDMS and PDMS/DVB coatings for analytes in equilibrium and having molecular weights A – ≤ 100 g/mol; B – between 100 and 120 g/mol; C – between 120 and 150 g/mol; D – between 150 and 180 g/mol and E – between 180 and 215 g/mol.

In order to verify the possibility that these high molecular weight components for which PDMS/DVB performs slightly better than DVB/CAR/PDMS are not retained in the DVB/PDMS layer as originally thought, but rather partition to CAR/PDMS layer of the DVB/CAR/PDMS coating and are hence not efficiently desorbed, extraction time profile interpretation was adopted. Figure 3.12 shows 5, 30, 60 and 120 min extraction time uptakes for homologous series of 1-alcohols, and the trend observed in this figure was consistent for other series of structurally related compounds. The results show several important findings. First of all, for metabolites having mid molecular weights (1-nonanol in Figure 3.12a), the extraction kinetics for the two coatings is similar even though these components are likely to partition into both inner and outer layers of the DVB/CAR/PDMS coating, indicating that

mass transfer through the boundary layer rather than coating thickness largely affects the extraction kinetics [94-95]. However, for the later eluting members (see the example of 1-pentadecanol and 1-heptadecanol in Figure 3.12), a significant deviation in performance of the two coatings is observed with the PDMS/DVB providing significantly better sensitivity enrichments as extraction time increases. The prominent increase of performance characteristics of the PDMS/DVB coating with respect to the DVB/CAR/PDMS coating as the extraction time increases is attributed to the fact that more time is allowed for high molecular weight compounds to partition into the CAR/PDMS layer of DVB/CAR/PDMS from which they are not desorbed effectively. With this finding, it is clear what causes limiting molecular weight range for the DVB/CAR/PDMS coating. However, these results indicate for the first time the importance of 'tuning' extraction time based on physicochemical properties of priority analytes to eliminate undesirable adsorption of high molecular weight analytes into the sorbent from which they are not desorbed efficiently and hence, allow best sensitivity, accuracy and desorption efficiency obtainable with DVB/CAR/PDMS.

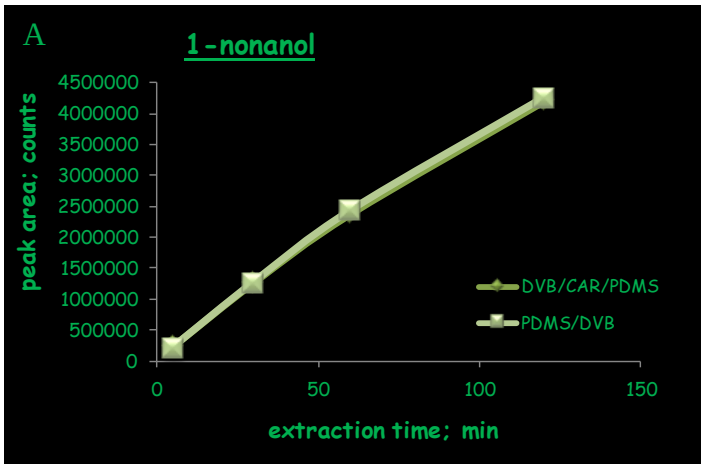

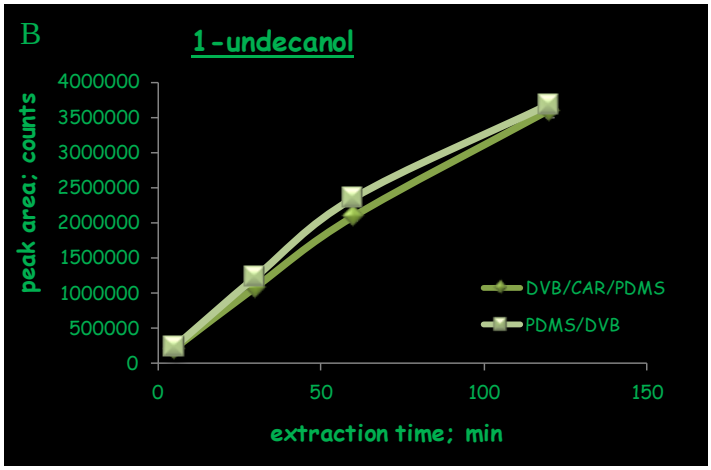
B
1-undecanol
peak area; counts
4000000
3500000
3000000
2500000
2000000
1500000
1000000
500000
0
0
50
100
150
extraction time; min
DVB/CAR/PDMS
PDMS/DVB

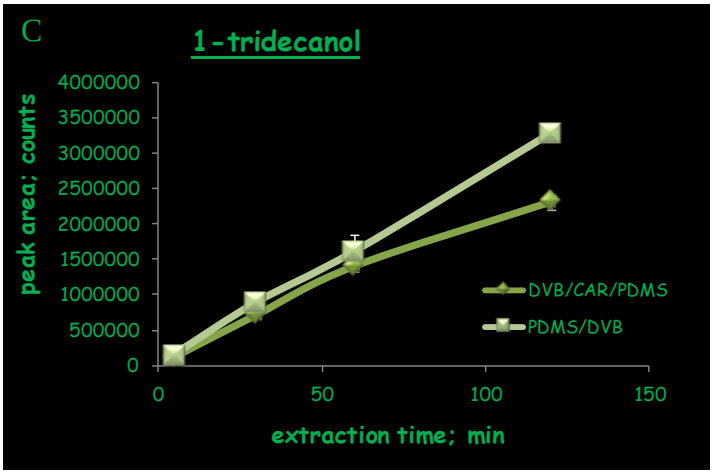
C
1-tridecanol
peak area; counts
4000000
3500000
3000000
2500000
2000000
1500000
1000000
500000
0
0
50
100
150
extraction time; min
DVB/CAR/PDMS
PDMS/DVB

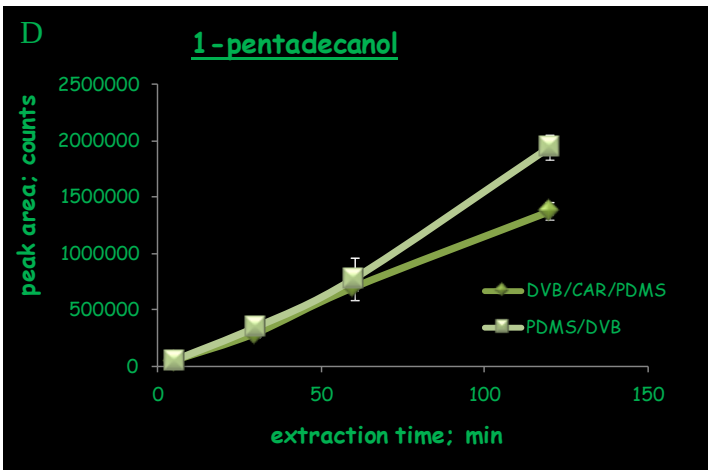
D
1-pentadecanol
peak area; counts
2500000
2000000
1500000
1000000
500000
0
0
50
100
150
extraction time; min
DVB/CAR/PDMS
PDMS/DVB

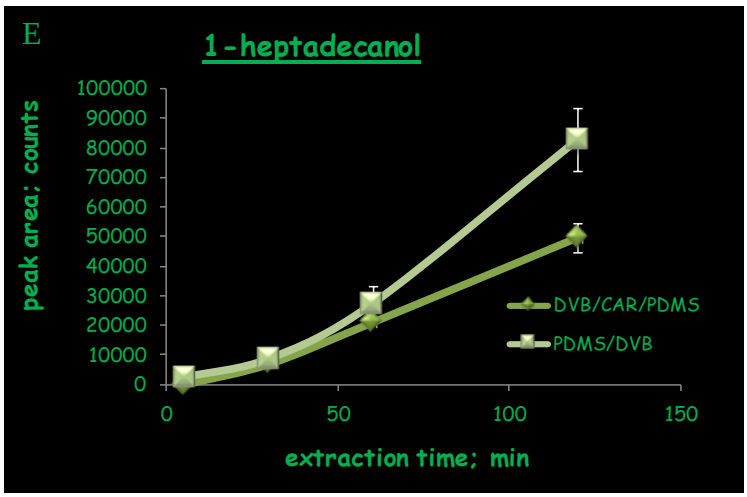

Figure 3.12. 5, 30, 60 and 120 min extraction time uptakes of 1-alcohols (A – 1-nonanol, B – 1-undecanol, C – 1-tridecanol, D – 1-pentadecanol and E – 1-heptadecanol) corresponding to HS-SPME extraction performed with DVB/CAR/PDMS and PDMS/DVB coatings.

These and additional extraction time profiles in Figure 3.13 also confirmed that equilibrium time is longer for polar compounds as compared to the nonpolar ones. For example, for compounds of similar molecular weights including nonane, nonanal and 1-nonanol, equilibrium was reached within 5 min and 60 min for nonane and nonanal, respectively, and not reached at all within 120 min of extraction with 1-nonanol. Since the aqueous phase is agitated and the coating is very thin, the limiting step now becomes diffusion in the headspace (from the headspace/water interface to the coating/headspace interface). In headspace, diffusion coefficients are four orders of magnitude larger than in liquid phase, but concentrations, therefore concentration gradients become smaller and smaller as Henry's constants decrease. As a result, the transport of analytes through the headspace is very slow and it may take quite a long time to achieve the equilibrium [116].

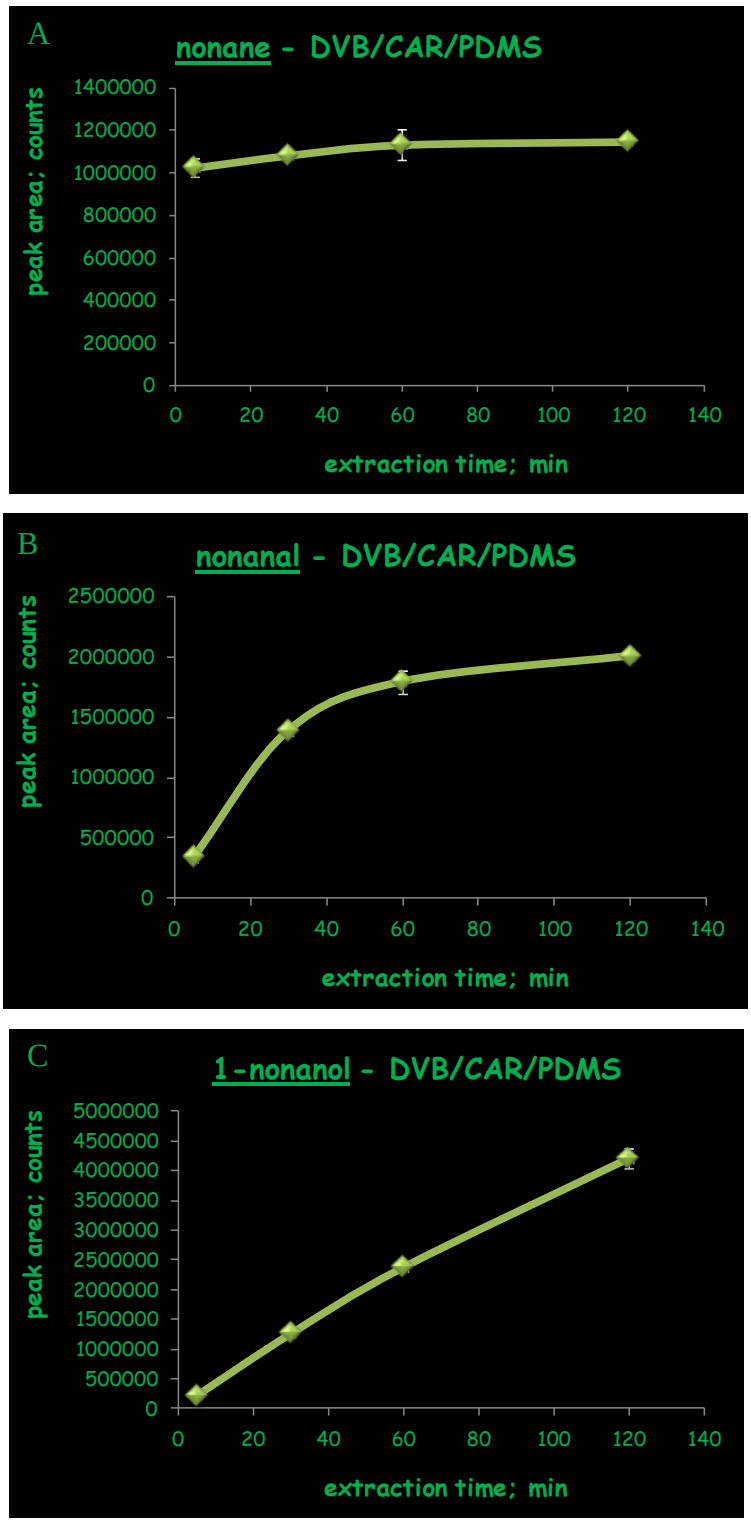

Figure 3.13. DVB/CAR/PDMS extraction time profiles of nonane (plot A), nonanal (plot B) and 1-nonanol (plot C).

3.4.6 *Determination of linear dynamic range*

Considering that extraction coverage and sensitivity of DVB/CAR/PDMS coating were optimum for the widest metabolite molecular weight range investigated, this coating was used for determination of linear dynamic range. The determination of linear dynamic range could encounter wide applicability in both targeted and discovery-based metabolomics studies, given the wide range of metabolite concentrations and considering the high water content in biological systems [8,165]. In quantitative studies, solid SPME coatings have frequently been criticized for poor linearity given the limited adsorption capacity and potential displacement of low K_{fs} compounds with high K_{fs} analytes at high extraction times in highly concentrated samples [95,166]. The objective here was to consider a wide range of metabolite concentrations and introduce high levels of high K_{fs} metabolites (despite the solubility issues) that potentially cause displacement in order to force coating saturation in a multi-component system. Consequently, 9-point calibration standard curves (same concentration ratios as implemented in coating evaluation mix, triplicate analysis per calibration point) were considered for 60 min HS-SPME extraction condition (linearity and repeatability (expressed in terms of % RSD, n=5 aqueous standards having metabolite concentrations that were employed in coating evaluation study) presented in Table 3.4).

Table 3.4. Determination of linear dynamic range (LDR, 9-point calibration curve, each point run in triplicates) and method repeatability for actual spiking metabolite concentrations employed in coating evaluation study for experimental design involving DVB/CAR/PDMS coating and 60 min HS-SPME extraction.

analyte name	range tested (pg/mL)	r^2	concentration (pg/mL)	repeatability (% RSD, n=5)
octane	0.7-1344	0.997	205	4.3
nonane	0.1-1425	0.998	217	2.9
undecane	0.1-1344	0.995	205	2.4
tridecane	0.1-1353	0.996	206	4.2
***alpha*-pinene**	0.1-1292	0.998	197	4.1

limonene	0.2-3207	0.997	489	1.9
(*Z*)-β-farnesene	83-169890	0.998	25908	2.7
(*E*)-β-farnesene	83-169890	0.996	25908	2.2
(*E,E*)-*a*-farnesene	83-169890	0.993	25908	3.3
2-hexanone	12-6225	0.999	949	2.7
2-heptanone	0.8-6574	0.997	1003	1.6
2-nonanone	0.4-6734	0.998	1027	1.5
2-undecanone	0.8-6764	0.996	1031	3.2
2-tridecanone	0.4-6725	0.992	1026	3.0
2-pentadecanone	2-27488	0.994	4192	4.4
2-heptadecanone	4-30358	0.918	9259	7.4
hexanal	0.4-6342	1.000	17096	2.5
heptanal	0.4-6545	0.999	967	2.1
octanal	0.4-6909	0.999	998	3.1
nonanal	0.4-6880	0.999	1054	2.4
undecanal	0.4-6764	0.996	1049	1.7
dodecanal	2-27229	0.995	1031	1.3
tridecanal	2-28393	1.000	4152	2.8
ethyl butanoate	14-6938	1.000	4330	5.8
ethyl heptanoate	1-6880	0.997	17687	1.8
ethyl nonanoate	1-7171	0.995	17687	2.5
ethyl undecanoate	1-9464	1.000	1058	1.5
ethyl tridecanoate	2-16989	0.994	1049	3.1
ethyl palmitate	9-37153	0.774	1094	10.9
ethyl stearate	154-39535	0.733	1443	8.1
1-pentanol	774-396233	1.000	2591	1.3
1-heptanol	162-83069	0.999	11332	3.7
1-nonanol	99-50724	0.998	12058	2.9
1-undecanol	3-49897	0.999	463	2.6
1-tridecanol	5-86598	0.997	50000	2.1
1-pentadecanol	163-167609	0.884	50000	6.8
1-heptadecanol	2732-174872	0.510	60426	10.0
2-pentanol	67-137285	0.947	12668	5.6
2-hexanol	149-76453	1.000	7735	1.6
2-octanol	53-27347	0.999	7609	1.2
2-dodecanol	2-29332	0.998	13206	1.8
2-hexadecanol	85-87017	0.896	51121	7.6
(*R*)-(-)-carvone	55-112107	0.996	53336	1.8
***cis*-citral; neral**	227-115982	0.996	20936	5.9

***trans*-citral; geranial**	57-115982	0.996	11659	8.1
eucalyptol	6-3039	1.000	4170	2.1
***cis*-linalool oxide**	640-327867	1.000	4473	2.6
***trans*-linalool oxide**	640-327867	0.999	26540	2.6
linalool	38-77719	0.998	11852	5.5
***trans*-geraniol**	2602-333109	0.993	50799	5.1
***cis, trans*-farnesol**	2859-365997	0.992	55815	15.6
(*Z,Z*)-farnesol	2859-365997	0.992	55815	16.8

As illustrated in Table 3.4, excellent linearity was obtained for the majority of compounds with the exception of highest molecular weight and most hydrophobic metabolites and 2-pentanol (calibration curves presented in Figure 3.14). For hydrophobic compounds, linearity was poor due to poor solubility in aqueous medium (in particular precipitation during dilution of spike) and competitive adsorption onto vial walls even when calibration points below solubility were considered for selected analytes (2-heptadecanone, 1-pentadecanol, 2-hexadecanol). However, in the case of 2-pentanol, representing one of the most polar, smallest molecular weight and $K_{fs}V_f$ analytes, coating saturation and displacement did take place in CAR/PDMS layer of DVB/CAR/PDMS coating above 69 ng/mL (linear regression coefficient 0.995 up to 69 ng/mL). In order to address non-linearity and increase SPME applicability in complex multi-component systems, a modification of extraction conditions was required and thus, the calibration curve was performed with 30 min HS-SPME extraction time. As a consequence, wider linear range (0.1-137 ng/mL) and excellent regression coefficient of 0.999 were obtained.

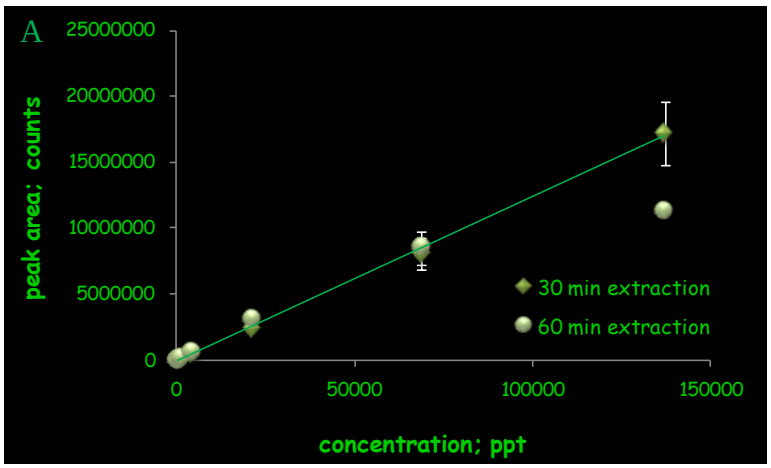
A
25000000
20000000
15000000
10000000
5000000
0
peak area; counts
30 min extraction
60 min extraction
0
50000
100000
150000
concentration; ppt

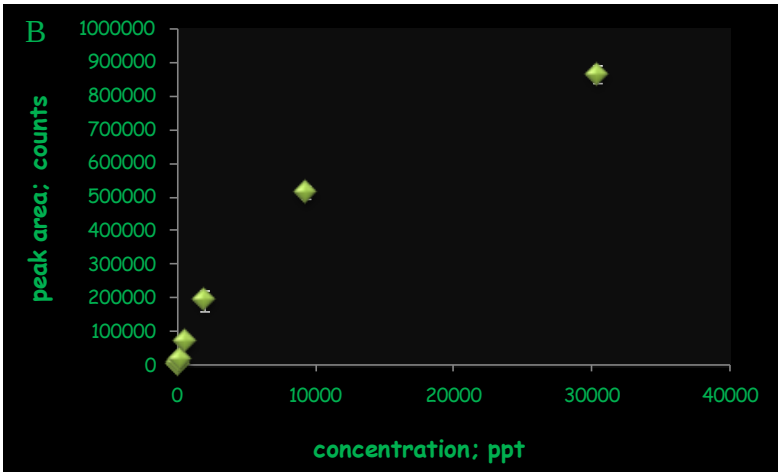
B
1000000
900000
800000
700000
600000
500000
400000
300000
200000
100000
0
peak area; counts
0
10000
20000
30000
40000
concentration; ppt

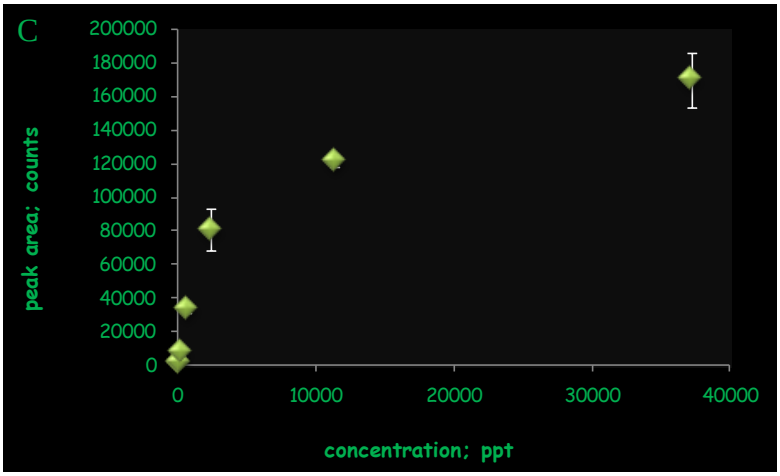
C
200000
180000
160000
140000
120000
100000
80000
60000
40000
20000
0
peak area; counts
0
10000
20000
30000
40000
concentration; ppt

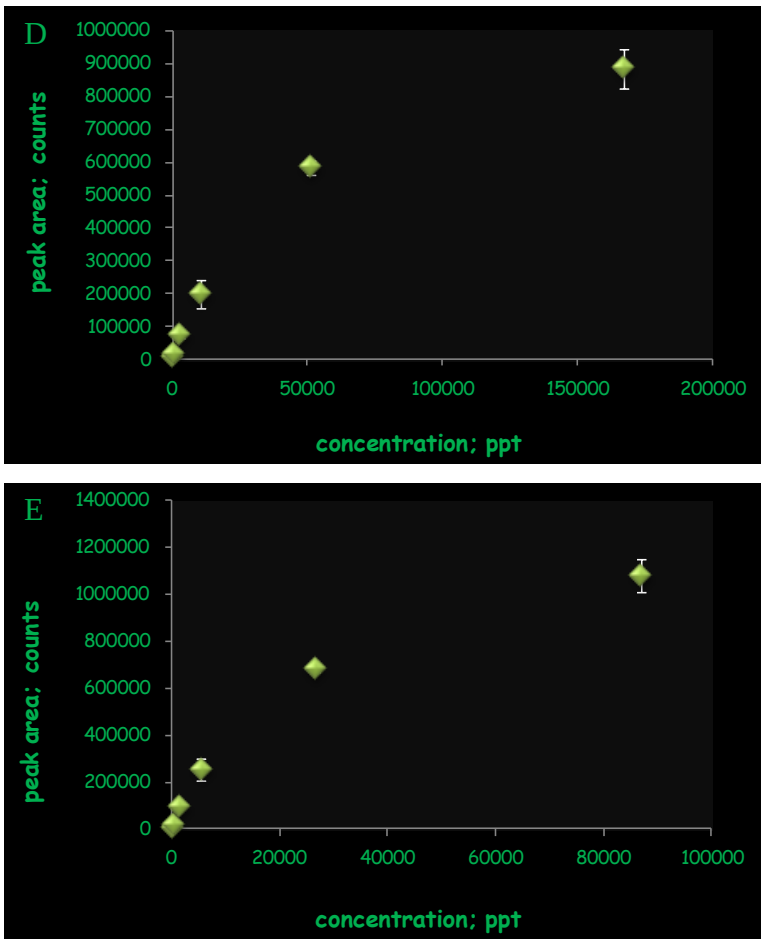

Figure 3.14. SPME calibration curves for 2-pentanol (plot A, 60 and 30 min extraction times employed), 2-heptadecanone (plot B), ethyl palmitate (plot C), 1-pentadecanol (plot D) and 2-hexadecanol (plot E) for aqueous samples spiked with 52 metabolites and analyzed with DVB/CAR/PDMS fibre coating.

As far as analysis of extremely heterogeneous and biochemically rich metabolomics samples is concerned, where the choice of sample preparation strategy is crucial for collection of interpretable data and visualization of interanalyte relationships, low SPME recovery for hydrophilic compounds and hydrophobic constituents' adsorption onto walls of extraction apparatus and organic matter should also result in minimization of displacement [100-101]. The competing phase which is in practice always present in different forms in real samples (humic material, proteins, polycarbohydrates, etc.) decreases free concentration of hydrophobic analytes to a significant extent such that undesirable displacement effect is likely reduced. On the other hand, more

hydrophilic components well dissolved in aqueous samples are expected to exist in higher free concentrations, but as demonstrated by the experimentally determined fibre constants in Table 3.3, they suffer from poor affinity towards the coating and are more likely to be displaced during competitive adsorption process. Nevertheless, in practice saturation (solid coating)/swelling (liquid coating) effects should be infrequent, but the concept requires further clarification and inclusion of real samples.

However, from the practical point of view, a more strict quality control procedure may be implemented at least in targeted metabolomics approaches to assure the system is free of such effects by introducing a small molecular weight (C_5 range or lower, having smaller molecular weight and K_{fs} than target metabolites) 'saturation' marker at different concentrations and monitoring the linearity for those types of metabolomics samples having variable composition. If a satisfactory linearity is not obtained, then the uptake of less volatile, hydrophobic and high K_{fs} analytes can be reduced by implementing shorter extraction time as demonstrated here for a multi-analyte system and by Gorecki et al. for a 6-component aqueous mixture composed of acetone, methyl isobutyl ketone, methyl ethyl ketone, 2-propanol, 2-methyl-2-propanol and tetrahydrofuran [167]. Alternatively, the uptake of 'displacing' analytes may be decreased and hence, inter-analyte displacement minimized by performing static SPME sampling as pointed out by Gorecki et al. [167]. For those compounds having large distribution constants, large amount of molecules has to be transferred through the headspace to the fibre coating and this results in long equilibration times especially when the conditions of mass transfer in the liquid phase are poor. Therefore, the implementation of static sampling attributes to longer equilibration times of analytes having large K_{fs}, while the analytes having small K_{fs} will still reach equilibrium in short times.

3.5 *Conclusions*

The wide volatility, hydrophobicity, polarity and molecular weight range of components considered in this systematic study allowed comprehensive evaluation of performance characteristics of commercial coatings in terms of extraction sensitivity, extraction selectivity and desorption efficiency. The $K_{fs}V_f$ data was generated for 52 components and four best performing coatings including PDMS, PA, PDMS/DVB and DVB/CAR/PDMS and the results demonstrated high quality log K_{fs} - log K_{ow} correlations. The results reported clearly indicate that current commercially available coatings exhibit poor-group type selectivity and that the magnitude of $K_{fs}V_f$ values is determined by analyte volatility and hydrophobicity rather than polarity of analytes and their specific interactions with the extraction phase. Alternatively, PA coating was slightly more selective in comparison to PDMS in the extraction of polar analytes, including 1-alcohols and 2-alcohols. Nevertheless, the magnitudes of the reported fibre constants for polar analytes are low in comparison to nonpolar compounds regardless of the coating type employed; hence, the development of novel extraction phase chemistries for improved extraction capacity of polar analytes is required. In addition, design of highly selective coatings more useful for direct and specific analysis requires reduction in the non-specific adsorption characteristics of current commercially available coatings. The implementation of DVB/CAR/PDMS coating resulted in a satisfactory overall extraction coverage and best extraction efficiency for the widest molecular weight range of examined analytes, the latter performance criterion translating into molecular weight threshold of up to 185 g/mol for which this coating provides best extraction capacity. Also, the determination of linear dynamic range with DVB/CAR/PDMS coating revealed that inter-analyte displacements were infrequent for a 52-component mixture; however, polar and low K_{fs} analytes, such as 2-pentanol, herein are likely to be displaced due to competitive adsorption. The implementation of shorter extraction times to minimize the

uptake of high K_{fs} ‘displacing’ compounds can extend method linearity and minimize displacements in multi-component mixtures.

4. *Ex vivo* headspace solid phase microextraction coupled with comprehensive two-dimensional gas chromatography – time-of-flight mass spectrometry for metabolite profiling in apples: Implementation of GCxGC structured separations for optimization of SPME procedure in complex samples

4.1 *Background and objectives of research*

In response to the ever increasing interest in development of reliable methods competent with obtaining a more complete and unbiased metabolomic snapshot for subsequent identification, quantification and profiling studies, the purpose of the current investigation was to test the feasibility of HS-SPME for fingerprinting of volatile and semivolatile metabolites in complex samples. In particular, the current study is focussed on the development and optimization of SPME – GCxGC-ToFMS methodology for metabolite profiling of apples (*Malus ×domestica* Borkh.). For the first time, GCxGC attributes in terms of molecular structure-retention relationships and utilization of two-dimensional separation space on orthogonal GCxGC setup were exploited in the field of SPME coating selection for complex sample analysis. Consequently, commercially available coatings were compared in terms of extraction selectivity and extraction sensitivity by considering a wider and more diverse spectrum of physicochemical properties of metabolites present in a complex biological system.

4.2 *Optimization of GCxGC column combination*

Most of the applications focussed on global screening of biochemically rich food and plant samples with GC instrumentation employ either non-polar (5%-

phenyl-methylpolysiloxane) or polar (polyethylene glycol) capillary columns for separation of constituents [39,44,46,49,60,70]. In the current study, Rxi-5SilMS column was employed in the first dimension volatility-based separation due to its good thermal stability, high upper temperature limit and low bleed as well as wide accessibility of literature RI libraries. In order to operate GCxGC system under two independent separation mechanisms, DB-17 and Supelcowax secondary dimension columns were tested to allow for polarity-based separation and specific analyte-stationary phase intermolecular interactions. Such a GCxGC system can be considered orthogonal considering that compounds are separated by two different retention mechanisms [79]. The benefits of 'reversed polarity mode' have also been realized in the GCxGC separation of food samples, particularly in achieving better overall chromatographic behaviour and separation of the polar sample constituents [79].

Peak apex plots corresponding to separation of apple constituents on GCxGC system employing the Rxi-5SilMS/DB-17 and Rxi-5SilMS/ Supelcowax column combinations following HS-SPME with DVB/CAR/PDMS coating are presented in Figure 4.1.

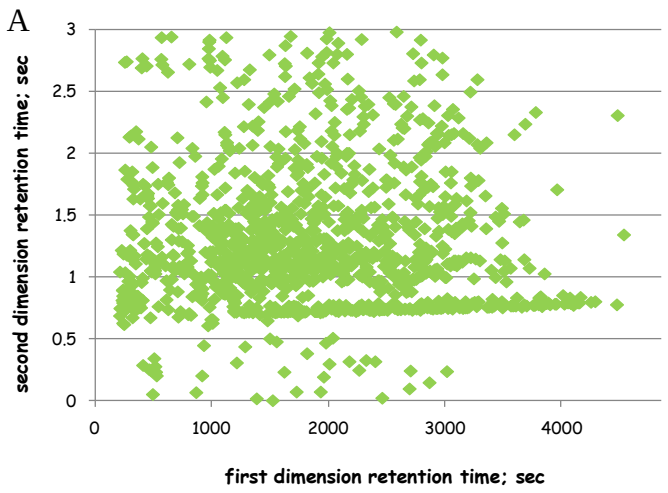

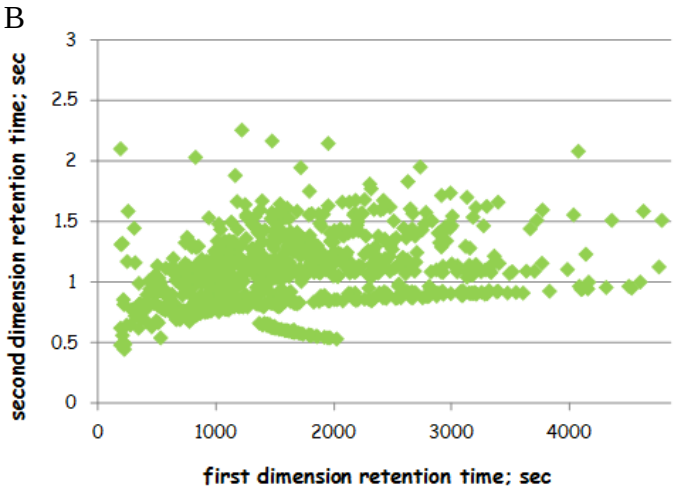

Figure 4.1. Peak apex plots corresponding to separation of apple constituents on GCxGC system employing the Rxi-5SilMS column in the first dimension separation and A – Supelcowax and B – DB-17 columns in second dimension.

As can be seen from the figure, widely differing separation profiles of volatile and semivolatile metabolites were obtained in the tested systems as a result of distinct analyte-stationary phase interactions. Overall, the employment of Supelcowax column in the second dimension resulted in more efficient exploitation of the available two-dimensional space. Considering the poor separation efficiency with DB-17 in the second dimension observed especially for analytes of mid- to high polarity, the overall 2D separation became rather unsatisfactory. On the other hand, the specific interactions with polyethylene glycol resulted in strong retention of polar metabolites, including 1-octen-3-ol, furfuryl acetate and phenylethyl alcohol with second dimension retention times of 2.855, 3.905 and 4.505 s, respectively, as compared to retention times of 1.055, 1.490 and 1.680 s, respectively, when DB-17 column was employed. With the employment of DB-17, chromatographic coelution in the first dimension was not compensated by the separation provided in the second dimension. This significantly affected the efficacy of automated ChromaTOF spectral deconvolution procedure to locate coeluting trace analytes and retrieve correct information on sample composition with minimum analyst supervision. For example, at a signal-to-noise (S/N) threshold value set at 50 for automated

peak finding and mass spectral similarity requirement of 800 ('unknowns' having lower match factors were filtered from the ChromaTOF peak table), the employment of Supelcowax and DB-17 resulted in detection of 1199 and 781 metabolite features.

4.3 *Extraction selectivity and sensitivity of commercial coatings in complex sample analysis*

The investigation of SPME coating performance was pursued by taking into account the extraction of constituents from a real complex sample in order to properly identify correlations between analyte structural properties and extraction selectivity. This was accomplished by taking advantage of the presence of structurally ordered GCxGC chromatograms obtained by employing two independent separation mechanisms in the two dimensions that enable recognition of the chemical patterns on the basis of retention time coordinates of detected analytes [84,86]. As such, the peak apex plots demonstrating GCxGC retention of extracted metabolites on available GCxGC separation plane as well as commercial SPME coating performance in terms of number of captured metabolite features (S/N and similarity thresholds 50 and 750, respectively) in real apple matrix extract are presented in Figures 4.2 and 4.3, respectively.

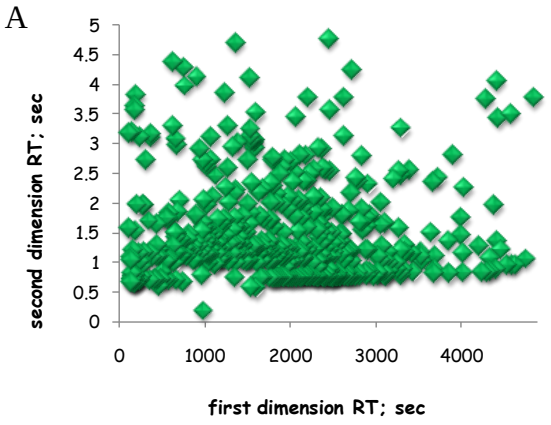

B

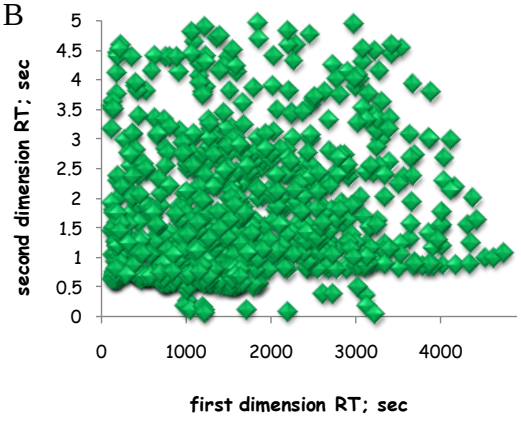
second dimension RT; sec
5
4.5
4
3.5
3
2.5
2
1.5
1
0.5
0
0
1000
2000
3000
4000
first dimension RT; sec

C

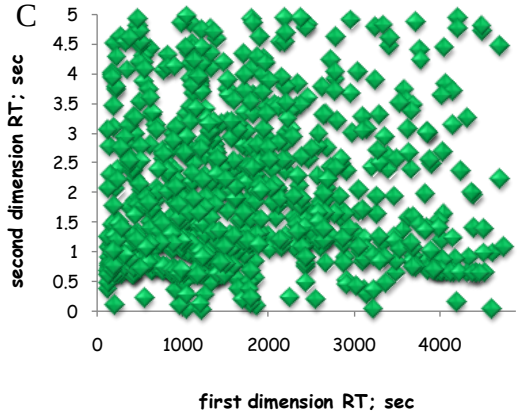
second dimension RT; sec
5
4.5
4
3.5
3
2.5
2
1.5
1
0.5
0
0
1000
2000
3000
4000
first dimension RT; sec

D

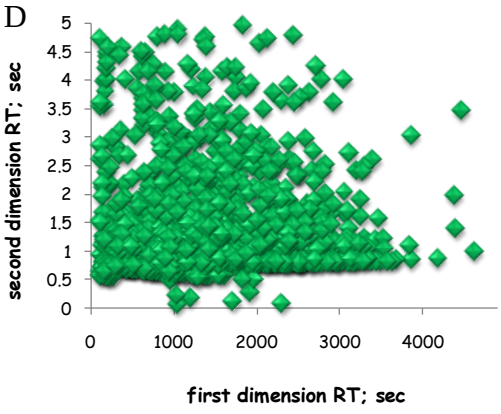
second dimension RT; sec
5
4.5
4
3.5
3
2.5
2
1.5
1
0.5
0
0
1000
2000
3000
4000
first dimension RT; sec

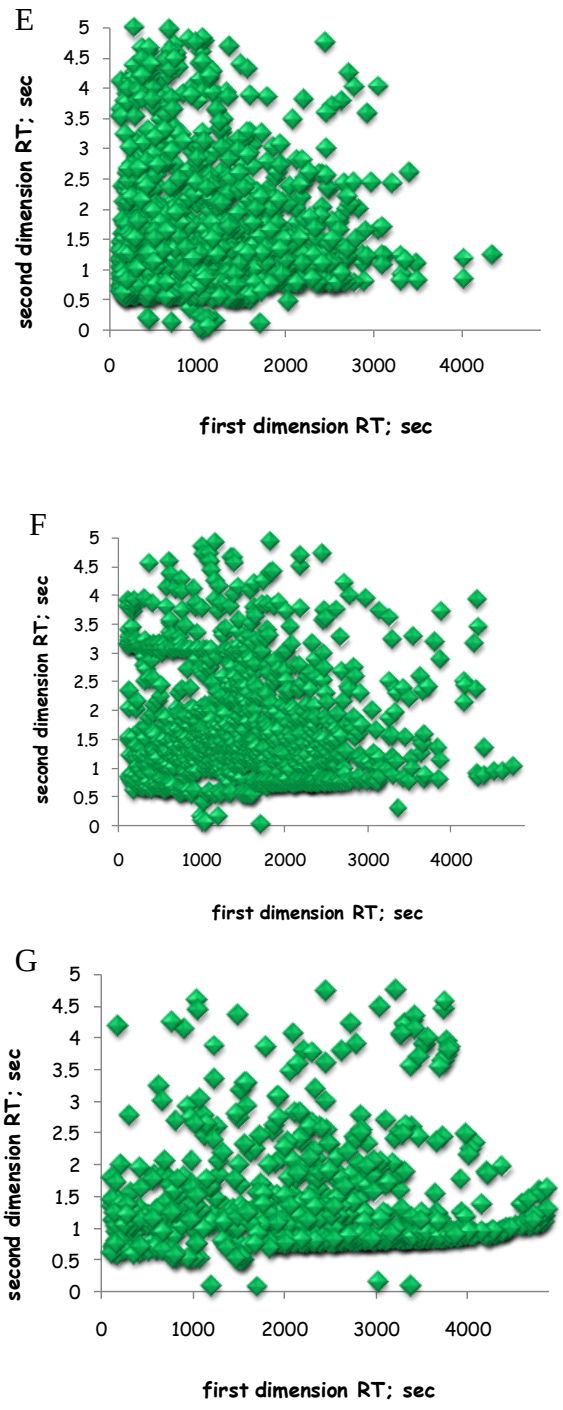

Figure 4.2. GCxGC peak apex plots generated from retention time coordinates of extracted metabolites by PDMS (plot A), PA (plot B), CW (plot C), DVB/CAR/PDMS (plot D), CAR/PDMS (plot E), PDMS/DVB (plot F) and carbopack Z/PDMS (plot G) coatings in real apple matrix. The peak finding algorithm was operated above S/N threshold of 50 and ChromaTOF peak tables

were manually filtered to exclude blank peaks and 'unknowns' for which library similarity match factor was lower than 750.

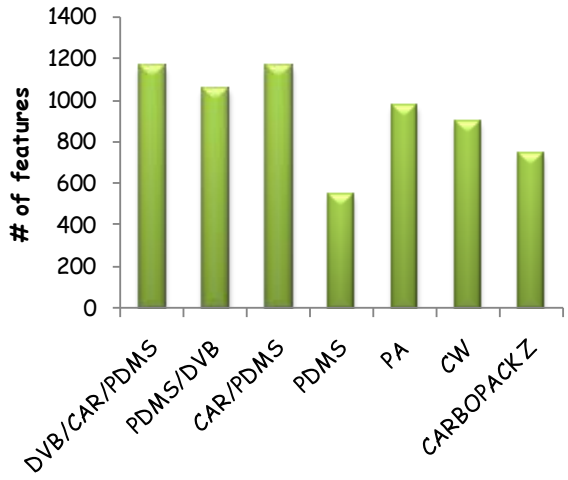

Figure 4.3. The comparison between coatings in terms of number of extracted metabolite features (similarity threshold 750).

Consequently, the implementation of PDMS, PA, CW, DVB/CAR/PDMS, PDMS/DVB, CAR/PDMS and carbopack Z/PDMS coatings resulted in the capturing of 549, 977, 897, 1163, 1053, 1167 and 745 metabolite features, respectively. It is evident from the presented data that selected SPME coatings (such as solid sorbents, including DVB/CAR/PDMS, PDMS/DVB and CAR/PDMS) are capable of providing a rich extraction coverage by capturing hundreds of chemically diverse metabolites for subsequent identification, quantification as well as sample fingerprinting approaches prevalent in the rapidly growing field of metabolomics. In order to eliminate peaks with lower mass spectral similarity factors and minimize potential misinterpretation of coating selectivities, the tables were post-processed to exclude metabolites having similarities lower than 800 and this resulted in 423, 648, 628, 830, 786, 723 and 461 features for PDMS, PA, CW, DVB/CAR/PDMS, CAR/PDMS, PDMS/DVB and carbopack Z/PDMS coatings (peak apex plots presented in

Figure 4.4 and plot illustrating the comparison of coatings in terms of number of captured metabolites presented in Figure 4.5).

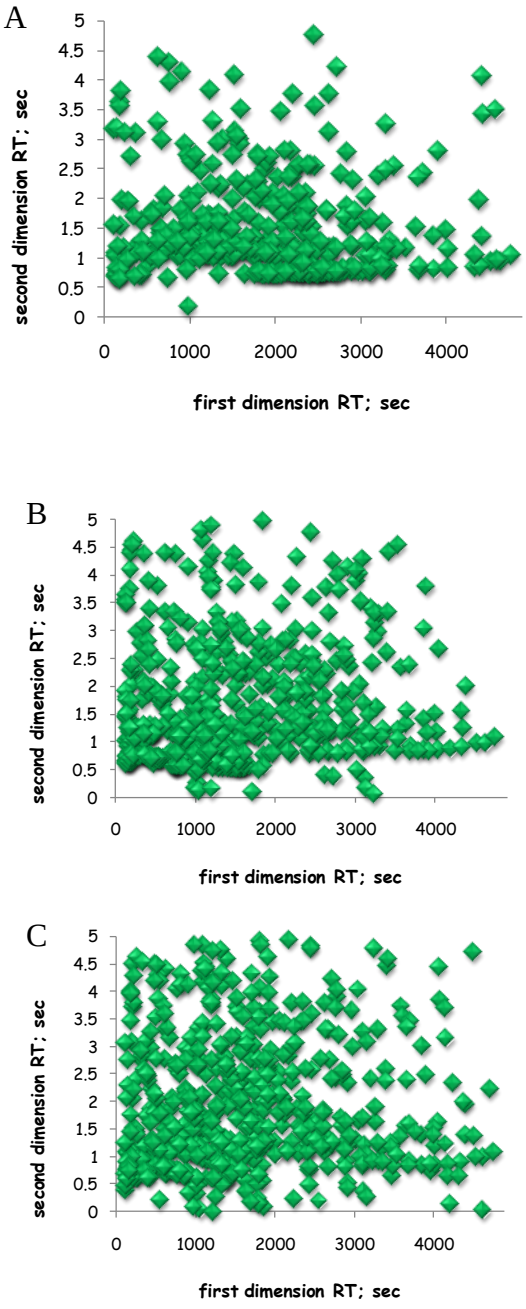

D

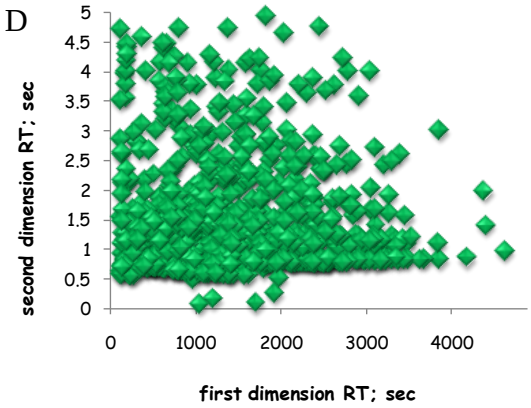
second dimension RT; sec
5
4.5
4
3.5
3
2.5
2
1.5
1
0.5
0
0
1000
2000
3000
4000
first dimension RT; sec

E

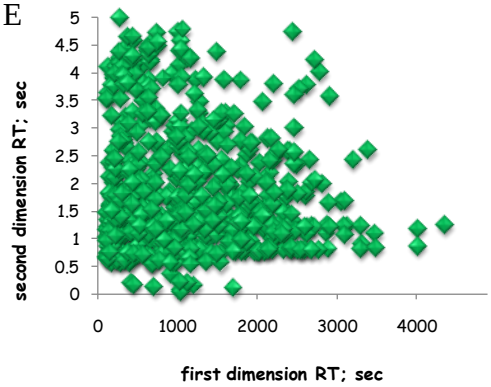
second dimension RT; sec
5
4.5
4
3.5
3
2.5
2
1.5
1
0.5
0
0
1000
2000
3000
4000
first dimension RT; sec

F

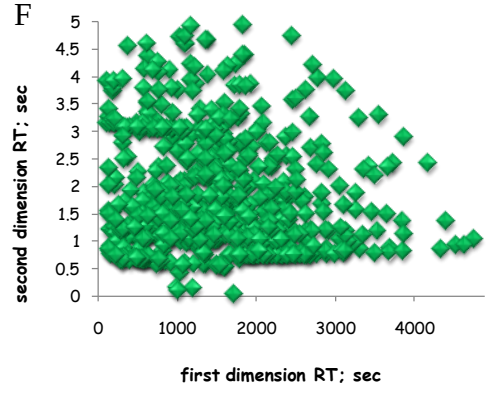
second dimension RT; sec
5
4.5
4
3.5
3
2.5
2
1.5
1
0.5
0
0
1000
2000
3000
4000
first dimension RT; sec

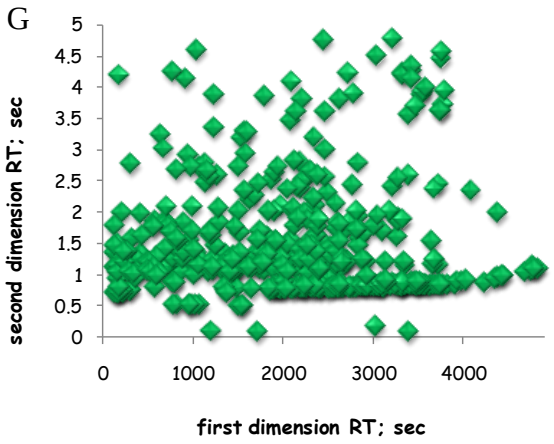

Figure 4.4. GCxGC peak apex plots generated from retention time coordinates of extracted metabolites by PDMS (plot A), PA (plot B), CW (plot C), DVB/CAR/PDMS (plot D), CAR/PDMS (plot E), PDMS/DVB (plot F) and carbopack Z/PDMS (plot G) coatings in real apple matrix. The peak finding algorithm was operated above S/N threshold of 50 and ChromaTOF peak tables were manually filtered to exclude blank peaks and 'unknowns' for which library similarity match factor was lower than 800.

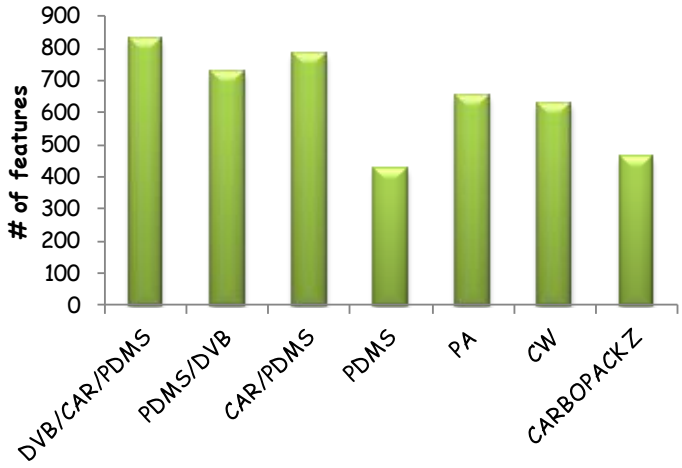

Figure 4.5. The comparison between coatings in terms of number of extracted metabolite features (similarity threshold 800).

Analyte structure-SPME coating selectivity trends are obvious on a polarity scale (second dimension axis) for liquid sorbents such as PDMS, PA and CW, the observation being consistent with spiked aqueous sample analysis. For

example, poor extraction coverage was observed for PDMS extraction phase when highly retained metabolites in the second dimension were concerned, whereas PA and CW coatings demonstrated better polar metabolite capture. Nonetheless, solid sorbents including DVB/CAR/PDMS, PDMS/DVB and CAR/PDMS, which consist of a solid material (porous polymer or porous carbon) suspended into a liquid polymer, exhibited coating-specific performance characteristics across the volatility range and boiling point scale (first dimension axis), which were independent of analyte polarity and can be interpreted in terms of adsorbent strength and desorption efficiency. These results are in agreement with the relevant extraction mechanism as the organic molecules are extracted based on physical trapping and the interaction of analyte with a solid particle [94-95]. Consequently, and in agreement with analysis of spiked water samples, coatings containing CAR/PDMS layer comprised of small micropores showed superior performance in volatile analyte capture as compared to PDMS/DVB.

A significant number of metabolite signatures were apparently captured by CAR/PDMS coating although the corresponding peak apex plot illustrates a high degree of discrimination against high-molecular weight metabolites (Figure 4.4e). A closer examination of filtered peak tables indicated that the highest apparent number of extracted metabolite features (Figure 4.2e and Figure 4.3) for this coating (first processing with similarity threshold of 750) resulted from multiple and replicate peak table entries corresponding to highly volatile metabolites. Considering the high sorbent strength and improved volatile analyte retention, the high extraction efficiencies for highly volatile analytes caused severe overloading of second dimension column and modulator and non-linear chromatography resulting in incorrect operation of ChromaTOF peak finding algorithm to locate individual overloaded peaks or those undergoing overloaded peak overlap. Figure 4.6 presents the zoomed-in sections for extracted ion chromatograms corresponding to modulated ethyl butanoate peak in spiked aqueous sample analysis illustrating the peak shapes for a representative volatile analyte obtained with DVB/CAR/PDMS and

CAR/PDMS coatings. It is clear that the slower desorption process from thicker CAR/PDMS layer of commercial CAR/PDMS coating distorts the peak shape for small molecular weight analytes and that significant peak tailing and broadening in first dimension was observed in obtained chromatograms [94-95]. This had the most extreme negative impact on nonpolar analytes, as the peak tailing in the first dimension resulted in poor chromatographic resolution and severe chromatographic overlap with slices of other coeluting non-polar compounds.

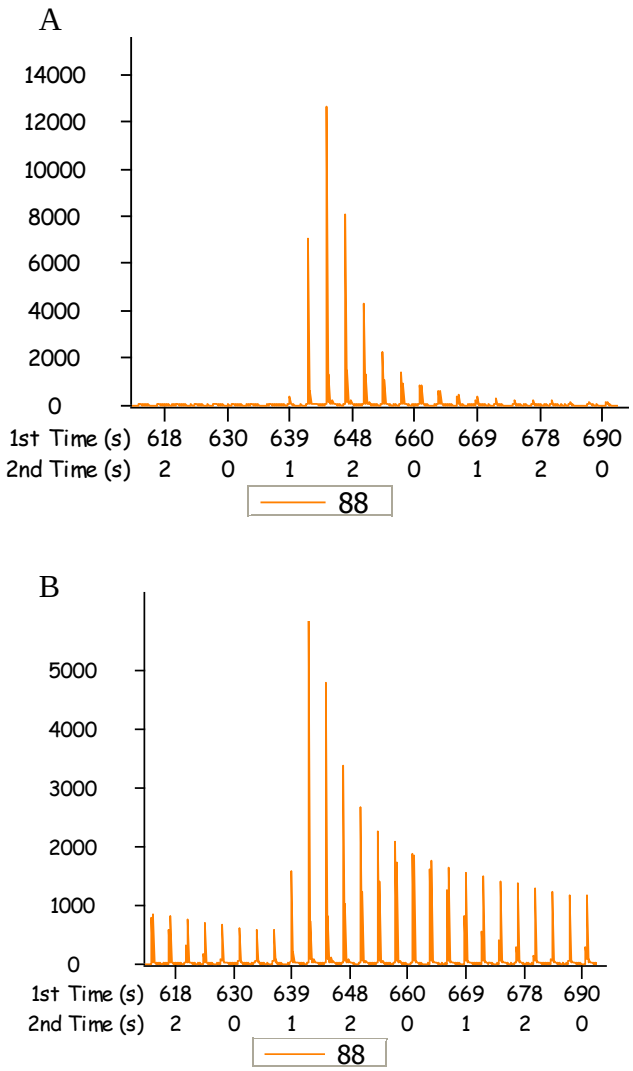

Figure 4.6. Extracted ion chromatogram corresponding to modulated ethyl butanoate peak illustrating the desorption efficiency obtained for

DVB/CAR/PDMS (plot A) and CAR/PDMS (plot B) coatings in spiked water sample analysis.

The plot presenting the comparison of commercial coatings in terms of precision (presented in Figure 4.7) also illustrates this effect to a certain extent. The loss of precision when employing carbon-based coatings, such as CAR/PDMS and carbopack Z/PDMS was detected, translating into the small number of analytes with precision between 0-5% and on the other hand, a significant number of peaks having precision of 10-20% and 20-35% (19 and 6 for CAR/PDMS and 20 and 4 for carbopack Z/PDMS for 10-20% and 20-35% RSD ranges, respectively). A more detailed interpretation of the data identifies these peaks as low-mid boiling point analytes, especially in the case of CAR/PDMS coating and in some cases with carbopack Z/PDMS coating.

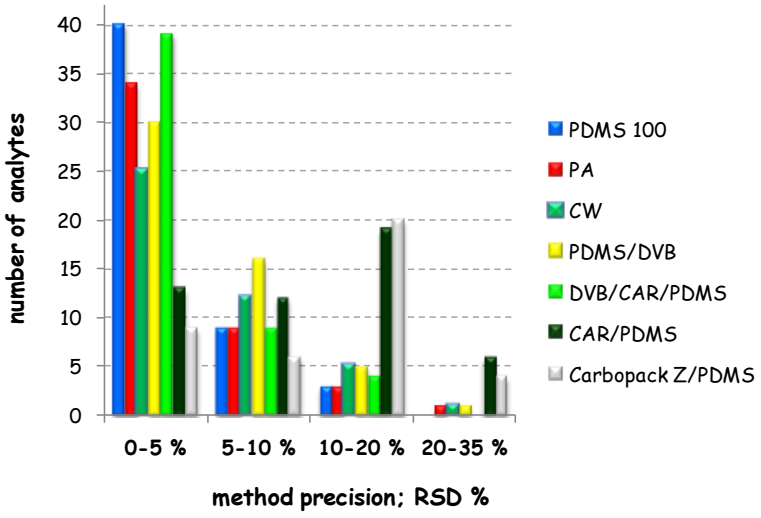

Figure 4.7. Precision of commercial coatings expressed in terms of relative standard deviation (RSD %, *n*=3) for spiked aqueous sample analysis.

In addition to peak apex plots, the extraction sensitivity and selectivity of commercially available coatings were also investigated for a group of 20 chemically diverse analytes (listed in Table 4.1 along with their physicochemical properties) that have been identified in existing literature as

being representative of highly polar compounds in food and/or correlated to particular food and apple quality traits (CAR/PDMS and carbopack Z/PDMS coatings were excluded from the comparison due to distorted one-dimensional peak profiles) [42,46,49,70,79,82].

Table 4.1. Selected metabolites identified and evaluated in HS-SPME extracts of apple samples and used for evaluation of SPME coating selectivity and sensitivity. Physicochemical properties and literature RI values were adapted from references [154-156]. The retention data reported for Rxi-5SilMS/DB-17 GCxGC column combination.

analyte name (synonym)	^1t_R: s	^2t_R: s	MW	log K_{ow}	*m/z*	RI_{exp}	RI_{lit}
2-Butenal	300	0.785	70.09	0.60	70	650	na
Benzaldehyde	944	1.530	106.12	1.71	106	964	964
1-Octen-3-ol	988	1.055	128.21	2.60	57	979	978
6-Methyl-5-hepten-2-one	1000	1.220	126.20	2.06	108	983	986
Benzonitrile	1004	1.670	103.12	1.54	103	985	983
2-Furanmethanol, acetate (Furfuryl acetate)	1024	1.490	140.14	1.10	81	992	996
(2E,4E)-2,4-Heptadienal	1084	1.340	110.15	1.86	81	1012	1013
1-Methyl-4-(1-methylethyl)-benzene (para-Cymene)	1108	1.135	134.22	4.00	119	1021	1025
Benzenemethanol (Phenylmethanol)	1156	1.685	108.14	1.08	79	1037	1040
Benzeneacetaldehyde (Phenyl acetaldehyde)	1180	1.685	120.15	1.54	91	1045	1045
(3E)-3,7-Dimethyl-1,3,6-octatriene (trans-β-Ocimene)	1184	1.025	136.23	4.80	93	1047	1046
5-Ethyldihydro-2(3H)-furanone (gamma-Hexalactone)	1212	2.315	114.14	0.60	56	1056	1060
1-Phenylethanone (Acetophenone)	1248	1.655	120.15	1.67	105	1068	1068
Benzeneethanol (Phenylethanol)	1388	1.680	122.16	1.57	91	1116	1113
1-Methoxy-4-(2-propenyl)benzene (Estragole)	1632	1.420	148.20	3.47	148	1200	1201
(2E,4E)-2,4-Nonadienal	1680	1.300	138.21	2.84	81	1217	1218
5-Butylhydro-2(3H)-furanone (gamma-Octalactone)	1792	1.760	142.20	1.59	85	1258	1263
(2E)-1-(2,6,6-Trimethyl-1,3-cyclohexadien-1-yl)-2-buten-1-one ((E)-β-Damascenone)	2124	1.410	190.28	4.21	69	1383	1379
(5E)-6,10-Dimethyl-5,9-undecadien-2-one (Geranyl acetone)	2292	1.265	194.31	4.36	69	1450	1450
4-(2,6,6-Trimethyl-1-cyclohexen-1-yl)-3-buten-2-one (β-Ionone)	2376	1.390	192.30	4.42	177	1484	1490

Results of the extraction sensitivity data are presented in Figure 4.8. In addition to the coating-specific boiling point scale distribution for solid coatings and the basic selectivity trends along the polarity scale for liquid sorbents,

several additional interesting points were identified here. Thus, despite the fact that solid coatings are characterized by high adsorbent capacity and retention capability for volatile compounds and that their extraction efficiencies are dependent on analyte size, the results presented in Figure 4.8 indicate that rewarding SPME enrichments were obtained with PA fibre coating for substituted aromatic compounds including benzaldehyde, benzonitrile, phenylmethanol and acetophenone with molecular weights of 106.12, 103.12, 108.14 and 120.15 g/mol, respectively, as the use of this phase provided comparable and in some cases significantly better extraction efficiencies as compared to solid adsorbents. Clearly, this violates molecular weight distribution presented in Chapter 3 and it illustrates that in addition to molecular weight considerations, the size and shape of the molecule represents a significant criterion in the outcome of the coating selection process. In this particular case, poor recoveries for solid adsorbents including DVB/CAR/PDMS and PDMS/DVB may be attributable to strong interactions of investigated analytes with adsorbent surface to the extent that these analytes are not desorbed efficiently. However, with the increasing size of the substitution group, the degree of analyte-adsorbent interaction decreases such that for representative analytes including benzeneacetaldehyde and phenylethanol, comparable extraction efficiencies between solid adsorbents and PA extraction phase were achieved. Based on the results presented in Figures 4.4, 4.5 and 4.8, DVB/CAR/PDMS coating still provided the most balanced coverage and the highest number of captured metabolite signatures, and was therefore adopted for future analyses.

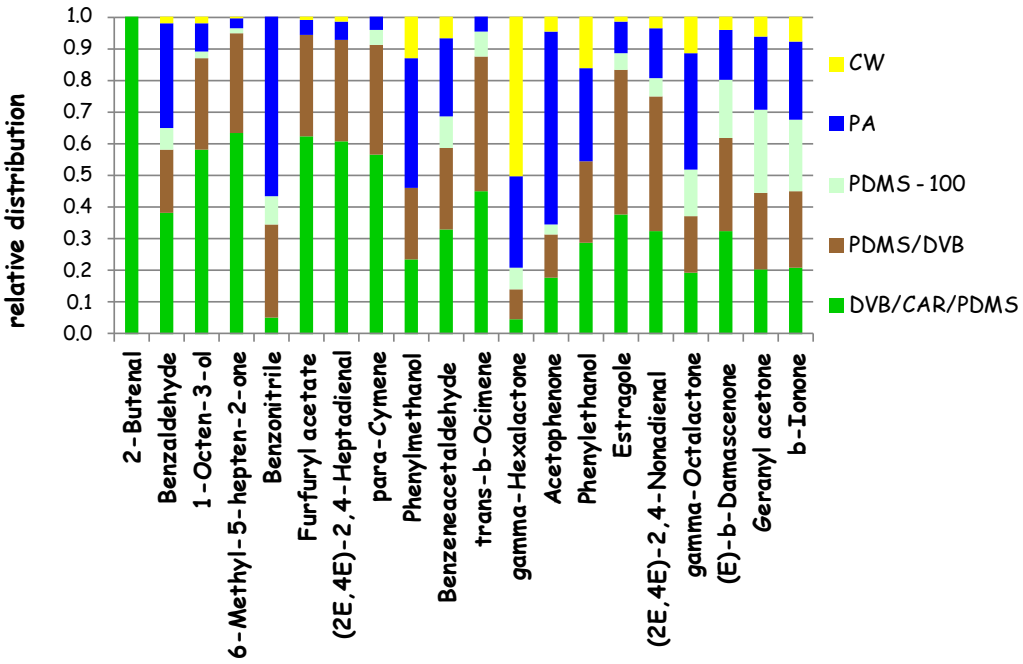

Figure 4.8. The comparison of commercial SPME coatings in terms of extraction efficiency and selectivity for representative volatile and semivolatile metabolites extracted from apple samples. The extracted responses were normalized with respect to extraction enrichment obtained with DVB/CAR/PDMS coating.

4.4 *Concluding remarks on SPME coating selection and how it impacts quality of GCxGC data*

Given a high degree of discrimination against high-molecular weight analyte capture and tailing one-dimensional peak profile that are both attributed by ineffective desorption, CAR/PDMS coating is not a good candidate for SPME-GCxGC hyphenation. Considering the poor mass spectral quality for individual slices corresponding to tailing one-dimensional peak profile, the latter manifestation results in inability of automated software to correctly construct one-dimensional peaks. Hence, the combination of second dimension peaks corresponding to a particular one-dimensional entity requires manual intervention, and in most extreme cases, quantitative representation of one-

dimensional peaks corresponding to volatile analytes is neither precise nor accurate. The peak shapes for these early eluting compounds desorbed from this strong sorbent could be improved by using a higher capacity stationary phase and a sufficiently low initial column temperature to effectively retain and focus these analytes [168]. However, considering the absence of solvent effects for beneficial band focussing in SPME analysis, volatile compounds are much more difficult to focus at the column head and slow desorption and transfer to the column lead to even more severe band broadening, as reported in this study. The use of this coating may still be considered for one-dimensional GC-MS applications, provided the effect of tailing on the detection of minor constituents can be resolved with the use of mass spectrometry as additional separation dimension. However, the implementation of this coating in GCxGC applications defeats the purpose of preserving the first dimension separation which is facilitated by careful adjustment of modulation period and oven programming rate settings in order to modulate first dimension peak at least four times. In the case of carbopack Z/PDMS coating, non-Gaussian tailing and broadening peak profiles for small-mid boiling point analytes for which the coating was unselective anyways possibly due to the small degree of microporosity (pore size approximately 100 Å) were observed in addition to at least two peak maxima per selected early eluting chromatographic peaks. A similar trend was observed by Poerschmann et al. during the temperature programmed desorption from 7-µm PDMS fibre coatings as they noted the presence of two 'desorption humps' per chromatographic peak [159]. These observations also limit the applications of this coating in SPME-GCxGC analysis.

The results obtained clearly indicate that the selection of particular SPME conditions, including the choice of extraction phase, has a dramatic impact on the outcome of GCxGC-ToFMS analysis. In particular, improper parameter settings for both techniques can result in lower chromatographic resolution and overall distortion of the generated chromatograms. For example, under a fixed/optimum set of GCxGC experimental settings that affect

resolution obtained in the first dimension including those corresponding to temperature programming rate and modulation period, the ineffective SPME injection accompanied by additional band broadening and poor desorption efficiency (as in the case of CAR/PDMS) can sacrifice the resolution advantages in GCxGC. Under those circumstances, for compounds having similar boiling points, the analyte fractions corresponding to tailing one-dimensional peak profile will be combined during each modulation cycle with the consequence of partially losing resolution already achieved in the first dimension separation. In addition, it is worth mentioning that GCxGC-ToFMS features in terms of two-dimensional separation space coverage obtained on orthogonal setup and molecular structure retention relationships seem to offer valuable tools for evaluation of extraction sensitivity and selectivity of future extraction phase chemistries. Considering the fact that selected SPME coatings extract large numbers of physicochemically diverse metabolites, the ability to relate the positions of peaks in the 2D separation plane to the trends in chemical properties of the sample set is perhaps the most important underlying characteristic of SPME-GCxGC-ToFMS hyphenation. As such, simply the choice of a suitable stationary phase in the second dimension and column ensemble specifically capable of targeting molecular properties of investigated sample leads to the desired separation selectivity in GCxGC-ToFMS. Thus, the conjunction with nonselective characteristics of currently available SPME extraction phases attributes to accomplishing the full characterization of the entire sample as the ultimate objective of metabolomics studies and provides an insightful and more easily interpretable approach to the optimization of SPME efficiency controlling parameters. On the other hand, the increased sensitivity attainable by GCxGC through zone compression provides the ability to comprehensively examine secondary chromatography effects that are often manifested by isovolatility and streaking curves arising from the tailing nature of the peaks for analytes that are, for example, slowly released from the injector and products of decomposition reactions [169]. Thus, the tailing nature of the one-dimensional peak profile in secondary chromatography instances whose

origins can be effectively studied with GCxGC as opposed to a traditional GC experiment where it is expected to be manifested by a raised baseline, can be employed to facilitate the characterization of new coatings in terms of desorption efficiency and the stability of components that they extract.

In addition, based on these and results obtained in Chapter 3 for a 52-component system, new advancements should be encouraged in the area of SPME coating development given the poor selectivity of existing coatings. Poor selectivity requires instruments offering a high number of separation dimensions, such as GCxGC-ToFMS for global metabolomics, although as pointed out by Chin et al. this may present significant drawbacks in developments of odour-driven analytical identification systems incorporating GC-olfactometry and GCxGC [170]. In such circumstances, poor selectivity of sample preparation procedure combined with numerous chromatographic coelutions in the first dimension makes the identification of potent odourants be a challenging task, even with the implementation of GCxGC-ToFMS [170]. Nevertheless, the nonselective adsorption characteristics of coatings such as DVB/CAR/PDMS aid in less biased and more comprehensive characterization of metabolome and hence, should open up unique opportunities in advanced fingerprinting of biological systems.

5. *Ex vivo* headspace and direct immersion solid phase microextraction in advanced metabolite fingerprinting of apples

5.1 *Background and objectives of research*

In this study, HS-SPME extraction time profiles were conducted on a complex sample such as apple homogenate in order to provide additional experimental supporting evidence on the potential presence of inter-analyte displacements in complex biological mixtures and to find potential correlations between analyte physicochemical properties and occurrence of displacements. Adopting apple as a sample matrix is advantageous in such an investigation due to the natural occurrence of a number of high K_{fs} metabolites including esters and sesquiterpene hydrocarbons that are present in high concentrations and characterized by high hydrophobicities and high Henry's constants which attribute to their high headspace concentrations. Consequently, a thorough and comprehensive examination of inter-analyte displacements was carried out by performing global evaluation of extraction time uptakes for identified metabolites present both in trace and high concentration levels in the system under investigation. Understanding displacements in HS-SPME is not only important for broadening the scope of scientific knowledge but also in the area of implementation of HS-SPME during quality controlled analysis of metabolomics samples since robustness of commercially available coatings during direct immersion exposure has not been actively studied. Also, considering that the performance of global metabolomics studies necessitates quality controlled analysis conditions and analysis of pooled extracts from high number of biological replicates, understanding the complex inter-analyte interactions during adsorption onto solid extraction phase in the HS-SPME process is necessary.

In addition to examination of inter-analyte displacements, the current study also aimed to compare metabolite coverage during *ex vivo* HS-SPME and DI-SPME extraction modes in order to identify the route toward less biased and more complete description of metabolome. The attributes of coupling SPME to GCxGC-ToFMS and advantages of such multidimensional analytical approach were also addressed.

5.2 *HS-SPME analysis of apple homogenate with DVB/CAR/PDMS fibre coating: occurrence of inter-analyte displacements in complex mixtures*

Data processing strategy employed included the automated data processing with peak finding algorithm operated at and/or above S/N ratio of 50. Peak tables generated in this way were post-processed to eliminate peaks with mass spectral match factors lower than 800 which resulted in reduction of data dimensionality from 5118 peaks to 1040 peaks. The peak table was submitted to further data reduction by sorting peaks according to S/N and eliminating blank peaks as well as those originating from column and extraction phase bleed. Consequently, starting from highest to lowest S/N ratio, manual peak picking was conducted in order to label peaks according to quality of peak shapes and accuracy in quantification which was affected by quality of chromatographic separation, modulator effectiveness and ability of automated deconvolution software to deconvolute spectra of chromatographically coeluting peaks. In total, the final evaluation included 153 compounds including *i)* 134 major components that were either present in high concentrations or exhibit high HS-SPME selectivity and with S/N ratio ranging from 128259 for ethyl butanoate to 1003.5 for (2E,4E)-2,4-octadienal; *ii)* 14 minor compounds that were either present in trace levels in the sample matrix and/or exhibit poor HS-SPME selectivity and having S/N ratios ranging from 129 for benzophenone to 75 for ethyl citrate; *iii)* two components including 2-

methylbenzaldehyde and (2Z)-2-penten-1-ol that were manually selected on the basis of high retention in the second dimension and relevance to representative polar compounds in food matrix; and *iv)* 3 components including 2-pentanol, linalool and 1-nonanol that were evaluated in a 52-component aqueous sample mixture from Chapter 3. Figure 5.1 illustrates peak apex plot with retention time coordinates of evaluated analytes and Table 5.1 lists the names of analytes evaluated along with their retention time coordinates, experimental and literature RI values, mass spectral similarity and S/N ratio.

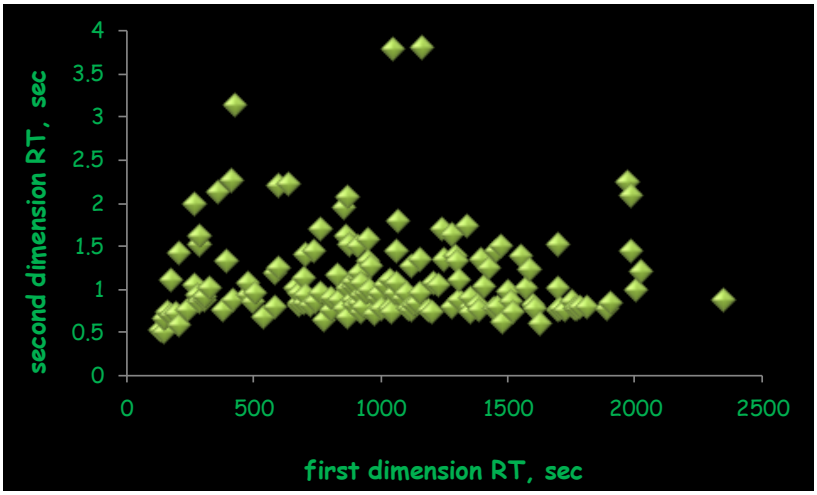

Figure 5.1. Peak apex plot demonstrating retention time coordinates of evaluated compounds in global extraction time profile evaluation.

Table 5.1. The list of metabolite names included in global processing of HS-SPME extraction time profiles. Also included are the first and second dimension retention time coordinates, experimental and literature RI values, mass spectral similarity (SIM) and quantification ions.

analyte name (synonym)	^1t_R; s	^2t_R; s	RI_{exp}	RI_{lit}	SIM	*m/z*
Acetaldehyde	140	0.510	na		963	42
1-Pentene	152	0.480	na		857	42
2-Propenal	152	0.635	na		931	56
2-Methyl-2-propanol	164	0.720	na		936	59
1-Propanol	176	1.100	na		911	59
2-Methylpropenal	180	0.675	na		939	70
Ethyl Acetate	200	0.710	608	618	952	61

1-Methoxybutane (Butyl methyl ether)	208	0.560	617	616	908	45
2-Methylpropanol (Isobutanol)	212	1.405	621	626	914	33
2-Methylbutanal	244	0.745	654	659	905	58
1-Penten-3-ol	268	1.975	679	682	854	67
1-Penten-3-one	272	1.040	683	683	882	55
Pentanal (Valeraldehyde)	284	0.915	696	695	956	58
2-Ethylfuran	288	0.845	700	702	883	81
3-Pentanol	292	1.505	702	703	878	59
2-Pentanol	292	1.610	702	700	902	45
Ethyl propanoate	308	0.850	710	707	915	57
Propyl acetate	312	0.895	713	712	933	61
Butyl formate	332	0.995	723	737	922	56
2-Methylbutanol	364	2.120	740	731	950	70
1-Chloropentane	384	0.735	750	754	892	70
(2E)-2-Pentenal	400	1.305	758	751	908	83
1-Pentanol	416	2.250	767	759	948	55
2-Methylpropyl acetate (Acetic acid, 2-methylpropyl ester)	424	0.850	771	768	932	73
(2Z)-2-Penten-1-ol	428	3.120	773	767	876	57
Ethyl butanoate	480	0.910	800	803	931	88
Hexanal	480	1.050	800	801	845	82
Propyl propanoate	500	0.840	809	814	970	75
1-Methoxyhexane (Methyl hexyl ether)	540	0.665	826	832	888	56
Ethyl 2-methylbutanoate (Butanoic acid, 2-methyl-, ethyl ester)	592	0.775	849	842	957	102
(2E)-2-Hexenal (Leaf aldehyde)	592	1.175	849	850	894	83
Butyl acetate	512	0.940	814	819	947	61
(2Z)-2-Hexenal [a]	600	1.235	853	852	944	83
(3Z)-3-Hexen-1-ol (Leaf alcohol)	604	2.195	854	853	882	67
1-Hexanol	644	2.205	872	867	942	69
4-Pentenyl acetate (5-Acetoxy-1-pentene)	672	0.995	884	890	882	68
2-Methylbutyl acetate (1-Butanol, 2-methyl-, acetate)	684	0.805	889	873	945	70
2-Butylfuran	684	0.825	889	894	850	81
2-Heptanone	684	0.945	889	898	921	58
Propyl butanoate	704	0.815	898	895	944	101
(4Z)-4-Heptenal	704	1.110	898	902	935	84
Heptanal	712	0.925	902	906	944	55
2-Heptanol	712	1.390	902	913	945	45
Butyl propanoate	728	0.810	909	910	844	75
Methoxybenzene (Anisole)	744	1.430	917	918	946	108
Pentyl acetate	748	0.845	919	915	935	61
Hexyl formate	768	0.930	928	929	946	56
(2E,4E)-2,4-Hexadienal (Sorbic aldehyde)	768	1.675	928	914	936	81
alpha-Pinene (2,6,6-Trimethyl-bicyclo[3.1.1]hept-2-ene)	780	0.625	933	933	920	93
Propyl 2-methylbutanoate (Butanoic acid, 2-methyl-, propyl ester)	808	0.750	946	942	915	103
unidentified component (hit # 1 (Z)-3-Methyl-2-pentene)	808	0.885	946	na	802	84

(2E)-2-Heptenal	832	1.145	957	956	927	83
1-Ethyl-3-methylbenzene (m-Ethyltoluene)	840	0.855	961	963	920	105
(4E)-4-Hepten-1-ol	860	1.945	970	na	855	81
3-Methylbutyl propanoate (1-Butanol, 3-methyl-, propanoate)	864	0.765	972	969	942	57
1-Heptanol	868	1.595	974	970	926	70
Benzaldehyde (Phenyl methanal)	872	2.055	976	964	951	106
2,2,6-Trimethylbicyclo(3.1.1)hept-2-ene (beta-Pinene)	876	0.660	978	978	845	93
1-Octen-3-one	876	0.990	978	980	899	70
1-Octen-3-ol	884	1.515	981	978	948	57
3-Octanone	892	0.865	985	986	902	72
2,3-Octanedione	892	1.020	985	986	808	99
6-Methyl-5-hepten-2-one	892	1.075	985	986	946	108
2-Pentylfuran (2-Amylfuran)	904	0.795	991	991	951	81
6-Methyl-5-hepten-2-ol (Sulcatol)	912	1.490	994	995	920	95
Ethyl hexanoate	920	0.815	998	1003	894	88
cis-2-Cyclooctenol	920	1.110	998	na	819	126
3-Octanol	920	1.170	998	999	942	59
Isobutyl 2-methylbutanoate (Butanoic acid, 2-methyl-, 2-methylpropyl ester) [a]	928	0.720	1002	1004	867	85
Octanal	928	0.915	1002	1006	952	84
(1-Methoxyethyl)benzene (1-Phenylethyl methyl ether)	928	1.050	1002	na	867	121
Pentyl propanoate	936	0.790	1006	1006	919	75
Hexyl acetate	948	0.935	1012	1000	923	73
(2E,4E)-2,4-Heptadienal	952	1.560	1014	1013	916	81
1,2-Dichlorobenzene	956	1.310	1016	1022	922	146
1,2,3-Trimethylbenzene (Hemimellitene)	964	0.970	1020	1023	849	105
1-Methoxy-4-methylbenzene (p-Methylanisole)	968	1.260	1022	1022	909	122
1-Methyl-4-(1-methylethenyl)cyclohexene (Limonene)	984	0.700	1030	1030	931	68
2,2,6-Trimethylcyclohexanone	996	0.885	1036	1035	845	82
unidentified component (hit # 1 2-Propylphenol)	1004	0.935	1040	na	832	107
Butyl 2-methylbutanoate	1008	0.760	1042	1042	915	130
(2Z)-2-Octenal [a]	1020	1.040	1048	1046	na	83
2-Methylbutyl butanoate (Butanoic acid, 2-methylbutyl ester)	1040	0.755	1058	1060	922	71
(2E)-2-Octenal	1040	1.095	1058	1059	951	70
1-Chlorooctane	1048	0.720	1062	1064	924	91
alpha-Methylbenzenemethanol (alpha-Phenylethanol)	1056	3.770	1066	1061	850	107
(1,1-Dimethylethoxy)-benzene (tert-Butoxybenzene)	1060	0.945	1068	1074	933	94
cis-5-Ethenyltetrahydro-à,à,5-trimethyl-2-furanmethanol (cis-Linalool oxide)	1068	1.065	1072	1069	878	94
1-Octanol	1068	1.435	1072	1076	937	56
2-Methylbenzaldehyde	1072	1.775	1074	1067	895	91
2-Ethyl-1,3-dimethylbenzene	1092	0.875	1084	1097	912	119
1,3,3-Trimethylbicyclo[2.2.1]heptan-2-one (Fenchone)	1104	0.930	1090	1090	917	81
Propyl hexanoate	1112	0.770	1094	1094	837	99
3,7-Dimethyl-1,6-octadien-3-ol (Linalool)	1124	1.250	1100	1101	854	93
2-Methylbutyl 2-methylbutanoate (Butanoic acid, 2-methyl-, 2-methylbutyl ester)	1128	0.740	1102	1104	913	85

Hexyl propanoate	1132	0.795	1104	1106	923	84
Heptyl acetate	1144	0.820	1111	1114	892	61
unidentified component (hit # 1 1-Methyl-3-(1-methylethyl)-benzene (m-Cymene))	1160	0.935	1120	na	879	119
(2E,4E)-2,4-Octadienal	1160	1.330	1120	1113	873	81
Phenylethyl Alcohol (Benzeneethanol, 2-Phenylethanol)	1168	3.800	1124	1117	842	91
Pentyl 2-methylbutanoate (Butanoic acid, 2-methyl-, pentyl ester) [b]	1192	0.735	1138	1126	905	103
Hexyl 2-methylpropanoate (Propanoic acid, 2-methyl-, hexyl ester)	1208	0.730	1147	1150	920	89
1,7,7-Trimethylbicyclo[2.2.1]heptan-2-one (Camphore)	1212	1.060	1149	1145	924	95
(2E)-2-Nonenal	1236	1.035	1162	1163	898	83
Benzyl acetate (Phenylmethyl acetate)	1244	1.685	1167	1167	923	108
1-Nonanol	1256	1.320	1173	1176	929	70
Butyl hexanoate	1284	0.785	1189	1193	899	117
Naphthalene	1288	1.630	1191	1191	946	128
alpha,alpha,4-Trimethyl-3-cyclohexene-1-methanol (alpha-Terpineol)	1300	1.360	1198	1195	927	59
1-Methoxy-4-(2-propenyl)benzene (Estragole)	1304	1.315	1200	1201	975	148
Decanal	1316	0.865	1207	1208	955	57
1-Methoxy-4-propylbenzene (4-Propylanisole, Dihydroanethole)	1316	1.100	1207	1207	859	121
3,5-Dimethylbenzaldehyde	1348	1.715	1226	na	831	134
(3Z)-3-Hexenyl 2-methylbutanoate	1356	0.780	1230	1231	921	67
Hexyl 2-methylbutanoate (Butanoic acid, 2-methyl-, hexyl ester)	1360	0.730	1233	1239	920	103
unidentified component (hit # 1 1,7,7-Trimethylbicyclo[2.2.1]hept-2-ene (2-Bornene))	1360	0.875	1233	na	860	93
(Z)-3-hexenyl-2-methylbutanoate [a]	1384	0.800	1247	1247	844	67
2-Methylbutyl hexanoate (Hexanoic acid, 2-methylbutyl ester)	1392	0.745	1251	1246	936	99
1-Methoxy-4-(1Z)-1-propenyl-benzene (cis-Anethole) [a]	1400	1.335	1256	1253	na	148
(2E)-2-Decenal	1412	1.015	1263	1265	921	70
1-Decanol	1432	1.230	1274	1278	804	70
Pentyl hexanoate	1452	0.765	1286	1280	819	99
1-Methoxy-4-(1E)-1-propenyl-benzene (trans-Anethole)	1456	1.435	1288	1288	940	148
2-Octylfuran	1464	0.780	1293	1297	862	81
2-Methylnaphthalene	1476	1.495	1300	1299	889	142
(3Z)-3-Tridecene [a,b]	1488	0.600	1308	1294	832	69
2-Methylpropanoic acid anhydride	1508	0.960	1321	na	825	71
n-Hexyl trans-2-methyl-2-butenoate (Hexyl tiglate) [a]	1520	0.845	1328	1329	836	101
2-Methyl-heptylbutanoate [b]	1528	0.725	1333	1317	844	103
unidentified component (hit # 1 3-Hydroxy-2,4,4-trimethylpentyl 2-methylpropanoate)	1556	1.360	1351	na	855	71
(2E)-2-Undecenal	1580	0.990	1367	1378	901	70
3-Hydroxy-2,4,4-trimethylpentyl 2-methylpropanoate	1592	1.220	1374	1376	885	71
Hexyl hexanoate	1608	0.800	1385	1390	829	117
Butyl octanoate	1612	0.760	1387	1387	851	145
Tetradecane	1632	0.595	1400	1400	928	57
3-Methylbutyl octanoate (Octanoic acid, 3-methylbutyl ester)	1704	0.740	1447	1450	930	70

(5E)-6,10-Dimethyl-5,9-undecadien-2-one (Geranyl acetone)	1704	1.000	1447	1450	935	43
2,3-Dimethylnaphthalene [a]	1704	1.500	1447	1439	825	141
unidentified component (hit # 1 (1,1-Dimethylpropyl)benzene)	1708	0.760	1450	na	839	119
unidentified component (hit # 1 (3E,6E)-3,7,11-Trimethyl-1,3,6,10-dodecatetraene)	1728	0.750	1463	na	815	93
1-(1,5-Dimethyl-4-hexenyl)-4-methylbenzene (alpha-Curcumene)	1760	0.835	1484	1480	909	132
(3Z,6E)-3,7,11-Trimethyl-1,3,6,10-dodecatetraene ((Z,E)-alpha-Farnesene)	1768	0.755	1489	1496	930	93
5-(1,5-Dimethyl-4-hexenyl)-2-methyl-1,3-cyclohexadiene (alpha-Zingiberene)	1776	0.760	1495	1496	878	93
(3E,6E)-3,7,11-Trimethyl-1,3,6,10-dodecatetraene ((E,E)-alpha-Farnesene)	1788	0.780	1503	1504	936	93
unidentified component (hit # 1 (2E,6E)-3,7,11-Trimethyl-2,6,10-dodecatrien-1-ol)	1816	0.785	1523	na	859	93
Hexyl octanoate	1896	0.755	1580	1579	942	84
1-[2-(Isobutyryloxy)-1-methylethyl]-2,2-dimethylpropyl 2-methylpropanoate	1908	0.825	1589	na	856	71
Benzophenone (Diphenylmethanone)	1976	2.235	1639	1627	833	105
Methyl (3-oxo-2-pentylcyclopentyl)acetate (Methyl dihydrojasmonate)	1992	1.430	1652	1650	945	83
Ethyl citrate (1,2,3-Propanetricarboxylic acid, 2-hydroxy-, triethyl ester) [b]	1992	2.075	1652	1655	853	157
1-(4-Isopropylphenyl)-2-methylpropyl acetate	2012	0.975	1667	na	821	191
Hexyl salicylate (Benzoic acid, 2-hydroxy-, hexyl ester) [a]	2032	1.195	1682	1679	800	120
unidentified component (hit # 1 (Z,Z,Z)-9,12,15-Octadecatrienoic acid)	2356	0.855	1921	na	820	79

From the category of 134 major components that were present in high concentration levels in apple sample or exhibited high HS-SPME selectivity that was manifested by overloading of the second dimension column and modulator even after 1 min of extraction, 1 min to 180 min extraction time uptakes revealed no occurrence of inter-analyte displacements. Representative analogues from this series constitute the compounds including ethyl butanoate, estragole, ethyl 2-methylbutanoate, ethyl hexanoate, propyl acetate, propyl 2-methylbutanoate, butyl hexanoate, butyl propanoate, hexanal, 2-methylbutyl acetate, 2-methylbutanol, pentyl acetate, 1-hexanol, hexyl acetate, propyl butanoate, butyl 2-methylbutanoate, butyl acetate, hexyl 2-methylbutanoate, and hexyl propanoate. As can be seen, these components constitute a diverse spectrum of physicochemical properties and the equilibration time is a function of analyte hydrophobicity, and based on the extraction time profiles presented in

Figure 5.2, equilibrium was reached within 15 or 30 min in the majority of cases.

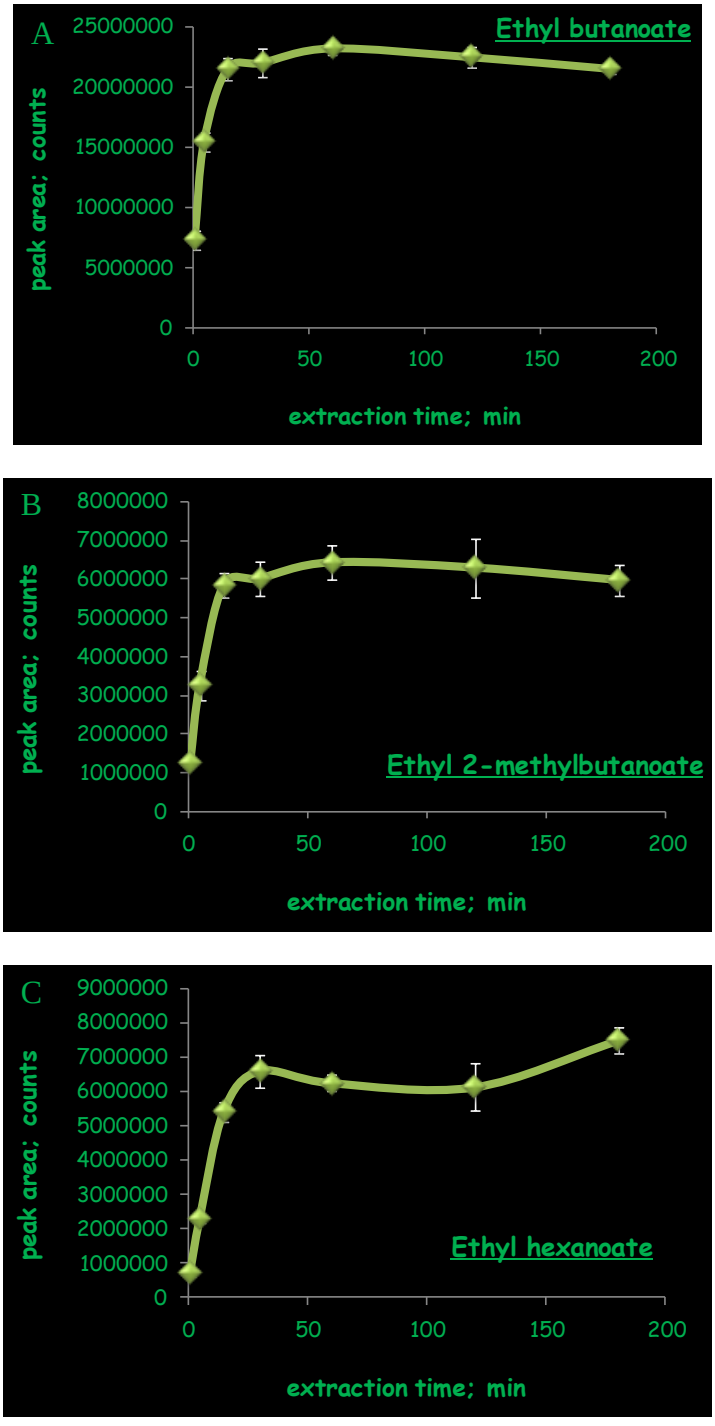

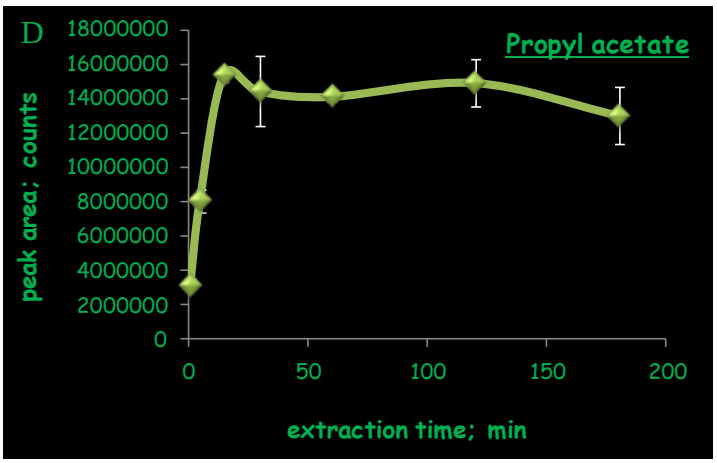
D
Propyl acetate
peak area; counts
18000000
16000000
14000000
12000000
10000000
8000000
6000000
4000000
2000000
0
0
50
100
150
200
extraction time; min

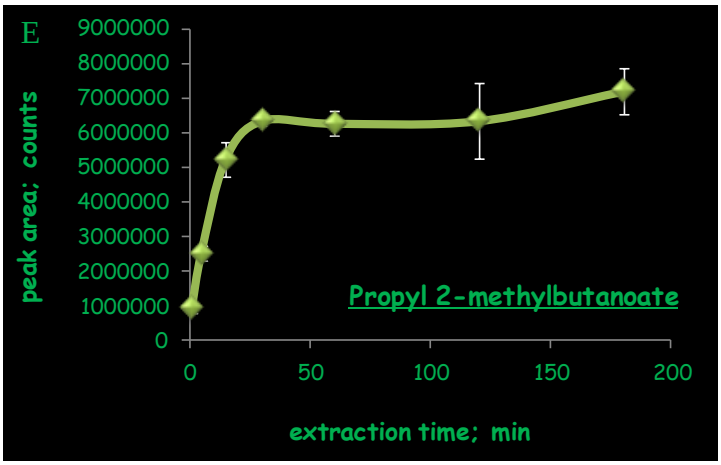
E
peak area; counts
9000000
8000000
7000000
6000000
5000000
4000000
3000000
2000000
1000000
0
Propyl 2-methylbutanoate
0
50
100
150
200
extraction time; min

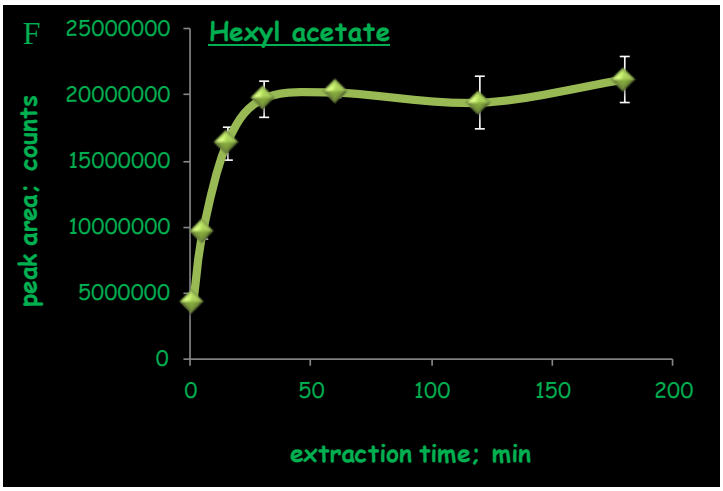
F
Hexyl acetate
peak area; counts
25000000
20000000
15000000
10000000
5000000
0
0
50
100
150
200
extraction time; min

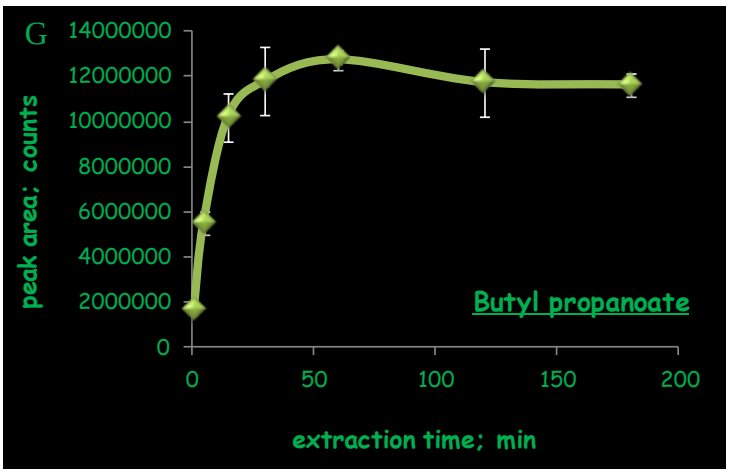

Figure 5.2. 1 min to 180 min extraction time uptakes of major components in apple matrix that exhibited high HS-SPME sensitivity and overloaded GCxGC system. A – ethyl butanoate, B – ethyl 2-methylbutanoate, C – ethyl hexanoate, D – propyl acetate, E – propyl 2-methylbutanoate, F – hexyl acetate, G – butyl propanoate

The category of 134 major components also included compounds having low-medium polarity and characterized by high hydrophobicities and high K_{fs} values. Such compounds characterized by long equilibration times due to the fact that more material needs to be transported through the boundary layer to fibre coating, such as hexyl hexanoate having retention time of 1608 s (Figure 5.3) exhibited no displacements.

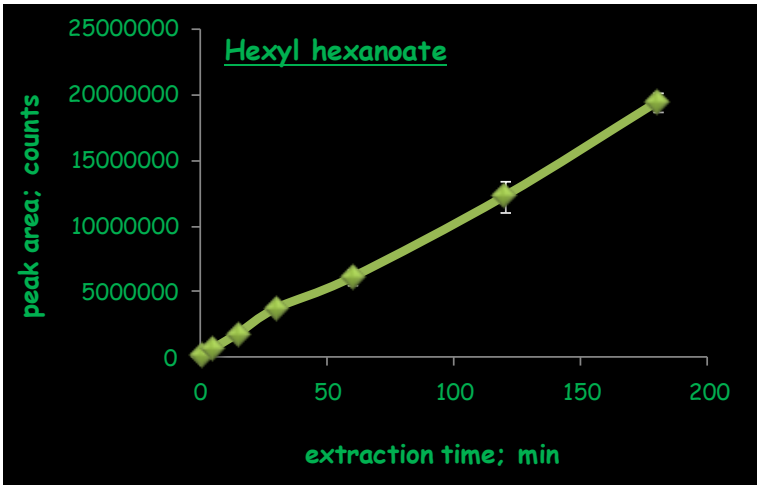

Figure 5.3. Extraction time profile of hexyl hexanoate in HS-SPME analysis of apple homogenate with DVB/CAR/PDMS coating.

The global evaluation of extraction time profiles in HS-SPME analysis also included minor and trace compounds characterized by lowest S/N ratios as per quantification ion assigned by ChromaTOF software, which was also manually verified during manual post-processing procedure that the peak table was subjected too. These 14 compounds that are either present at trace levels in the sample matrix and/or exhibit poor HS-SPME selectivity had S/N ratios ranging from 129 for benzophenone to 75 for ethyl citrate. The majority of these metabolites were characterized by high retention on the second dimension column and high polarity, hence low fibre constants can also be assumed based on the conclusions deducted in Chapter 3, where the negative correlation between retention in second dimension and fibre constants was obvious. In addition, selected metabolites were also characterized by high hydrophobicities, which attributed to poor HS-SPME sensitivity as the mass transfer from sample matrix to headspace is the limiting step in whole SPME procedure. Representative members from high hydrophobicity class included one unidentified component (hit # 1 (Z,Z,Z)-9,12,15-octadecatrienoic acid) (first and second dimension retention times 2356 and 0.855 s, respectively), hexyl salicylate (first and second dimension retention times 2032 and 1.195 s, respectively) and 1-(4-isopropylphenyl)-2-methylpropyl acetate (first and second dimension retention times 2012 and 0.975 s, respectively). Corresponding extraction time profiles from Figure 5.4 emphasize long equilibration times and absence of displacements.

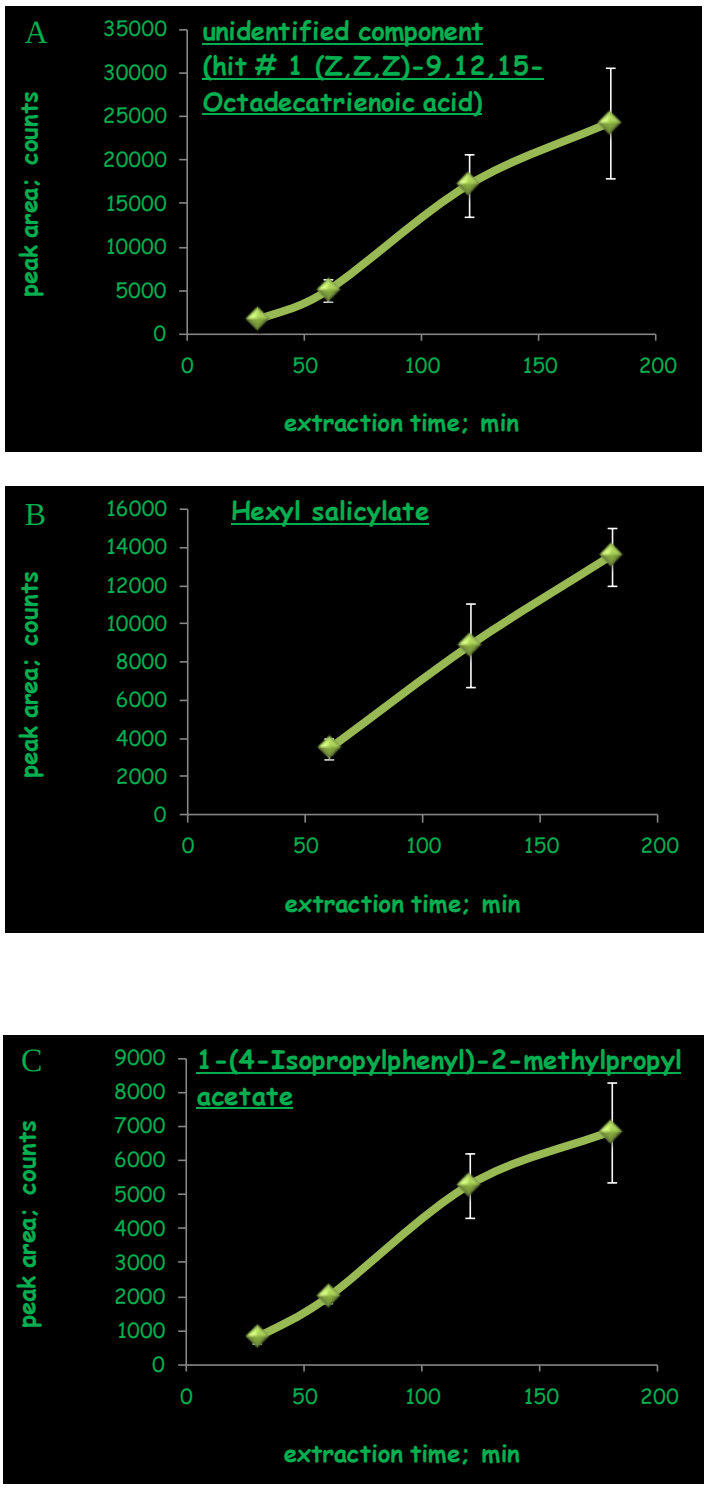

Figure 5.4. Extraction time uptakes corresponding to analytes that are representative of lowest S/N ratios and characterized by high hydrophobicities. A – unidentified component (hit # 1 (Z,Z,Z)-9,12,15-octadecatrienoic acid), B – hexyl salicylate and C – 1-(4-isopropylphenyl)-2-methylpropyl acetate.

For polar and low K_{fs} compounds strongly retained on BP 20 second dimension column that were characterized by low S/N ratios, equilibration times overall were very long and for the majority of compounds, equilibrium was not reached within 180 min of extraction. The long equilibration is attributed to slow transport of analytes through the headspace [116]. Even though diffusion coefficients in headspace are four orders of magnitude higher as compared to the aqueous phase, concentrations, therefore concentration gradients become smaller and smaller as Henry's constants decrease [116]. The relevant extraction time uptakes obtained showed no occurrence of displacement and the plots for representative analytes from this subset including benzeneethanol (first and second dimension retention times 1168 and 3.8 s, respectively), alpha-phenylethanol (first and second dimension retention times 1056 and 3.77 s, respectively), (2Z)-2-penten-1-ol (first and second dimension retention times 428 and 3.12 s, respectively), 1-pentanol (first and second dimension retention times 416 and 2.25 s, respectively), benzophenone (first and second dimension retention times 1976 and 2.235 s, respectively), (3Z)-3-hexen-1-ol (first and second dimension retention times 604 and 2.195 s, respectively) are illustrated in Figure 5.5.

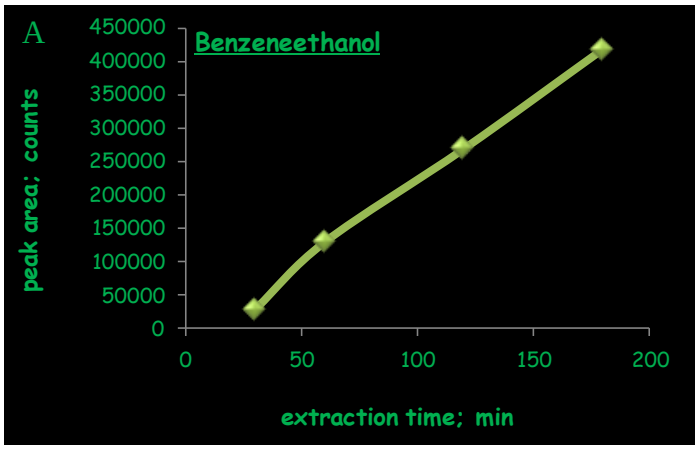

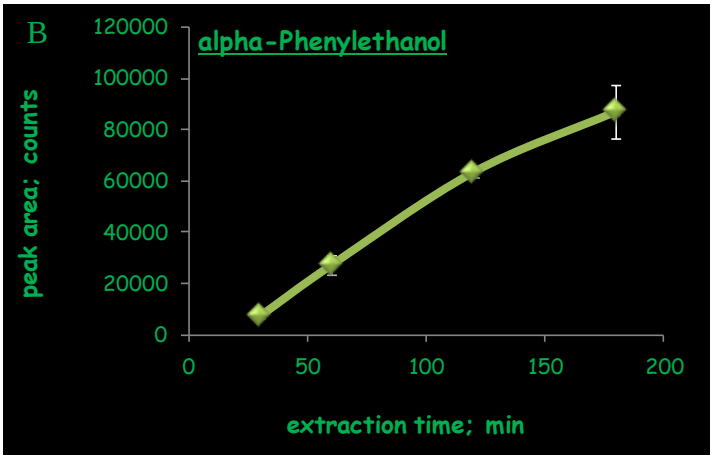
B
alpha-Phenylethanol
peak area; counts
120000
100000
80000
60000
40000
20000
0
0
50
100
150
200
extraction time; min

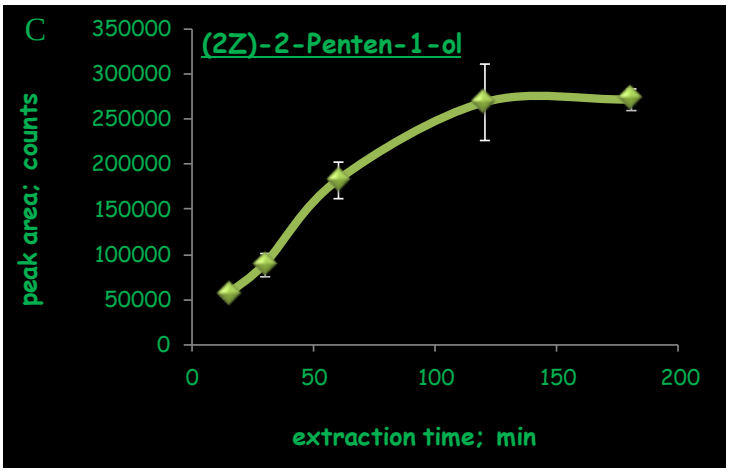
C
(2Z)-2-Penten-1-ol
peak area; counts
350000
300000
250000
200000
150000
100000
50000
0
0
50
100
150
200
extraction time; min

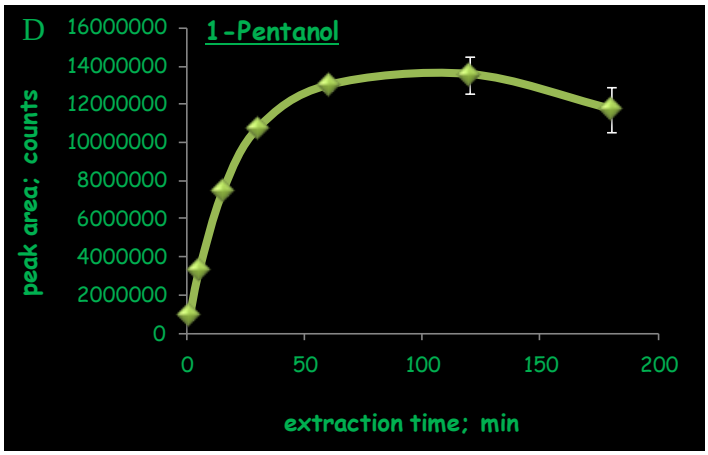
D
1-Pentanol
peak area; counts
16000000
14000000
12000000
10000000
8000000
6000000
4000000
2000000
0
0
50
100
150
200
extraction time; min

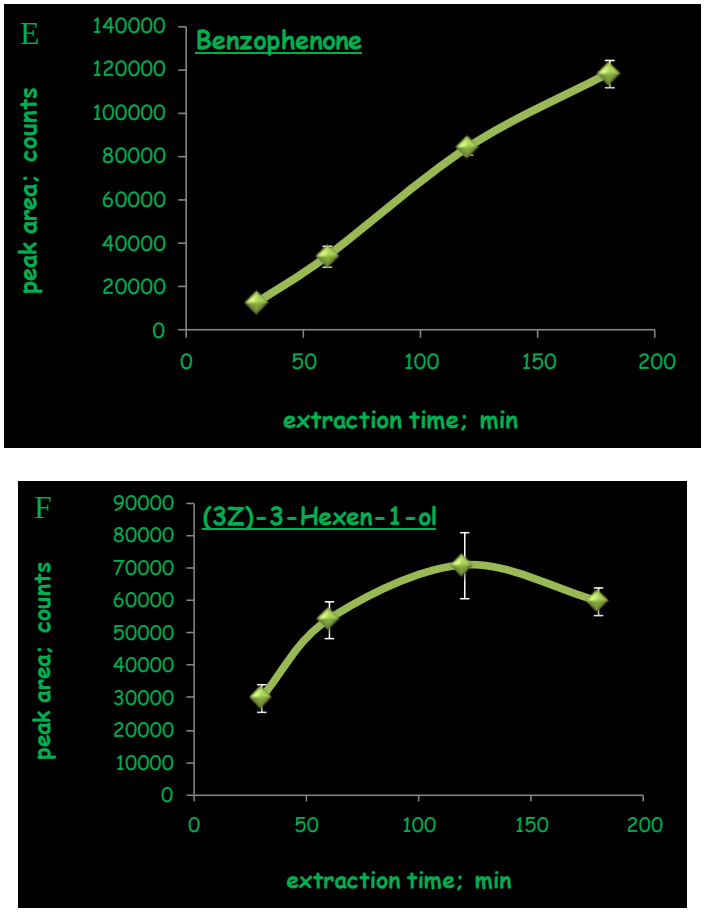

Figure 5.5. HS-SPME extraction time profiles of representative polar compounds in apple matrix including A – benzeneethanol, B – alpha-phenylethanol, C – (2Z)-2-penten-1-ol, D – 1-pentanol, E – benzophenone, F – (3Z)-3-hexen-1-ol.

Finally, it is important to address the components for which extraction time profiles revealed the presence of inter-analyte competition for adsorption sites and occurrence of displacements. The only compounds for which reduction in extracted amounts was observed with simultaneous increments in extraction time are acetaldehyde (first and second dimension retention times 140 and 0.51 s, respectively), 2-methyl-2-propanol (first and second dimension retention times 164 and 0.72 s, respectively), 1-methoxybutane (first and second dimension retention times 208 and 0.56 s, respectively), 2-methylpropanol (first and second dimension retention times 212 and 1.405 s respectively), and 3-pentanol (first and second dimension retention times 292 and 1.505 s,

respectively). Therefore, for only 5 out of 153 evaluated components, inter-analyte displacements were occurring and resulted in a significant reduction in extracted response after reaching distribution equilibrium (Figure 5.6).

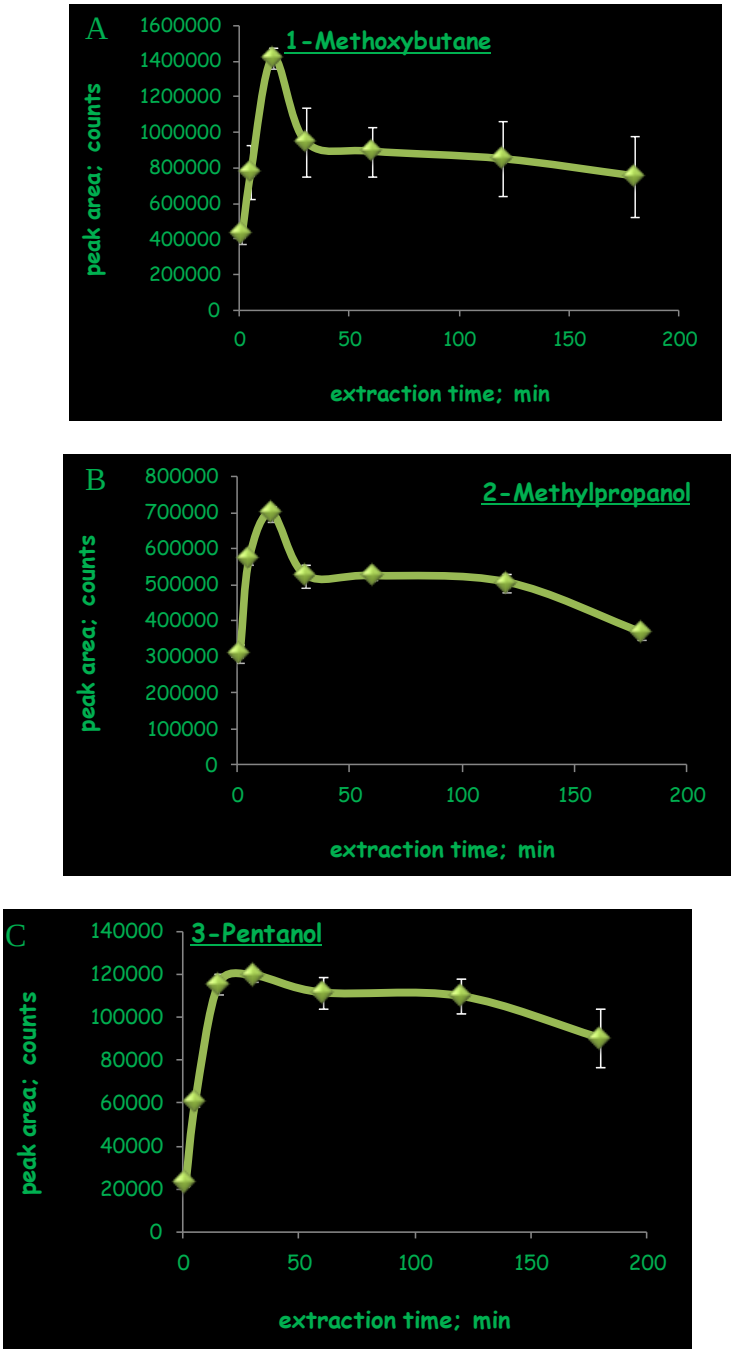

Figure 5.6. HS-SPME extraction time profiles of compounds in apple homogenate for which occurrence of inter-analyte displacement was detected. A – 1-methoxybutane, B – 2-methylpropanol, and C – 3-pentanol.

Equilibration times for these compounds ranged between 5 and 15 min, followed by the gradual decrease in response. However, it is important to emphasize that all of these compounds share similar physicochemical properties considering they are all early eluters on the first dimension column and they are characterized by medium to high polarities and hence low fibre constants. Most important, these results are in line with those obtained in Chapter 3, where nonlinear dependency was apparent for 2-pentanol, a C_5 member of homologous series of 2-alcohols and one the lowest K_{fs} compounds. Molecular weights for the displaced compounds in the analysis of apple homogenate range from 44 to 88 g/mol, with the extent of inter-analyte displacement being more prominent with the decreasing molecular weight and K_{fs} value.

It is important to point out that the literature information concerned with identification of analytes that are likely to be displaced in SPME analysis of food and environmental samples with solid coatings and correlation between the extent of inter-analyte displacement and physicochemical properties is rather inconsistent. For example, in their study on SPME combined with GC and olfactometry-mass spectrometry for characterization of cheese aroma compounds, Frank et al. saw no displacement for compounds in Parmesan cheese and for low to medium concentration compounds in strong, typical-flavoured blue cheese including sulfur aroma compounds, 2,6-diethylpyrazine, aroma impact benzene and phenol derivatives (methoxy methylbenzene, 4-methyl phenol, ethyl and propyl phenol and phenylethyl alcohol), lactones and sesquiterpenes [171]. However, inter-analyte displacements were observed for macro-concentration components including 2-pentanone, 2-hexanone, 2-heptanone, butanoic acid, hexanoic acid, 2-heptanol, methyl butanol and acetic acid. In Pecorino cheese, displacements for butanoic acid, acetic acid, acetoin, 2-pentanone and ethyl butanoate were detected. The authors employed CAR/PDMS fibre coating in HS mode for 16 h extraction at 22 ^{o}C above 7 g of grated cheese. While during the evaluation of components in apple homogenate, phenylethyl alcohol exhibited no displacement as well, 2-heptanone and methyl butanol were not displaced either even though the latter

compound was overloading GCxGC system. Therefore, the results by Frank et al. do not agree with the study conducted in current global evaluation of extraction time profiles in which displacements were observed for volatile and medium to high polarity compounds having low K_{fs} values and short equilibration times. In a study by Contini et al. on the effect of the matrix volatile composition in the HS-SPME analysis of extra virgin olive oil, the authors employed PDMS/DVB fibre coating in HS-SPME mode for 90 min at 40 ^{o}C above 10 g olive oil in 20 mL vial [172]. When all compounds were analyzed simultaneously, only ethanol, Z-3-hexenyl acetate, nonanal, acetic acid, E-2-nonenal and 1-nonanol were not influenced by the presence of other compounds. Linearity in the calibration curves for 42 other compounds was lost at concentrations of mixture ranging between approximately 5 and 50 ppm. Therefore, the authors concluded that PDMS/DVB fibre was not suitable for quantitative extraction of all volatiles usually found in extra virgin olive oil at overall concentrations of about 10-50 ppm. However, as reported in Chapter 3, Gorecki et al. implemented PDMS/DVB fibre coating in HS mode above an aqueous solution spiked with several polar organic compounds [167]. During the analysis of their relatively simple mixture, they observed nonlinearity in calibration curves for acetone, tetrahydrofuran, 2-butanone, 2-propanol and 2-methyl-2-propanol, with the latter compound also being displaced during analysis of apple homogenate.

Even though in such a challenging mixture it is impossible to determine the components that are responsible for displacement, the results obtained clearly demonstrate that nonpolar high Henry's constant compounds that are present in high concentration levels in headspace, characterized by high fibre coating/sample matrix distribution constants and released from sample matrix into headspace after disruption of fruit are not displaced but are likely to displace the components mentioned above. In addition, a good correlation in physicochemical properties of 'displaced' analytes between analysis of a 52-component aqueous solution and apple homogenate composed of 100s of constituents characterized by a diverse spectrum of functionalities suggests that

introduction of small molecular weight 'saturation' marker in metabolomics mixture is a valid approach for detection of nonlinear behavior in quantitative metabolomics. The 'displacement' marker should possess similar physicochemical properties to the components for which nonlinear dependence between analyte concentration and equilibrium extracted amount was detected above, and the employment of the polar component in C_5 range is the best option considering that for lower alkyl chain members, modulator effectiveness was not optimum. In fact, the most effective thermal GCxGC interfaces implemented for enabling modulation process and performing GCxGC separations employ a cryogenically generated cold spot in order to trap the material eluting from the primary column [173-174]. A cryogen, which may typically include liquid carbon dioxide (CO_2) or cold nitrogen gas, cools a segment of a GC column and traps the analytes in a local cold spot. After periodically removing cryogen by interrupting its delivery, the temperature of the trapping capillary, which in the case of commercial GCxGC system employed in this study is a thin film second dimension column, is increased for effective remobilization and reinjection of analytes for further second dimension separation. However, the main drawback of currently available modulators is difficulty in trapping highly volatile analytes (C_1-C_6) and ineffective modulation for such species, which in the majority of cases leads to poor enhancement of peak amplitude and errors in quantification [173]. For example, Harynuk et al. reported ineffective modulator effectiveness in GCxGC separation of highly volatile compounds such as propane when the setup resembling the commercial modulator hardware and employing gaseous nitrogen cooled in low temperature liquid nitrogen dewar was used as the cryogen [173]. One solution toward improvement of the second dimension peak shapes and increase of cryotrapping efficiency for highly volatile analytes is employment of thick film capillary column as the modulation column [175]. However, such modifications would also result in difficulties in modulation, remobilization and reinjection of heavier analytes [175]. Alternatively, and as Harynuk and Pursch have demonstrated, trapping capillaries have to be cooled

with a jet of liquid nitrogen [173,175]. However, the majority of commercial modulators, including dual-stage quad-jet thermal modulator employed here, are not capable of ensuring optimum modulator effectiveness for constituents in complex samples that exhibit a wide range of volatilities. This was also evident during quantification of early eluting compounds present in HS-SPME extract of apple homogenate and especially relevant to analytes in $< C_5$ range, including those for which the inter-analyte displacements resulted in gradual reduction of extracted amounts after reaching distribution equilibrium.

This observation points out that the adsorptive properties of DVB/CAR/PDMS coating are well tuned to the actual high-resolution GCxGC-ToFMS system. The physicochemical properties of analytes for which occurrence of inter-analyte displacements was detected due to the limited adsorption capacity of a solid sorbent are synchronized with the properties of compounds exhibiting suboptimum modulator effectiveness. In other words, complications in SPME calibration of low affinity 'displaced' analytes due to nonlinear dependencies between extracted amounts and sample concentrations in the presence of high K_{fs} coextracts are synchronized with errors in quantification attributed by suboptimum modulator effectiveness. The compounds exhibiting such physicochemical properties and suffering from both inter-analyte displacements and suboptimum modulator performance should therefore be excluded from the final data matrix in global metabolomics studies.

5.3 *HS-SPME and GCxGC-TOFMS in analysis of volatile and semivolatile metabolites: sensitivity enhancement*

With the objective of confirming the expected superiority of GCxGC-ToFMS in terms of improved signal intensity due to re-focusing of the analyte in the modulator, spiked water samples were also submitted to one-dimensional GC-ToFMS analysis. The comparison between the two techniques for selected

structurally related compounds in terms of S/N enhancement and similarity spectral match factors is documented in Table 5.2.

Table 5.2. Comparison between GC-ToFMS and GCxGC-ToFMS for selected members of series-related compounds (60 min HS-SPME extraction of spiked water samples) in terms of signal intensity and mass spectral identification potential.

	GC-ToFMS		GCxGC-ToFMS		
analyte name	S/N	spectral match factor	S/N	spectral match factor	S/N enhancement factor[a]
2-hexanone	1057	942	11892	950	11
2-nonanone	4999	925	55268	937	11
2-tridecanone	3280	na	26596	921	8
2-heptadecanone	1546	882	17206	892	11
ethyl butanoate	1344	880	16906	947	13
ethyl nonanoate	3913	919	53616	942	14
ethyl tridecanoate	3483	920	34283	944	10
ethyl palmitate	578	917	8496	930	15
ethyl stearate	12	na	177	850	15
1-pentanol	3418	937	14768	960	4
1-nonanol	2271	936	13697	940	6
1-tridecanol	1469	939	8412	957	6
1-pentadecanol	741	na	5550	914	7
1-heptadecanol	20	na	202	916	10

na data not available

[a] ratio of S/N GCxGC-ToFMS/GC-ToFMS

As far as the identification potential of GCxGC-ToFMS is concerned, overall higher mass spectral match factors were obtained as compared to one-dimensional analysis mode, especially for higher MW compounds, including ethyl stearate, 1-pentadecanol and 1-heptadecanol, for which the HS-SPME extraction sensitivity in pre-equilibrium conditions was poor due to slow mass transfer from sample matrix to fibre coating. These were often indistinguishable from the background in the 1D GC-ToFMS chromatogram due to their low signal intensity and needed to be manually located, followed by the library

searching procedure, which frequently resulted in many instances of erroneous hit assignment. The comparison between the two techniques in terms of analyte detectability also revealed superior GCxGC-ToFMS performance characteristics with S/N enhancement factors ranging between 4 and 15. This is in good agreement with experimentally observed gains in analyte detectability reported in the literature [79, 176]. However, one should keep in mind that the signal intensity in GCxGC is strongly dependent on the number of modulations, analyte polarity and the choice of column combination [82,176]. As a result, based on the well comprehended retention behaviour of numerous polar compounds, poor S/N enhancement factors were obtained for alcohols as they frequently tail on non-polar stationary phases, which is likely resulted from the interactions of their hydroxyl groups with active sites present in the capillary column wall [82]. Therefore, in order to take full advantage of the GCxGC improved detectability characteristic, the reverse polar/non-polar column combinations should be considered for polar analytes along with modulation period optimization for trace analyte determination.

5.4 *Considerations on SPME methodology for metabolomic profiling – comparison between HS- and DI-SPME extraction modes*

Considering that HS-SPME extraction mode is selective and sensitive for highly volatile compounds and that its implementation results in biased metabolome coverage and discrimination against high molecular weight as well as polar analyte capture, DI-SPME mode was also tested in order to identify the route toward unbiased metabolome coverage. The performance characteristics of the two extraction formats for 60 min extraction at 30 ^{o}C are illustrated in the peak apex plots in Figure 5.7 and can be briefly summarized in terms of 555 and 906 captured metabolites for HS- and DI-SPME modes, respectively, found above the S/N and similarity thresholds of 200 and 800, respectively.

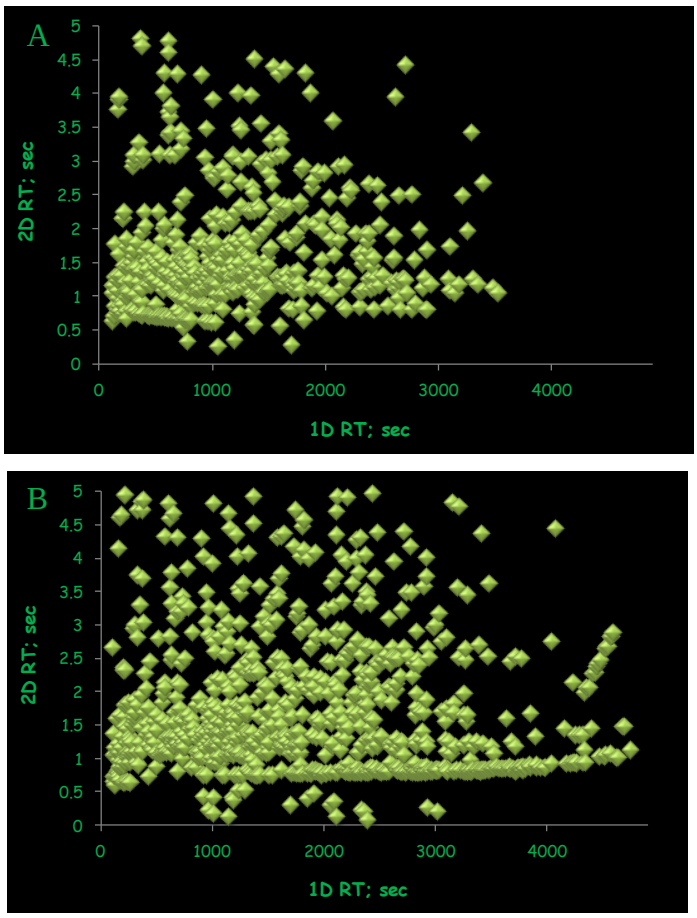

Figure 5.7. Comparison between HS-SPME (plot A) and DI-SPME (plot B) extraction modes for metabolite profiling in apples. Peak apex plots demonstrate retention time coordinates on two-dimensional retention time plane for 555 and 906 captured metabolites found by ChromaTOF software above S/N threshold of 200 for HS- and DI-SPME modes, respectively.

DI-SPME provided more balanced metabolite coverage and the discrimination against high molecular weight and polar metabolites was accounted for. With the use of DI-SPME, polar and high MW metabolites were effectively extracted (refer to Figure 5.8), including 1,3-octanediol (^1t_R and ^2t_R 1830 and 4.575 s), (2E,4E)-2,4-hexadienal (^1t_R and ^2t_R 755 and 3.320 s), (2E,4E)-2,4-heptadienal (^1t_R and ^2t_R 1025 and 2.740 s), 1-octen-3-ol (^1t_R and ^2t_R 980 and 2.840 s), benzenemethanol (^1t_R and ^2t_R 1155 and 4.670 s), benzeneethanol (^1t_R and ^2t_R 1385 and 4.510 s), 4-methyl-4-vinylbutyrolactone (^1t_R and ^2t_R 1155 and 0.125 s), octanoic acid (^1t_R and ^2t_R 1595 and 2.505 s), cis-jasmin lactone (^1t_R and ^2t_R 2360

and 3.355 s), gamma-tetradecalactone (^1t_R and ^2t_R 3275 and 2.630 s), isopropyl palmitate (^1t_R and ^2t_R 3540 and 1.065 s), and hexadecanoic acid (^1t_R and ^2t_R 3420 and 4.355 s).

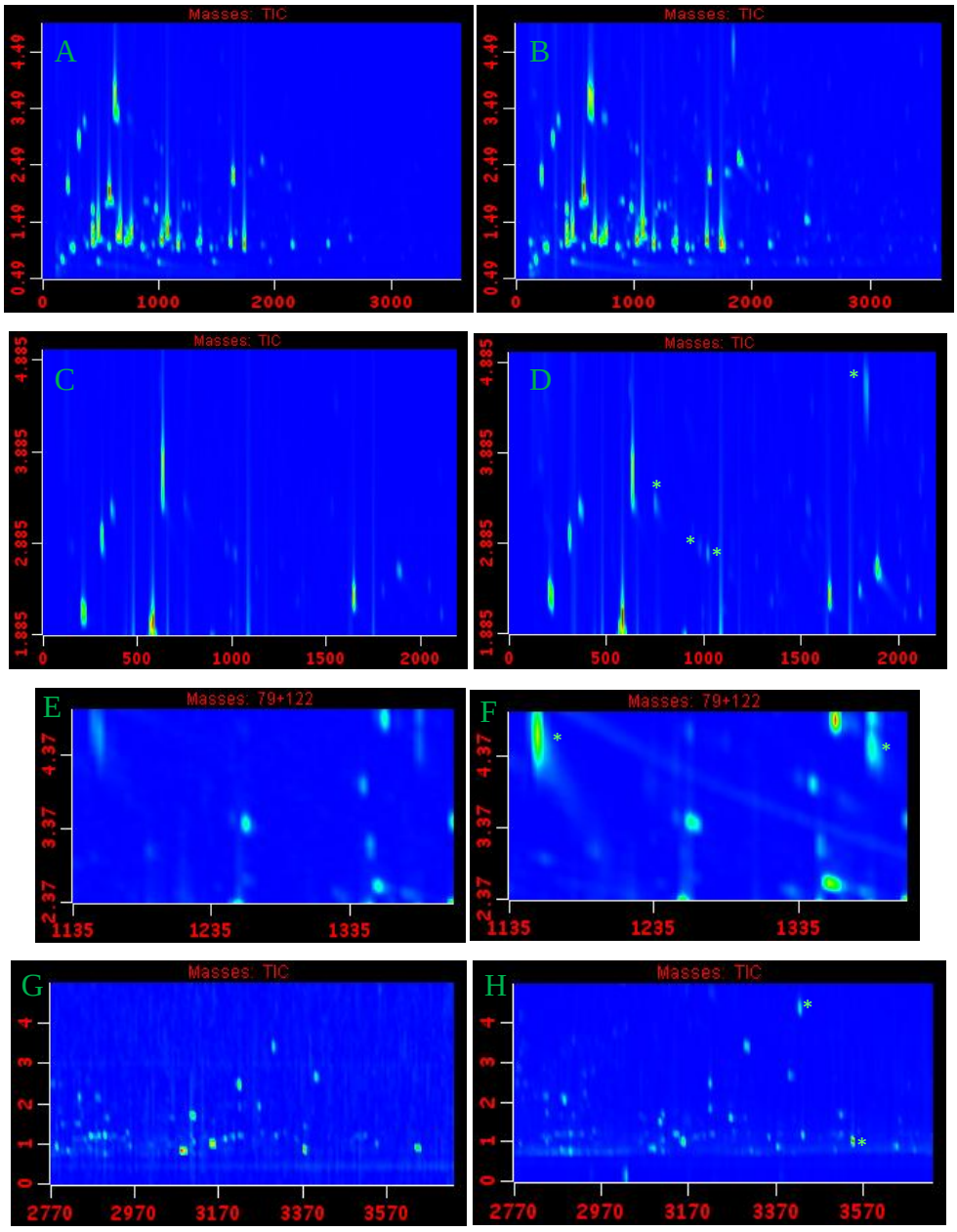

Figure 5.8. Comparison between HS-SPME (plots to the left (A, C, E, G)) and DI-SPME (plots to the right (B, D, F, H)) extraction modes for metabolite profiling in apples. Plots A and B represent total ion current GCxGC contour plots demonstrating comparison between two modes. The peaks labeled by asterisk in TIC and extracted ion chromatograms corresponding to DI-SPME extracts represent the following metabolites: plot D: 1,3-octanediol (^1t_R and ^2t_R 1830 and 4.575 s), (2E,4E)-2,4-hexadienal (^1t_R and ^2t_R 755 and 3.320 s),

(2E,4E)-2,4-heptadienal (^1t_R and ^2t_R 1025 and 2.740 s) and 1-octen-3-ol (^1t_R and ^2t_R 980 and 2.840 s); plot F: benzenemethanol (^1t_R and ^2t_R 1155 and 4.670 s) and benzeneethanol (^1t_R and ^2t_R 1385 and 4.510 s); plot H: isopropyl palmitate (^1t_R and ^2t_R 3540 and 1.065 s) and hexadecanoic acid (^1t_R and ^2t_R 3420 and 4.355 s).

These results are well correlated with those obtained in a recent study aimed at the detailed investigation of volatiles in South African red wines, in which the authors proceeded to implementation of solid phase extraction due to the failure of HS-SPME to extract several influential semi-volatile constituents, including lactones and phenols [177-178]. Since the use of HS-SPME accelerates the extraction of analytes characterized by high Henry's law constants and hence attributes to shorter equilibration times, the resultant overloading of narrow bore thin film second dimension column hindered the identification of trace minor compounds suffering from overloaded peak overlap. In addition to assuring a rewarding metabolic picture and the lower degree of discrimination achieved through more efficient capture of high molecular weight and more polar metabolites, DI-SPME is to be pursued in future studies and in *in vivo* SPME studies. The convenient introduction of the miniaturized SPME assembly in living systems provides unique opportunities for direct tissue sampling of endogenous compounds, including those that are representative of apple quality traits.

5.5 *GCxGC-ToFMS attributes in metabolomic profiling of apples and analyte identification in ex vivo DI-SPME extract*

The surface plot of total ion current (TIC) GCxGC-ToFMS chromatogram of DI-SPME apple extract obtained following 60 min extraction at 30 ^oC is represented in Figure 5.9. The data presented and the number of peak entries in both non-processed and filtered peak tables indicate that DI-SPME apple extract represents a chromatographically challenging material. The use of a suitable column ensemble in GCxGC led to the effective exploitation of available two

dimensional separation space and the consequent achievement of exceptional resolving power.

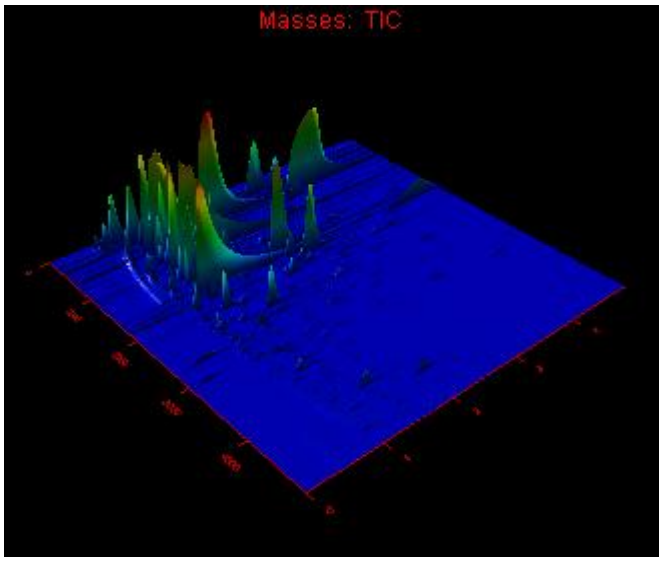

Figure 5.9. Surface plot of total ion current (TIC) GCxGC-ToFMS chromatogram corresponding to 60 min DI-SPME extraction of apple sample.

The advantage of increased separation efficiency and resolving power obtainable with GCxGC-ToFMS is illustrated in the zoomed-in portions of the contour plots of extracted ion chromatograms presented in Figure 5.10. In Figure 5.10 a, at least four peaks (with $^{2}t_{R}$ of 0.930, 1.215, 2.055 and 2.420 s including the identified pentyl salicylate with experimental RI value of 1572) are coeluting in the first dimension among those that passed the specified ChromaTOF S/N threshold in addition to many more trace compounds that are aligned vertically. Similarly, Figure 5.10 b illustrates another example of chromatographic coelution in the primary dimension separation, while the four components including 2-methylbutyl hexanoate, 1-methoxy-4-(1Z)-1-propenyl-benzene, phenylethyl acetate and 5-butyldihydro-2(3H)-furanone are successfully resolved after the submission of the corresponding first dimension fraction to second dimension for further separation. The mass spectral match factors were 955, 961, 935 and 923, respectively, while calculated experimental retention index was 1252.

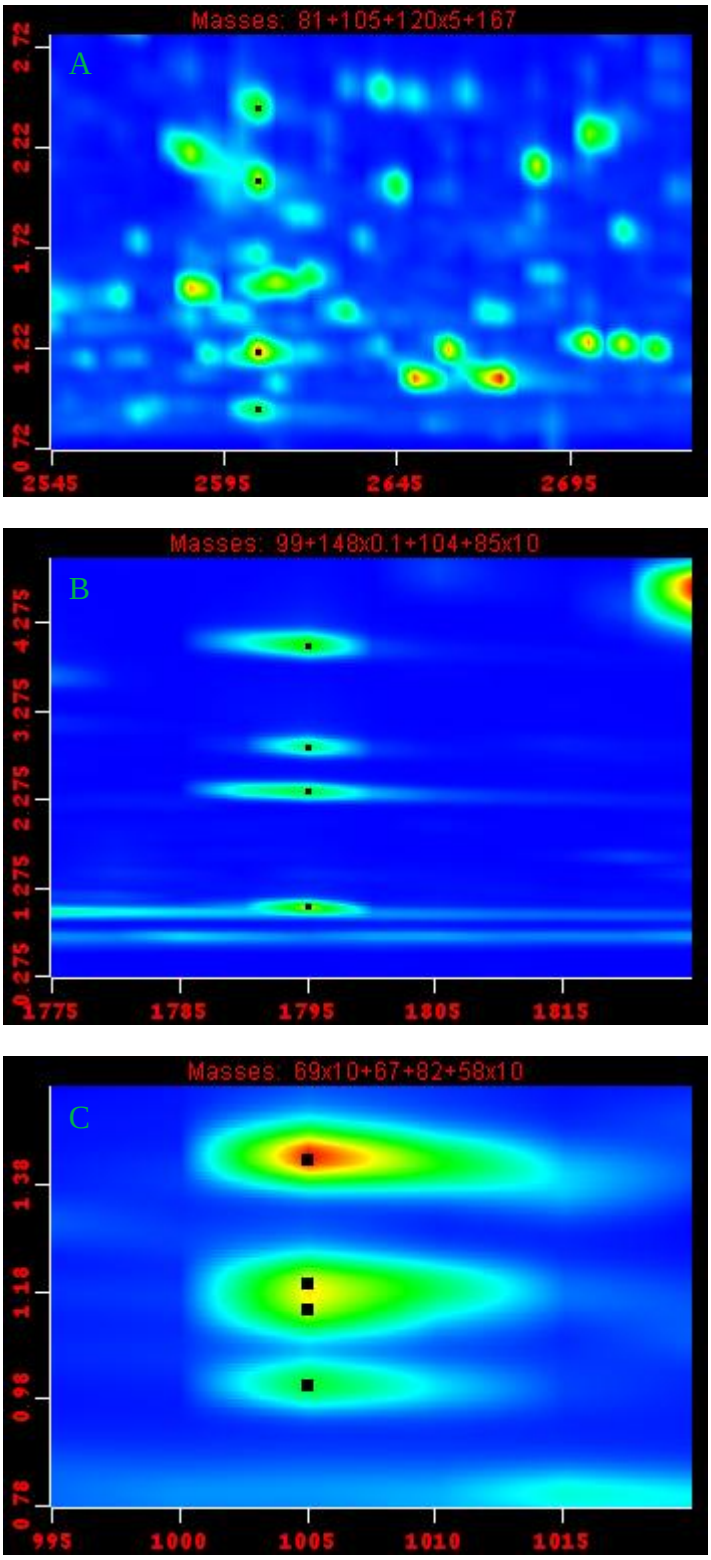

Figure 5.10. Contour plots of extracted ion chromatograms demonstrating chromatographic coelution in first dimension for A – four peaks with first

dimension retention time of 2605 s and second dimension retention times of 0.930, 1.215, 2.055 and 2.420 s and found above S/N 200 including identified pentyl salicylate, B – four peaks including 2-methylbutyl hexanoate, 1-methoxy-4-(1Z)-1-propenyl-benzene, phenylethyl acetate and 5-butyldihydro-2(3H)-furanone with first dimension retention time of 1795 s and second dimension retention times of 1.085, 2.380, 2.880 and 4.015 s, respectively and C – four peaks tentatively identified as beta-myrcene, trans-herboxide, 2-pentylfuran and 2-octanone having first dimension retention time of 1005 s and second dimension retention times of 1.010, 1.150, 1.200 and 1.430 s, respectively.

Finally, the last example illustrates insufficient resolving power of the first dimension separation for beta-myrcene, trans-herboxide, 2-pentylfuran and 2-octanone with the first dimension retention time of 1005 s and the second dimension retention times of 1.010, 1.150, 1.200 and 1.430 s, respectively. These plots illustrate that even though SPME and in particular HS-SPME mode of its implementation is regarded as the extraction methodology capable of reducing matrix effects and generating clean chromatograms, its hyphenation with GCxGC and mass spectrometry as additional separation dimension (see example of trans-herboxide and 2-pentylfuran in Figure 5.10 c) is a conceivable solution in analysis of complex naturally existing matrices. The nonselective adsorption properties attribute to extraction of a large range of physicochemicaly diverse analytes, hence requiring the employment of high-resolution instrumentation that traditional one-dimensional GC-MS is not capable of ensuring.

Data collected from DI-SPME-GCxGC-ToFMS analysis of apple samples were submitted to automated ChromaTOF data processing procedure, which employed S/N threshold of 200 for the 'unique mass' to find all the peaks followed by the mass spectral deconvolution to mathematically separate spectra of co-eluted peaks and perform modulated peak combination [78]. The resultant peak table consisted of 2,581 entries and was subjected to further data reduction procedure on the basis of mass spectral purity requiring a mass spectral similarity threshold of 800. The table retrieved in the process consisted of 1,081 entries and was submitted to a manual verification procedure in order to *i)* filter out column bleed and fibre bleed peaks, *ii)* remove duplicate entries

observed under non-linear chromatography and/or suboptimum chromatography and modulator effectiveness regimes that adversely affected modulated peak recombination (retrieval of 703 entries), and *iii)* confirm/revise the identification based on retention index comparison and/or molecular structure-retention relationships facilitating a *priori* identification of structurally related peaks [86]. The base peaks were used for the calculation of experimental RI values which were compared to literature databases. Considering that modulation causes a certain degree of inaccuracy in the first dimension retention time and that the literature RI were complied for one-dimensional GC systems employing stationary phases from various manufacturers, maximum acceptable difference of 30 for the absolute RI was adopted [78].

The extensive manual data authentication resulted in the compilation of 399 volatile and semivolatile metabolites that are documented in Table 5.3. As can be seen from the presented table, the minimum reporting peak criteria were established based on the guidelines of the Metabolomics Standards Initiative (MSI) Chemical Analysis Working Group (CAWG) advising both mass spectral and RI information for compounds identification. The exceptions were metabolites, which were *i)* reported given they passed mass spectral similarity criterion of 900 since their literature RI values were not available, and *ii)* identified on the basis of GCxGC structured retentions. The latter identification approach was especially crucial for larger molecular weight members of the homologous series, as the corresponding hits are not present in commercial libraries. For example, a series of gamma-lactones including gamma-tridecalactone, gamma-pentadecalactone and gamma-hexadecalactone was tentatively identified by adopting structured separation approach and combining it with mass spectral similarity for lighter members. For gamma-lactone series including gamma-hexalactone, gamma-octalactone, gamma-nonalactone, gamma-decalactone, gamma-undecalactone and gamma-dodecalactone, the linear relationship between first and second dimension retention time was characterized by regression coefficient of 0.949 (Figure 5.11).

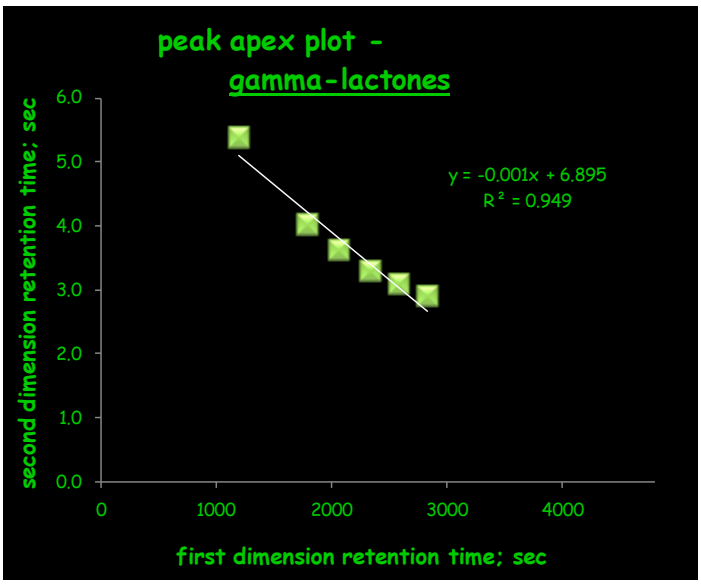

Figure 5.11. Apex plot showing the relationship between first and second dimension retention times for homologous series of gamma-lactones including gamma-hexalactone, gamma-octalactone, gamma-nonalactone, gamma-decalactone, gamma-undecalactone and gamma-dodecalactone.

Even though very strict peak reporting criteria were employed and ChromaTOF data processing involved the adoption of S/N and mass spectral similarity parameters of 200 and 800, respectively, in order to reduce data dimensionality, the results presented in Table 5.3 are rewarding. For example, the implementation of novel DI-SPME – GCxGC-ToFMS methodology enabled the identification of important metabolites, including butyl acetate, hexyl acetate, 1-hexanol, (2E)-2-hexenal and estragole found to dominate apple volatile composition, 2-methylbutyl acetate and butyl 2-methylbutanoate found to contribute to characteristic apple-like aroma as well as high odour impact constituents such as *trans-beta*-damascenone, hexanal, (3Z)-3-hexenal, methyl 2-methylbutanoate, ethyl 2-methylbutanoate and linalool [48,70]. On the other hand, the number of tentatively identified compounds in Table 5.3 exceeds the performance characteristics of classic one dimensional-GC setups, the majority of which are reporting on average 100 peaks for HS-SPME approaches coupled to GC-MS [42,49]. As a result of the powerful combination of DI-SPME and GCxGC-ToFMS, several metabolites were identified in the current study that

have not been previously reported to constitute volatile metabolome profile of apples. These include benzenemethanol, benzeneacetaldehyde, 2,6-dimethyl-5-heptenal (bergamal), cis- and trans-linalool oxides, cis- and trans-rose oxides, nerol oxide, alpha-terpineol, anisylacetone, para-methoxycinnamaldehyde, ethylhexyl cinnamate and *trans-beta*-ionone.

Table 5.3. Volatile and semivolatile metabolites identified in apple samples submitted to DI-SPME – GCxGC-ToFMS procedure. ChromaTOF data processing parameters involved S/N and similarity thresholds of 200 and 800, respectively and data post-processing was performed to confirm/revise identification based on *i)* literature RI values and/or *ii)* GCxGC molecular structure retention relationships.

analyte name (synonym)	^1t_R; s	^2t_R; s	RI_{exp}	RI_{lit}
Acetaldehyde	125	0.640	Na	
Ethyl alcohol	130	1.040	Na	
Ethylcyclopropane	135	0.595	Na	
1-Propanol [b]	150	1.590	600	574
2-Methylpropenal (Isobutenal) [b]	155	0.805	605	577
Butanal [b]	165	0.820	615	600
2-Methylfuran [b]	170	0.765	620	609
1-Methoxybutane [b]	180	0.675	630	616
Ethyl Acetate [b]	180	0.855	630	618
2-Methyl-1-propanol (Isobutanol) [b]	185	1.645	635	626
Acetic acid [b]	185	4.600	635	641
Butyronitrile (1-Cyanopropane) [d]	190	1.155	640	640
2-Butenal (Crotonaldehyde) [b]	205	1.315	655	657
1-Butanol [b]	210	2.360	660	660
2-Methylbutanal [b]	215	0.880	665	659
1-Hydroxy-2-propanone (Acetol) [b]	220	4.935	670	674
Benzene [b]	230	0.930	680	667
1-Penten-3-ol [b]	230	2.320	680	682
2-Pentanone [b]	235	1.065	685	687
1-Penten-3-one [b]	235	1.225	685	683
Pentanal (Valeraldehyde) [b]	245	1.085	695	695
2,3-Pentanedione (Acetylpropionyl) [b]	245	1.430	695	696
2-Ethylfuran [b]	250	1.000	700	702
Ethyl propanoate [b]	265	1.080	708	707
Trimethoxymethane (Trimethyl orthoformate) [d]	270	1.265	711	702
Methyl butanoate [b]	280	1.095	716	720
Butyl formate [b]	285	1.230	719	737
Vinylfuran (2-Ethenylfuran) [b]	290	1.500	722	723
3-Penten-2-one [b]	310	1.865	732	733

2-Methyl-1-butanol [b]	310	2.995	732	731
(2E)-2-Methyl-2-butenal (Tiglic aldehyde) [b]	320	1.680	738	738
2-Methyl-3-pentanone [b]	330	1.100	743	742
(2E)-2-Pentenal [b]	340	1.795	749	751
Toluene [b]	360	1.220	759	763
1-Pentanol [b]	365	3.295	762	759
2-Methylthiophene [b]	370	1.455	765	770
(2Z)-2-Penten-1-ol [b]	370	4.850	765	767
Isobutyl acetate (2-Methyl-1-propyl acetate) [b]	380	1.125	770	768
3-Methyl-2-butenol (Prenol) [c]	380	4.725	770	772
Methyl 2-methylbutanoate [b]	385	1.095	773	769
2,3-Hexanedione (Acetylbutyryl) [b]	405	1.670	784	781
3-Methyl-2-butenal (Prenal) [b]	405	2.255	784	783
2-Hexanone [b]	415	1.350	789	792
Cyclopentanone [b]	415	2.040	789	791
3-Buten-1-ol acetate (2-Vinylethyl acetate) [b]	425	1.515	795	797
Hexanal [b]	435	1.390	800	801
(3Z)-3-Hexenal [b]	435	1.735	800	797
Octane [c]	440	0.725	802	800
Ethyl butanoate [b]	440	1.195	802	803
Propyl propanoate [b]	460	1.150	809	814
Butyl acetate [b]	480	1.325	816	819
2-Methyl-4-pentenal [d]	495	1.540	821	798
1-Methoxyhexane [b]	510	0.875	826	832
Pentyl formate (Amyl formate) [b]	510	1.420	826	823
(2E)-2-Butenyl acetate [b]	510	1.645	826	824
Furfural (2-Furancarboxaldehyde) [b]	530	2.780	833	845
Isopropyl butanoate (Butanoic acid, 1-methylethyl ester) [b]	555	1.055	841	837
Ethyl (2E)-2-butenoate [b]	560	1.565	843	839
Ethyl 2-methylbutanoate [b]	575	1.075	848	842
(2E)-2-Hexenal (Leaf aldehyde) [b]	580	2.125	850	850
(3Z)-3-Hexen-1-ol (Leaf alcohol) [b]	590	4.320	853	853
Ethylbenzene [b]	600	1.295	857	857
3-Ethylthiophene [d]	610	1.515	860	854
5-Hexen-1-ol [b]	615	4.805	862	879
1,4-Dimethylbenzene (p-Xylene) [c]	625	1.325	866	867
(2E)-2-Hexen-1-ol [b]	625	4.580	866	864
Isobutyl propanoate (Propanoic acid, 2-methylpropyl ester) [b]	630	1.105	867	866
2-Methylbutanoic acid [b]	635	2.465	869	881
1-Hexanol [b]	635	3.785	869	867
2-Methylbutyl acetate (1-Butanol, 2-methyl-, acetate) [b]	655	1.230	876	873
3-Methylbutyl acetate (1-Butanol, 3-methyl-, acetate) [b]	665	1.275	879	871
(4Z)-4-Hexen-1-ol [c]	665	4.665	879	874
4-Penten-1-yl acetate (5-Acetoxy-1-pentene) [b]	675	1.535	883	890
3-Heptanone [b]	680	1.315	884	885

Styrene (Ethenylbenzene) [b]	690	1.905	888	891
2-Butylfuran [b]	695	1.205	890	894
1-Nonene [b]	700	0.790	891	892
Cyclohexanone [b]	700	2.135	891	901
4-Heptanol [b,e]	700	4.305	891	879
(4Z)-4-Heptenal [b]	715	1.695	897	902
Propyl butanoate [b]	720	1.170	898	895
Ethyl pentanoate [b]	725	1.185	900	901
Heptanal [b]	725	1.400	900	906
(2Z)-2-Pentenyl acetate [b,e]	730	1.575	902	909
2-Heptanol [b]	730	2.415	902	913
2-Butoxyethanol (Butyglycol) [b]	740	3.430	905	903
Butyl propanoate [b]	750	1.220	908	910
(2E,4E)-2,4-Hexadienal (Sorbic aldehyde) [b]	755	3.320	910	914
3-Methyl-3-butenyl acetate [b]	760	1.550	911	883
Pentyl acetate [b]	765	1.340	913	915
Methoxybenzene (Anisole) [b]	765	2.485	913	918
3-Methyl-2-butenyl acetate (Prenyl acetate) [c]	790	1.615	921	920
Methyl hexanoate [b]	800	1.290	924	922
Hexyl formate [b]	810	1.440	927	929
alpha-Pinene (2,6,6-Trimethyl-bicyclo[3.1.1]hept-2-ene) [b]	820	0.860	930	933
Bicyclo[4.2.0]octa-1,3,5-triene (Cardene)	835	1.565	935	na
Ethyl (2E)-2-methyl-2-butenoate (Ethyl tiglate) [b]	845	1.445	938	938
(1S)-1,5-Dimethyl-6,8-dioxabicyclo[3.2.1]octane ((-)-(1S,5R)-Frontalin) [b]	855	1.335	941	949
Propyl 2-methylbutanoate [b]	865	1.075	944	942
Propylbenzene (Isocumene) [b]	885	1.265	951	948
Butyl 2-methylpropanoate [b]	890	1.065	952	953
2-Methylpropyl butanoate [b]	900	1.090	956	953
(2E)-2-Heptenal [b]	900	1.880	956	956
1-Ethyl-3-methylbenzene (m-Ethyltoluene) [b]	910	1.300	959	963
Benzaldehyde (Phenyl methanal) [b]	910	4.285	959	964
5-Methyl-2-furancarboxaldehyde (5-Methylfurfural) [b]	930	0.430	965	960
6-Methyl-6-hepten-2-one [b]	930	1.755	965	966
5-Ethyl-2(3H)-furanone (2-Ethylbutenolide) [b]	935	4.015	967	954
3-Methylnonane [c]	950	0.745	971	972
1-Heptanol [b]	950	3.030	971	970
1-Ethyl-2-methylbenzene (o-Ethyltoluene) [b]	960	1.380	975	980
1-Octen-3-one [b]	965	1.580	976	980
(1-Methylethenyl)benzene (alpha-Methylstyrene) [b]	975	1.725	979	988
3-(Methylthio)propanol [b]	980	0.220	981	982
Hexyl acetate [b]	980	1.245	981	1000
1-Octen-3-ol [b]	980	2.840	981	978
6-Methyl-5-heptene-2-one [b]	990	1.760	984	986
3-Octanone [b]	995	1.310	986	986

2,3-Octanedione [b]	995	1.650	986	986
Methoxymethylbenzene [b]	995	2.120	986	984
3-Methylene-7-methyl-1, 6-octadiene (beta-Myrcene) [b]	1005	1.010	989	991
2-Ethenyl-2-methyl-5-(1-methylethenyl)tetrahydrofuran (trans-Herboxide) [b]	1005	1.150	989	988
2-Pentylfuran (2-Amylfuran) [b]	1005	1.200	989	991
2-Octanone [b]	1005	1.430	989	989
1,3,5-Trimethylbenzene (Mesitylene) [c]	1010	1.400	990	994
Furfuryl acetate (2-Furanmethanol, acetate) [b]	1015	3.920	992	996
6-Methyl-5-hepten-2-ol (Sulcatol) [b]	1020	2.780	994	995
Hexanoic acid [b]	1025	0.165	995	979
(2E,4E)-2,4-Heptadienal [b]	1025	2.740	995	1013
Butyl butanoate [b]	1030	1.200	997	999
trans-2-(2-Pentenyl)furan [b]	1035	1.450	998	1000
1-Methyl-3-vinylbenzene (3-Methylstyrene) [d]	1035	1.765	998	973
3-Octanol [b]	1035	2.020	998	999
Ethyl hexanoate [b]	1040	1.185	1000	1003
Isobutyl 2-methylbutanoate (Butanoic acid, 2-methyl-, 2-methylpropyl ester) [b]	1050	1.020	1003	1004
Octanal [b]	1050	1.385	1003	1006
(3Z)-3-Hexenyl acetate [b]	1050	1.555	1003	1008
2-Octanol [b]	1050	2.190	1003	1004
Pentyl propanoate (Amyl propanoate) [b]	1065	1.170	1008	1006
(2E,4E)-2,4-Heptadienal [b]	1075	2.820	1011	1013
Hexyl acetate [b]	1080	1.405	1013	1012
(2E)-2-Hexenyl acetate [b]	1090	1.520	1016	1017
1-Methoxy-4-methylbenzene (p-Methylanisole) [b]	1100	2.170	1019	1022
4-Methyl-5-vinylthiazole [d]	1115	2.975	1024	999
2-Cyclohexene-1,4-dione [b]	1120	2.545	1025	1032
1-Methyl-4-(1-methylethenyl)cyclohexene (Limonene) [b]	1130	1.050	1029	1030
Benzocyclopentane (Indane) [b]	1135	1.615	1030	1034
1,2,3-Trimethylbenzene (Hemimellitene) [c]	1135	1.685	1030	1023
2-Ethylhexanol [b]	1135	2.555	1030	1030
2,2,6-Trimethylcyclohexanone [b]	1140	1.375	1032	1035
Propyl (2E)-2-methyl-2-butenoate (Propyl tiglate) [b]	1150	1.370	1035	1035
Dihydro-5-methyl-5-vinyl-2(3H)-furanone (4-Methyl-4-vinylbutyrolactone) [b]	1155	0.125	1037	1041
Benzenemethanol (Benzyl alcohol) [b]	1155	4.670	1037	1040
(3E)-3-Octen-2-one [b]	1160	1.790	1038	1036
Butyl 2-methylbutanoate [b]	1170	1.130	1041	1042
Benzeneacetaldehyde [b]	1170	4.430	1041	1045
Pentyl 2-methylpropanoate (Pentyl isobutyrate) [b]	1195	1.065	1049	1054
5-Ethyldihydro-2(3H)-furanone (gamma-Hexalactone) [b]	1200	0.360	1051	1060
2,6-Dimethyl-5-heptenal (Bergamal) [b]	1205	1.425	1052	1053
(2E)-2-Octenal [b]	1220	1.800	1057	1059
2-Methylbutyl butyrate [b]	1225	1.105	1059	1056

1-Phenylethanone (Acetophenone) [b]	1235	4.030	1062	1068
(1,1-Dimethylethoxy)-benzene (tert-Butoxybenzene) [b]	1250	1.500	1067	1074
(2E)-2-Octen-1-ol [b]	1250	3.540	1067	1067
(3E,5E)-3,5-Octadien-2-one [b]	1255	2.350	1068	1068
cis-5-Ethenyltetrahydro-à,à,5-trimethyl-2-furanmethanol (cis-Linalool oxide) [b]	1260	1.780	1070	1069
(5Z)-5-Octen-1-ol [b]	1260	3.470	1070	1073
1-Octanol [b]	1265	2.695	1071	1076
4-Methylbenzaldehyde (p-Tolualdehyde) [c]	1290	3.615	1079	1086
1-Ethenyl-3-ethyl-benzene (m-Ethylstyrene) [d]	1300	1.655	1083	1064
trans-5-Ethenyltetrahydro-à,à,5-trimethyl-2-furanmethanol (trans-Linalool oxide) [b]	1305	1.840	1084	1086
2-Nonanone [b]	1320	1.400	1089	1093
(3Z)-3-Hexenyl propanoate [b]	1340	1.355	1095	1101
Ethyl heptanoate [b]	1345	1.165	1097	1101
3,7-Dimethyl-1,6-octadien-3-ol (Linalool) [b]	1350	2.265	1098	1101
Undecane [c]	1355	0.760	1100	1100
6-Methyl-3,5-heptadiene-2-one [d]	1355	2.630	1100	1084
2-Methylbutyl 2-methylbutanoate [b]	1360	1.040	1102	1104
Hexyl propanoate [b]	1365	1.200	1103	1106
Nonanal [b]	1365	1.385	1103	1107
4-Methyl-2-(2-methyl-1-propenyl)tetrahydro-2H-pyran (cis-Rose oxide) [b]	1380	1.200	1108	1112
(2E,4E)-2,4-Octadienal [b]	1380	2.510	1108	1113
Heptyl acetate [b]	1385	1.245	1110	1114
Phenylethyl alcohol (Benzeneethanol) [b]	1385	4.510	1110	1117
1,3-Diethenylbenzene (m-Vinylstyrene) [d]	1390	2.270	1112	1086
1-(4-Methyl-3-cyclohexen-1-yl)ethanone (4-Acetyl-1-methylcyclohexene) [b]	1410	2.340	1119	1135
2-Ethylhexanoic acid (2-Butylbutanoic acid) [b]	1425	1.615	1124	1126
4-Methyl-2-(2-methyl-1-propenyl)tetrahydro-2H-pyran (trans-Rose oxide) [b]	1430	1.190	1125	1130
1,7-Dioxaspiro[5.5]undecane [b]	1440	1.305	1129	1108
Butyl 3-hydroxybutanoate [d]	1440	3.565	1129	1111
2-Butenoic acid, 2-methyl-, butyl ester, (2E)- (Butyl tiglate) [b]	1450	1.340	1132	1133
Pentyl 2-methylbutanoate (Amyl 2-methylbutanoate) [d]	1465	1.075	1137	1126
2,6,6-Trimethyl-2-cyclohexene-1,4-dione (4-Oxoisophorone) [b]	1475	3.120	1141	1143
1,2-Dihydronaphthalene [b]	1485	2.095	1144	1156
Hexyl 2-methylpropanoate (Hexyl isobutanoate) [b]	1495	1.065	1147	1150
3,6-Dihydro-4-methyl-2-(2-methyl-1-propenyl)-2H-pyran (Nerol oxide) [b]	1505	1.445	1151	1152
(2E,6Z)-2,6-Nonadienal [b]	1505	2.070	1151	1153
1-Methoxy-4-vinylbenzene (p-Methoxystyrene) [b]	1505	2.830	1151	1159
2-Ethylhexyl acetate [b,e]	1510	1.150	1153	1159
Isopentyl valerate (Isoamyl valerate) [c]	1515	1.085	1154	1151
Pentylbenzene (1-Phenylpentane) [b]	1520	1.235	1156	1156

1,2,3,4-Tetrahydronaphthalene (Tetralin) [b]	1520	1.690	1156	1163
(2E)-2-Nonenal [c]	1525	1.720	1158	1163
Benzyl acetate (Phenylmethyl acetate) [b]	1530	3.295	1159	1167
1-(3-Methylphenyl)ethanone (m-Methylacetophenone) [b]	1560	3.385	1169	1176
1-Nonanol [b]	1565	2.425	1171	1176
5-Methyl-2-(1-methylethyl)-cyclohexanol (Menthol) [b]	1580	2.205	1176	1184
4-Ethylbenzaldehyde [b]	1585	3.060	1178	1181
5-Hexenyl butyrate [b]	1595	1.300	1181	1183
Octanoic Acid [b]	1595	2.505	1181	1192
1-(4-Methylphenyl)ethanone (p-Methylacetophenone) [c]	1600	3.390	1183	1188
2-(2-Butoxyethoxy)ethanol (Butoxydiethylene glycol) [b]	1605	3.680	1185	1184
Butyl hexanoate [b]	1620	1.160	1190	1193
Hexyl butanoate [b]	1625	1.205	1192	1195
Benzoic acid [b]	1625	4.320	1192	1185
(3Z)-3-Dodecene [d]	1630	0.825	1193	1195
alpha,alpha,4-Trimethyl-3-cyclohexene-1-methanol (alpha-Terpineol) [b]	1630	2.480	1193	1195
Ethyl octanoate [b]	1640	1.170	1197	1202
1-Methoxy-4-(2-propenyl)benzene (Estragole) [b]	1640	2.330	1197	1201
1-(2-Methylphenyl)ethanone (o-Methylacetophenone) [c]	1650	2.240	1200	1188
1-Methoxy-4-propylbenzene (p-Propylanisole, Dihydroanethole) [b]	1660	1.835	1204	1207
Decanal [b]	1665	1.335	1205	1208
(2E,4E)-2,4-Nonadienal [b]	1685	2.330	1213	1218
2,6,6-Trimethyl-1-cyclohexen-1-carboxaldehyde (beta-Cyclocitral) [b]	1695	1.800	1216	1219
Benzothiazole (Benzosulfonazole) [b]	1710	0.295	1221	1226
(3Z)-3-Hexenyl 2-methylbutanoate [b]	1730	1.160	1229	1231
Hexyl 2-methylbutanoate [b]	1750	1.150	1236	1239
Hexyl (2E)-2-butenoate [b]	1765	1.385	1241	1245
1-Phenoxy-2-propanol (2-Phenoxy-1-methylethanol) [d]	1775	2.025	1245	1215
(2E)-3,7-Dimethyl-2,6-octadien-1-ol (Geraniol) [b]	1790	3.265	1250	1255
2-Methylbutyl hexanoate [b]	1795	1.085	1252	1246
1-Methoxy-4-(1Z)-1-propenyl-benzene (cis-Anethole) [b]	1795	2.380	1252	1253
Phenylethyl acetate [b]	1795	2.880	1252	1257
5-Butyldihydro-2(3H)-furanone (gamma-Octalactone) [b]	1795	4.015	1252	1263
4-Methoxybenzaldehyde (p-Anisaldehyde) [b]	1800	0.895	1254	1257
Hexylbenzene [b]	1810	1.225	1257	1251
1-(2,4-Dimethylphenyl)ethanone (2,4-Dimethylacetophenone) [b]	1815	2.915	1259	1252
(2E)-2-Decenal [b]	1820	1.650	1261	1265
1,3-Octanediol [b]	1830	4.575	1264	1275
(2E)-3,7-Dimethyl-2,6-octadienal (Geranial) [b]	1835	2.075	1266	1268
1-Decanol [b]	1850	2.215	1271	1278
Nonanoic acid [b]	1860	0.385	1275	1289
1-(4-Ethylphenyl)ethanone (p-Ethylacetophenone) [b]	1870	3.000	1279	1274
(E)-1-Methoxy-4-(1-propenyl)benzene (trans-Anethole) [c]	1885	2.640	1284	1288

2-Undecanone [b]	1905	1.340	1291	1294
1-Methylnaphthalene [b]	1905	2.700	1291	1297
(3E)-3-Tridecene [c,d]	1910	0.825	1293	1293
(2E,4Z)-2,4-Decadienal [c]	1910	2.070	1293	1290
Tridecane [c]	1930	0.790	1300	1300
Undecanal [b]	1945	1.305	1306	1309
1,3-Isobenzofurandione (1,3-Dihydro-1,3-dioxo-isobenzofuran)	1950	1.590	1308	na
(2E,4E)-2,4-Decadienal [b]	1970	2.180	1315	1322
n-Hexyl trans-2-methyl-2-butenoate (Hexyl tiglate) [c]	2000	1.285	1327	1329
2-Methyl-heptylbutanoate [d]	2015	1.050	1333	1317
1,1,6-Trimethyl-1,2-dihydronaphthalene [b]	2060	1.655	1350	1354
1-(4-Methoxyphenyl)ethanone (p-Methoxyacetophenone, 4-Acetylanisole) [b]	2065	0.295	1352	1356
5-Pentyldihydro-2(3H)-furanone (gamma-Nonalactone) [b]	2075	3.610	1356	1362
(2Z)-3,7-Dimethyl-2,6-octadienyl acetate (Neryl acetate) [b]	2080	1.505	1358	1361
Heptylbenzene (1-Phenylheptane) [b]	2090	1.210	1362	1356
(2Z)-2-Undecenal [c]	2095	1.595	1363	1371
3-Hydroxy-2,4,4-trimethylpentyl 2-methylpropanoate [b]	2110	2.140	1369	1376
Decanoic acid [b]	2110	3.730	1369	1376
3-Methyltridecane [b]	2115	0.785	1371	1371
Butyl benzoate [b]	2115	2.085	1371	1376
(2E)-1-(2,6,6-Trimethyl-1,3-cyclohexadien-1-yl)-2-buten-1-one (trans-beta-Damascenone) [b]	2130	1.830	1377	1379
Biphenyl (Phenylbenzene, Lemonene) [b]	2130	2.910	1377	1380
1-(4-Methoxyphenyl)-2-propanone (4-Methoxyphenylacetone, p-Acetonylanisole) [b]	2135	4.920	1379	1384
Benzyl 3-methylbutanoate [b]	2145	2.025	1383	1399
Hexyl hexanoate [b]	2150	1.120	1385	1390
1-Ethylnaphthalene [b]	2165	2.460	1390	1395
(3Z)-3-Tetradecene [d]	2170	0.840	1392	1394
2-Dodecanone [b]	2170	1.315	1392	1393
2-Methyl-1,1'-biphenyl (1-Methyl-2-phenylbenzene, o-Phenyltoluene) [b]	2175	2.250	1394	1396
3,4-Dihydro-2H-1-benzopyran-2-one (3,4-Dihydrocoumarin) [c]	2180	3.350	1396	1386
1,2-Dimethoxy-4-(2-propenyl)benzene (Methyleugenol, 4-Allylveratrole) [b]	2185	2.910	1398	1403
Tetradecane [b]	2195	0.795	1402	1400
1,3-Dimethylnaphthalene [b]	2195	2.460	1402	1405
Dodecanal [b]	2210	1.290	1408	1410
2,6-Dimethylnaphthalene [b]	2225	2.585	1414	1409
2-Methyl-1H-isoindole-1,3(2H)-dione (n-Methylphthalimide) [b]	2235	0.905	1418	1425
1,1'-(1,4-Phenylene)bis-ethanone (p-Acetylacetophenone) [b]	2260	1.820	1428	1451
2,6-Bis(1,1-dimethylethyl)phenol [b]	2265	1.680	1430	1433
5-Methyl-2-benzofuran-1,3-dione (4-Methylphthalic anhydride)	2265	3.615	1430	na
Pentyl benzoate (Amyl benzoate) [b]	2280	1.935	1436	1442

1,7-Dimethylnaphthalene [b]	2280	2.680	1436	1428
(5E)-6,10-Dimethyl-5,9-undecadien-2-one (Geranyl acetone) [b]	2305	1.605	1446	1450
1,1'-(1,3-Phenylene)bis-ethanone (1,3-Diacetylbenzene)	2305	1.960	1446	na
3-Methylbutyloctanoate [c]	2310	1.070	1448	1449
Diisopropyl hexanedioate (Diisopropyl adipate) [b]	2310	1.655	1448	1464
2,3-Dimethylnaphthalene [b]	2310	2.760	1448	1439
(6E)-7,11-Dimethyl-3-methylene-1,6,10-dodecatriene ((E)-beta-Farnesene) [b]	2320	1.070	1452	1452
alpha-6-Pentylpyrone [b]	2320	3.780	1452	1463
n-Butyl 6-hydroxycaproate	2330	4.305	1456	na
2,6-bis(1,1-Dimethylethyl)-2,5-cyclohexadiene-1,4-dione (2,6-di-tert-Butyl-para-benzoquinone) [b]	2335	1.480	1458	1462
1-Phenyl-1-hexanone (Caprophenone) [b]	2335	2.300	1458	1428
5-Hexyldihydro-2(3H)-furanone (gamma-Decalactone) [b]	2345	3.295	1462	1469
1-[4-(Ethoxymethyl)phenyl]ethanone	2350	0.225	1464	na
Octylbenzene (1-Phenyloctane) [b]	2350	1.200	1464	1466
Undecanoic acid [b]	2350	2.535	1464	1465
Butyl o-hydroxybenzoate (Butyl salicylate) [b]	2360	2.165	1468	1474
Tetrahydro-6-(2Z)-2-pentenyl-2H-pyran-2-one (cis-Jasmin lactone) [b]	2360	3.355	1468	1490
Diisobutyl succinate [d]	2375	1.675	1474	1450
1-Dodecanol [c]	2375	1.925	1474	1476
(3E)-4-(2,6,6-Trimethyl-1-cyclohexen-1-yl)-3-buten-2-one (trans-beta-Ionone) [b]	2380	1.815	1476	1470
1-(1,5-Dimethyl-4-hexenyl)-4-methylbenzene (alpha-Curcumene) [b]	2385	1.260	1478	1480
(3E)-4-(2,2,6-Trimethyl-7-oxabicyclo[4.1.0]hept-1-yl)-3-buten-2-one (alpha-Ionone epoxide) [d]	2385	2.055	1478	1463
4-Methyl-1,1'-biphenyl (1-Methyl-4-phenylbenzene, p-Phenyltoluene) [b]	2390	2.680	1480	1487
1-Propylnaphthalene [b]	2400	2.240	1484	1490
Dodecanenitrile (1-Cyanoundecane) [b]	2405	1.795	1486	1486
6-Pentyltetrahydro-2H-pyran-2-one (delta-Decalactone) [b]	2405	3.435	1486	1494
3-Methyl-1,1'-biphenyl ((3-Methylphenyl)benzene, m-Phenyltoluene) [c]	2415	2.670	1490	1490
4-(4-Methoxyphenyl)-2-butanone (Anisylacetone, Rasberry ketone methyl ether) [c]	2420	3.305	1492	1501
2-Tridecanone [c]	2425	1.290	1494	1495
Pentadecane [c]	2440	0.805	1500	1500
Butylated Hydroxytoluene (2,6-di-tert-Butyl-4-cresol) [b]	2440	1.580	1500	1503
(3E,6E)-3,7,11-Trimethyl-1,3,6,10-dodecatetraene ((E,E)-alpha-Farnesene) [b]	2445	1.130	1502	1504
2,4-bis(1,1-Dimethylethyl)phenol (1-Hydroxy-2,4-di-tert-butylbenzene) [b]	2450	4.955	1504	1519
Tridecanal [c]	2460	1.280	1509	1516
Dibenzofuran (2,2'-Biphenylene oxide) [b]	2465	3.715	1511	1517
1,1'-(1,2-Ethanediyl)bis-benzene (1,2-Diphenylethane, Dihydrostilbene) [b]	2475	2.430	1515	1519
Methyl dodecanoate (Methyl laurate) [b]	2490	1.195	1522	1527
4,4,7a-Trimethyl-5,6,7,7a-tetrahydro-1-benzofuran-2(4H)-	2490	4.385	1522	1537

one (Dihydroactinidiolide) [b]				
6-Methyl-2H-1-benzopyran-2-one (6-Methylcoumarin, Toncarine) [b]	2525	1.875	1537	1557
2,3,6-Trimethylnaphthalene [b]	2535	2.460	1541	1537
1,4,5-Trimethylnaphthalene	2575	2.545	1559	na
2-Methylpentadecane [c]	2590	0.795	1565	1564
3-(4-Methoxyphenyl)-2-propenal (para-Methoxycinnamaldehyde) [c]	2595	2.080	1567	1567
5-Heptyldihydro-2(3H)-furanone (gamma-Undecalactone) [b]	2595	3.080	1567	1577
Nonylbenzene [b]	2600	1.190	1570	1571
Pentyl salicylate [b]	2605	2.055	1572	1575
1-Tridecanol [b]	2615	1.830	1576	1580
3,3'-Dimethylbiphenyl (1-Methyl-3-(3'-methylphenyl)benzene) [c]	2630	2.520	1583	1583
1-[2-(Isobutyryloxy)-1-methylethyl]-2,2-dimethylpropyl 2-methylpropanoate	2640	1.235	1587	na
4,4'-Dimethylbiphenyl (1-Methyl-4-(4'-methylphenyl)benzene) [c]	2640	2.500	1587	1590
1-Hexadecene [b]	2655	0.850	1593	1592
Ethyl dodecanoate [c]	2655	1.125	1593	1598
2-Tetradecanone [c]	2660	1.280	1596	1597
Hexadecane [c]	2675	0.810	1602	1600
Dodecyl acetate [b]	2690	1.175	1609	1610
Tetradecanal [b]	2700	1.255	1613	1614
2,6-bis(1,1-Dimethylethyl)-4-(1-oxopropyl)phenol [b]	2720	1.230	1622	1635
Benzophenone [b]	2725	4.400	1624	1627
Isopropyl dodecanoate (Isopropyl laurate) [b]	2730	1.050	1627	1617
Dibenzo[a,e]pyran (Xanthane) [b]	2755	3.480	1638	1637
Methyl (3-oxo-2-pentylcyclopentyl)acetate (Methyl dihydrojasmonate) [b]	2775	2.520	1647	1650
Phenyl benzoate	2785	4.170	1651	na
n-Hexyl-6-hydroxycaproate	2790	3.480	1653	na
Undecylcyclopentane [b]	2795	0.865	1656	1656
1,1'-Oxybis-octane (Dioctyl ether, 1-(Octyloxy)octane) [c]	2815	0.885	1664	1657
Decylbenzene (1-Phenyldecane) [b]	2835	1.185	1673	1675
5-Octyldihydro-2(3H)-furanone (gamma-Dodecalactone) [c]	2835	2.895	1673	1681
1-Tetradecanol [c]	2840	1.760	1676	1680
Hexyl salicylate [c]	2840	1.960	1676	1679
Tetradecanenitrile (Myristonitrile) [c]	2875	1.695	1691	1695
2-Pentadecanone [b]	2885	1.270	1696	1697
Heptadecane [c]	2895	0.810	1700	1700
2-Ethylhexyl benzoate [d]	2905	1.685	1704	1674
[(Z)-2-Phenylethenyl]benzene (cis-Stilbene)	2905	3.575	1704	na
Pentadecanal [c]	2925	1.245	1713	1710
2-Methylphenyl benzoate (o-Tolyl benzoate)	2925	3.720	1713	na
Methyl tetradecanoate (Methyl myristate) [b]	2945	1.175	1722	1727
1,2,3,4-Tetrahydroanthracene [b]	2995	2.950	1744	1749
3,5-di-tert-Butyl-4-hydroxybenzaldehyde (4-Formyl-2,6-di-	3005	2.985	1749	1774

tert-butylphenol) [b]				
Tetradecanoic acid [b]	3025	0.190	1758	1760
3-Methylheptadecane [c]	3045	0.815	1767	1772
1-Pentadecanol [c]	3060	1.695	1773	1778
5-Nonyldihydro-2(3H)-furanone (gamma-Tridecalactone) [f]	3060	2.750	1773	na
1-Octadecene [b]	3095	0.865	1789	1790
2-Hexadecanone [c,d]	3100	1.260	1791	1782
2-Hexyl-1-octanol	3100	1.540	1791	na
2-Ethylhexyl salicylate (Benzoic acid, 2-hydroxy-, 2-ethylhexyl ester) [b]	3105	1.735	1793	1805
3,5-di-tert-Butyl-4-hydroxyacetophenone (1-(3,5-Ditert-butyl-4-hydroxyphenyl)ethanone)	3110	2.810	1796	na
Octadecane [c]	3120	0.805	1800	1800
Hexadecanal [b]	3135	1.245	1808	1811
Isopropyl tetradecanoate (Isopropyl Myristate) [b]	3155	1.055	1819	1817
6,10,14-Trimethyl-2-pentadecanone (Hexahydrofarnesyl acetone) [b]	3185	1.180	1835	1843
1-Phenylnaphthalene [c]	3205	3.550	1846	1842
Pentadecanoic acid [b]	3220	4.780	1854	1851
2-Methyloctadecane [b]	3235	0.815	1862	1867
1-Hexadecanol [c]	3265	1.650	1878	1884
5-Decyldihydro-2(3H)-furanone (gamma-Tetradecalactone) [b,f]	3275	2.630	1884	1893
2-Heptadecanone [c]	3305	1.255	1900	1902
Nonadecane [c]	3310	0.825	1903	1900
1-Nonadecene [b]	3330	0.800	1913	1895
Methyl hexadecanoate (Methyl palmitate) [b]	3355	1.170	1926	1925
(9E)-9-Hexadecen-1-ol	3375	1.240	1936	na
Hexadecanoic acid [b]	3420	4.355	1959	1957
5-Undecyldihydro-2(3H)-furanone (gamma-Pentadecalactone) [f]	3480	2.530	1990	na
Eicosane [c]	3500	0.835	2000	2000
Hexadecyl acetate (Palmityl acetate) [c]	3510	1.165	2005	2009
Isopropyl hexadecanoate (Isopropyl Palmitate) [b]	3540	1.065	2022	2023
1-Octadecanol [c]	3650	1.580	2081	2086
5-Dodecyldihydro-2(3H)-furanone (gamma-Hexadecalactone) [f]	3675	2.450	2095	na
Heneicosane [c]	3685	0.840	2100	2100
Methyl (9Z)-9-octadecenoate (9-Octadecenoic acid (Z)-, methyl ester) [d]	3690	1.250	2103	2077
Methyl octadecanoate (Methyl stearate) [c]	3730	1.165	2126	2128
Docosane [c]	3860	0.850	2200	2200
2-Ethylhexyl (2E)-3-(4-methoxyphenyl)-2-propenoate (Ethylhexylcinnamate) [b]	4045	2.745	2312	2321
bis(2-Ethylhexyl)hexanedioate (Octyl adipate) [d]	4165	1.430	2385	2381

na – data not available

[a] – calculated retention index using retention time corresponding to base peak

[b] – both library searching and retention index employed for identification

[c] – assigned name is not first library hit; proper hit is unavailable in hit table/library; identification based on library searching, retention index and structurally ordered GCxGC chromatograms
[d] – literature retention index only available on 100% Dimethylpolysiloxane column
[e] – assigned name is not first library hit based on mass spectral examination and estimated retention index from NIST library
[f] – assigned name is not first library hit; proper hit is unavailable in library and identification is based on GCxGC structure

5.6 *Concluding remarks*

The global evaluation of extraction time profiles in HS-SPME analysis conducted with DVB/CAR/PDMS coating revealed the occurrence of inter-analyte displacements for only five compounds among the diverse set of 153 evaluated components having a diverse range of volatilities, polarities and affinities toward the employed extraction phase. Considering that reduction in SPME response with respect to extraction time in biochemically rich apple homogenate constituted by hundreds of components was detected for metabolites with molecular weights between 44 and 88 g/mol and having medium to high polarities and low fibre constants, a good correlation with 52-component spiked aqueous solution was achieved. In the latter scenario, nonlinear dependency was apparent for 2-pentanol, a C_5 member of homologous series of 2-alcohols and one the lowest K_{fs} compounds. Hence, the introduction of small molecular weight 'saturation' marker in comparative metabolomics analyses of biological samples having variable compositions is a valid approach for detection of nonlinear behavior and for ensuring accurate quantitative analysis. The employment of the polar component in C_5 range is the conceivable solution considering that modulation parameters usually employed in order to obtain a satisfactory modulator effectiveness for the

overall volatility range are suboptimum for early eluting compounds in the majority of cases.

On the other hand, the comparison between HS- and DI-SPME extraction modes revealed the attainment of a less biased and more comprehensive metabolic snapshot and improved capture of more polar and high molecular weight metabolites when direct immersion mode was employed. Considering nonselective adsorption properties of DVB/CAR/PDMS extraction phase and consequent rewarding metabolite coverage ensured with simultaneous implementation of DI-SPME mode, multidimensional instruments, such as the GCxGC-ToFMS employed here, are required for comprehensive characterization of metabolomics samples. The field of employment of *in vivo* DI-SPME for sampling of endogenous metabolites with minimum perturbation toward the biological system under question should hence open the doors for unique investigations in the field of global metabolite analysis.

6. *In vivo* DI-SPME sampling of apples: evaluating the precision of metabolomics platforms

6.1 *Background and objectives of research*

In conventional analytical chemistry, it is customary to report figures of merit for a particular optimized and validated method implemented in quantitative determination of a single analyte or a group of analytes [179]. Reporting such performance characteristics is in the line of good analytical practice and furthermore it provides credibility to the analytical method. When multiple analytes are quantitated, figures of merit, including precision, analysis time and limit of detection, are made by treating each analyte separately. Such reporting criteria are feasible for a limited number of analytes, hence making the implementation of the approach useless in establishing the quality of data acquired during global metabolomics workflow. Nevertheless, the reporting of simple numbers that have the potential to emphasize the performance characteristics of whole metabolomics platform is of utmost importance. Comprehensive characterization of the quality of *in vivo* DI-SPME – GCxGC-ToFMS global metabolomics platform is the focus of the experiments and data interpretations reported herein.

Reports that summarize the quantification of the analytical precision in metabolomics experiments have been performed, although such global evaluations of the analytical precision of a whole metabolomics platform are rare and unsurprisingly have not involved the inclusion of *in vivo* SPME sampling step hyphenated to GCxGC-ToFMS. In the current study, global measure, evaluation and interpretation of the analytical precision in employed *in vivo* DI-SPME – GCxGC-ToFMS platform were comprehensively investigated by considering both the analytical and biological sources of variation. Data interpretation was facilitated by establishing the correlation between analytical

precision and physicochemical properties of selected physicochemically diverse metabolites for which tentative annotation of identity was established through high quality mass spectral and retention index comparisons and occurrence of GCxGC molecular structure-retention relationships.

6.2 *Global evaluation of analytical precision, comparison with results obtained in ex vivo assay and potential of in vivo SPME in quantitative metabolomics*

6.2.1 *Global evaluation of analytical precision of in vivo DI-SPME – GCxGC-ToFMS metabolomics platform – October 2009 sampling*

Global evaluation of intra-fruit repeatability from the October 2009 sampling season was conducted by implementing a sampling approach in which three DVB/CAR/PDMS fibre coatings were penetrated to equal distances inside the fruit cortex. The insertion positions were made as to profile the metabolome from all possible sides of apple cortex or in another words, the three sampling positions were spread apart equal distances from each other. The picture illustrating the design of the sampling approach is presented in Figure 6.1.

Figure 6.1. Sampling design approach from October 2009 featuring intra-fruit repeatability experiment in which apple metabolome was profiled from all possible sides of the fruit cortex.

The ChromaTOF data processing procedure was initiated with automated processing of the three samples by adopting 100 as S/N threshold for peak finding algorithm. The corresponding automated procedure retrieved 7982 one-dimensional peak entries and was therefore subjected to further data reduction by employing the criterion of mass spectral similarity between experimentally obtained and true EI mass spectral fragmentation patterns. Consequently, facilitation of similarity threshold of 800 resulted in occurrence of 1540 one-dimensional peak entries, which corresponded to metabolite features that further needed to be screened in order to select exclusively high peak shape-quality true metabolites while simultaneously eliminating column fibre and extraction phase bleed peaks. Peak table screening was conducted for metabolites having S/N above or equal to 200. During the process of peak selection for quantitative determination of analytical precision, duplicate peak table entries whose origin is attributed to non-linear chromatography, second dimension column and modulator overloading, poor modulator effectiveness, poor resolution power and peak tailing as a result of analyte-stationary phase incompatibility were filtered out as well. In general, metabolite features for which these performance characteristics were not satisfactory to the point that accurate quantification was not possible were eliminated. Consequently, manual peak picking resulted in a table composed of 357 true metabolites having retention time coordinates as shown in Figure 6.2 and for which the quantitative evaluation of the analytical precision in terms of intra-fruit repeatability was conducted. During this process, the quality of mass spectral deconvolution was carefully assessed in order to detect outlying deconvolutions by confirming the correct assignment of quantification ion and its ‘uniqueness’ with respect to ions of chromatographically overlapping components. Additional manual supervision tasks involved the verification of reliability associated with the second dimension peak combination into respective one-dimensional entries based on mass spectral quality and GC elution window.

The modification of incorrect second dimension peak integration was also conducted in the process in order to ensure as accurate as possible estimation of analytical precision.

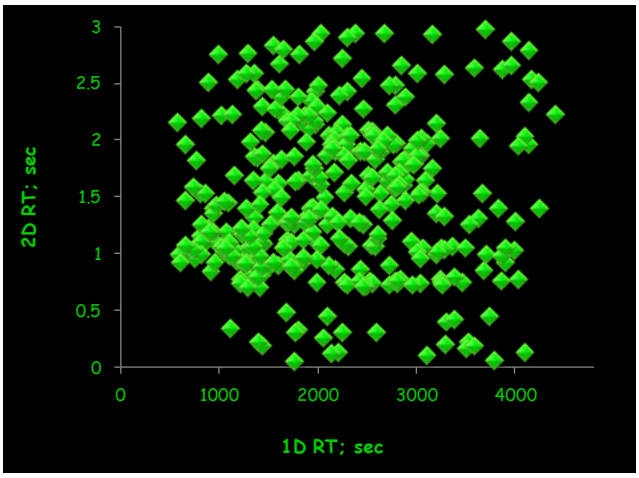

Figure 6.2. Peak apex plot with retention time coordinates of 357 true metabolites included in global evaluation of the analytical precision.

The median RSD for intra-fruit repeatability experiment involving three DVB/CAR/PDMS fibre coatings and 357 metabolites was 22.0% with minimum and maximum RSD values of 0.3 and 102.3%, respectively. In order to determine the quality of the metabolomics workflow, Food and Drug Administration (FDA) guidance was considered as a benchmark and hence its requirement on 15% RSD for analytical variability in targeted bioanalysis was adopted [100]. Even though the maximum RSD was unsatisfactory, this preliminary experiment demonstrated that the proposed *in vivo* DI-SPME metabolomics methodology has the potential to generate rewarding analytical results considering that 41.5% of peaks pass the strict FDA 15% RSD requirements.

However, a maximum RSD of 102.3% was quite unsatisfactory and these numerical values deserve to be accompanied by thorough data interpretation, which requires tentative identification of analyte identity for reliable deduction of trends. Consequently, 53 compounds whose retention on

two-dimensional separation plane is illustrated in peak apex plot in Figure 6.3 were tentatively identified with the aid of mass spectral similarity, retention index and/or GCxGC structurally ordered separations. The metabolites and their retention properties as well as the results of intra-fruit repeatability are listed in Table 6.1.

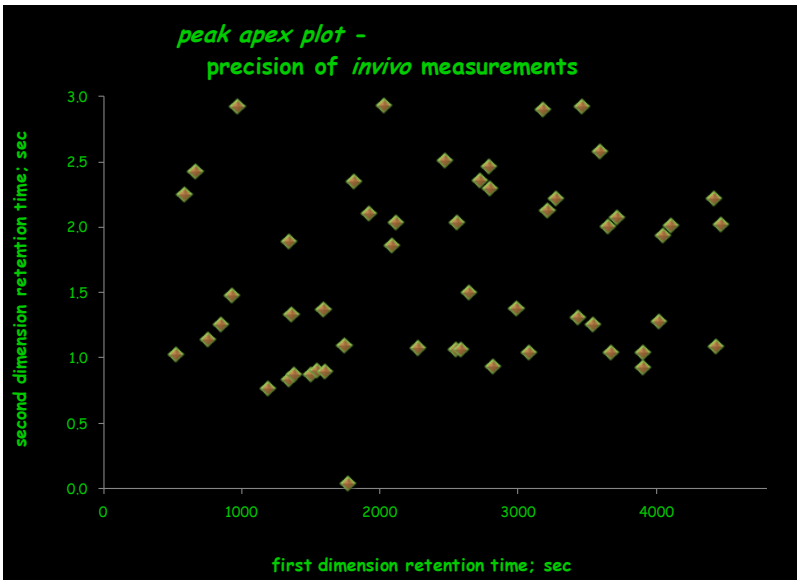

Figure 6.3. The peak apex plot of retention time coordinates corresponding to tentatively identified metabolites that were included in global evaluation of intra-fruit repeatability for *in vivo* DI-SPME – GCxGC-ToFMS metabolomics platform.

Table 6.1. Tentatively identified metabolites and their retention properties for the experiment involving global evaluation of intra-fruit repeatability of *in vivo* DI-SPME – GCxGC-ToFMS metabolomics platform.

analyte name; *(synonym)*	^1t_R; s	^2t_R; s	RI_{exp}	RI_{lit}	RSD; %
acetic acid, propyl ester	525	1.020	718	na	**13.2**
2-methyl-1-butanol	588	2.245	741	731	**25.0**
1-pentanol	666	2.420	770	759	**28.4**
Hexanal	759	1.135	803	801	**13.2**
2-vinyl-5-methylfuran	852	1.250	831	na	**24.7**
2-hexenal	930	1.475	855	850	**20.8**
trans-2-hexenol	972	2.915	867	na	**19.1**
2,6,6-trimethylbicyclo[3.1.1]hept-2-ene, *(alpha-pinene)*	1194	0.760	934	933	**7.2**
6,6-dimethyl-2-methylene-bicyclo(3.1.1)heptane,	1344	0.825	979	978	**0.3**

(beta-pinene)					
1-octen-3-ol	1347	1.885	980	978	**11.7**
6-methyl-5-hepten-2-one	1362	1.320	985	986	**9.3**
2-methyl-6-methylene-2,7-octadiene, *(beta-myrcene)*	1380	0.865	990	991	**11.7**
1-methyl-4-(1-methylethenyl)cyclohexene, *(limonene)*	1509	0.870	1030	1030	**11.0**
butyl 2-methylbutanoate	1545	0.905	1042	na	**23.6**
2-octenal	1596	1.365	1058	1059	**3.7**
1-isopropyl-4-methyl-1,4-cyclohexadiene, *(gamma-terpinene)*	1602	0.890	1059	1058	**12.2**
Nonanal	1743	1.090	1104	1107	**4.1**
cis,cis-4,6-octadienol	1767	0.035	1112	na	**14.4**
butyl-3-hydroxybutanoate	1818	2.345	1129	na	**16.8**
4-ethylbenzaldehyde	1920	2.100	1164	1181	**9.0**
(2E)-3-phenyl-2-propenal, *(trans-cinnamaldehyde)*	2034	2.930	1202	na	**14.9**
4-isopropylbenzaldehyde, *(cumaldehyde)*	2091	1.855	1223	na	**6.6**
1-benzofuran-2(3H)-one, *(2-coumaranone)*	2124	2.030	1234	na	**15.6**
2-undecanone	2283	1.070	1291	1294	**19.8**
5-pentyldihydro-2(3H)-furanone, *(gamma-nonalactone)*	2469	2.505	1361	1362	**13.4**
2-dodecanone	2556	1.065	1394	1393	**23.4**
1,2-dimethoxy-4-(2-propenyl)benzene, *(methyl eugenol)*	2562	2.030	1397	1403	**21.3**
Dodecanal	2589	1.060	1407	1410	**28.9**
1,3-diacetylbenzene	2646	1.495	1430	na	**4.3**
5-hexyldihydro-2(3H)-furanone, *(gamma-decalactone)*	2730	2.355	1465	1469	**12.5**
6-pentyltetrahydro-2H-pyran-2-one, *(delta-decalactone)*	2793	2.460	1490	1494	**10.7**
1-(4-methoxyphenyl)-3-butanone, *(rasberry ketone methyl ether)*	2799	2.295	1493	na	**10.6**
1,3,6,10-dodecatetraene, 3,7,11-trimethyl-, (3E,6E)-, *(farnesene <(E,E)-, alpha->)*	2826	0.925	1504	1504	**13.8**
1-tridecanol	2991	1.370	1574	1580	**14.4**
Tetradecanal	3078	1.040	1612	1614	**46.4**
phenyl benzoate	3180	2.890	1659	na	**25.4**
dihydro-5-octyl-2(3H)-furanone, *(gamma-dodecalactone)*	3219	2.125	1677	1681	**10.7**
6-heptyltetrahydro-2H-pyran-2-one, *(delta-dodecalactone)*	3279	2.220	1704	1708	**16.3**
1-pentadecanol	3435	1.305	1779	1784	**14.7**
valeric acid, 2-pentadecyl ester	3462	2.915	1791	na	**34.8**
2,6,10-dodecatrien-1-ol, 3,7,11-trimethyl-, acetate, *(farnesyl acetate)*	3546	1.245	1833	1832	**55.0**
4-(1-methyl-1-phenylethyl)phenol, *(4-cumylphenol)*	3597	2.575	1858	na	**6.6**
5-decyldihydro-2(3H)-furanone, *(gamma-tetradecalactone)*	3657	2.000	1888	na	**22.6**
2-heptadecanone	3681	1.040	1900	1915	**43.0**
6-nonyltetrahydro-2H-pyran-2-one, *(delta-tetradecalactone)*	3717	2.070	1919	1920	**31.9**

Octadecanal	3909	1.040	2014	2024	**66.4**
1-methylethyl hexadecanoate, *(isopropyl palmitate)*	3912	0.915	2016	na	**32.8**
1-octadecanol	4023	1.275	2060	na	**60.7**
5-undecyldihydro-2(3H)-furanone, *(gamma-pentadecalactone)*	4056	1.935	2073	na	**72.1**
6-undecyltetrahydro-2H-pyran-2-one, *(delta-hexadecalactone)*	4110	2.010	2095	na	**63.7**
2-ethylhexyl-4-methoxycinnamate	4422	2.220	na	na	**48.2**
Eicosanal	4440	1.080	na	na	**77.5**
6-dodecyltetrahydro-2H-pyran-2-one, *(delta-heptadecalactone)*	4470	2.015	na	na	**102.3**

As it can be seen from the corresponding peak apex plot and metabolite entry table, the selected metabolites comprised a diverse array of volatilities and specific interactions with the second dimension column. In addition to chemical diversity, a particular emphasis during metabolite selection procedure was placed on inclusion of as many metabolites as possible that are members of homologous groups of compounds. Hence, groups of series related compounds were individually evaluated in order to deduct the correlation between molecular weight and the analytical precision. The detailed examination of boiling point-analytical precision dependencies are illustrated in Figure 6.4 for homologous series of aldehydes, 1-alcohols, 2-alkenals, 2-ketones, delta-lactones, gamma-lactones and terpenoids.

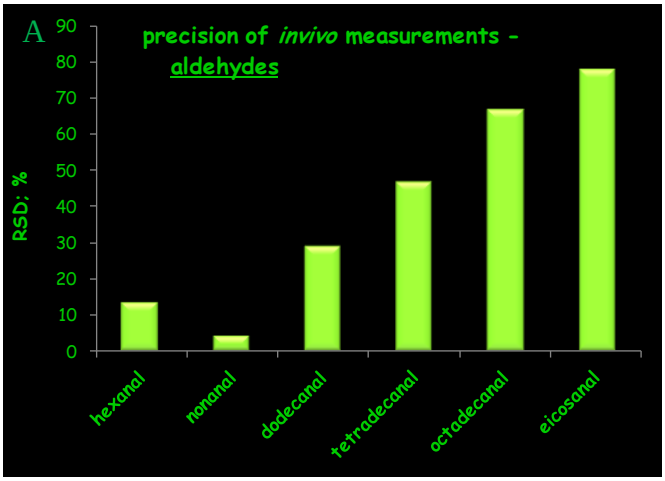

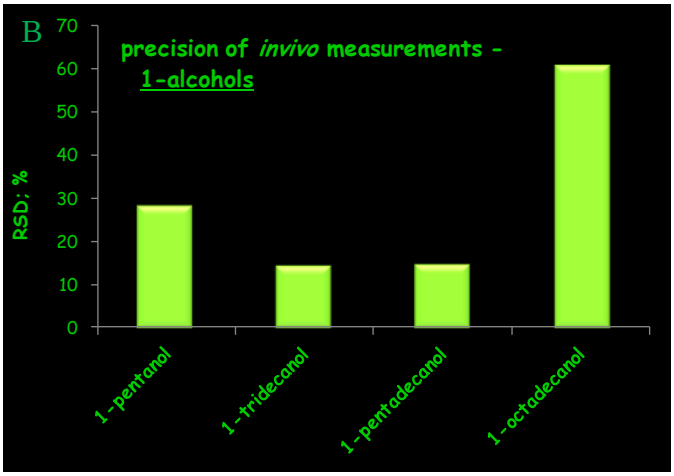
B
precision of *invivo* measurements -
1-alcohols
RSD; %
70
60
50
40
30
20
10
0
1-pentanol
1-tridecanol
1-pentadecanol
1-octadecanol

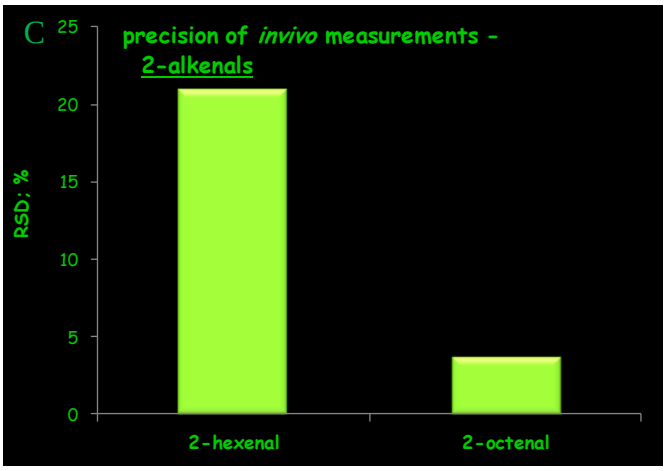
C
precision of *invivo* measurements -
2-alkenals
RSD; %
25
20
15
10
5
0
2-hexenal
2-octenal

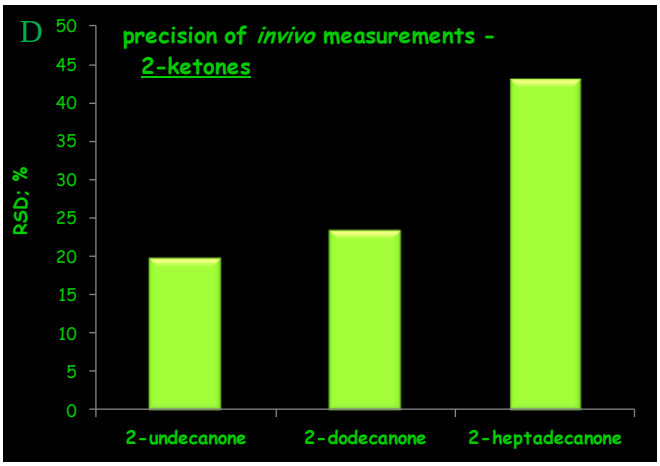
D
precision of *invivo* measurements -
2-ketones
RSD; %
50
45
40
35
30
25
20
15
10
5
0
2-undecanone
2-dodecanone
2-heptadecanone

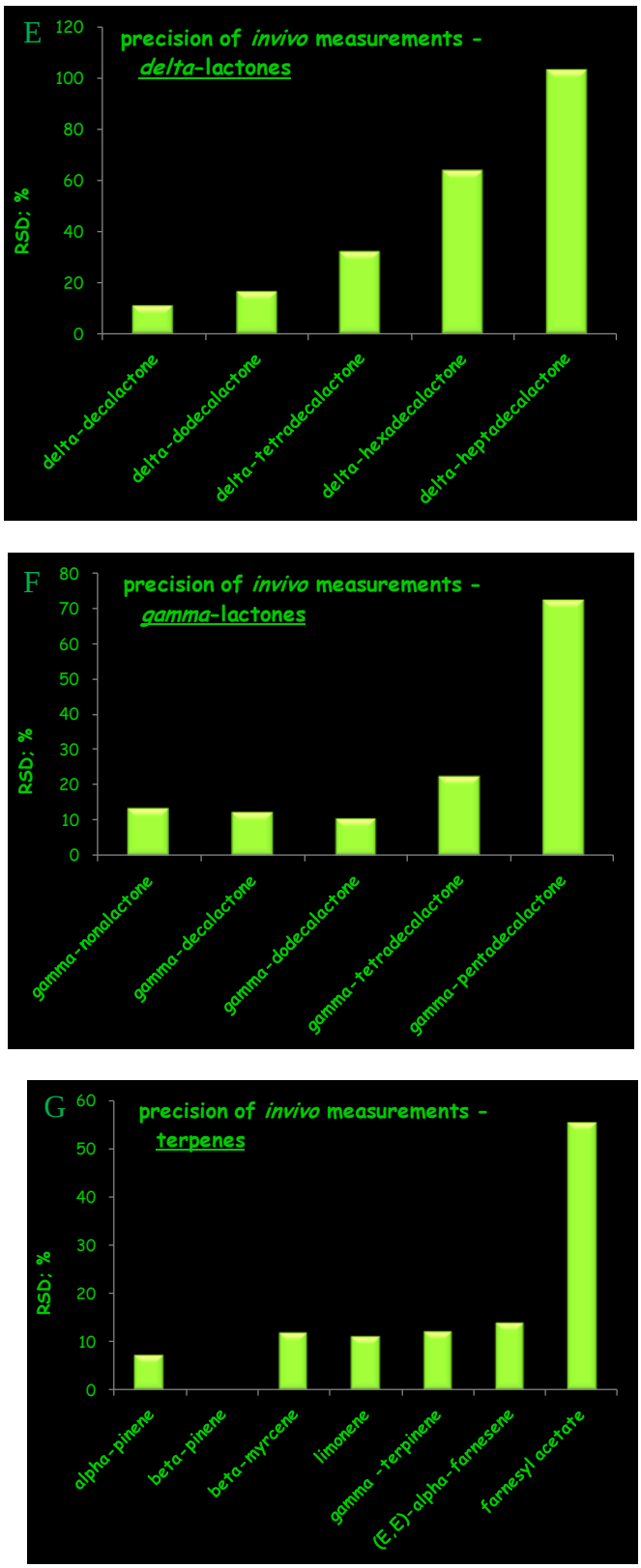

Figure 6.4. Dependencies between molecular weight and analytical precision of *in vivo* DI-SPME – GCxGC-ToFMS assay for several homologous groups of

metabolites including A – aldehydes, B – 1-alcohols, C – 2-alkenals, D – 2-ketones, E – delta-lactones, F – gamma-lactones, and G – terpenoids.

The results obtained clearly demonstrate significant correlations between metabolite molecular weights and analytical precision as well as the consistency in RSD distribution relative to increasing boiling point for all groups of evaluated compounds. The trend exhibited showed increasing RSD with increasing boiling point within a particular structurally related group of metabolites. These results may be attributed to one of the following factors: *i)* poor inter-fibre repeatability; *ii)* negligible variations in extraction timing for high K_{fs} compounds for which equilibrium was not attained resulting in high relative errors in amount of analyte extracted; *iii)* differences in mass transfer for high K_{fs} compounds between the three sampling positions; *iv)* adsorption of macromolecules on the surface of solid extraction phase affecting the analyte uptake; *v)* differences in spatial intra-compartmental distribution of analytes; and *vi)* environment-induced differences in spatial distribution of analytes.

The first possible option was considered as in the history of SPME, occasionally, unacceptable inter-fibre repeatability results were observed and based on our experience, they were more frequently encountered in the case of solid coatings. In extreme cases, the microscopic observation of solid coatings indicated discoloration trends along the 1-cm coating length and for example in the case of DVB/CAR/PDMS coating, the outer layer of DVB/PDMS frequently seemed non-uniformly applied over CAR/PDMS layer. This inconsistency in applying a uniformly thick DVB/PDMS layer has the potential not only to affect extraction sensitivity, but also length of equilibrium time and desorption efficiency when high molecular weight compounds contact the stronger sorbent. However, this option was ruled out based on the performance characteristics of the three coatings in spiked aqueous sample analysis which pointed out excellent inter-fibre repeatability across the volatility and polarity ranges as shown in Figure 6.5.

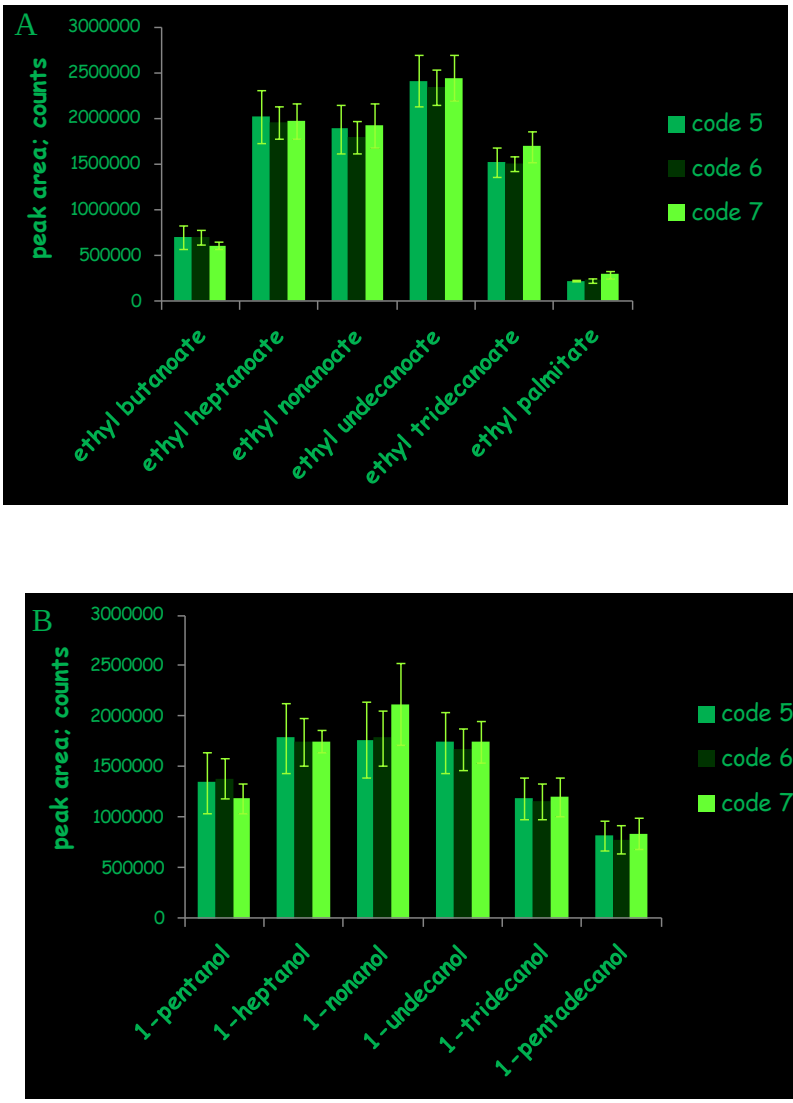

Figure 6.5. Performance characteristics of the three DVB/CAR/PDMS coatings in *ex vivo* analysis of A – ethyl esters and B – 1-alcohols in spiked water samples. The coatings were employed in *in vivo* sampling during October 2009 season.

The second possibility for increasing analytical variation with respect to molecular weight in a particular series of compounds may be attributed to small variations in extraction time during manual SPME operation that result in large relative errors in extracted amounts when the extraction is performed in the steep regions of a typical extraction time profile curve [94-95]. Based on the extraction time uptakes corresponding to spiked aqueous samples and apple

homogenate, 60 min extraction condition represents an extraction time point in the steep part of the extraction time profile curve for heavy and high K_{fs} metabolites for which high RSD was observed during *in vivo* assay. However, precise timing was enforced during *in vivo* sampling with all three SPME coatings and the length of extraction time itself is reasonable so that the effect of extraction time variations on the order of few seconds on the analytical variability for high K_{fs} compounds can be considered negligible. The third option above is related to the potential differences in the mass transfer rates of high K_{fs} metabolites between the investigated tissue and the fibre coatings at three different positions of sampling. The amount of analyte extracted by SPME coating is governed by analyte distribution constant between the SPME coating and sample matrix if the equilibrium is reached, or when short exposure times are implemented the rate of mass transfer between sample matrix and extraction phase affects the analyte uptake by the fibre [94-95]. Provided that within 60 min of exposure time, high molecular weight metabolites do not reach equilibrium in the tissue matrix, the extraction efficiencies for such compounds are governed by mass transfer rates, which are otherwise defined by analyte diffusion coefficients in the sample matrix and agitation conditions. This assumption is supported by extraction time profiles presented in Chapters 3 and 5, which illustrate slow equilibration in HS-SPME analysis of liquid samples. Furthermore, the diffusion path length *in vivo* is greater than the one existing in a liquid medium as a consequence of the tortuosity of the diffusion route when analyte molecules come in contact with matrix components through which passage does not occur and that obstruct free diffusion significantly [180]. During the process of developing one of the variants of diffusion-based calibration methods, called kinetic calibration using dominant pre-equilibrium desorption in which calibration of SPME responses *in vivo* is performed on the basis of isotropic relationship between analyte absorption from the matrix to the extraction phase and desorption of preloaded internal standard from the extraction phase to the sample matrix, Zhou et al. investigated desorption kinetics of preloaded pesticide standards *in vivo* [180]. The authors adopted the

experimental design in which four PDMS fibre coatings were preloaded with pesticide internal standards at four different concentrations while loading was performed from aqueous solutions spiked with pesticides at concentrations of 1.0, 2.0, 4.0 and 8.0 μg/mL for 20 min. Desorption kinetics was examined by exposing the preloaded fibre coatings at four different positions located 1 cm apart with respect to each other along the leaf of the jade plant. The linear relationship between the preloaded pesticide amounts and those remaining in the fibre coating after 20 min of desorption in the tissue was claimed by the authors [180]. The linear relationship characterized by correlation coefficients of 0.990, 0.994, 0.999 and 0.999 for target pesticides including carbofuran, propoxur, carbaryl and aldicarb, respectively, indicates independence of desorption rate on the sampling position in the leaf while simultaneously implying that extraction kinetics should not be affected by sampling position either considering the symmetric relationship between the two rates. Therefore, the correlation associated with decreasing precision in a particular group of structurally related compounds with respect to increasing molecular weight of analytes for which equilibration was not reached should not be influenced by differences in sampling positions either in the current global metabolomics study. The three fibre coatings were inserted from directions perpendicular to the fruit stem and penetrated to equal distances from the surface of the fruit, hence such possibility was eliminated considering the impressively regulated intra- and inter-compartmentalization and organization of complex plant structures.

Adsorption of macromolecules on the surface of solid extraction phase has the potential to affect analyte uptake, reproducibility, desorption efficiency and representativeness of sample extract once non-volatile and thermally labile compounds undergo reactions in the injector leading to their decomposition and formation of volatile end products [181]. Therefore, the extraction efficiency of individual coatings was compared for representative low and high boiling point analogues of structurally related compounds. The results are illustrated in

Figure 6.6 for members of homologous groups of terpenoids, delta-lactones and aldehydes.

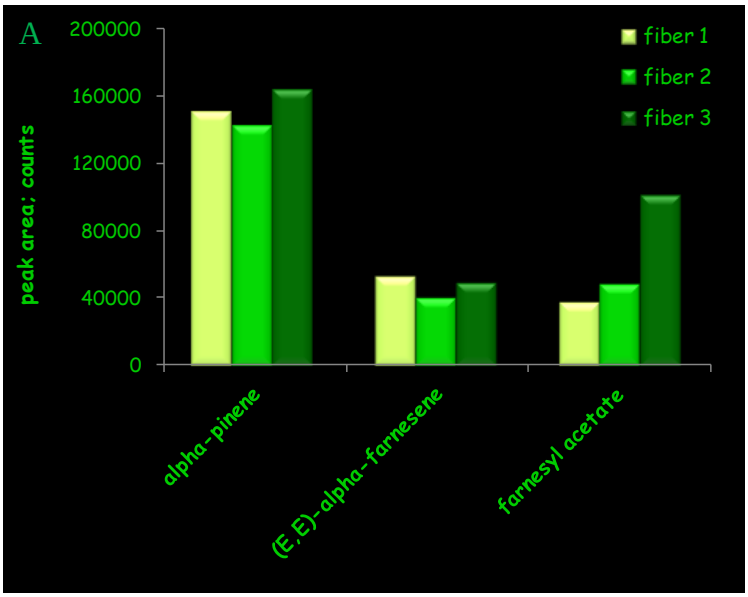

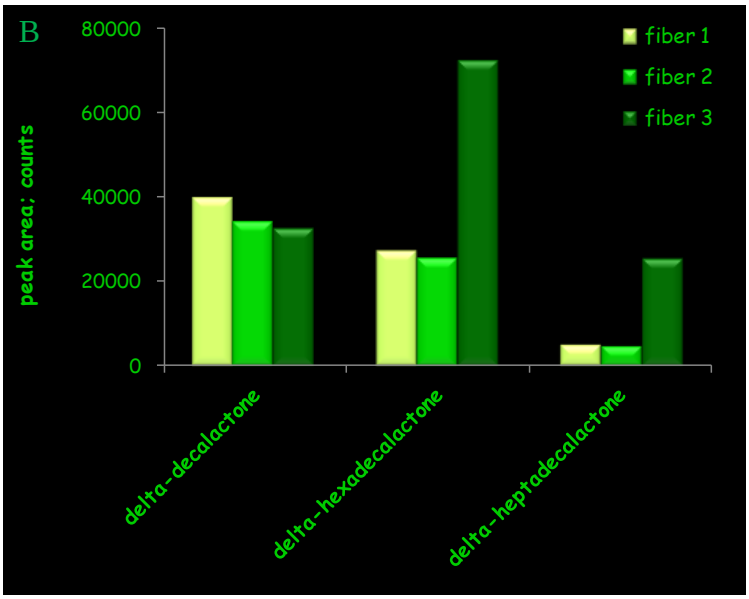

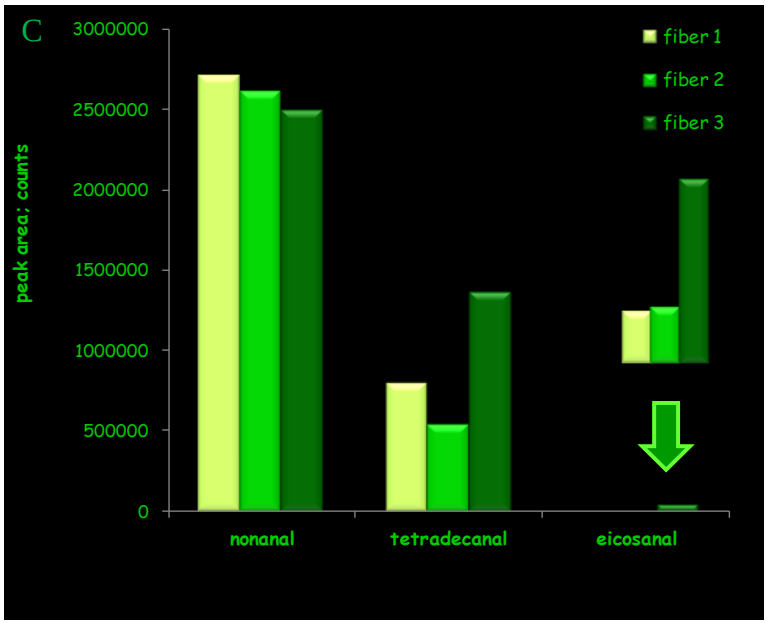

Figure 6.6. Comparison of the extraction efficiencies of three fibre coatings employed in *in vivo* DI-SPME – GCxGC-ToFMS assay for selected low and high boiling point members of homologous groups of A – terpenoids, B – delta-lactones and C – aldehydes.

The trends in extraction efficiency between the three employed fibre coatings in Figure 6.6 clearly illustrate that the fibre coating with code 3 always exhibited higher extraction efficiency for highest molecular weight members of homologous series with the effect being more pronounced with increasing molecular weight in a homologous series. However, the plots presented in Figure 6.7 for selected metabolites for which the annotation of analyte identity was not conducted, show a completely reversed correlation. Namely, the same fibre coating for which highest extraction efficiency was obtained for highest molecular weight members of homologous series presented in Figure 6.6 exhibited lowest extraction efficiency for selected unidentified heavy metabolites in Figure 6.7. Therefore, considering that the extraction efficiency for high molecular weight compounds was differentially affected for the coatings inserted at different positions, the unsatisfactory reproducibility of *in vivo* assay should not be attributed to extraction phase fouling with matrix interferences, but rather complex processes of anatomical and physiological nature in plant metabolomics.

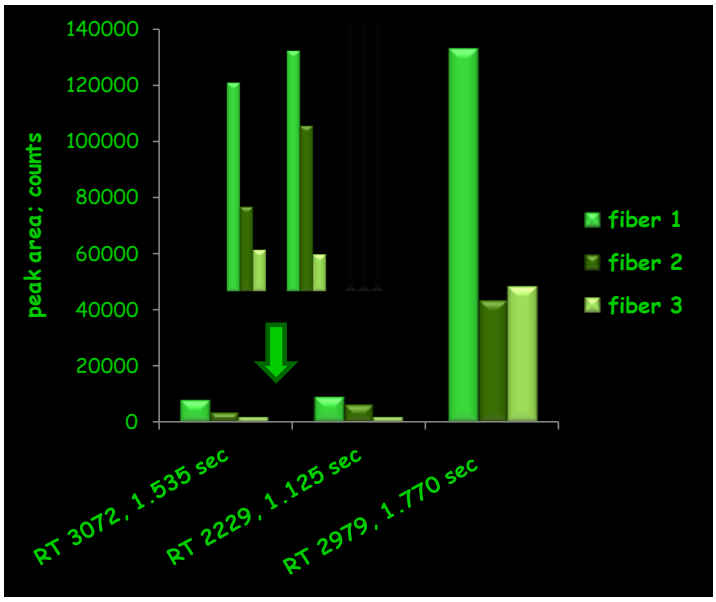

Figure 6.7. The extraction efficiencies for three SPME coatings employed in *in vivo* assay and obtained for unidentified high molecular weight compounds that were used in global evaluation of precision.

The considerations on plant anatomy and physiology were addressed in the introductory section 1.3.2, where it was thoroughly emphasized that the anatomic and physiological complexity of plants has to be considered in studies focused on plant metabolism [14]. Each plant organ, tissue and compartment is composed and characterized by a specific set of metabolites that are present in specific distributions and are very often differentially affected by external stimuli. For example, the analysis of glucosinolate distribution within *Arabidopsis thaliana* revealed a non-uniform distribution throughout the leaf tissue and the authors concluded that the accumulations of these compounds close to the leaf margin and the middle vein strongly influences the feeding preference of larvae [182]. The comparison of leaf phloem sap samples obtained from petiole recesses and leaf disks that were taken from the same leaf of *Cucurbita maxima* also attributed to differing GC-MS metabolite profiles with respect to levels of carbohydrates [5]. Similarly, Moing et al. developed a multi-platform metabolomics assay in order to monitor the spatial and developmental metabolite alterations in melon [183]. The authors implemented

HS-SPME analysis with PDMS/DVB fibre coating to elucidate the melon volatile profile among other probed metabolites, including mineral elements and those metabolites amenable to LC-MS analysis. Significant inter-compartmental metabolite localizations were detected and reported in line with findings deducted in afore-mentioned references, except that the spatial distribution of volatile metabolites was correlated to the suppressed or expressed contents of their primary and secondary metabolite precursors in the same compartmental divisions. For example, the presence of six isoprenoids including ß-carotene correlated significantly to the spatial distribution of ß-cyclocitral, ß-ionone, dihydro-ß-ionone and dihydropseudoionone reflecting therefore their biosynthesis from carotenoid degradation and clear dependence between localization of products and precursors in melon fruit tissue. A close link between alanine and serine and the production of ethyl hexanoate was also identified. All of these factors suggest the impressive potential of spatial metabolomics to reveal interactions between primary metabolism and volatile bouquet that can be implemented for future flavour design efforts in melon fruit [183]. However, brute force has been applied for dissecting different melon layers and the sample preparation procedure has been initiated by cutting two slices of 1 cm thickness in the equatorial plane of each fruit, removing skin and seeds and taking five concentric mesocarp rings of flesh from the periphery (outer mesocarp) to the centre (inner mesocarp). The rings corresponding to different positions were deep frozen and stored at -80 ^{o}C until grinding in liquid nitrogen. Considering that *in vivo* SPME has been widely acknowledged for its potential in studies requiring spatial resolution advantages, the eliminated sample handling steps including harvesting, metabolism quenching, homogenization and storage are additionally advantageous [141]. The question arising now is whether the differentially affected extraction efficiencies for high molecular weight metabolites between the three positions that are contributing to unsatisfactory intra-fruit repeatability are the result of differences in spatial localization of metabolome. Since the perpendicular direction of inserted fibre coatings with respect to apple stem and consistent exposure depth should ensure

in vivo sampling of same compartments within apple, such a conclusion would be reasonable under the circumstance of having the inconsistent radius of apple around the stem which could be resulted by uneven size of the fruit, however such observations were not visually present at the site of sampling.

Alternatively, the intra-compartmental variations in metabolite content have been extensively reported in particular in response to environmental stimuli [101]. For example, and as reported in the introductory section 1.1.4.1, Rudell and coworkers conducted metabolic profiling of 'Granny Smith' apple peel in order to evaluate metabolomic alterations resulting from prestorage Ultraviolet – white light irradiation [52]. The authors reported irradiation-induced alterations in metabolic pathways associated with ethylene synthesis, flavonoid pigment synthesis, acid metabolism and fruit texture. Rudell et al. also performed global metabolite profiling in 'Granny Smith' apples that were exposed to artificial UV-white light after harvest [43]. The authors hypothesized that postharvest UV-vis irradiation will reduce scald susceptibility and in fact, they determined that scald was eliminated on the side of the fruit directly exposed to artificial light and as far as the opposite fruit side was concerned, the scald was reduced with increasing treatment time. Correlations between scald status and light treatment duration as well as induced changes in metabolome including decreasing α-farnesene content with light treatment duration were reported. Indeed, pre-harvest light environment was determined as one of the crucial factors having the potential to alter the scald incidence [43]. However, in addition to artificial light, scald incidence was found to be reduced on sunlight-exposed portions of apples and enhanced by bagging the fruit to limit sunlight exposure during fruit ripening [43]. The increased sunlight exposure has been linked with heightened phenolic levels in exposed peel [43]. In general the synthesis of phenylpropanoid compounds and isoprenoid pigments and many other metabolites originating from other pathways was provoked following fruit exposure to both sunlight and artificial light. Other authors also cautioned toward appropriate definition of organ positions with respect to environmental and growing conditions, including sun

and shade [15]. In addition to apple, alterations in metabolite content, including the volatile profile resulting from enhanced light environment, have been detected in strawberry fruit [37]. For example, Watson et al. observed a considerable variation in the content of volatile metabolites even within a single crop as a result of environmental conditions as explained below [37,184]. In order to assess the alterations in metabolome as a result of management practices, they determined contents of 3 non-volatile and 13 volatile metabolites by employing atmospheric pressure chemical ionization coupled to gas phase analysis and direct liquid-mass spectrometry for analysis of two groups of metabolites, respectively [184]. More specifically, the effect of environmental conditions, including harvest date and shading effect, was investigated with respect to levels of non-volatile metabolites, including sucrose, glucose and citric acid, while the group of volatile metabolites included acetaldehyde, acetic acid, methyl acetate, ethyl acetate, hexenal, hexanal, methyl butanoate, 2-heptanone, ethyl butanoate, ethyl methyl butanote, furanone, ethyl hexanoate, and ethyl methyl hexanoate [184]. Shading was induced at three treatments of 0%, 25% and 47% by employing shade netting. While based on their studies, the concentration of sucrose and glucose was inversely proportional to the level of shading, shade treatments had no significant effect on the fruit citric acid concentration [184]. On the other hand, among volatile metabolites, the contents of hexanal, hexenal, ethyl methyl butanoate and methyl butanoate were significantly affected when comparing control fruit with those submitted to 47% shading treatment [184]. The data obtained suggested that brief light integral has a significant effect on strawberry flavour quality, considering that 47% shading treatment caused a significant reduction in the concentration of hexanal, hexenal, ethyl methyl butanoate and methyl butanoate as compared to control fruit of the same harvest. In line with the results obtained during *in vivo* sampling here, extraction efficiencies for the volatile metabolites that were considered in this study and simultaneously for which tentative identification was verified in Table 6.1 were monitored for three employed fibre coatings

inserted in three positions. The results for 2-hexenal and hexanal are illustrated in Figure 6.8.

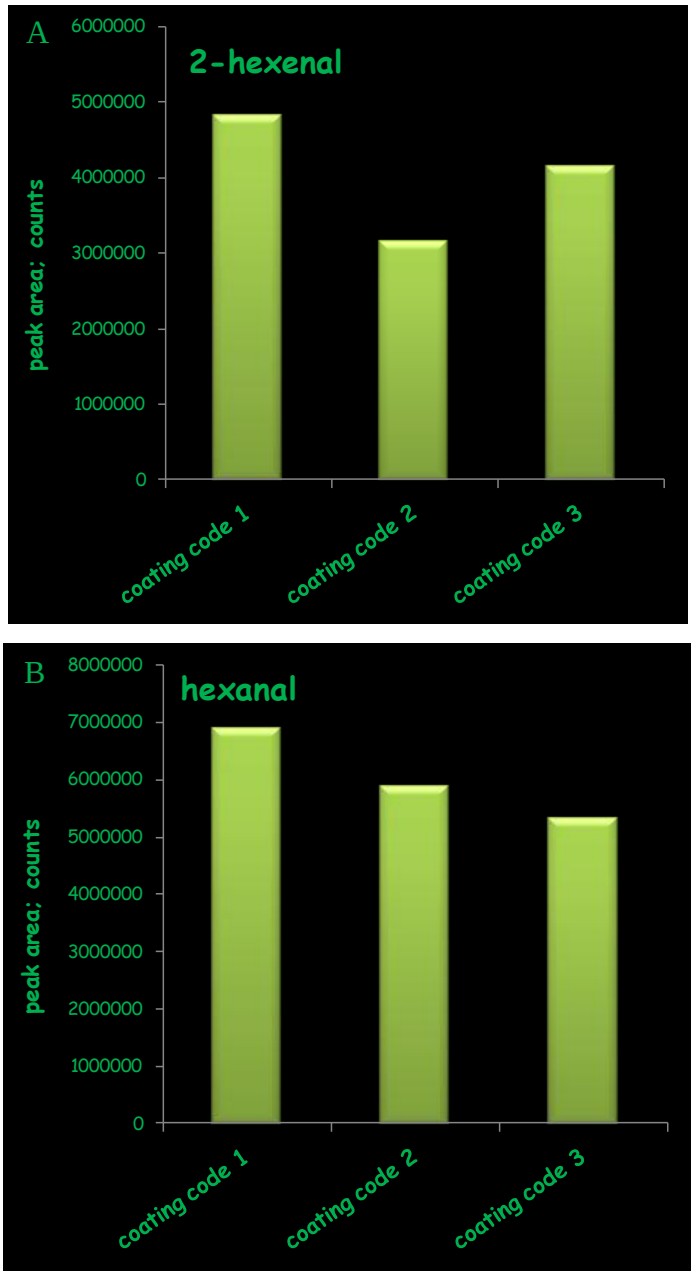

Figure 6.8. Extraction efficiencies for 2-hexenal (plot A) and hexanal (plot B) during *in vivo* DI-SPME sampling of 'Honeycrisp' apples.

The fibre coating 1 that was inserted into fruit cortex such that the SPME sampling side was facing east at the time of sampling and was accessible to

sunlight, indeed extracted slightly higher amounts of these volatile compounds, which is in agreement with results reported by Watson et al. However, only one replicate was performed per each sampling position which limits the implementation of statistical analysis in order to determine whether these differences are indeed significant. On the other hand, fibre coating 3 for which the corresponding sampling side was facing inward towards the apple tree and hence was exposed to an environment in which sunlight exposure should be inhibited, was extracting lower amounts of these volatile metabolites.

One of the possible factors that Watson et al. considered to be responsible for the reduction in volatile metabolite content with respect to shading interval is reduction in photosynthetic processes and consequent reduction in the amounts of primary metabolite precursors from which volatile compounds are produced [184]. Alternatively, such changes in metabolome could be resulted by the direct influence of shading on the fruit. Finally, it was concluded that the mechanisms by which shading periods incident on the crop alter concentrations of flavour compounds remain to be elucidated. The definite elucidation of these mechanisms is greatly hindered by the difficulty in interpreting data obtained under uncontrollable growing conditions such as variable light integral and fruit-to-fruit variability with respect to maturity and developmental level which all represent disadvantages of any *ex vivo* protocol. Miniaturization and on-site compatibility advantages of SPME along with *in vivo* sampling inducing minimum perturbation toward the investigated system permit repeated and multiple samplings of individual organisms, hence eliminating the manifestation of biological inter-species variations in data interpretation.

6.2.2 *Global evaluation of intra- and inter-fruit repeatability in in vivo DI-SPME – GCxGC-ToFMS metabolomics platform – September 2010 sampling*

Considering that considerable variations in extraction efficiencies of selected metabolites, in particular high boiling point compounds were detected between three different fibre coatings inserted considerable distances apart in fruit cortex, the *in vivo* sampling of 2010 harvest season involved a substantially different sampling approach. As explained in the experimental section, the experimental design involved insertion of three SPME fibre coatings per biological specimen while all sampling positions were facing west and were located 1.5 cm apart with respect to each other. Intra- and inter-fruit repetability was evaluated by activating data processing method in terms of peak finding and similarity thresholds of 50 and 700, respectively. Consequently, manual picking of high quality metabolites and elimination of false outlying features was performed on HC-O-3-code-17 sample since the peak table generated by software in this case resulted in the highest number of entries (15097). The mass spectral unknowns were filtered to eliminate peaks with hits having similarity lower than 700 and consequently 4932 peaks were obtained. The dimensionality of peak table was further reduced to result in a total of 111 one-dimensional peak entries having S/N and similarity greater than 200 and 800, respectively. The peak apex plot demonstrating retention time coordinates of metabolites included in global evaluation of intra- and inter-fruit repeatability is presented in Figure 6.9. The median of intra-fruit repeatability data involving three fibre coatings and one apple (HC-O-5) was 37.1% with minimum of 0.7% for unidentified compound with retention time coordinates of 1106 and 1.71 s and maximum of 125.6% for metabolite with first and second dimension retention times of 3108 and 0.910 s, respectively. As a result, unsatisfactory precision was obtained for selected compounds as well.

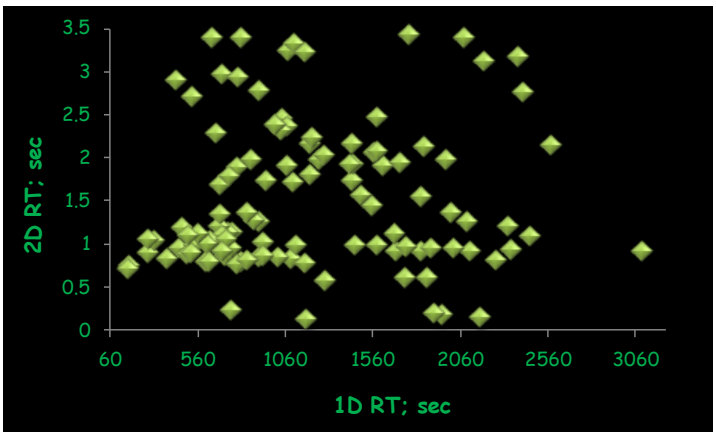

Figure 6.9. Peak apex plot demonstrating retention time coordinates of metabolites included in global evaluation of intra- and inter-fruit repeatability in September 2010 harvesting season.

Therefore, it is crucial to compare the two *in vivo* sampling designs in terms of analytical precision obtained. This is illustrated in Figure 6.10 for members of homologous series of esters.

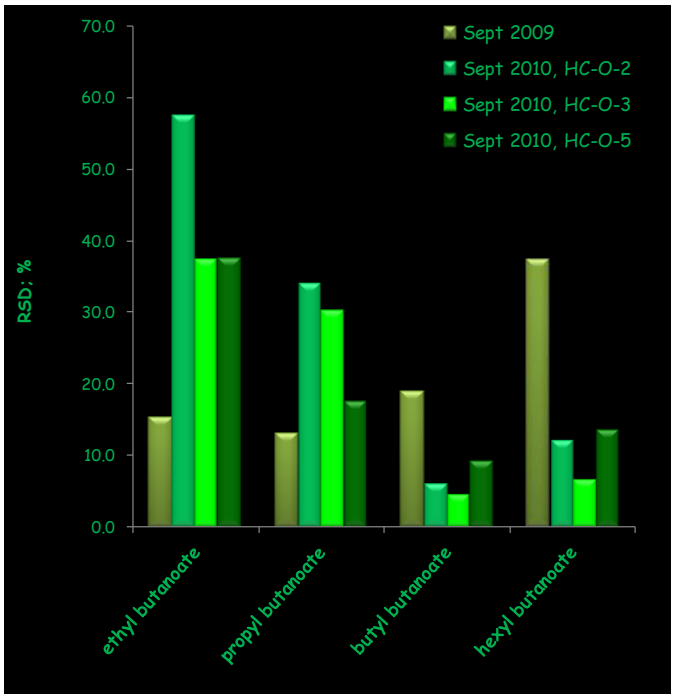

Figure 6.10. Comparison of analytical precision corresponding to *in vivo* sampling designs from 2009 and 2010 harvesting years for series-related compounds.

The figure clearly illustrates that for September 2010 sampling design in which fibre sampling positions were placed 1.5 cm distance apart from each other, RSD improved significantly for high molecular weight compounds. This is also illustrated in Figure 6.11 for hexyl butanoate, the highest molecular weight compound for which the RSDs obtained for three fibre coatings per each of the sampled apples including HC-O-2, HC-O-3 and HC-O-5 were 12.0, 6.5 and 13.5%, respectively, while the median RSD was 12.0%. This is a significant improvement as compared to sampling from 2009 harvesting year, since RSD for the same compound was 37.3%. The extraction performance of the employed coatings in sampling of this particular metabolite in HC-O-2, HC-O-3 and HC-O-5 apples is illustrated in Figure 6.11. In addition to excellent intra-fruit repeatability, the figure also illustrates excellent inter-fruit repeatability characterized by RSD of 16.5% for this metabolite.

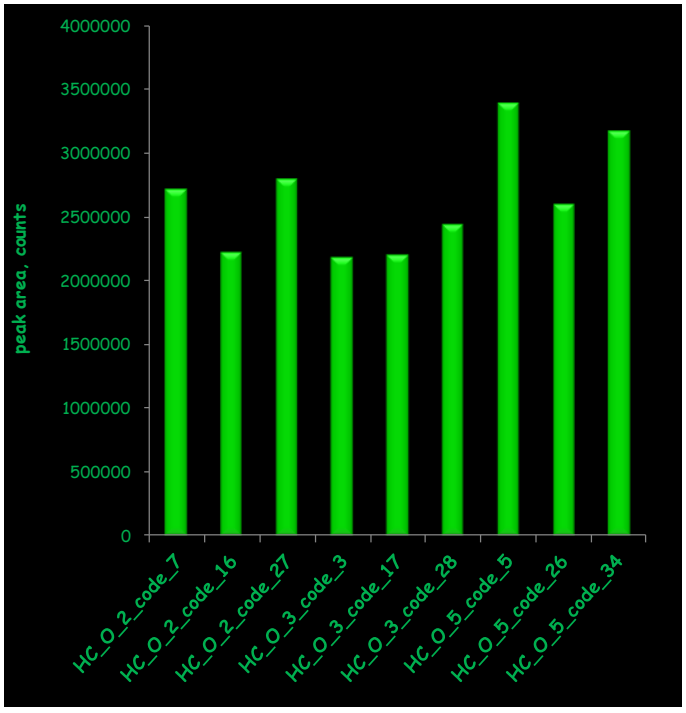

Figure 6.11. The extraction efficiencies of employed DVB/CAR/PDMS coatings in *in vivo* sampling of hexyl butanoate.

The performance characteristics of the coatings in terms of intra- and inter-fruit repeatability for butyl butanoate were also rewarding. For HC-O-2, HC-O-3 and HC-O-5 apples, RSDs determined on the basis of three exposed fibre coatings per apple were 5.9, 4.5 and 9.0%, respectively, while the RSD corresponding to sampling design from October 2009 was 18.6%. Inter-fruit repeatability for sampling design from 2010 resulted in RSD of 5.9%, as seen in Figure 6.12.

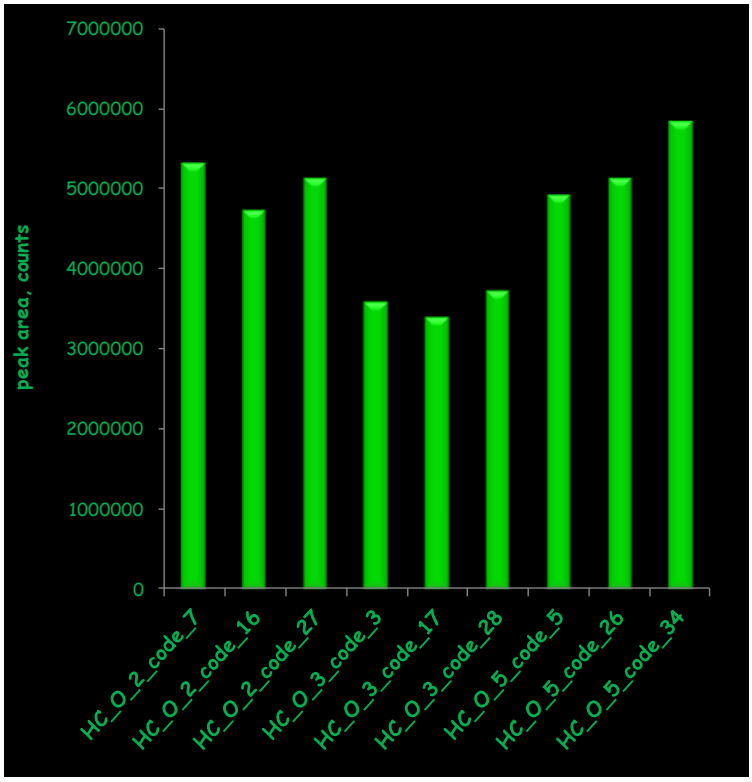

Figure 6.12. The extraction efficiencies of employed DVB/CAR/PDMS coatings in *in vivo* sampling of butyl butanoate.

However, in addition to satisfactory performance characterstics for higher molecular weight metabolites, Figure 6.10 also illustrates poor intra-fruit repeatability for most volatile compounds in the corresponding homologous series. For example, intra-fruit repeatability for ethyl butanoate is characterized by 57.5, 37.2 and 37.3%, while for propyl butanote, RSDs of 34.1, 30.0 and 17.4% were obtained for apples HC-O-2, HC-O-3 and HC-O-5, respectively.

For these two compounds, intra-fruit repeatability was characterized by 15.1 and 12.8% RSD, respectively in October 2009 sampling design. The poorer performance characteristics of *in vivo* sampling design from September 2010 harvesting year in terms of analytical precision for intra-fruit determinations of these early eluting compounds are also illustrated in Figure 6.13, where metabolites are presented with respect to GC elution order. Selected metabolites are also differentially affected, hence, while sampling design from September 2010 harvesting season resolved limitations associated with high analytical variability observed for higher molecular weight compounds, intra-fruit repeatability for highly volatile compounds was poorer. These results provide directions for future DI-SPME *in vivo* platforms, which should incorporate further examinations of analytical precision with respect to sampling position.

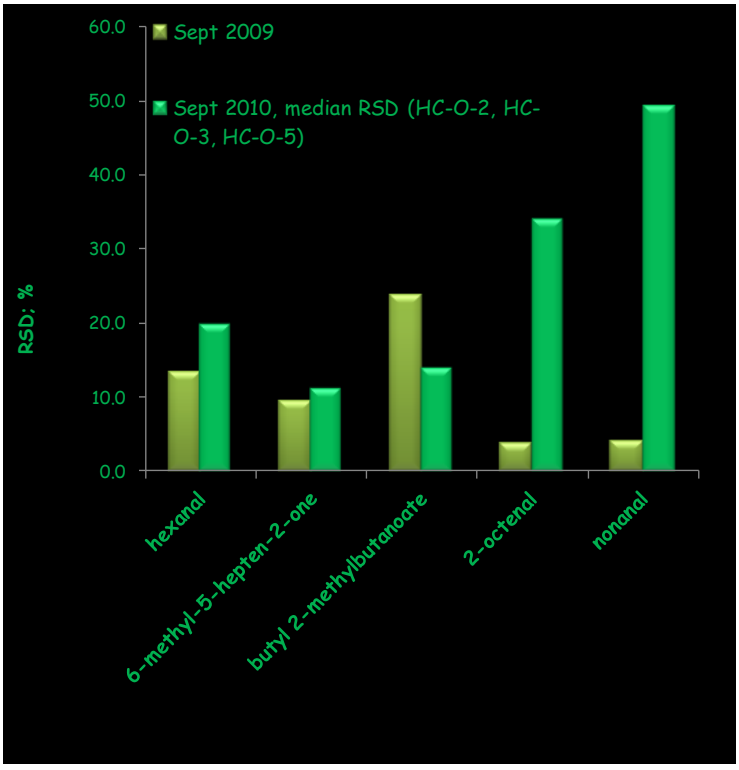

Figure 6.13. Comparison of analytical precision corresponding to *in vivo* sampling designs from 2009 and 2010 harvesting years for selected early eluting metabolites.

While the results of inter-fruit repeatability obtained during *in vivo* assay in September 2010 for butyl butanoate and hexyl butanoate were rewarding as mentioned above, global evaluation including a diverse spectrum of compounds is required. For 9 SPME fibre coatings exposed to HC-O-2, HC-O-3 and HC-O-5 apples, median RSD was 55.6% with minimum of 10.6 and maximum of 214.8%. However, this is to be expected considering that in global metabolomics, biological variability significantly exceeds analytical variability. As mentioned in a study by Watson et al, significant strawberry fruit-to-fruit variation in volatile metabolite content was detected and attributed to different maturity levels of fruits as well as to multiple harvests [184]. The effect of uneven maturity on high fruit-to-fruit variability is a valid explanation for the trend observed herein, since maturity issues of 'Honeycrisp' apples have been reported as illustrated in introduction [58]. In addition, the apples considered in evaluation of fruit-to-fruit variation were located significant distances apart from each other and in addition, HC-O-2, HC-O-3 and HC-O-5 apples were also grown on different branches and subbranches to such extent that sunlight availability was substantially different. For example, HC-O-2 was located on the main branch within the tree. The sub-branch corresponding to HC-O-3 was further away from the tree trunk, growing from the HC-O-2 branch and closer to the ground. HC-O-5 subbranch was also a part of the branch on which HC-O-2 was located. Different locations with respect to the tree, nutrient availability and light supplement have the potential to induce significant alterations in metabolome profile.

Even in a study reported by Tikunov et al., fruit-to-fruit variation within genotype ranged from 8 (2E-heptenal) to 35 (2-methylbutanol) % RSD, while biological variation between genotypes ranged between 28% and 198% [185]. However, the method employed by the authors involved the implementation of SPME in headspace extraction mode and only 13 highly volatile compounds were included in the evaluation. *In vivo* DI-SPME methodology implemented in the current research project represents state-of-the-art approach in global metabolite analysis not only because hundreds of components were included in

determination of analytical figures of merit, but for its promising potential in the field of spatial and temporal metabolomics studies of plant systems.

6.2.3 *Comparison of in vivo DI-SPME and ex vivo HS-SPME metabolomics assays in terms of analytical precision*

For comparative purposes, intra-fruit repeatability of *ex vivo* HS-SPME metabolomics assay was also evaluated by considering the identified analytes that are listed in Table 6.1., provided that they were effectively extracted by HS-SPME mode whose employment as explained before results in biased representation of metabolome and intensified discrimination against high molecular weight and polar analyte coverage. A total of 40 compounds were included in evaluation of intra-fruit repeatability of HS-SPME extracts, including selected metabolites that were additionaly included in the determination of quality of HS-SPME metabolomics assay. The experiment was also designed to determine the long term stability of samples after they were thawed, placed in extraction vessels and stored on autosampler tray before extraction. Prolonged tray storage was purposely enforced in order to monitor the stability of selected components in a complex matrix of highly dynamic nature, and in accordance with ensuring an acceptable degree of throughput, which is a crucial prerequisite in metabolomics, considering the large numbers of samples to be analyzed. The median RSD corresponding to intra-fruit repeatability and long term stability of HS-SPME extracts (n = 10) was 13.6% with minimum and maximum RSDs of 2.5 and 88.6% for 2-hexenal and limonene, respectively. Therefore, for 55% of analytes, RSDs were lower than 15%, while selected compounds exhibited unusual profiles with respect to storage time (Figure 6.14). Figure 6.14 illustrates unstable response with respect to storage time on tray for 6-methyl-5-hepten-2-one, *beta*-myrcene, (2E)-2-octenal, *trans-beta*-damascenone and (*Z,Z*)-farnesol adversely affecting

RSDs for these compounds that are represented by 35.2, 27.3, 20.9, 41.2 and 37.5%, for the compounds illustrated, respectively.

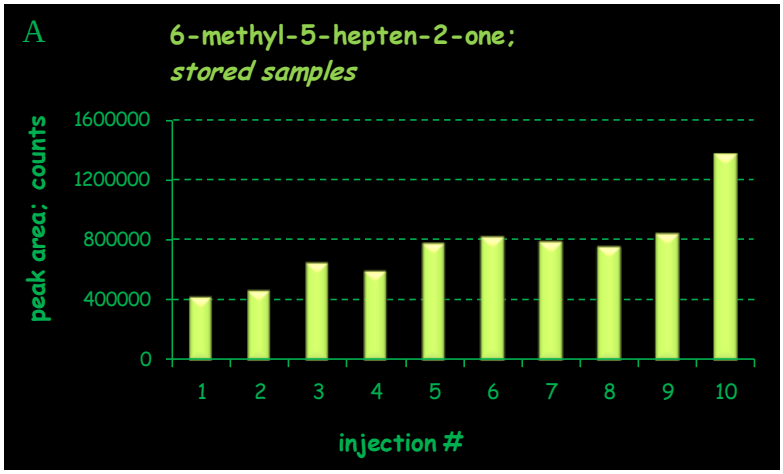

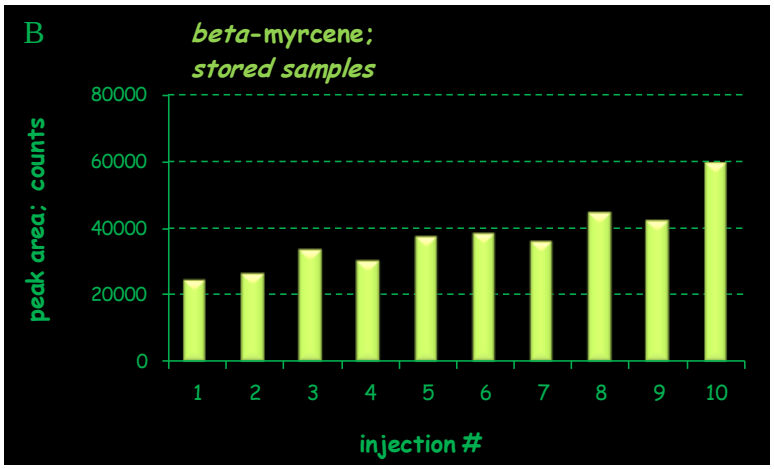

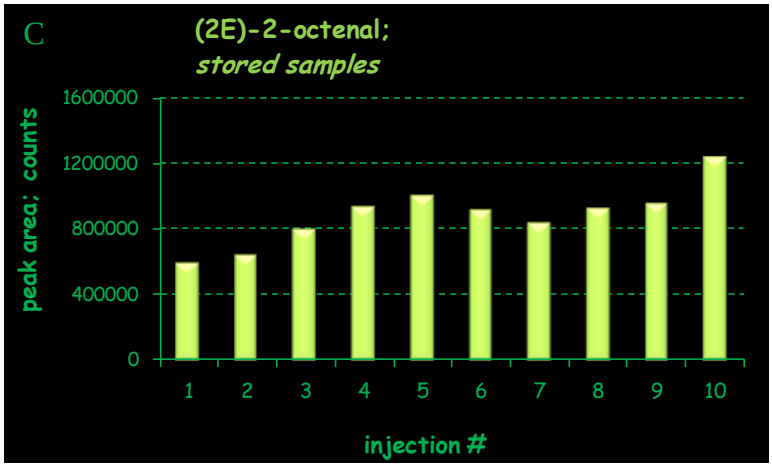

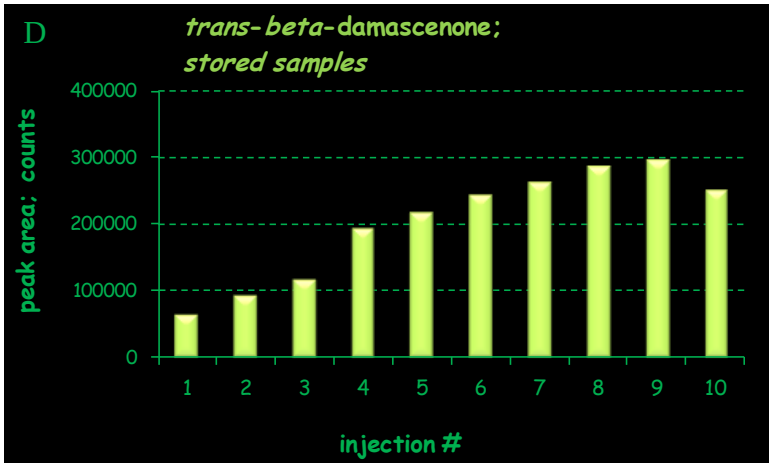

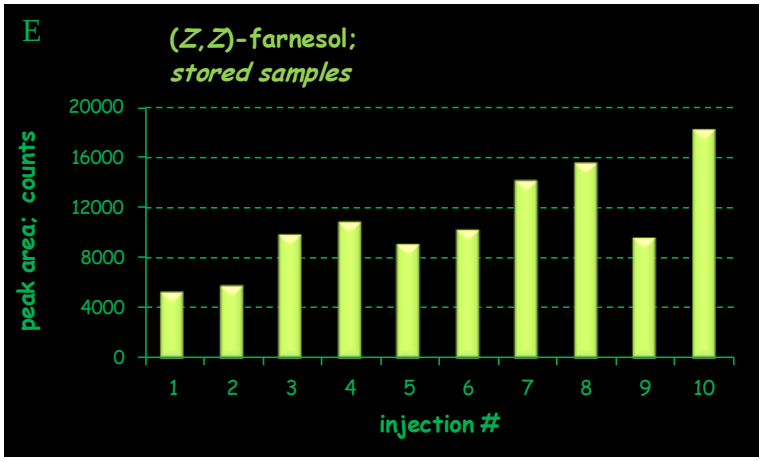

Figure 6.14. Intra-fruit repeatability and stability of selected metabolites detected in HS-SPME extracts of apple samples stored on tray for prolonged time periods. A - 6-methyl-5-hepten-2-one, B - *beta*-myrcene, C - (2E)-2-octenal, D - *trans*-*beta*-damascenone and E - (*Z*,*Z*)-farnesol.

The increasing extracted responses with respect to storage time on tray are likely related to complexity, heterogeneity, and dynamic nature of investigated matrix composed of thousands of chemically diverse analytes. These issues with sample incompatibility with respect to storage have been reported in a number of studies as emphasized in Section 1.3.2. Issues related to alterations of volatile metabolite composition of fruit during storage and likelihood of leakage, cross-contamination, and loss of sample integrity are well documented for periods following metabolism quenching and sample

preparation and prior to extraction [5,15]. Considering that even freeze storage is not exempt from such drawbacks, it is not surprising that such alterations occur in samples stored at room temperature. Vanderhaegen and coworkers published a review on the chemistry of beer aging and reported the nature and extent of changes occurring in the chemical composition of this food commodity during storage [186]. The authors identified a number of reactions responsible for the formation and/or decomposition of selected groups of metabolites, including carbonyl compounds, acetals, esters and sulfur compounds. The decomposition and/or formation mechanisms of these compounds have been associated with occurrence of:

i) aging reactions producing carbonyl compounds including oxidation of higher alcohols, Strecker degradation of amino acids, aldol condensation, oxidation of unsaturated fatty acids and formation of *trans*-*beta*-damascenone;

ii) acetalization of aldehydes;

iii) Maillard reaction;

iv) synthesis and hydrolysis of volatile esters;

v) degradation of polyphenols.

Even though beer as a sample matrix is a completely separate story, selected reaction pathways are common to many biological systems and interestingly, the contents of *trans*-*beta*-damascenone presented in Figure 6.14 above have also been reported to increase in beer with respect to aging time [186]. This particular compound belongs to a class of carotenoid-derived carbonyl compounds and its precursors in beer have been associated with allene triols and acetylene diols formed by the degradation of neoxanthin. The authors also proposed that the compound formation might be related to chemical hydrolysis of glycosides [186]. On the other hand, several studies also confirmed the increase of (2E)-nonenal and other linear C_4-C_{10} alkenals and alkanals in beer during storage [186]. In this study, the levels of (2E)-2-octenal were also enhanced during tray storage of apple samples (Figure 6.14) and the fact that

plots in Figure 6.15 show perfect intra-fruit reproducibility and long term stability for the same compounds when samples are analyzed by HS-SPME immediately after thawing, makes the interpretation undertaken here valid. The RSDs for 6-methyl-5-hepten-2-one, *beta*-myrcene, (2E)-2-octenal, *trans-beta*-damascenone and (*Z*,*Z*)-farnesol detected in freshly analyzed samples were 7.0, 6.7, 7.3, 6.6 and 19.5%, respectively.

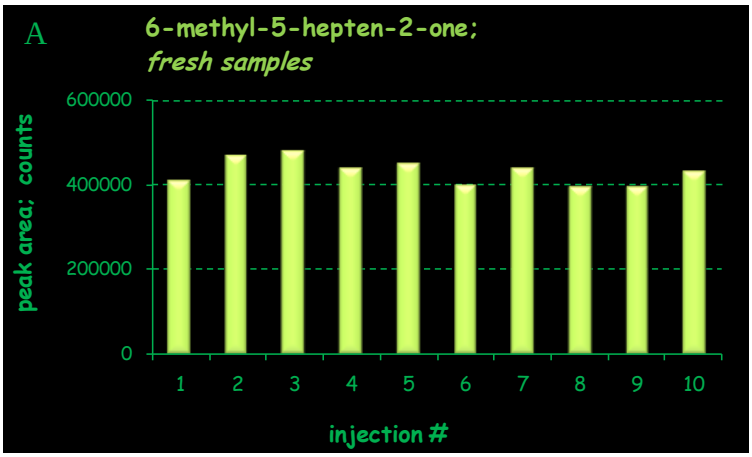

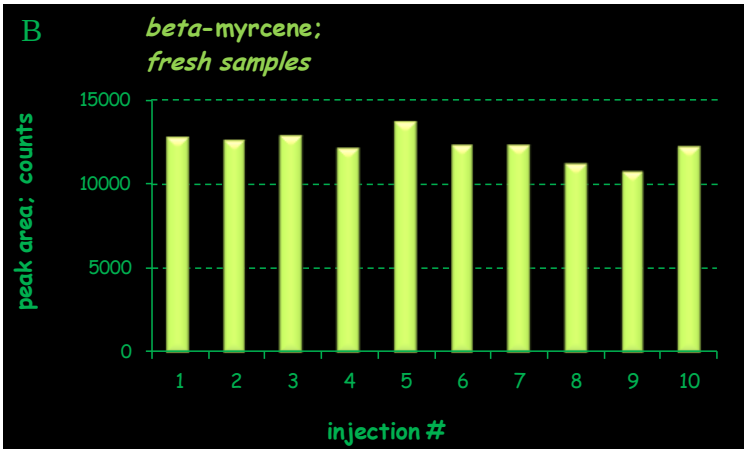

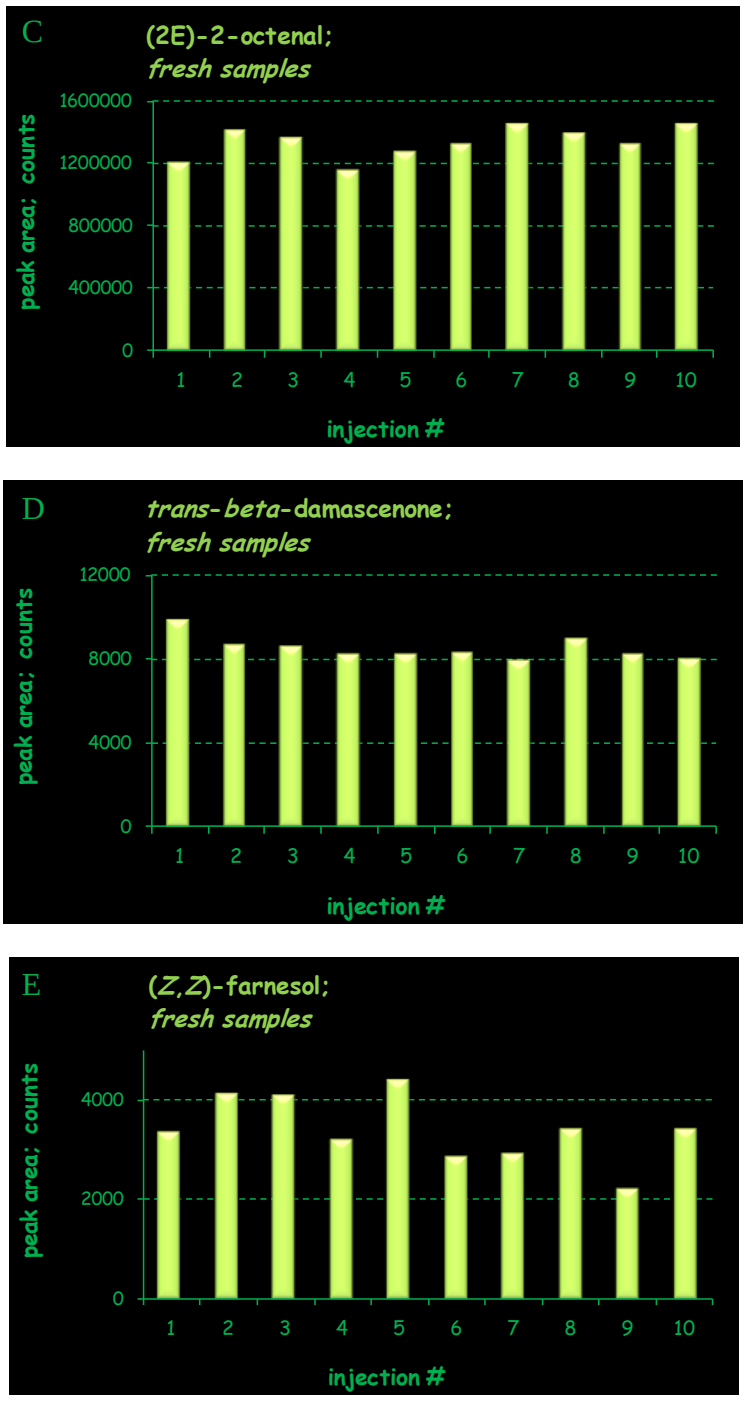

Figure 6.15. Intra-fruit repeatability and stability of selected metabolites detected in HS-SPME extracts of apple samples analyzed immediately after thawing. A - 6-methyl-5-hepten-2-one, B - *beta*-myrcene, C - (2E)-2-octenal, D - *trans*-*beta*-damascenone and E - (*Z*,*Z*)-farnesol.

These complex formation and degradation mechanisms occurring in samples analyzed by *ex vivo* assay despite the conduction of suitable metabolism quenching steps also result in unsatisfactory fruit-to-fruit variation, which is for selected metabolites significantly higher as compared to implemented *in vivo* sampling approaches (Table 6.2 and Figure 6.16).

Table 6.2. Intra-fruit and fruit-to-fruit variation in selected volatile and semivolatile metabolites determined in *ex vivo* (fresh samples and samples stored on autosampler tray) and *in vivo* (September 2009 and 2010 sampling sets) extracts.

		analyte name			
		6-methyl-5-hepten-2-one	beta-myrcene	(2E)-2-octenal	*trans*-beta-damascenone
intra-fruit	*in vivo*, 2009 sampling, *n*=3	**9.3**	**11.7**	**3.7**	nd
	in vivo, 2010 sampling, *n*=3	**9.8**	**14.5**	**39.9**	**32.1**
	ex vivo HS-SPME, *n* = 10	**35.2**	**27.3**	**20.9**	**41.2**
	ex vivo HS-SPME fresh samples, *n* = 10	**7.0**	**6.7**	**7.3**	**6.6**
inter-fruit	*in vivo*, 2010 sampling, *n* = 9	**35.7**	**43.7**	**34.7**	**47.6**
	ex vivo HS-SPME, *n* = 10	**27.6**	**23.8**	**11.1**	**60.1**

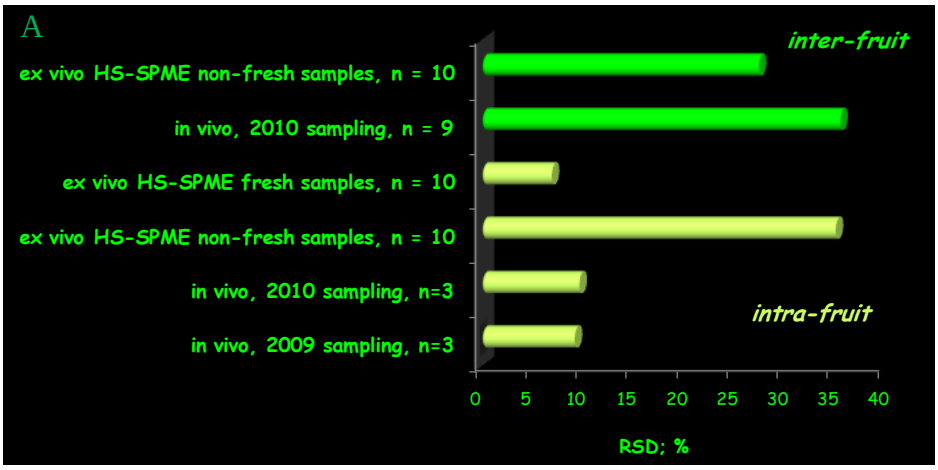

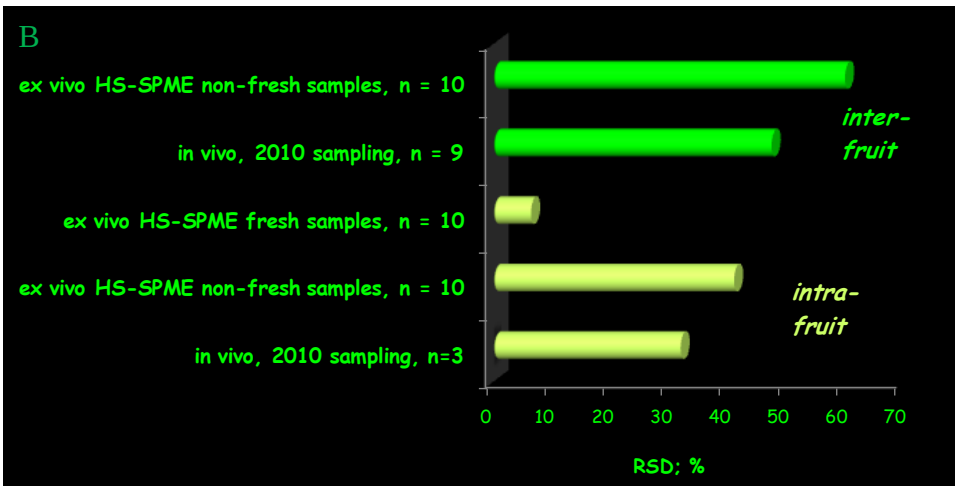

Figure 6.16. Intra- and inter-fruit variability for 6-methyl-5-hepten-2-one (plot A) and *trans-beta*-damascenone (plot B) and corresponding to performance of *ex vivo* assays for stored and freshly analyzed samples and *in vivo* assays from sampling designs conducted in 2009 and 2010.

Accordingly, for 6-methyl-5-hepten-2-one, intra-fruit RSDs in *ex vivo* assay for stored and freshly analyzed samples were 35.2 and 7.0%, respectively, while *in vivo* assay yielded RSDs of 9.3 and 9.8%, for 2009 and 2010 sampling years, respectively. On the other hand, inter-fruit RSDs for stored samples in *ex vivo* assay and *in vivo* sampling design from 2010 were 27.6 and 35.7%, respectively. For *trans-beta*-damascenone, intra-fruit repeatability for *ex vivo* assay corresponding to stored and freshly analyzed samples was characterized by respective RSDs of 41.2 and 6.6%, while *in vivo* assay yielded RSD of 32.1% for 2010 sampling year. Fruit-to-fruit variation for this compound was characterized by 60.1 and 47.6% RSD for *ex vivo* method of prolonged tray storage and *in vivo* method from 2010, respectively.

6.2.4 *Statistical treatment of in vivo data: biomarkers of fruit ripeness*

In order to deduce whether substantial intra-fruit and intra-compartment variability detected during *in vivo* DI-SPME sampling of apples and subsequent submission of extracts to GCxGC-ToFMS analysis has the potential to

adversely affect the quality of statistical data interpretation, one-way analysis of variance (ANOVA) was conducted. Statistical treatment of data was performed on extracted SPME responses represented in terms of global means for each apple and corresponding to five metabolites; butyl propanoate, butyl butanoate, ethyl hexanoate, butyl 2-methylbutanoate and estragole. The choice of metabolites was influenced by the study performed by Schaffer and coworkers who generated a transgenic line of 'Royal Gala' apple that produces no detectable levels of ethylene resulting in apples having no ethylene-induced ripening attributes [60]. In response to the application of external ethylene, these fruits underwent a normal climacteric burst during which increasing concentrations of ester, polypropanoid, and terpene volatile metabolites were detected. The contents of butyl propanoate, butyl butanoate, ethyl hexanoate, butyl 2-methylbutanoate and estragole were also enhanced over an 8-day period, hence these targeted compounds were included in the statistical treatment of data. The metabolites along with their retention time coordinates, inter-fruit variations and results of statistical analysis are presented in Table 6.3.

Table 6.3. One-way ANOVA treatment of *in vivo* SPME extracted responses for butyl propanoate, butyl butanoate, ethyl hexanoate, butyl 2-methylbutanoate and estragole obtained for HC-O apple group (lower harvest maturity) and HC-L apple group (higher harvest maturity).

analyte name	Butyl propanoate	Butyl butanoate	Ethyl hexanoate	Butyl 2-methylbutanoate	Estragole
^1t_R; s	521.5	714	721	808.5	1106
^2t_R; s	0.905	0.860	0.890	0.785	1.720
interfruit RSD (HC-O, n=12); %	40.9	34.4	73.1	46.5	12.9
interfruit RSD (HC-L, n=12); %	38.3	30.2	52.1	24.6	26.7
F	7.4	10.9	14.4	27.6	10.4
F_{crit}	6.0	6.0	6.0	6.0	6.0
P	3.5	1.7	0.9	0.2	1.8

Table 6.3 and Figure 6.17 illustrate that at 95% confidence level, the levels of evaluated metabolites were significantly expressed in apples of later harvest maturity. These results clearly indicate that despite significant variability with respect to intra- and inter-fruit composition of selected metabolites manifested during *in vivo* sampling and attributed to spatially and environmentally influenced metabolite localizations, *in vivo* SPME has potential in obtaining high quality metabolomics data of major biologically relevant impact. Alignment and quantitation of other detected metabolites should be conducted in the future, with the aim of identifying new biomarkers of harvest maturity and fruit ripeness.

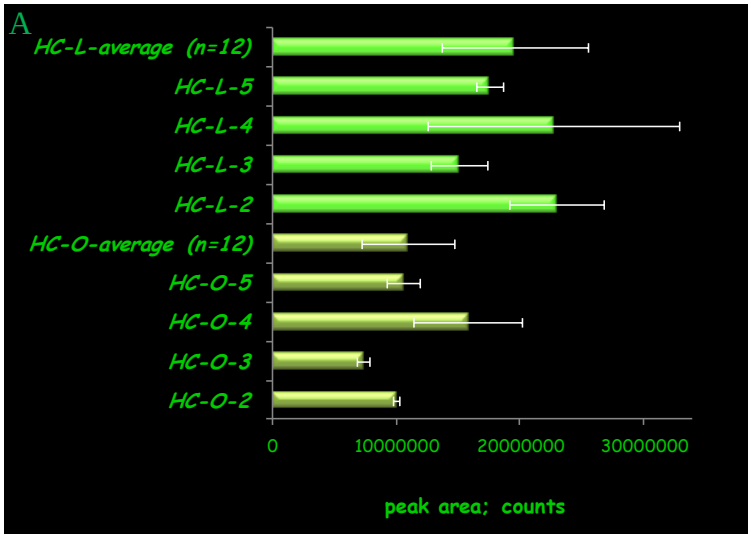

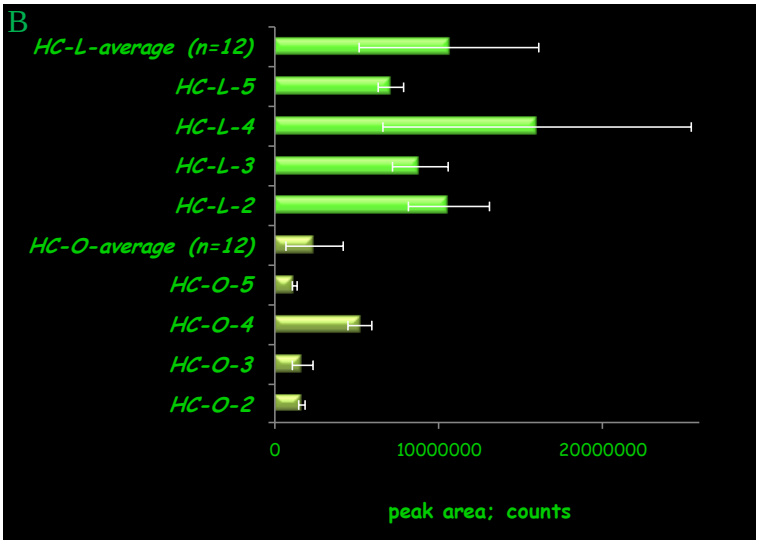

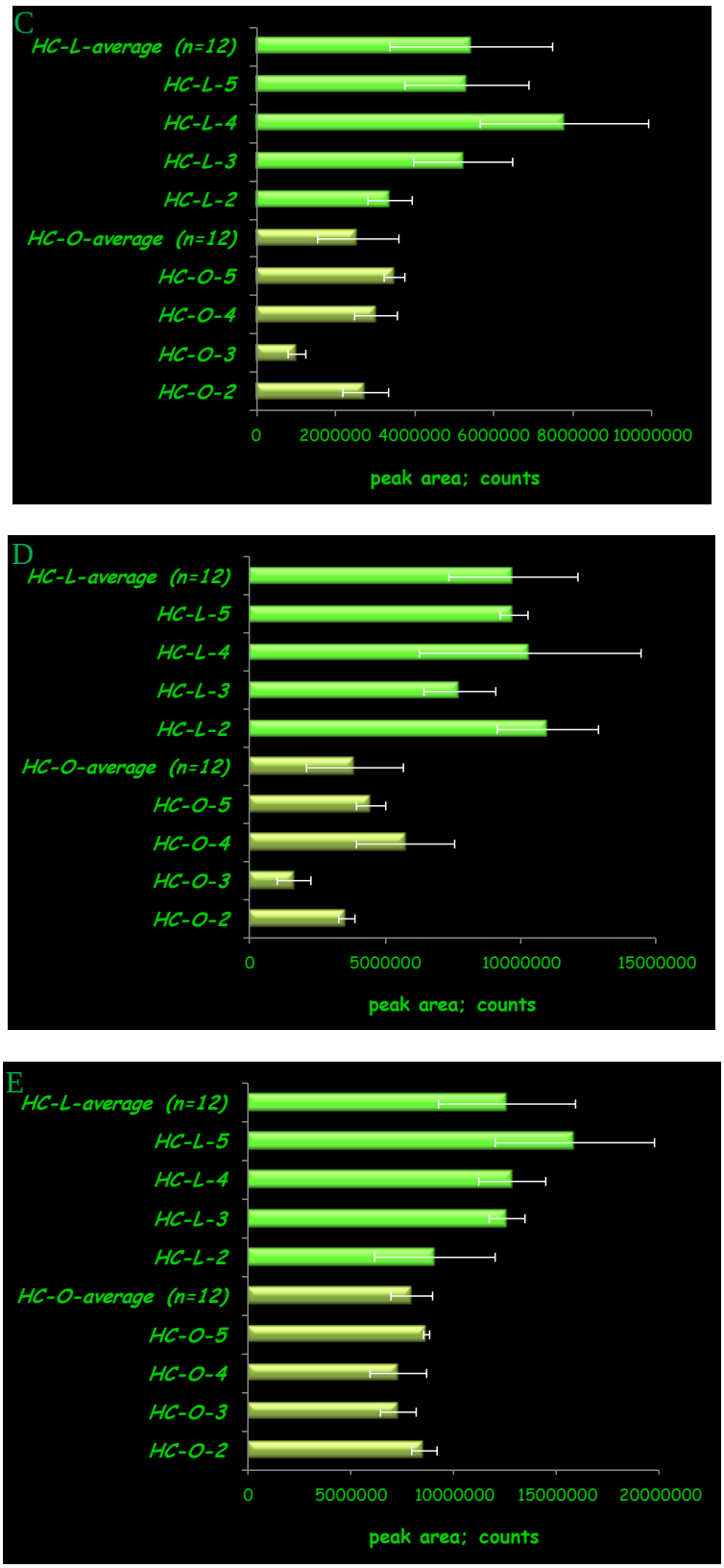

Figure 6.17. Extraction efficiencies for selected indicators of apple fruit ripeness including A - butyl butanoate; B - ethyl hexanoate; C - butyl

propanoate; D - butyl 2-methylbutanoate and E – estragole between two groups of samples of earlier (HC-O) and later (HC-L) harvest maturity.

In fact, a first approach at principal components analysis involved implementation of fully automated GCxGC-ToFMS data processing procedure with respect to alignment of metabolites and their relative quantification. The original ChromaTOF data processing (S/N 50, SIM 800) performed on 24 *in vivo* DI-SPME apple extracts revealed that the highest number of one-dimensional entries among all samples of earlier harvest maturity (HC-O) was encountered in HC-O-3-code-17 sample (total # of metabolite entries including the peaks that did not pass S/N and SIM criteria is 15,097). By applying the data reduction criteria consisting of SIM 700, 4,267 entries were preserved, which were further filtered to exclude column bleed peaks, fibre bleed peaks and blank peaks. Furthermore, peaks for which separation efficiency and modulator effectiveness were not satisfactory and thus resulted in a multitude of outlying deconvolutions were eliminated, as well as metabolite entries for which one-dimensional peaks were characterized by tailing and streaking peak profiles. Duplicate peak entries were preserved, provided that they met criteria of unique elution on two-dimensional retention time plane and that the one-dimensional peak shapes were not characterized by isovolatility curves. In summary, the data reduction resulted in preservation of 250 true high-quality metabolites that met S/N 100 criteria.

Alignment of metabolites in all 24 *in vivo* extracts was accomplished by employing completely automated 'compare-to-reference' ChromaTOF software option which relied on the following alignment criteria: *i)* one-dimensional RT shift 14 sec (the length of four modulation periods); *ii)* two-dimensional RT shift 0.1 sec; *iii)* mass spectral match threshold 500 (in order to eliminate as much as possible the appearance of missing values for the metabolites for which complexity of chromatographic profiles resulted in lower mass spectral purity) and *iv)* GCxGC similarity match for combination of second dimension peaks 600. Hence, manual interventions associated with second dimension peak

combination into respective one-dimensional peak entries and second dimension peak re-integration were eliminated, while the inspections of automated unique mass assignment and peak table sorting in Microsoft Excel had to still be conducted manually. The first and second retention time deviation criteria were selected based on the *i)* retention stability encountered for those metabolites in spiked water quality control standards (52 component metabolite mixture), for which severe second dimension retention time shifts were observed with Supelcowax and BP 20 narrow-bore second-dimension columns and *ii)* retention stability for several early eluting metabolites present in real *in vivo* samples. The employment of thicker stationary phase Stabilwax second dimension column attributed to rewarding performance characteristics when retention time stability is concerned: *i)* for spiked water samples, the maximum standard deviation for polar metabolites that were highly retained in second dimension (2-pentanol, 1-pentanol, *trans*-geraniol, *cis*, *trans*-farnesol and (*Z*,*Z*)-farnesol) was 1.8 sec (less than length of one modulation cycle) and 0.02 sec, for first and second dimensions, respectively with maximum second dimension retention time shift of 0.06 sec between spiked water samples analyzed prior to and after injection of *in vivo* extracts; *ii)* for early eluting compounds in actual *in vivo* extracts (including ethyl propanoate, propyl acetate, hexanal, ethyl butanoate and ethyl 2-methylbutanoate), the maximum standard deviation was 5 sec (less than length of two modulation periods) and 0.025 sec, for first and second dimension separations, respectively.

Submission of data to PCA analysis (SIMCA software) revealed the extraction of several principal components, among which the first and third PCs accounted for 53.9 and 6.4 % of the variance of the data set, respectively. The PCA scores plot is illustrated in Figure 6.18. Even though the figure illustrates certain degree of sample overlap and the presence of several outlying samples, the separation of two groups of apple samples having different degrees of apple maturity was established. The results are rewarding considering that the data processing, alignment and quantification procedures were fully automated. However, the preliminary successful differentiation of samples also represents

promising opportunities for future data interpretations with the aim of improving the quality of sample characterization and including examinations associated with stability of quality control standards, elimination of outlying deconvolutions and alignments, inter-fibre repeatability, sampling time, sampling temperature and sampling position, the latter variable having a pronounced effect on amounts extracted by SPME for selected metabolites due to anatomical and physiological complexity of natural living systems. With this end, *in vivo* SPME technique offers numerous unique opportunities for detection, identification and reliable quantification of new biomarkers of harvest maturity, fruit ripeness and many other global metabolomics topics in the field of plant biology.

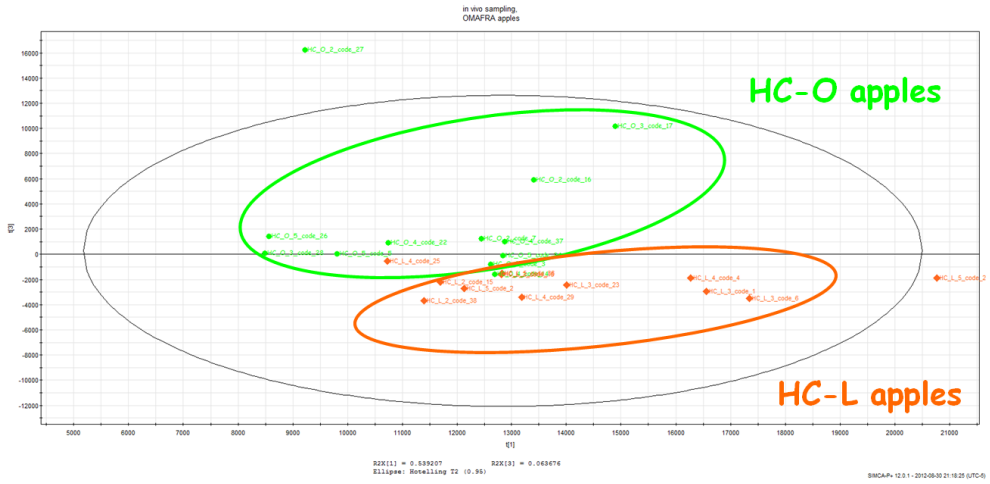

Figure 6.18. PCA scores plot representing the preliminary separation of groups of apple samples according to the degree of harvest maturity (HC-O and HC-L apples represent samples of earlier and later harvest maturity, respectively) and fruit ripeness. Twelve samples of each group were considered in the statistical analysis, while 250 true high-quality metabolites from *in vivo* SPME extracts (September 2010 sampling season) were automatically aligned and quantitated.

6.3 *Conclusions*

The studies conducted herein demonstrate the feasibility of *in vivo* DI-SPME – GCxGC-ToFMS metabolomics platform in obtaining reliable and readily interpretable data sets. Intra-fruit repeatability was found to be excellent for selected metabolites, and for others significant variations in contents were depicted with respect to sampling locations. Placing fibre coatings significant distances apart from each other adversely affects intra-fruit repeatability for high boiling point analytes, while close sampling positions result in unsatisfactory precision corresponding to highly volatile compounds. The important feature is that despite intra-compartmental analytical variations in metabolite contents induced by differences in spatial localization, environmental conditions or possibly SPME process itself, statistical interpretation of data may still be valid. After all, the intra-fruit and fruit-to-fruit repeatability obtained using traditional *ex vivo* HS-SPME assay revealed losses in representativeness of metabolome, the reason of which, *in vivo* SPME should present powerful future alternative for characterization of more 'true' metabolome.

7. Metabolome coverage in *in vivo* DI-SPME sampling of apples and comparison to *ex vivo* assay

7.1 *Background and objectives of research*

The objective of the current investigation is focused on comparison of metabolome coverage obtained with two different SPME metabolomics platforms, an *in vivo* assay performed directly on the site and *ex vivo* DI-SPME assay. *In vivo* DI-SPME assay was performed on living apple plants and hence requirements associated with harvesting, metabolism quenching and laborious sample manipulation steps that have the potential to adversely impact the integrity of metabolomics extract were eliminated. On the other hand, owing to less biased and more complete coverage of volatile and semivolatile metabolites obtained when *ex vivo* SPME sampling is performed in direct immersion mode, as opposed to sampling the headspace, a comparative study was conducted on DI-SPME *ex vivo* extracts. The sample preparation prior to *ex vivo* assay was ensuring the strict requirements imposed by metabolism quenching, including freezing in liquid nitrogen, addition of saturated sodium chloride solution during homogenization and in extreme cases, samples were analyzed immediately after thawing. For the comparison of *in vivo* and *ex vivo* assays on apples grown and harvested in September 2010, fibres employed in *in vivo* sampling were stored in dry ice at – 70 ^{o}C after extraction and during transportation to the laboratory. Upon arrival to the laboratory, they were stored in a freezer at – 30 ^{o}C until the time of analysis, hence extraction of freshly collected extracts was not possible due to the delays attributed to GCxGC-ToFMS instrumental problems. Similarly, apple homogenates for which metabolism was quenched were stored in dark at – 30 ^{o}C following laborious sample preparation steps. Even though analysis of fresh samples and extracts was not possible, the enforced circumstances resemble those encountered in a

real-life situation, when large sample sets need to be stored for periods of time depending on the throughput of analytical platform. In the case of *in vivo* sampling, multiple coatings containing collected extracts also need to be manually and individually desorbed, hence storage cannot be avoided. Determination of on-fibre stability for a particular storage regime should be the focus of future research efforts, and provided that results are satisfactory, the automation of desorption procedure for fibre coatings employed on site should be accomplished. These aspects impose crucial future considerations and were outside of scope of current study. On the other hand, during September 2011 sampling, SPME fibre coatings implemented *in vivo* and stored in dry ice were immediately desorbed upon arrival to the laboratory, whereas the sample preparation for *ex vivo* assay was timed so that *i)* one sample is analyzed fresh immediately after homogenization (no freezing and thawing) and *ii)* two samples are frozen in dry ice and stored there until thawing, extraction and GCxGC-ToFMS analysis were due.

7.2 *Data processing methodology*

The contour plots of GCxGC-ToFMS TIC chromatograms corresponding to two distinct sampling designs are illustrated in Figure 7.1. As it can be seen from Figure 7.1, substantially differing GCxGC-ToFMS profiles were obtained depending on the mode of SPME sampling.

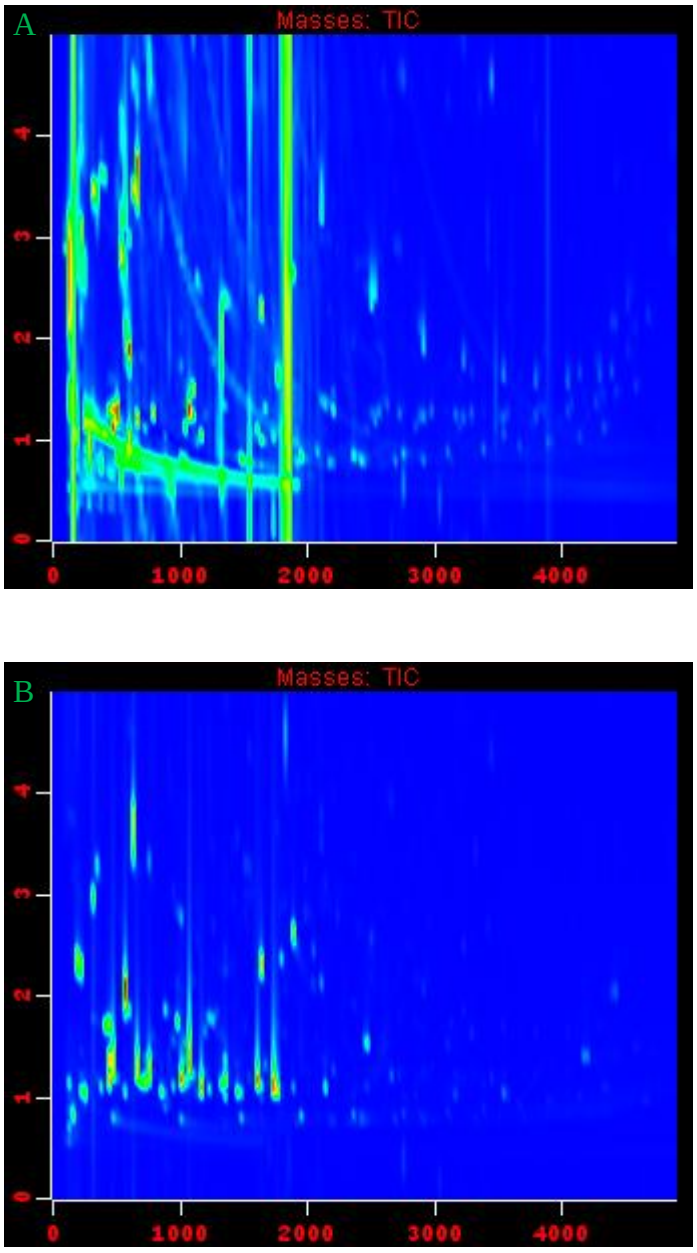

Figure 7.1. Contour plots of GCxGC-ToFMS TIC chromatograms corresponding to A – *in vivo* DI-SPME sampling and B – *ex vivo* DI-SPME sampling.

The two samples corresponding to *ex vivo* and *in vivo* DI-SPME extracts of the same apple, HC-L-1 were processed according to same data processing specifications. Automated ChromaTOF data processing procedure employed S/N threshold of 200 for the 'unique mass' to find all the peaks followed by the mass spectral deconvolution and modulated peak combination. The resultant

peak tables consisted of 5,404 and 2,581 entries for *ex vivo* and *in vivo* methods, respectively. The tables were subjected to further data reduction procedure on the basis of mass spectral purity requiring a mass spectral similarity threshold of 800 and this resulted in 1,508 metabolite features for *in vivo* method that needed to be screened for high quality true metabolites. The column bleed and fibre bleed peaks were first removed leading to 1,048 and 906 entries for *in vivo* and *ex vivo* assays, respectively (peak apex plots in Figure 7.2). Tentative identification of these peaks was performed on the basis of mass spectral similarity, retention index comparison and molecular structure-retention relationships in order to confirm or revise the identification based on these criteria. Even though the table of metabolites for which identity was annotated was not completely finalized for *in vivo* extract, employment of tentative identification procedure was a critical requirement for drawing reliable conclusions about the occurrence of differential metabolites in either SPME extract.

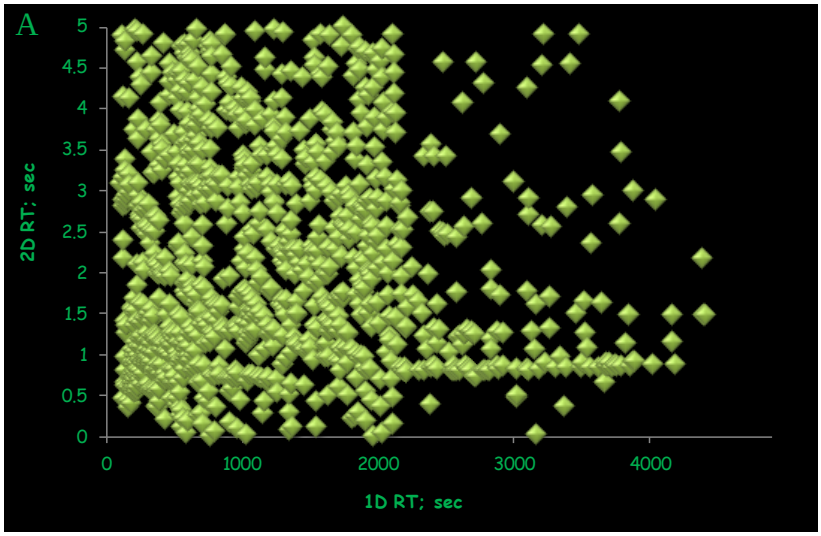

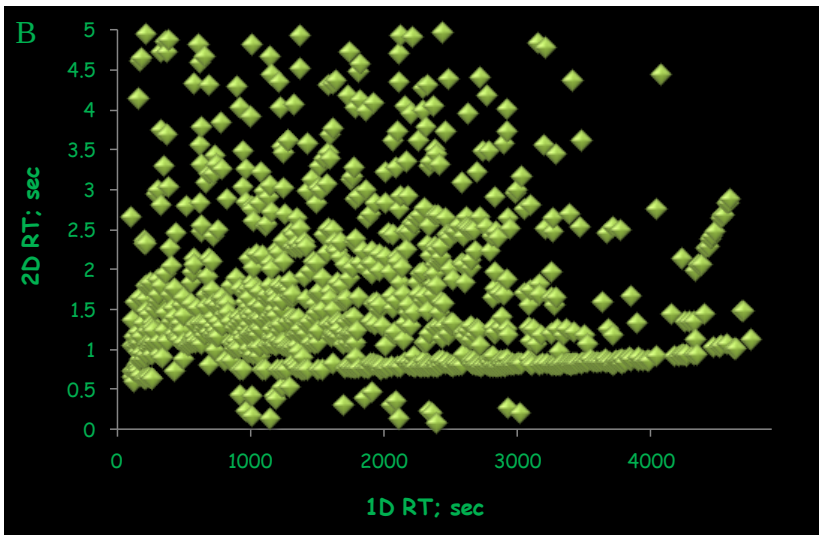

Figure 7.2. Peak apex plots demonstrating retention time coordinates of captured metabolites in *in vivo* (plot A) and *ex vivo* (plot B) apple extracts for S/N and mass spectral similarity thresholds of 200 and 800, respectively.

Subsequently, the tables corresponding to *in vivo* and *ex vivo* SPME sampling protocols were individually and manually screened in order to identify true and high quality metabolites and eliminate metabolite features for which resolution power, separation efficiency and modulation efficiency were not optimum and hence allow reliable chromatogram comparison. In addition, replicate entries in peak table were removed provided that they corresponded to incorrect operation of data processing software, which was in the majority of cases attributed to suboptimum separation and modulation efficiencies, non linear chromatography due to overloading and extensive peak tailing in first and second dimensions. Replicate peak table entries corresponding to peaks eluting in differing elution windows were preserved. The peak tables containing all of the metabolites that passed these requirements were constituted of 326 and 579 true metabolites corresponding to *in vivo* and *ex vivo* sampling protocols, respectively. Each individual metabolite present in either table was manually searched for in both chromatograms involved in the comparative study since retention time shifts in second dimension were severe to allow automated alignment of peaks. Consequently, two different peak tables were produced with metabolite entries that were labeled based on the results of the manual

searching procedure, which was relying on mass spectral comparison and elution window of a particular metabolite in order to label peak occurrence or absence of a metabolite manually searched for in the compared sample.

7.3 *Metabolites unique to in vivo sampling mode*

In total, 51 metabolites were unique to *in vivo* approach. The metabolites that were unique to *in vivo* sampling mode and for which successful annotation of analyte identity was established through implementation of mass spectral and retention index comparisons, GCxGC structured retentions and accessibility to literature RI databases are listed in Table 7.1 and selected extracted ion chromatograms for their 'unique' ion are presented in Figure 7.3.

Table 7.1. Tentatively identified metabolites that were unique to *in vivo* sampling approach.

analyte name	CAS #	RI_{exp}	RI_{lit}	similarity	structure
2,4,6-Trimethylphenol	527-60-6	1205	1204	824	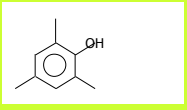
2-Phenoxyethanol	122-99-6	1223	1226	898	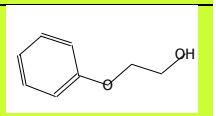
gamma-Butyrolactone	96-48-0	944	941	965	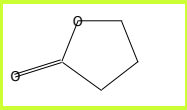
2-Methylbenzofuran	4265-25-2	1105	1109	879	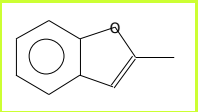
2,2'-Bifuran	5905-00-0	1037	1047	872	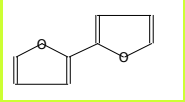
Butyl stearate	123-95-5	2385	2374	862	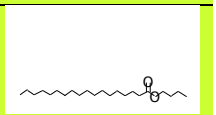

2-(2-Ethoxyethoxy)ethanol	111-90-0	1019	1006	953	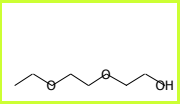

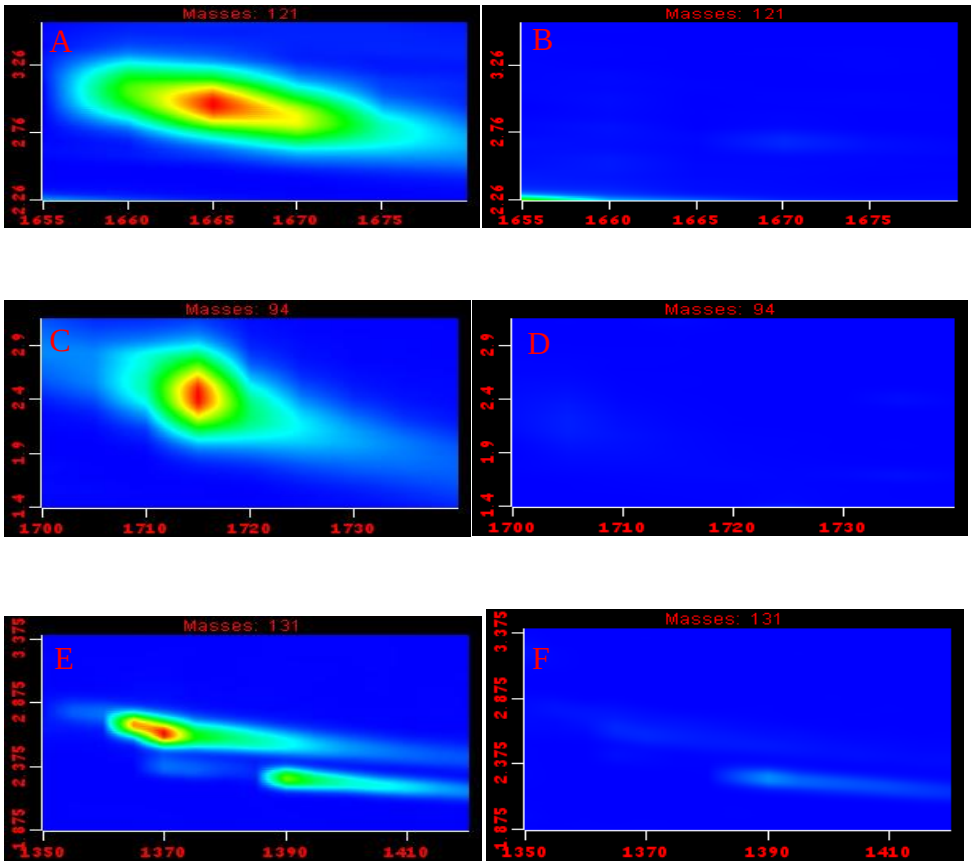

Figure 7.3. GCxGC extracted ion chromatograms corresponding to elution windows of metabolites unique to *in vivo* approach in *in vivo* (left plots) and *ex vivo* (right plots) extracts. A and B - 2,4,6-trimethylphenol, C and D - 2-phenoxyethanol, E and F - 2-methylbenzofuran.

All of these compounds exhibit structures of common secondary metabolites present in plant kingdom, and the reasons behind their unique occurrence in *in vivo* extracts, although at this point not completely understood can be attributed to a variety of reasons that were also briefly emphasized in the introductory section. First of all, harvesting of the plant material itself can initiate enzymatic degradation and oxidation and therefore, induce a significant impact on metabolome, especially if significant metabolism perturbation in the

investigated system is induced during the process. Freezing of the harvested apple samples was conducted within 10 s following harvesting as this process may also trigger enzymatic reactions that are associated with handling and wounding of the plant and hence result in breakdown of selected metabolites [101]. However, the important question is whether freezing after harvesting was fast enough, considering the impressive speed of metabolic processes [72]. Reported reaction times as low as 1 s and less require fast inhibition of enzymatic processes [72]. The second step following harvesting involved freezing in liquid nitrogen, a process that is not homogeneous and has the potential to lead to a number of issues including loss of metabolites, the emission of touch- or wound-induced metabolites and non-reversible loss of metabolites by absorption to cell walls [72-73]. For example, modification of the volatile profile in strawberries upon freezing was reported [15]. Following freezing, apples intended for *ex vivo* sample preparation were stored in dry ice during transportation and before homogenization. In-laboratory sample preparation procedure was quite laborious and required at least 25 min per apple (frozen fruit disruption, weighing, homogenization, transfer of homogenate into vials, placement of parafilm around screw caps of storage vials, labeling of vials, glassware and equipment washing and preparation for next sample to be prepared) during which time remaining samples were stored in dry ice. In fact, multiple delays were sometimes required for completion of sample preparation procedure for all apples. However, it is well known that loss of sample integrity may be encountered during deep freeze storage, the reason for which sample preparation and homogenization should be conducted immediately after freezing [5,15]. The disruption of fruit tissue and homogenization processes are also prone to production of artifacts and induction of metabolite degradations. In this regard, quenching of metabolic activity is not only essential for stopping metabolic turnover in the running pathways, but also to ensure inhibition of enzyme activities that could potentially lead to destruction of metabolite after tissue disruption [102]. The possibility of decomposition of metabolites following fruit disruption has for instance been communicated by the example

of determination of pyrophosphate levels in plants [102]. Pyrophosphatase activity in leaves has been reported to be so high to the extent that within 0.05 s, all the pyrophosphate in a leaf extract is hydrolyzed. Such conversions are not encountered in intact tissues since a majority of the pyrophosphatase activity is located in the plastids, while pyrophosphate is located in cytosol [102]. Following tissue disruption, the pyrophosphatase comes in contact with pyrophosphate leading to its complete destruction. Secondary metabolites do not exhibit such rapid decomposition reactions, although some like primary metabolites are highly susceptible to degradation by enzymes that come in contact with them after tissue disruption [102]. Hence, conversion of glucosinolates into isothiocyanates has been reported to occur in *Arabidopsis*. Indeed major differences in the analysis of intact versus disrupted leaves have been reported, as in the latter scenario destruction of tissue compartmentalization during the crushing of fresh plant organs releases hydrolytic enzymes responsible for a vast majority of reactions [5]. In the context of metabolite classes considered in this study, it is important to emphasize that volatile compounds themselves are classified as 'primary' or 'secondary' depending on their occurrence in the intact tissue for the former class or their occurrence being resulted by tissue disruption in the latter category [62]. While the analysis of intact fruit resembles instantaneous snapshot of true and representative metabolome at a particular biological state, the analysis of disrupted fruit resembles volatile profile indicative of flavour perception during eating [62]. The employment of knives and scalpels during fruit disruption, the former being used in the current study, induces wound stresses and activation of reactions on the exposed surfaces [15]. As a result, immediately after weighing appropriate amounts of disrupted apple fruit tissue in the current study, the pieces were soaked in saturated sodium chloride solution and exposure length of surfaces was dependent on the time required to weigh and cut the frozen material. In addition to fruit disruption, homogenization process can induce contamination and volatilization of certain components [15]. With respect to volatile and semivolatile metabolites that are not observed in *ex vivo* extracts in

the current study, there is a high probability of these metabolites being destroyed during homogenization since the process was detected to induce decomposition of important flavour compounds within minutes of its performance [97]. In fact, homogenization process represents the most vulnerable stage of any metabolomics platform [5]. Finally, the storage of *ex vivo* samples before extraction often results in cross-contamination and loss of sample integrity even when deep freeze storage conditions are employed [5]. Pre-extraction thawing of plant sample also triggers undesirable metabolite conversions and leads to significant losses in extract integrity [5]. For example, Tohge et al. reported that pre-extraction incubation of the disrupted tissue at 37 ^{o}C for 1 hr revealed that metabolome of plants including *Arabidopsis thaliana* leaves, *Solanum lycopersicum* fruits and *Oryza sativa* leaves was significantly altered, whereas such occurrences were not detected by incubation process after the addition of extraction buffer [102]. Finally, an essential requirement for preservation of metabolome integrity is performance of extraction step that is able to prevent hydrolytic, oxidative, photodegradative, and enzymatic conversions of metabolites. Based on results presented in Chapter 6, a series of degradation mechanisms resulted in the formation and decomposition of selected metabolites with respect to tray storage period, therefore, extraction process itself is not free of such processes. In fact, the occurrence of 2,4,6-trimethylphenol in unique *in vivo* profile suggests that this compound might have underwent oxidation since many metabolites including phenols are highly sensitive to oxidation and hydrolysis [5].

Therefore, all preparative and manipulative procedures during sample collection, metabolism quenching, sample preparation and extraction steps of traditional *ex vivo* sample preparation workflow are prone to metabolome alterations that are in most severe cases manifested by destruction of important metabolites as demonstrated here. What needs to be addressed at this point is whether *in vivo* SPME still has unique metabolic fingerprint when both *in vivo* and *ex vivo* extracts are analyzed immediately following arrival to the laboratory and sample preparation, respectively. The relevant data processing

and interpretation from September 2011 sampling season has not yet been completed, however, selected differences in extracted metabolome coverages were spotted. For instance, contour plots of GCxGC-ToFMS extracted ion chromatograms corresponding to *in vivo* and *ex vivo* retention time windows of *in vivo*-specific metabolite with annotated analyte identity are presented in Figure 7.4. The metabolite, 1,4-diacetylbenzene (p-acetylacetophenone) having first and second dimension retention times of 1736 and 3.404 s, respectively, and experimental and literature RI indices of 1455 and 1451, respectively, is unique to metabolite profile obtained *in vivo*. Tikunov et al. detected a number of acetophenone derivatives, including acetophenone itself and 4-methylacetophenone, in HS-SPME extracts of tomato samples analyzed as a part of large-scale profiling and comparative multivariate analysis platform [185]. The authors reported that the biosynthetic pathway for these acetophenone derivatives is still unclear, however, 4-methylacetophenone and acetophenone clustered with terpenoids (including *cis*- and *trans*-linalool oxides, limonene, ocimenol, α-terpineol, 2-caren-10-al, p-cymen-8-ol) and cyclic carotenoid volatiles (ß-damascenone, ß-ionone and ß-cyclocitral), respectively in metabolite-metabolite correlation matrix composed of 322 compounds. In their study, the clustering of metabolites in particular compound classes was determined by their biosynthetic pathways and metabolite precursors from which they are derived. Therefore, metabolites sharing common biosynthesis pathway and biochemical precursor clustered in the same group, and grouping of acetophenone and 4-methylacetophenone with the above-mentioned groups of volatiles may provide future basis for elucidating their biochemical origin and roles [185]. Interestingly, ß-cyclocitral was found to be specific to metabolome obtained via *ex vivo* DI-SPME assay, as mentioned in following sections.

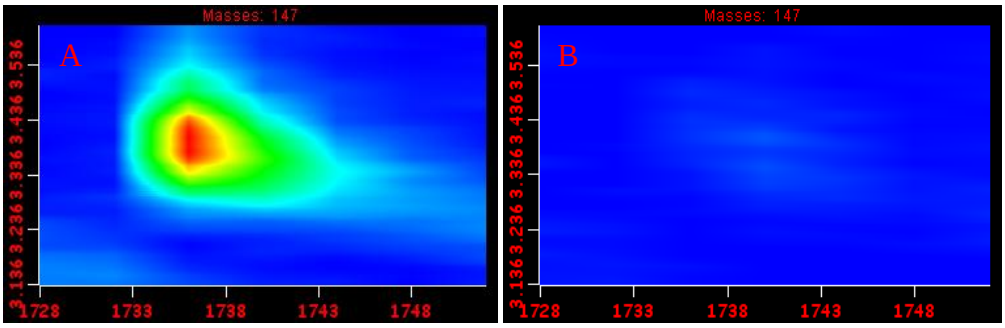

Figure 7.4. Contour plots of GCxGC extracted ion chromatograms corresponding to elution windows of 1,4-diacetylbenzene, a metabolite unique to *in vivo* approach in *in vivo* (left plot) and *ex vivo* (right plot) extracts. Desorption of *in vivo* extracts was done immediately after arrival to the laboratory.

7.4 *Metabolites unique to ex vivo sampling mode*

On the other hand, the number of differential metabolites that were unique to *ex vivo* DI-SPME approach was significantly higher. 241 metabolites were unique to *ex vivo* approach and although all of them could not be screened and interpreted individually from biological point of view, some important classes were easily interpretable. The first class involves analytes including (2E)-2-heptenal, (2Z)-2-octenal, (2E,4E)-2,4-nonadienal, (2E)-2-pentenal, (2E,4E)-2,4-heptadienal, (3E,5E)-3,5-octadien-2-one and (2E,6Z)-2,6-nonadienal. All of these compounds whose extracted ion chromatograms are illustrated in Figure 7.5 represent an important class of metabolites that are derived from unsaturated fatty acids, including oleic acid, linoleic acid and linolenic acid [187]. Unsaturated fatty acids cannot be considered as stable food components as they are readily oxidized to hydroperoxides, which subsequently degrade to a multitude of volatile by-products [187]. The process of lipid peroxidation was reported to occur even in foods having trace levels of unsaturated fatty acids or in foods in which only a small portion of lipid was subjected to oxidation. Several studies reported that volatile bouquet formed

during autoxidation of unsaturated fatty acids such as oleic acid, linoleic acid and linolenic acid is constituted mainly by aldehydes and ketones [187].

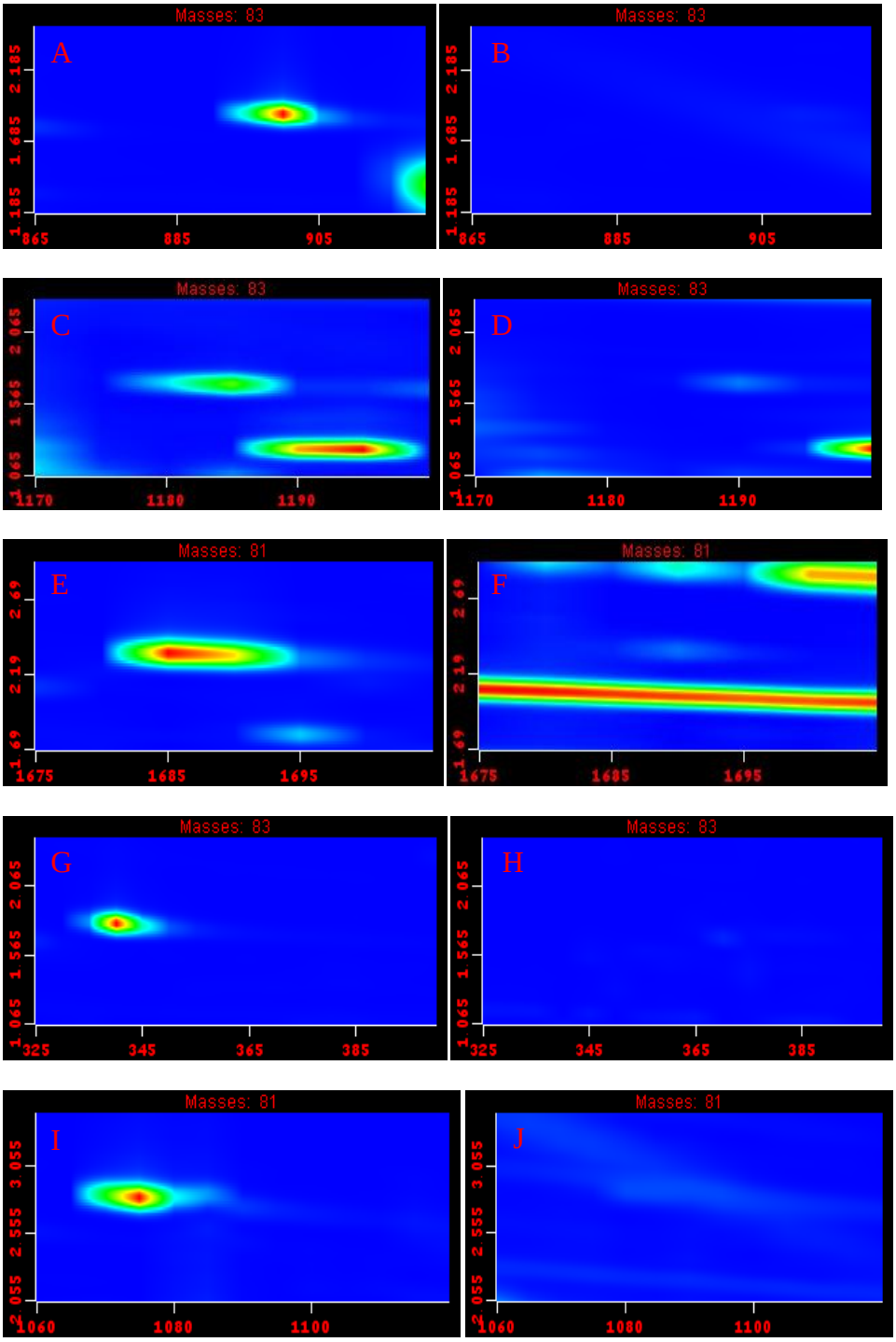

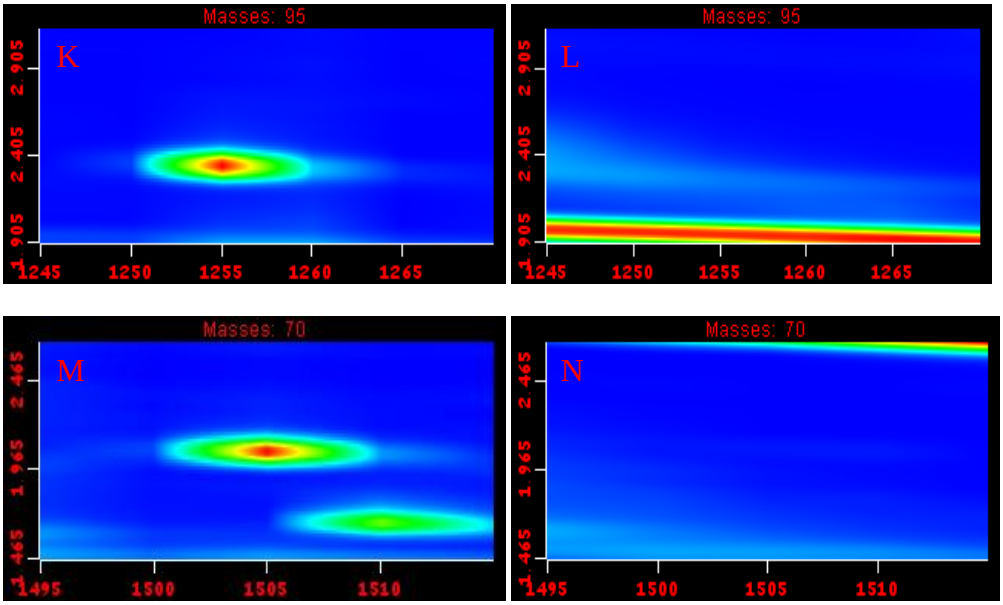

Figure 7.5. GCxGC extracted ion chromatograms corresponding to elution windows of metabolites unique to *ex vivo* approach in *ex vivo* (left plots) and *in vivo* (right plots) extracts. A and B - (2E)-2-heptenal, C and D - (2Z)-2-octenal, E and F - (2E,4E)-2,4-nonadienal, G and H - (2E)-2-pentenal, I and J - (2E,4E)-2,4-heptadienal, K and L - (3E,5E)-3,5-octadien-2-one, M and N - (2E,6Z)-2,6-nonadienal.

Biosynthetic pathways in apples involved in the production of aroma compounds from fatty acids involve ß-oxidation, hydroxyacid cleavage and lipoxygenase to form aldehydes, ketones, acids, alcohols, lactones and esters [188]. In intact fruits, volatile end products are formed via the ß-oxidation biosynthetic pathway, whereas when fruit tissue is disrupted, lipoxygenase pathway is responsible for their formation [188]. In intact fruit, enzymes in the lipoxygenase (LOX) biosynthetic pathway and their substrates possess specific subcellular locations which in turn prevent the formation of volatile end products [188]. On the other hand, during disruption and homogenization of fruit tissue, linoleic and linolenic acids are oxidized to various C_6 and C_9 aldehydes. Consequently, the occurrence of differential metabolites from Figure 7.5 that are unique to *ex vivo* approach and known to be derived from unsaturated fatty acids may be resulted by the activation of lipoxygenase enzymes during fruit disruption and homogenization. Considering that both *in*

vivo and *ex vivo* extracts had to be stored prior to final GCxGC-ToFMS analysis since the analysis of samples was delayed as a consequence of instrumental problems, it is important to determine whether oxidation products of unsaturated fatty acids are still unique to *ex vivo* approach for the extracts and samples that are analyzed immediately after sampling and sample preparation. Even though data from September 2011 sampling is not fully processed to reveal the complete picture, GCxGC contour plots corresponding to extracted ion chromatograms zoomed in the area of chromatographic elution (first and second dimension retention times 944 and 1.584 s) of unidentified (hit # 1 (2E,4E)-2,4-heptadienal) degradation product of unsaturated fatty acids are still showing differences in metabolome profile (Figure 7.6). Considering that *ex vivo* sample was submitted to GCxGC-ToFMS analysis immediately after sample preparation procedure, which omitted freezing of homogenate in dry ice and thawing of the sample in water bath, results show that rapid degradations of metabolome integrity are likely to be encountered during *ex vivo* metabolomics assay despite the incorporation of metabolism quenching.

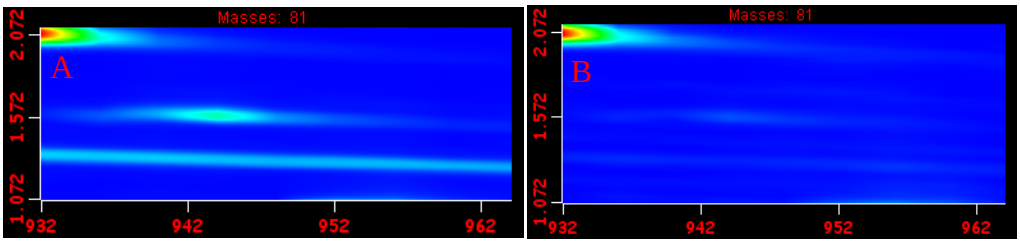

Figure 7.6. GCxGC extracted ion chromatograms corresponding to elution windows of unidentified unsaturated fatty acid degradation product (hit # 1 (2E,4E)-2,4-heptadienal) unique to *ex vivo* approach in *ex vivo* (left plot) and *in vivo* (right plot) extracts. GCxGC-ToFMS analysis was conducted immediately after sample preparation of *ex vivo* sample while freezing and thawing processes were omitted from assay.

Similarly, two volatile metabolites that were specifically unique to the *ex vivo* DI-SPME sampling protocol are 6-methyl-3,5-heptadiene-2-one and 2,6,6-trimethyl-1-cyclohexen-1-carboxaldehyde (ß-cyclocitral) having first and second dimension retention times of 1355 and 2.630 s and 1695 and 1.800 s,

respectively, and known to be produced during the process of oxidative degradation of carotenoids [187]. Dehydrolycopene and β-carotene have been identified as the precursors of these compounds [187]. The relevant enlarged sections of corresponding GCxGC extracted ion chromatogram plots are illustrated in Figure 7.7.

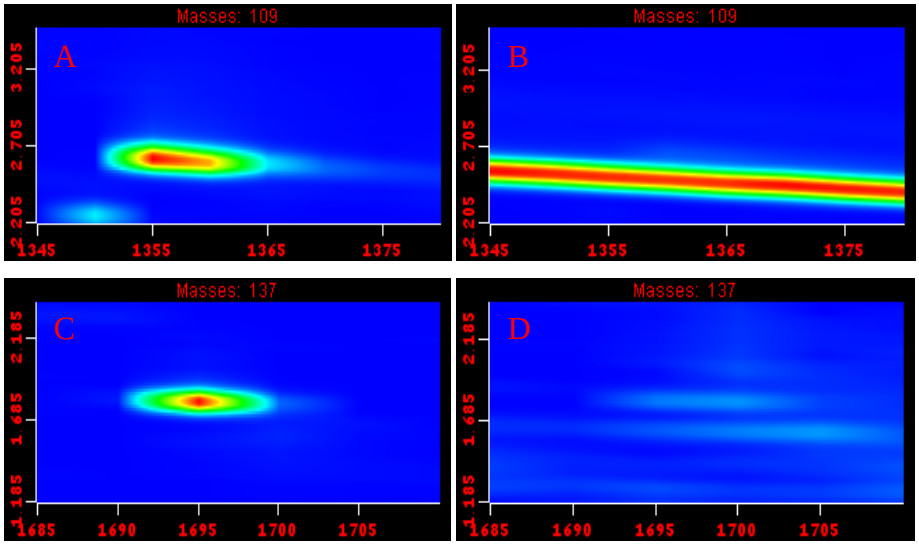

Figure 7.7. GCxGC extracted ion chromatograms corresponding to elution windows of metabolites unique to *ex vivo* approach in *ex vivo* (left plots) and *in vivo* (right plots) extracts. A and B - 6-methyl-3,5-heptadiene-2-one (experimental RI 1100, literature RI 1084), C and D - ß-cyclocitral (experimental RI 1216, literature RI 1219).

That activation of enzymes indeed takes place during sample preparation steps of *ex vivo* DI-SPME metabolomics platform is supported by the occurrence of monoterpene 5-methyl-2-(1-methylethyl)-cyclohexanol (menthol) as a part of metabolome composition that is unique to *ex vivo* extract. The retention time coordinates of the compound are 1580 and 2.205 s, the experimental and literature retention indices are 1176 and 1184, respectively. The corresponding extracted ion chromatogram is presented in Figure 7.8.

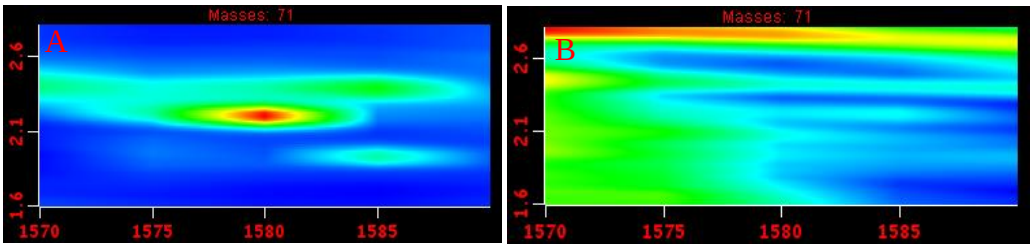

Figure 7.8. GCxGC extracted ion chromatograms corresponding to elution windows of menthol, a metabolite unique to *ex vivo* approach in *ex vivo* (left plot) and *in vivo* (right plot) extracts.

The formation of this compound is enabled by the presence and activation of cytochrome P450 enzymes [67]. In fact, P450 cytochrome oxidases are involved in numerous metabolic pathways related to volatile biosynthesis [67]. Biological relevance behind the unique occurrence of menthol in *ex vivo* DI-SPME apple extract here is attributed to 3-hydroxylation of limonene by a P450 enzyme, which is considered as the first step in menthol biosynthesis in plants. Nevertheless, the activation of this enzyme is also important during biosynthetic processes responsible for the generation of fatty acid volatiles. For example, two different P450 enzymes, 9-LOX and 13-LOX can introduce a peroxide into linoleic acid and subsequent cleavage of hydrocarbon chain by hydroperoxide lyases produces nonadienal and 3-cis-hexenal, the former being also unique to *ex vivo* extract based on Figure 7.5.

7.5 *Implementation of in vivo approach: challenges and concluding remarks*

Despite the amazing potential of *in vivo* SPME metabolomics platform to generate distinct metabolome profile corresponding to instantaneous and accurate metabolism snapshot, several drawbacks of the technique were identified during its implementation. The most significant drawback of the methodology is associated with occurrence of a multitude of reactions in GC

injector during thermal desorption of *in vivo* extracts. The mode of *in vivo* extraction via direct immersion and direct exposure of the extraction phase to the complex matrix result in attachment of non volatile interferences on the surface of the extraction phase. The coextraction of nonvolatile and thermally labile matrix components and their attachment on the coating surface was accounted for by brief dipping of the fibre coating in the aqueous water solution, which was conducted after extraction and before desorption. Such a design was implemented in sampling sets corresponding to October 2009 and September 2010 sampling years and most of the generated GCxGC profiles resembled the one illustrated in Figure 7.9.

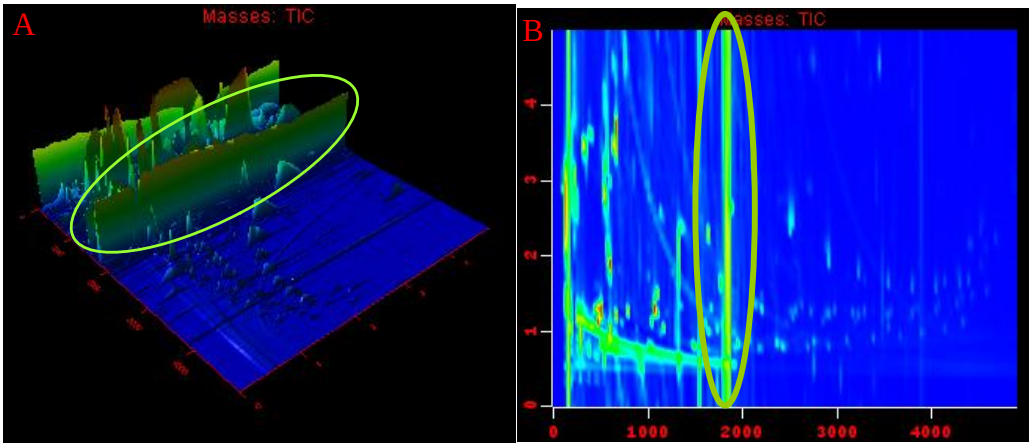

Figure 7.9. Typical TIC GCxGC-ToFMS surface (plot A) and contour (plot B) plots corresponding to *in vivo* extracts obtained in sampling years 2009 and 2010.

The circled portion of these chromatograms represents the area of elution of the major compound, which based on the GCxGC profiles in extracted ion chromatograms from Figure 7.10 not only overloads second dimension column and modulator, but occupies a substantial portion of available GCxGC separation space. Based on the library searching procedure (mass spectrum shown in Figure 7.10 b) and retention index comparison (retention time coordinates 1815 and 0.225 s, experimental and literature RI 1259 and 1256, respectively), the compound was tentatively identified as 5-(hydroxymethyl)-2-

furancarboxaldehyde or 2-hydroxymethyl-5-furfural, one of the major by-products of Maillard reaction occurring during thermal treatment of carbohydrates in the presence of amines [187].

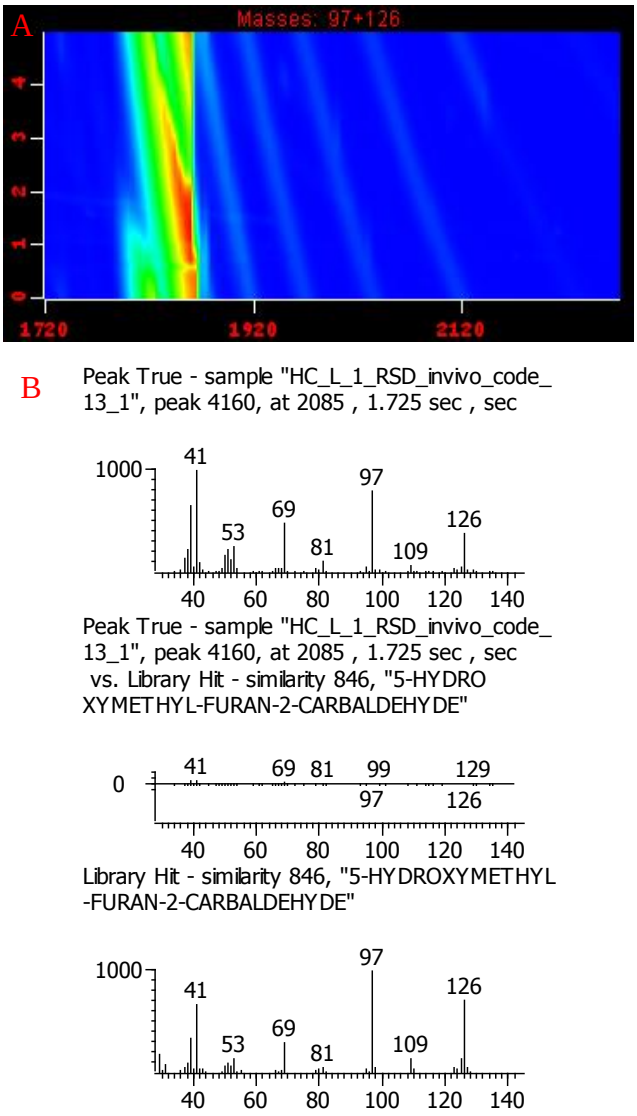

Figure 7.10. GCxGC extracted ion chromatogram (plot A) and mass spectra (plot B, experimental mass spectrum is upper plot, library mass spectrum is lower plot and the difference between the two spectra is middle plot) corresponding to 2-hydroxymethyl-5-furfural.

Several additional metabolites also exhibited tailing, broadening and overloading peak profiles both in the first and second dimension that were

indicative of their formation in the injector. In fact, based on data interpretation presented in Chapter 2, the increased sensitivity attainable by GCxGC through zone compression provided the ability to comprehensively examine such secondary chromatography effects often manifested by isovolatility and streaking curves arising from the tailing nature of the peaks, which are products of decomposition reactions [169]. Hence, the visual inspection of GCxGC chromatographic profiles corresponding to *in vivo* extracts can be effectively employed toward the investigation of stability of extracted components. As a result, sampling design from September 2011 season involved increasing duration of washing step (10 s immersion), which resulted in overall decreased formation of artifacts formed in the injector during desorption (Figure 7.11). However, despite the efforts employed with regards to increasing the wash step, it was determined that visually and microscopically observed artifacts on the surface of extraction phase which were often manifested in browning and caramelization spots, are highly associated with the obtained GCxGC profiles with respect to the formation of degradation products. For example, for one of the fibre coatings for which such defects were microscopically detectable, resultant chromatographic profile was not clean and the occurrence of Maillard reaction products was detected, despite the implementation of longer washing step. However, once DVB/CAR/PDMS coatings were overcoated with outer PDMS layer (project outside of scope of this thesis), the formation of Maillard reaction artifacts was reduced and overall chromatographic profiles were cleaner as compared to DVB/CAR/PDMS coatings. However, the uniformity of externally coated PDMS layer had a pronounced effect on obtained GCxGC profiles with respect to occurrence of Maillard reaction.

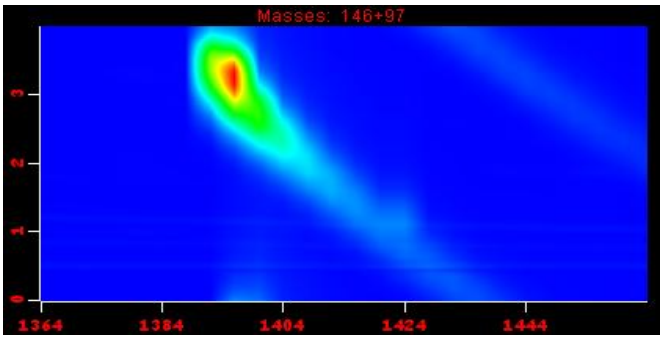

Figure 7.11. GCxGC extracted ion chromatogram corresponding to 2-hydroxymethyl-5-furfural in *in vivo* SPME extract for which washing step duration was 10 s.

The above mentioned instances of reactions occurring in the injector due to incompatibility of commercial coatings with direct immersion extraction have two important adverse implications in global metabolomics: *i)* production of artifacts leads to loss of metabolome integrity and representativeness and *ii)* complications in identification and quantification of many additional metabolites present at trace levels that are chromatographically coeluting with major 'artifact' peaks. In such instances, high reliability was placed on the deconvolution procedure of ChromaTOF software to locate these peaks and deconvolute their mass spectra, but the procedure was successful only in limited number of cases as 100s of trace components are overlapping with Maillard reaction products (Figure 7.12).

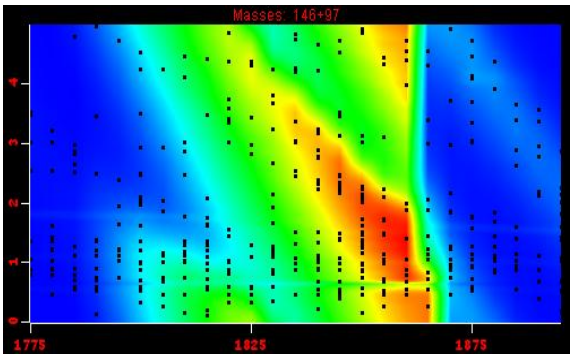

Figure 7.12. Elution window of 2-hydroxymethyl-5-furfural peak in *in vivo* extract illustrating chromatographic coelution of hundreds of metabolites.

The latter implication above also resulted in obtaining lower number of high quality true metabolites in *in vivo* extract after the completion of processes associated with manual post-processing of peak tables and manual peak picking (326 and 579 true metabolites corresponding to *in vivo* and *ex vivo* sampling protocols, respectively passed the peak picking criteria). On the other hand, the chromatographic profiles of *ex vivo* DI-SPME extracts were cleaner and no occurrence of such high severity degradation reactions was detected, possibly due to the apple sample dilution. Alternatively, potential residual enzymatic activity, which was reported to take place in plant extracts and to be more enhanced with respect to the water content, may be responsible for this [100]. For example, t'Kindt and coworkers reported activation of invertase in *Arabidosis thaliana* that led to the hydrolysis of sucrose into glucose and fructose [100].

Design of SPME coatings with improved compatibility with direct immersion analysis of food samples should be encouraged and current research efforts in our laboratory are aiming in that direction. Despite these drawbacks, the implementation of *in vivo* SPME metabolomics platform undoubtedly minimizes drawbacks encountered in traditional sample preparation. Such drawbacks are manifested in production of inaccurate and unrepresentative metabolome profiles as a consequence of manipulative sample preparation steps resulting in perturbation of metabolism, wounding and activation of enzymes that produce 'artifacts'. The occurrence of several differential metabolites that are specific to *in vivo* approach requires further data interpretation and inclusion of sampling sets from 2011 harvesting season in which the production of Maillard reaction products was minimized. Nevertheless, the results presented here illustrate rewarding accomplishments of *in vivo* SPME assay in obtaining more representative metabolism snapshot.

8. Conclusions

The objective of current research project was full exploitation of advantages offered by solvent-free, green and environmentally friendly SPME sample preparation methodology in the field of global metabolite analysis of naturally complex sample matrices. In particular, its solvent-free implementation, on-site compatibility, non-exhaustive extraction nature and miniaturized format led to the efficient employment of extraction technique directly at the site of the investigated system. Hence, *in vivo* DI-SPME assay was developed for sampling of living plants with minimum perturbation while simultaneously ensuring elimination of manipulative sample preparation and metabolism quenching steps that are a part of any *ex vivo* metabolomics assay. It is worth emphasizing that *in vivo* SPME sampling of metabolome profile composed of volatile and semivolatile metabolites amenable to GC analysis has not so far been conducted in sampling of endogenous tissue compounds. Rather, volatile emissions of intact plants were profiled, thus limiting the assay to determination of highly volatile metabolome profile that is often not representative of true organism biological state. In addition, the comparative literature evaluation of *ex vivo* and *in vivo* emission profiles often involved reporting metabolic differences for which *ex vivo* assay did not incorporate metabolism quenching step.

The *in vivo* DI-SPME technique was coupled to multidimensional GCxGC-ToFMS instrument in the quest for comprehensive complex sample characterization and high-resolution metabolite fingerprinting and profiling of ‘Honeycrisp‘ apples. Considerable efforts were placed on evaluation of performance characteristics of commercially available SPME fibre coatings in terms of extraction selectivity, extraction sensitivity and desorption efficiency in the analysis of 52-component spiked water samples and apple homogenate. In the process, drawbacks of commercial coatings were identified and DVB/CAR/PDMS selected for future *ex vivo* HS-SPME, *ex vivo* DI-SPME and DI-SPME *in vivo* implementations. This extraction phase attributed to

attainment of excellent metabolite coverage, characterized by highest number of captured metabolites and excellent volatile metabolite extraction recovery. The comparison of *ex vivo* HS-SPME and DI-SPME extraction modes revealed the capture of less biased and more complete metabolome profile with DI-SPME mode, since the discrimination against high molecular weight and polar metabolites was compensated for. At the end of these optimization experiments, it was concluded that the assay combining nonselective adsorptive properties of DVB/CAR/PDMS extraction phase and DI-SPME mode of its implementation provides rich metabolite coverage composed of hundreds of chemically diverse compounds. Hence, full potential of SPME in the field of global metabolite analysis requires hyphenation of technique with high-resolution instrumentation such as GCxGC-ToFMS.

On the other hand, the comparative study on the metabolome coverage between *ex vivo* and *in vivo* DI-SPME modes of sampling revealed improved extraction coverage when the latter mode was implemented. However, manual peak picking for selection of high quality metabolites above S/N and similarity thresholds of 200 and 800, respectively, revealed that metabolome coverage obtained in *in vivo* assay was characterized by lower number of peaks in comparison to *ex vivo* assay (326 and 579 true metabolites for *in vivo* and *ex vivo* sampling protocols, respectively). Lower number of high quality true metabolites is attributed to initiation of Maillard reactions in GC injector resulting in the production of volatile end products whose precursors were coextracted with metabolites of interest during direct immersion extraction. The one-dimensional peak profiles corresponding to these artifacts were indicative of decomposition and formation reactions during thermal desorption of *in vivo* extracts.

Therefore, full future implementation of *in vivo* SPME in global metabolomics will require improvement of matrix-compatibility of SPME coatings during direct immersion extraction in order to improve the representativeness of metabolome collected during *in vivo* SPME assay. In addition, these studies that are currently undertaken in our laboratory will

address coating robustness for multiple extraction cycles in order to enhance the number of possible *in vivo* sampling cycles per single coating and hence ensure cost-effective implementation of the methodology. Future studies focussed on advanced global metabolic profiling and fingerprinting of plant samples should also investigate the effects of perturbation that are potentially induced following the penetration of SPME assembly into the plant tissue. Depending on the extent of invasion, experiments investigating metabolome alterations and responsive pathways that result as a consequence of potential SPME 'invasions' should be properly designed.

Nevertheless, in its current stage of development, *in vivo* SPME offers unique opportunities for advanced fingerprinting and profiling of plant metabolome corresponding to biological systems in their natural environments. The studies conducted herein demonstrate the feasibility of *in vivo* DI-SPME – GCxGC-ToFMS metabolomics platform in obtaining reliable and readily interpretable data sets. The global determination of analytical precision for intra-fruit repeatability confirmed that the proposed *in vivo* DI-SPME metabolomics methodology has the potential to generate rewarding analytical results considering that 41.5% of peaks pass strict FDA 15% RSD requirements. Satisfactory intra- and inter-fruit repeatability was also reflected in the statistical evaluation of data using one-way ANOVA to determine whether the contents of selected biomarkers of apple maturity are statistically different between two groups of samples. Analytical precision of *in vivo* DI-SPME metabolomics platform was greatly influenced by intra- and inter-compartmental alterations in metabolite profile as a result of widely acknowledged spatial localizations that are attributed to environmental stimuli and growing conditions.

Based on the results of this study that were obtained using apple as an investigated system, widely differing GCxGC-ToFMS profiles were obtained depending on the mode of SPME sampling. *In vivo* SPME profile was composed of several unique metabolites whose 'uniqueness' to this sampling mode, origin, biosynthetic pathways and biological roles are to be further investigated in future. On the other hand, despite the incorporation of

appropriate metabolism quenching steps and minimization of sample storage, the metabolome profile obtained through implementation of *ex vivo* DI-SPME assay was characterized by presence of several volatile degradation products. Based on data interpretation, their occurrence is attributed to metabolome alterations that may take place during manipulative metabolism quenching and sample preparation steps, with fruit disruption and homogenization representing the most vulnerable steps of enzyme activation, metabolite conversions and loss of metabolism integrity. Finally, the comparative studies between traditional *ex vivo* and DI-SPME *in vivo* assays associated with metabolome coverage and global evaluation of analytical precision in terms of intra-fruit repeatability revealed losses in representativeness of metabolome when the former mode of sampling was employed. *In vivo* SPME hence offers unique features in the quest for collection and characterization of representative plant metabolome.

References

[1] H. Kanani, P. K. Chrysanthopoulos, M. I. Klapa, J. Chromatogr. B 871 (2008) 191-201.

[2] M. M. Koek, F. M. Van der Kloet, R. Kleemann, T. Kooistra, E. R. Verhejj, T. Hankemeier, Metabolomics 7 (2011) 1-14.

[3] P. Bais, S. M.Moon, K. He, R. Leitao, K. Dreher, T. Walk, Y. Sucaet, L. Barkan, G. Wohlgemuth, M. R. Roth, E. S. Wurtele, P. Dixon, O. Fiehn, B. M. Lange, V. Shulaev, L. W. Sumner, R. Welti, B. J. Nikolau, S. Y. Rhee, J. A. Dickerson, Plant Physiol. 152 (2010) 1807-1816.

[4] M. Steinfath, D.Groth, J. Lisec, J. Selbig, Physiol. Plant.132 (2008) 150-161.

[5] D. Ryan, K.Robards, Sep. Purif. Rev. 35 (2006) 319-356.

[6] J. W. Allwood, D.I. Ellis, R. Goodacre, Physiol. Plant.132 (2008) 117-135.

[7] R. D. Hall, I.D. Brouwer, M. A. Fitzgerald, Physiol. Plant. 132 (2008) 162-175.

[8] G. G. Harrigan, S. Martino-Catt, K. C. Glenn, Metabolomics 3 (2007) 259-272.

[9] R. D. Hall, New Phytol. 169 (2006) 453-468.

[10] A. D. Hegeman, Brief. Funct. Genomic. 9 (2010) 139-148.

[11] L. W. Sumner, P. Mendes, R. A. Dixon, Phytochem. 62 (2003) 817-836.

[12] K. Saito, F. Matsuda, Annu. Rev. Plant Biol. 61 (2010) 463-489.

[13] A. Ishihara, F. Matsuda, H. Miyagawa, K. Wakasa, Metabolomics 3 (2007) 319-334.

[14] U. Roessner, F. Pettolino, Top. Curr. Genomics 18 (2007) 253-278.

[15] J. W. Allwood, R. C. H. De Vos, A. Moing, C. Deborde, A. Erban, J. Kopka, R. Goodacre, R. D. Hall, Methods Enzymol. 500 (2011) 299-336.

[16] J. M. Hagel, P. J. Facchini, Phytochem. Rev. 7 (2008) 479-497.

[17] A. Aharoni, M. A. Jongsma, H. J. Bouwmeester, Phytochem. Rev. 10 (2005) 594-602.

[18] R. D. Hall, FOOD metabolomics: META-PHOR: A new European research initiative 18 (2007).

[19] V. L. W. Go, C. T. H. Nguyen, D. M. Harris, W-N. P. Lee, J. Nutr. (2005) 3016S-3020S.

[20] A. Aharoni, M. A. Jongsma, H. J. Bouwmeester, Trends Plant. Sci. 10 (2005) 594-602.
[21] A. Ishihara, F. Matsuda, H. Miyagawa, K. Wakasa, Metabolomics 3 (2007) 319-334.
[22] G. S. Catchpole, M. Beckmann, D. P. Enot, M. Mondhe, B. Zywicki, J. Taylor, N. Hardy, A. Smith, R. D. King, D. B. Kell, O. Fiehn, J. Draper, PNAS 102 (2005) 14458-14462.
[23] U. Roessner, C. Wagner, J. Kopka, R. N. Trethewey, L. Willmitzer, Plant J. 23 (2000) 131-142.
[24] J. Memelink, Trends Plant. Sci. 10 (2005) 305-307.
[25] H. Rischer, K-M. Oksman-Caldentey, Trends Biotechnol. 24 (2006) 102-104.
[26] A. M. Slisz, A. P. Breksa, D. O. Mischchuk, G. McCollum, C. M. Slupsky, J. Proteome Res. in press (2012).
[27] W-L. Yang, M. A. Bernards, Metabolomics 3 (2007) 147-159.
[28] S. Jan, T. Parween, T. O. Siddiqi, Radiat. Environ. Biophys. in press (2012).
[29] R. A. Dixon, D. R. Gang, A. J. Charlton, O. Fiehn, H. A. Kuiper, T. L. Reynolds, R. S. Tjeerdema, E. H. Jeffery, J. B. German, W. P. Ridley, J. N. Seiber, J. Agric. Food Chem. 54 (2006) 8984-8994.
[30] J. M. Cevallos-Cevallos, J. I. Reyes-De-Corcuera, E. Etxeberria, M. D. Danyluk, G. E. Rodrick, Trends Food Sci. Technol. 20 (2009) 557-566.
[31] L. V. T. Shepherd, P. Fraser, D. Stewart, Bioanalysis 3 (2011) 1143-1159.
[32] L. Tarpley, A. L. Duran, T. H. Kebrom, L. W. Sumner, BMC Plant Biol. 5 (2005) 1-12.
[33] J. J. Giovannoni, Plant Cell 16 (2004) S170-S180.
[34] F. Mounet, M. Lemaire-Charmley, M. Maucourt, C. Cabasson, J.- L. Giraudel, C. Deborde, R. Lessire, P. Gallusci, A. Bertrand, M. Gaudillere, R. Rothan, D. Roline, A. Moing, Metabolomics 3 (2007) 273-288.
[35] L. G. Deluc, J. Grimplet, M. D. Wheatley, R. L. Tillett, D. R. Quilici, C. Osborne, D. A. Schooley, K. A. Schlauch, J. C. Cushman, G. R. Cramer, BMC Genomics 8 (2007) 1-42.
[36] Q. F. Vorst, C. H. R. de Vos, A. Lommen, R. V. Staps, R. G. F. Visser, R. J. Bino, R. D. Hall, Metabolomics 1 (2005) 169-180.
[37] P. J. White, J. Exp. Bot. 53 (2002) 1995-2000.

[38] S. Park, N. Sugimoto, M. D. Larson, R. Beaudry, S. van Nocker, Plant Physiol. 141 (2006) 811-824.
[39] E. Aprea, H. Gika, S. Carlin, G. Theodoridis, U. Vrhovsek, F. Mattivi, J. Chromatogr. A 1218 (2011) 4517-4524.
[40] A. Vikram, B. Prithiviraj, H. Hamzehzarghani, AC. Kushalappa, J. Sci. Food Agric. 84 (2004) 1333-1340.
[41] Fruit and Vegetable Production, Statistics Canada, Agriculture Division, Crops Section, Ottawa, Ontario, Canada, June 2011.
[42] S. F. A. R. Reis, S. M. Rocha, A. S. Barros, I. Delgadillo, M. A. Coimbra, Food Chem. 113 (2009) 513-521.
[43] D. R. Rudell, J. P. Mattheis, Postharvest Biol. Technol. 51 (2009) 174-182.
[44] D. R. Rudell, J. P. Mattheis, M. L. A. T. M. Hertog, J. Agric. Food. Chem. 57 (2009) 8459-8466.
[45] T. Ahn, G. Paliyath, D. P. Murr, Food Res. Int. 40 (2007) 1012-1019.
[46] U. Vogler, A. S. Rott, C. Gessler, S. Dorn, Transgenic Res, 19 (2010) 77-89.
[47] E. Pesis, A. M. Ibáñez, M. L. Phu, E. J. Mitcham, S. E. Ebeler, A. M. Dandekar, J. Agric. Food. Chem. 57 (2009) 2786-2792.
[48] E. Róth, A. Berna, K. Beullens, S. Yarramraju, J. Lammertyn, A. Schenk, B. Nicolaï, Postharvest Biol. Technol. 45 (2007) 11-19.
[49] L. Ferreira, R. Perestrelo, M. Caldeira, J. S. Cámara, J. Sep. Sci. 32 (2009) 1875-1888.
[50] S. Saevels, J. Lammertyn, A. Z. Berna, E. A. Veraverbeke, C. D. Natale, B. M. Nicolaï, Postharvest Biol. Technol. 31 (2004) 9-19.
[51] J. C. Young, C. L. G. Chu, X. Lu, H. Zhu, J. Agric. Food Chem. 52 (2004) 8086-8093.
[52] D. R. Rudell, J. P. Mattheis, E. A. Curry, J. Agric. Food Chem. 56 (2008) 1138-1147.
[53] A. Hern, S. Dorn, Entomologia Experimentalis et Applicata 102 (2002) 145-151.
[54] A. Vikram, B. Prithiviraj, H. Hamzehzarghani, A. C. Kushalappa, J. Sci. Food Agric. 84 (2004) 1333-1340.
[55] B. D. Whitaker, J. F. Nock, C. B. Watkins, Postharvest Biol. Technol. 20 (2000) 231-241.
[56] J. R. DeEll, B. Ehsani-Moghaddam, Hort. Science 45 (2010) 414-417.
[57] J. R. DeEll, OMAFRA Horticulture News (2004).

[58] J. Cline, J. Gardner, OMAFRA Horticulture News (2009).
[59] A. Botton, G. Eccher, C. Forcato, A. Ferrarini, M. Zermiani, S. Moscatello, A. Battistelli, R. Velasco, B. Ruperti, A. Remina, Plant Physiol. 155 (2011) 185-208.
[60] R. J. Schaffer, E. N. Friel, E. J. F. Souleyre, K. Bolitho, K. Thodey, S. Ledger, J. H. Bowen, J.-H. Ma, B. Nain, D. Cohen, A. P. Gleave, R. N. Crowhurst, B. J. Janssen, J.-L. Yao, R. D. Newcomb, Plant Physiol. 144 (2007) 1899-1912.
[61] B. G. Defilippi, A. M. Dandekar, A. A. Kader, J. Agric. Food Chem. 53 (2005) 3133-3141.
[62] J. Song, C. F. Forney, Can. J. Plant Sci. 88 (2008) 537-550.
[63] R. D. Newcomb, R. N. Crowhurst, A. P. Gleave, E. H. A. Rikkerink, A. C. Allan, L. L. Beuning, J. H. Bowen, E. Gera, K. R. Jamieson, B. J. Janssen, W. A. Laing, S. McArtney, B. Nain, G. S. Ross, K. C. Snowden, E. J. F. Souleyre, E. F. Walton, Y.-K. Yauk, Plant Physiol. 141 (2006) 147-166.
[64] D. D. Rowan, Metabolites 1 (2011) 41-63.
[65] S. A. Goff, H. J. Klee, Sci. 311 (2006) 815-819.
[66] W. Schwab, R. Davidovich-Rikanati, E. Lewinsohn, Plant J. 54 (2008) 712-732.
[67] N. Dudareva, E. Pichersky, J. Gershenzon, Plant Physiol. 135 (2004) 1893-1902.
[68] D. Tieman, P. Bliss, L. M. Mcintyre, A. Blandon-Ubeda, D. Bies, A. Z. Odabasi, G. R. Rodríguez, E. van der Knaap, M. G. Taylor, C. Goulet, M. H. Mageroy, D. J. Snyder, T. Colquhoun, H. Moskowitz, D. G. Clark, C. Sims, L. Bartoshuk, H. J. Klee, Curr. Biol. 22 (2012) 1035-1039.
[69] S. A. Goff, H. J. Klee, Sci. 311 (2006) 815-819.
[70] F. Dunemann, D. Ulrich, A. Boudichevskaia, C. Grafe, W. E. Weber, Mol. Breeding 23 (2009) 501-521.
[71] Y. Ban, N. Oyama-Okubo, C. Honda, M. Nakayama, T. Moriguchi, Food Chem. 118 (2010) 272-277.
[72] W. B. Dunn, D. I. Ellis, Trend Anal. Chem. 24 (2005) 285-294.
[73] S. G. Villas-Bôas, S. Mas, M. Åkesson, J. Smedsgaard, J. Nielsen, Mass Spectrom. Rev. 24 (2005) 613-646.
[74] P. Donato, P. Q. Tranchida, P. Dugo, G. Dugo, L. Mondello, J. Sep. Sci. 30 (2007) 508-526.
[75] K. Maštovská, S. J. Lehotay, J. Chromatogr. A 1000 (2003) 153-180.

[76] J. W. Allwood, A. Erban, S. de Koning, W. B. Dunn, A. Luedemann, A. Lommen, L. Kay, R. Löscher, Metabolomics 5 (2009) 479-496.
[77] M. Herrero, E. Ibáñez, A. Cifuentes, J. Bernal, J. Chromatogr. A 1216 (2009) 7110-7129.
[78] S. M. Rocha, E. Coelho, J. Zrostlíková, I. Delgadillo, M. A. Coimbra, J. Chromatogr. A 1161 (2007) 292-299.
[79] M. Adahchour, J. Beens, U. A. Th. Brinkman, J. Chromatogr. A 1186 (2008) 67-108.
[80] P. Q. Tranchida, D. Sciarrone, P. Dugo, L. Mondello, Analytica Chimca Acta 716 (2012) 66-75.
[81] T. Čajka, J. Hajšlová, J. Cochran, K. Holadová, E. Klimánková, J. Sep. Sci. 30 (2007) 534-546.
[82] M. Adahchour, J. Beens, R. J. J. Vreuls, A. M. Betenburg, U. A. Th. Brinkman, J. Chromatogr. A 1054 (2004) 47-55.
[83] B. Mitrevski, P. Wynne, P. J. Marriott, Anal. Bioanal. Chem. 401 (2011) 2361-2371.
[84] J. Y. Gardner, D. E. Brillhart, M. M. Benjamin, L. G. Dixon, L. M. Mitchell, J-M. D. Dimandja, J. Sep. Sci. 34 (2011) 176-185.
[85] R. A. Shellie, W. Welthagen, J. Zrostliková, J. Spranger, M. Ristow, O. Fiehn, R. Zimmermann, J. Chromatogr. A 1086 (2005) 83-90.
[86] P. P. de Souza, Z. de L. Cardeal, R. Augusti, P. Morrison, P. J. Marriott, J. Chromatogr. A 1216 (2009) 2881-2890.
[87] M. F. Almstetter, P. J. Oefner, K. Dettmer, Anal. Bioanal. Chem. 402 (2012) 1993-2013.
[88] C. Ma, H. Wang, X. Lu, H. Wang, G. Xu, B. Liu, Metabolomics 5 (2009) 497-506.
[89] E.Gaquerel, A. Weinhold, I. T. Baldwin, Plant Physiol. 149 (2009) 1408-1423.
[90] M. F. Almstetter, I. J. Appel, M. A. Gruber, C. Lottaz, B. Timischl, R. Spang, K. Dettmer, P. J. Oefner, Anal. Chem. 81 (2009) 5731-5739.
[91] M. Kusano, A. Fukushima, M. Kobayashi, N. Hayashi, P. Jonsson, T. Moritz, K. Ebana, K. Saito, J. Chromatogr. B 855 (2007) 71-79.
[92] K. M. Pierce, J. L. Hope, J. C. Hoggard, R. E. Synovec, Talanta 70 (2006) 797-804.
[93] P. Wojtowicz, J. Zrostlíková, T. Kovalczuk, J. Schůrek, T. Adam, J. Chromatogr. A 1217 (2010) 8054-8061.

[94] J. Pawliszyn, in: J. Pawliszyn (Ed.), Solid Phase Microextraction: Theory and Practice, Wiley-VCH, New York, 1997.
[95] J. Pawliszyn, in: J. Pawliszyn (Ed.), Handbook of Solid Phase Microextraction, Chemical Industry Press, Beijing, 2009.
[96] T. Parliment, A. D. Harmon, in: R. Marsili (Ed.), Flavor, Fragrance, and Odor Analysis, Marcel Dekker, Inc., New York, 2002.
[97] J. G. Wilkes, E. D. Conte, Y. Kim, M. Holcomb, J. B. Sutherland, D. W. Miller, J. Chromatogr. A 880 (2000) 3-33.
[98] P. L. Buldini, L. Ricci, J. L. Sahrma, J. Chromatogr. A 975 (2002) 47-70.
[99] K. Ridgway, S. P. D. Lalljie, R. M. Smith, J. Chromatogr. A 1153 (2007) 36-53.
[100] R. t'Kindt, K. Morreel, D. Deforce, W. Boerjan, J. V. Bocxlaer, J. Chromatogr. B 877 (2009) 3572-3580.
[101] H. K. Kim, R. Verpoorte, Phytochem. Anal. 21 (2010) 4-13.
[102] T. Tohge, T. Mettler, S. Arrivault, A. J. Carroll, M. Stitt, A. R. Fernie, Front. Plant Sci. 2 (2011) 1-15.
[103] A. Oikawa, T. Otsuka, Y. Jikumaru, S. Yamaguchi, F. Matsuda, R. Nakabayashi, T. Takashina, K. Isuzugawa, K. Saito, K. Shiratake, J. Sep. Sci. 34 (2011) 3561-3567.
[104] A. Nongonierma, P. Cayot, J.-L. L. Quéré, M. Springett, A. Voilley, Food Rev. Int. 22 (2006) 51-94.
[105] W. Wardencki, J. Curyło, J. Namieśnik, J. Biochem. Biophys. Methods 70 (2007) 275-288.
[106] N. H. Snow, G. C. Slack, Trend Anal. Chem. 21 (2002) 608-617.
[107] D. Tholl, W. Boland, A. Hansel, F. Loreto, U. S. R. Röse, J.-P. Schnitzler, Plant J. 45 (2006) 540-560.
[108] C. L. Arthur, J. Pawliszyn, Anal. Chem. 62 (1990) 2145-2148.
[109] H. Lord, J. Pawliszyn, J. Chromatogr. A 885 (2000) 153-193.
[110] S. Risticevic, H. Lord, T. Górecki, C. L. Arthur, J. Pawliszyn, Nat. Protoc. 5 (2010) 122-139.
[111] G. A. Mills, V. Walker, J. Chromatogr. A 902 (2000) 267-287.
[112] C. Nerín, J. Salafranca, M. Aznar, R. Batlle, Anal. Bioanal. Chem. 393 (2009) 809-833.
[113] J. Pawliszyn, S. Liu, Anal. Chem. 59 (1987) 1475-1478.
[114] J. Pawliszyn, Anal. Chem. 75 (2003) 2543-2558.
[115] J. Pawliszyn, Can. J. Chem. 79 (2001) 1403-1414.

[116] Z. Zhang, J. Pawliszyn, Anal. Chem. 65 (1993) 1843-1852.
[117] F. Pragst, Anal. Bioanal. Chem. 388 (2007) 1393-1414.
[118] E. Baltussen, C. A. Cramers, P. J. F. Sandra, Anal. Bioanal. Chem. 373 (2002) 3-22.
[119] S. Risticevic, Y. Chen, L. Kudlejova, R. Vatinno, B. Baltensperger, J. R. Stuff, D. Hein, J. Pawliszyn, Nat. Protoc. 5 (2010) 162-176.
[120] S. Risticevic, V. H. Niri, D. Vuckovic, Anal. Bioanal. Chem. 393 (2009) 781-795.
[121] L. Setkova, S. Risticevic, J. Pawliszyn, J. Chromatogr. A 1147 (2007) 224-240.
[122] S. Risticevic, E. Carasek, J. Pawliszyn, Anal. Chim. Acta 617 (2008) 72-84.
[123] L. Setkova, S. Risticevic, J. Pawliszyn, J. Chromatogr. A 1147 (2007) 213-223.
[124] P. Q. Tranchida, M. Lo Presti, R. Costa, P. Dugo, G. Dugo, L. Mondello, J. Chromatogr. A 1103(2006) 162-165.
[125] C. Cagliero, C. Bicchi, C. Cordero, P. Rubiolo, B. Sgorbini, E. Liberto, Food Chem. 132 (2012) 1071-1079.
[126] A. L. Robinson, P. K. Boss, H. Heymann, P. S. Solomon, R. D. Trengove, J. Chromatogr. A 1218 (2011) 504-512.
[127] B. T. Weldegergis, A. de Villiers, C. McNeish, S. Seethapathy, A. Mostafa, T. Górecki, A. M. Crouch, Food Chem. 129 (2011) 188-199.
[128] E. Klimánková, K. Holadová, J. Hajšlová, T. Čajka, J. Poustka, M. Koudela, Food Chem. 107 (2008) 464-472.
[129] D. Ryan, R. Shellie, P. Tranchida, A. Casilli, L. Mondello, P. Marriott, J. Chromatogr. A 1054 (2004) 57-65.
[130] F. Bianchi, M. Careri, C. Conti, M. Musci, R. Vreuls, J. Sep. Sci. 30 (2007) 527-533.
[131] A. Williams, D. Ryan, A. O. Guasca, P. J. Marriott, E. Pang, J. Chromatogr. B 817 (2005) 97-107.
[132] M. Adahchour, J. Wiewel, R. Verdel, R. J. J. Vreuls, U. A. T. Brinkman, J. Chromatogr. A 1086 (2005) 99-106.
[133] L. T. Vaz-Freire, M. D. R. G. da Silva, A. M. C. Freitas, Anal. Chim. Acta 633 (2009) 263-270.
[134] C. Cordero, C. Bicchi, P. Rubiolo, J. Agric. Food. Chem. 56 (2008) 7655-7666.

[135] E. M. Humston, J. D. Knowles, A. McShea, R. E. Synovec, J. Chromatogr. A 1217 (2010) 1963-1970.
[136] S. Rochat, J-Y. de Saint Laumer, A. Chaintreau, J. Chromatogr. A 1147 (2007) 85-94.
[137] Z. L. Cardeal, M. D. R. G. Silva, P. J. Marriott, Rapid Commun. Mass Spectrom. 20 (2006) 2823-2836.
[138] K. W. Cheong, C. P. Tan, H. Mirhosseini, S. T. Chin, Y. B. C. Man, N. S. A. Hamid, A. Osman, M. Basri, Food Chem. 125 (2011) 1481-1489.
[139] T. Cajka, J. Hajslova, F. Pudil, K. Riddellova, J. Chromatogr. A 1216 (2009) 1458-1462.
[140] X. Zhang, K. D. Oakes, S. Wang, S. Cui, J. Pawliszyn, C. D. Metcalfe, M. R. Servos, Trends Anal. Chem. 32 (2012) 31-39.
[141] G. Ouyang, D. Vuckovic, J. Pawliszyn, Chem. Rev. 111 (2011) 2784-2814.
[142] D. Vuckovic, S. Risticevic, J. Pawliszyn, Angew. Chem. Int. Ed. 50 (2011) 2-13.
[143] F. Augusto, A. L. P. Valente, Trends Anal. Chem. 21 (2002) 428-438.
[144] R. X. Loi, M. C. Solar, J. D. Weidenhamer, J. Chem. Ecol. 34 (2008) 70-75.
[145] G. Flamini, P. L. Cioni, Food Chem. 120 (2010) 984-992.
[146] G. Flamini, P. L. Cioni, I. Morelli, Flavour Fragr. J. 17 (2002) 147-149.
[147] E. E. Stashenko, S. A. Ordóñez, N. A. Marín, J. R. Martínez, J. Chromatogr. Sci. 47 (2009) 817-821.
[148] F. M. Musteata, J. Pawliszyn, J. Proteome Res. 4 (2005) 789-800.
[149] O. Dalby, J. W. Birkett, J. Chromatogr. A 1217 (2010) 7183-7188.
[150] C. Mardones, D. V. Baer, J. Silva, M. J. Retamal, J. Chromatogr. A 1215 (2008) 1-7.
[151] S. Magdic, A. Boyd-Boland, K. Jino, J. Pawliszyn, J. Chromatogr. A 736 (1996) 219-228.
[152] D. D. Roberts, P. Pollien, C. Milo, J. Agric. Food Chem. 48 (2000) 2430-2437.
[153] M. A. S. Avila, R. Breiter, Chromatographia 66 (2007) 369-376.
[154] L. Mondello, The FFNSC mass spectra library: an innovative and reliable peak assignment procedure.
[155] NIST Chemistry WebBook; http://webbook.nist.gov/chemistry/.
[156] ChemSpider: The free chemical database; http://www.chemspider.com/.

[157] J. O'Reilly, Q. Wang, L. Setkova, J. P. Hutchinson, Y. Chen, H. L. Lord, C. M. Linton, J. Pawliszyn, J. Sep. Sci. 28 (2005) 2010-2022.
[158] J. J. Langenfeld, S. B. Hawthorne, D. J. Miller, Anal. Chem. 68 (1996) 144-155.
[159] J. Poerschmann, J. Microcolumn Sep. 12 (2000) 603-612.
[160] B. Shurmer, J. Pawliszyn, Anal. Chem. 72 (2000) 3660-3664.
[161] A. Paschke, P. Popp, J. Chromatogr. A 999 (2003) 35-42.
[162] S. Endo, S. T. J. Droge, K. Goss, Anal. Chem. 83 (2011) 1394-1400.
[163] E. L. Difilippo, R. P. Eganhouse, Environ. Sci. Technol. 44 (2010) 6917-6925.
[164] J. Poerschmann, T. Górecki, F. Kopinke, Environ. Sci. Technol. 344 (2000) 3824-3830.
[165] O. Fiehn, G. Wohlgemuth, M. Scholz, T. Kind, D. Y. Lee, Y. Lu, S. Moon, B. Nikolau, Plant J. 53 (2008) 691-704.
[166] T. Górecki, X. Yu, J. Pawliszyn, Analyst 124 (1999) 643-649.
[167] T. Górecki, P. Martos, J. Pawliszyn, Anal. Chem. 70 (1998) 19-27.
[168] N. H. Snow, J. Sinex, M. Danser, LC GC Eur. 23 (2010) 260-267.
[169] P. J. Marriott, T. Massil, H. Hügel, J. Sep. Sci. A 27 (2004) 1273-1284.
[170] S-T. Chin, G. T. Eyres, P. J. Marriott, J. Chromatogr. A 1218 (2011) 7487-7498.
[171] D. C. Frank, C. M. Owen, J. Patterson, Lebensm. Wiss. U. Technol. 37 (2004) 139-154.
[172] M. Contini, M. Esti, Food Chem. 94 (2006) 143-150.
[173] J. Harynuk, T. Górecki, J. Chromatogr. A 1019 (2003) 53-63.
[174] J. Beens, M. Adahchour, R. J. J. Vreuls, K. van Altena, U. A. Th. Brinkman, J. Chromatogr. A 919 (2001) 127-132.
[175] M. Pursch, P. Eckerle, J. Biel, R. Streck, H. Cortes, K. Sun, B. Winniford, J. Chromatogr. A 1019 (2003) 43-51.
[176] J. Zrostlíková, J. Hajšlová, T. Čajka, J. Chromatogr. A 1019 (2003) 173-186.
[177] B. T. Weldegergis, A. de Villiers, S. Seethapathy, C. McNeish, A. Mostafa, T. Górecki, Anal. Chim. Acta 129 (2011) 188-199.
[178] B. T. Weldegergis, A. M. Crouch, T. Górecki, A. de Villiers, J. Chromatogr. A 701 (2011) 98-111.
[179] A. K. Smilde, M. J. van der Werf, J.-P. Schaller, C. Kistemkaer, Analyst 134 (2009) 2281-2285.

[180] S. N. Zhou, W. Zhao, J. Pawliszyn, Anal. Chem. 80 (2008) 481-490.
[181] S. Risticevic, D. Vuckovic, J. Pawliszyn, in: B. Xing, N. Senesi, P. M. Huang (Eds.), Biophysico-chemical Processes of Anthropogenic Organic Compounds in Environmental Systems, John Wiley & Sons, Inc., Hoboken, 2011.
[182] S. Kueger, D. Steinhauser, L. Willmitzer, P. Giavalisco, Plant J. 70 (2012) 39-50.
[183] A. Moing, A. Aharoni, B. Biais, I. Rogachev, S. Meir, L. Brodsky, J. W. Allwood, A. Erban, W. B. Dunn, L. Kay, S. de Koning, R. C. H. de Vos, H. Jonker, R. Mumm, C. Deborde, M. Maucourt, S. Bernillon, Y. Gibon, T. H. Hansen, S. Husted, R. Goodacre, J. Kopka, J. K. Schjoerring, D. Rolin, R. D. Hall, New Phytol. 190 (2011) 683-696.
[184] R. Watson, C. J. Wright, T. McBurney, A. J. Taylor, R. S. T. Linforth, J. Exp. Bot. 53 (2002) 2121-2129.
[185] Y. Tikunov, A. Lommen, C. H. R. de Vos, H. A. Verhoeven, R. J. Bino, R. D. Hall, A. G. Bovy, Plant Physiol. 139 (2005) 1125-1137.
[186] B. Vanderhaegen, H. Neven, H. Verachtert, G. Derdelincks, Food Chem. 95 (2006) 357-381.
[187] H.– D. Belitz, W. Grosch, P. Schieberle, in: Food Chemistry, Springer-Verlag, Berlin, 2009.
[188] J. Dixon, E. W. Hewett, New Zeal. J. Crop Hort. 28 (2000) 155-173.